INTERACTIONS BETWEEN HEMP GLOBULINS AND DAIRY PROTEINS

A thesis presented in partial fulfilment of the
Requirements for the degree of

DOCTOR OF PHILOSOPHY
IN
FOOD TECHNOLOGY

at
Riddet Institute, Massey University,
Palmerston North,
New Zealand.

CHIH-CHIEH CHUANG
2021

ABSTRACT

Industrial Hemp (*Cannabis sativa* L.) is a sustainable protein source and is easily digested. However, the hemp globulins (HG), which constitute around 70% of total hemp seed protein, have low solubility in water at neutral pH. The insolubility of HG limits its usage in many food systems.

This work explored the interactions between hemp globulins (HG) and dairy proteins, and aimed to increase the functionality of HG. HG was extracted with a mild salt-extraction and heat treatment was avoided, so the native structure of HG was preserved. The composition of HG was studied and a phase diagram of HG solubilisation was obtained regarding pH and ionic strength.

Two methods were used to increase the solubility/colloidal stability of HG by introducing interactions between HG and sodium caseinate (SC). The first method is by heating HG and SC together at 90 °C and the ionic strength of 0.5 M. SC exhibited the chaperone-like activity and inhibited the formation of large aggregates of HG. The addition of SC did not change the denaturation kinetics of HG, but rather changed its aggregation pattern. The second method is by pH-cycling. HG and SC formed colloidally stable nanoparticles (Z-average diameter ≈ 130 nm) after adjusting the pH to 12, reacted for 1 hour and neutralised back to pH 7. The solubility of HG increased from ~20% to > 80% after the pH-cycling.

The mechanisms and molecular interactions of both processing methods (heating and pH-cycling) were proposed. During heating, SC interacted with HG via hydrophobic interactions and the aggregation regime of HG changed from diffusion-limited cluster aggregation to

reaction-limited cluster aggregation, while the kinetics of HG denaturation was unaffected. During the pH-cycling, hydrogen bond was one of the driving forces for assembly of HG|SC nanoparticles. HG partially unfolded at pH 12 and interacted with caseins during the neutralisation and the stable HG–SC nanoparticles were formed.

The pH-cycled HG-SC nanoparticles can be used to make Pickering emulsions. Concentrated emulsions were prepared, and the rheological properties of emulsions during storage can be tuned by controlling HG:SC ratio in the HG|SC nanoparticles, i.e. emulsions became more solid-like when there was more HG in the HG-SC nanoparticles. The internal structure and interactions within the emulsions were evaluated by fitting frequency sweep test data according to a co-operative theory of flow. The results suggested that the solid-like emulsion resulted from stronger short-range interactions between flocs of oil droplets, which developed during storage when there was more HG in the HG–SC nanoparticles.

In conclusion, the findings in this study advanced our understanding of the interactions between plant seed globulins and caseins during processing. Such knowledge will help to increase the functionalities of plant proteins by mixing plant and dairy proteins.

ACKNOWLEDGEMENTS

The PhD journey was long and persistent endeavour was necessary, which is not my strongest point. I could not finish the thesis without the kind support from everyone I met during the past few years.

I would like to thank my supervisors first. Dr Simon Loveday provided gentle guidance and the freedom to explore and helped me to aim for the goal. I learnt a lot from his scientific thinking. Dr Aiqian Ye gave many valuable advises, especially on the interfacial properties of proteins. Dr Skelte Anema at Fonterra Research and Development Centre has enormous knowledge on dairy proteins and gave critical insights. Dr Teresa Wegrzyn gave provoking ideas and useful tips in the lab.

I am grateful to the Riddet Institute for financial support and for providing a research environment. It was quite enjoyable to discuss and learn from my fellow students, Yu-Fang Chen, Jie Hong Chiang, Feng Ming Chian, Cai Ling Ang, Sewuese Okubanjo, Siqi Li, Marina Marinea and Lirong Cheng.

My parents Ching-Shu and Hsiu-Luan were encouraging and were always there for me.

I wish to show my gratitude to my wife Che for her love and support. It was stressful that both of us were doing our PhD, but we have almost made it now. Finally, I thank my daughter Amy (安牧), the smile on your face gives me hope every day.

TABLE OF CONTENTS

LIST OF TABLES

LIST OF FIGURES

LIST OF PUBLICATIONS

Peer-reviewed paper

Chuang, C.-C., Wegrzyn, T. F., Anema, S. G., & Loveday, S. M. (2019). Hemp globulin heat aggregation is inhibited by the chaperone-like action of caseins. *Food Hydrocolloids, 93,* 46-55. https://doi.org/10.1016/j.foodhyd.2019.01.061

Chuang, C.-C., Anema, S. G., Ye, A., & Loveday, S. M. (2020). Hemp globulin forms colloidal nanocomplexes with sodium caseinate during pH-cycling. Submitted to *Food Research International.*

Chuang, C.-C., Ye, A., Anema, S. G., & Loveday, S. M. (2020). Concentrated Pickering emulsions stabilised by hemp globulin–caseinate nanoparticles: tuning the rheological properties by adjusting the hemp globulin:caseinate ratio. *Food & Function* 10.1039/D0FO01745K

Presentation

Chuang, C.-C., Wegrzyn, T. F., Anema, S. G., & Loveday, S. M. Formation of hemp protein microparticles by phase separation. 7th International Symposium on "Delivery of Functionality in Complex Food Systems", Auckland, New Zealand. 5-8 November 2017 (poster presentation).

Chuang, C.-C., Anema, S. G., Ye, A., Wegrzyn, T. F., & Loveday, S. M. Improving colloidal stability of hemp globulins by making hemp-casein protein nanoparticles with a pH-cycling

method. 8th International Symposium on "Delivery of Functionality in Complex Food Systems", Porto, Portugal. 7-10 July 2019 (oral presentation).

Chuang, C.-C., Anema, S. G., Ye, A., Wegrzyn, T. F., & Loveday, S. M. Improving the functionality of plant proteins by blending with caseinates. Dairy Industry Workshop, Palmerston North, New Zealand. 28-29 August 2019 (oral presentation).

Chuang, C.-C., Anema, S. G., Ye, A., & Loveday, S. M. Hemp-casein nanoparticles can stabilise concentrated emulsions. 5th International Conference on "Food Structures, Digestion & Health", Rotorua, New Zealand. 30th September to 3rd October 2019 (poster presentation).

Chuang, C.-C., & Loveday, S. M. Hemp seed protein: prospects and pitfalls. NZIFST Conference, Palmerston North, New Zealand. 7 July 2021 (oral presentation).

LIST OF SYMBOLS AND ABBREVIATIONS

2D-PAGE	Two-dimensional SDS-PAGE
α-la	α-lactalbumin
β-lg	β-lactoglobulin
BSA	Bovine serum albumin
CCP	Colloidal calcium phosphate
CLSM	Confocal Laser Scanning Microscopy
DCR	Derived count rate
DLCA	Diffusion-limited cluster aggregation
DLS	Dynamic laser scattering
DSC	Differential scanning calorimetry
DSF	Differential scanning fluorimetry
DTT	Dithiothreitol
HG	Hemp globulins
NEM	N-ethylmaleimide
pI	Isoelectric point
PSD	Particle size distribution
RLCA	Reaction-limited cluster aggregation
SC	Sodium caseinate
SDS-PAGE	sodium dodecyl sulfate polyacrylamide gel electrophoresis
SO	Sypro Orange
SPI	Soy protein isolate
TEM	Transmission electron microscopy
WPI	Whey protein isolate

1. INTRODUCTION

Proteins are essential nutrients that can be hydrolysed, absorbed and reconstituted into structural proteins and enzymes to maintain our metabolism, and may also provide energy. Major protein sources are from animals or plants. Plant proteins, especially when the production is in commercial- and industrial-scale, are generally regarded as more sustainable protein sources than animal proteins (Poore & Nemecek, 2018). Increasing demand for high-quality protein is expected by 2050 due to the rapid growth of population and increasing living standards, and there will be a shortage of protein if no initiative is taken. Therefore, it has been proposed that plant-based diets should be considered (Sabaté & Soret, 2014).

However, there are also shortcomings when using plant proteins as the sole protein source. Firstly, the nutritional quality of plant protein is generally inferior compared to animal proteins. Most plant proteins are regarded as incomplete, which means that they do not contain the correct proportion of essential amino acids (Young & Pellett, 1994). In addition to the inherent nature of amino acid composition, there is another problem of protein digestibility. In general, when compared with plant-derived proteins, more amino acids are digested and absorbed when dairy proteins are consumed (Mathai, Liu, & Stein, 2017).

In order to solve the problem of poor protein quality of plant protein and the possible sustainable problem of animal proteins, partial replacement of animal-derived protein with plant protein had been proposed as one of the solutions to meet the demand for high-quality protein (Boland et al., 2013). By substituting part of the animal proteins by plant proteins,

we might “top up” the insufficient or less digestible amino acids in plant protein and lower the environmental pressure at the same time.

However, the utilisation of plant protein could be challenging because of the possible inferior functional properties. Proteins are often used to provide/stabilise structure in food systems such as gel, emulsion and foam (Foegeding & Davis, 2011). Unlike the water-soluble dairy proteins, proteins from plant seeds have low water solubility, which in turn affects other functionalities of plant proteins (Wouters, Rombouts, Fierens, Brijs, & Delcour, 2016). Therefore, various methods have been tried to increase the solubility of plant proteins, such as deamination (Hamada, 1994), enzymatic hydrolysis (Achouri, Zhang, & Shiying, 1998; Malomo & Aluko, 2015b; Yin et al., 2008), pH-cycling (Jiang, Chen, & Xiong, 2009), high-pressure homogenisation (Dong et al., 2011) and freeze-milling (T. Wang, Zhang, Wang, Wang, & Chen, 2015).

Mixing and introducing interactions between dairy and plant proteins together could be another solution to improve the functionalities of plant proteins. It had been proposed to make protein ingredients from mixtures of plant and dairy proteins to achieve functional synergy (Ipsen, 2017). Synergy in the protein functionalities had been reported in some dairy-plant protein blends, e.g. stronger gels (Jose, Pouvreau, & Martin, 2016; Roesch, Juneja, Monagle, & Corredig, 2004; D. Wong, Vasanthan, & Ozimek, 2013) and stable emulsions (Hinderink, Münch, Sagis, Schroën, & Berton-Carabin, 2019; Yerramilli, Longmore, & Ghosh, 2017) as summarised in Chapter 2.

This work seeks to improve the functionalities of plant seed proteins by introducing interactions with dairy proteins. The molecular interactions between plant and dairy proteins during the processing were also analysed.

The objectives were:

- Extract protein from plant seeds (pea, hemp and chia) and characterise their compositions and functionalities. Select one suitable plant protein source for detailed studies.
- Introduce interactions between the plant protein and dairy proteins (whey or casein fractions) to find the possible enhancement of the functionalities of plant proteins.
- Analyse the interactions between plant and dairy proteins.
- Find the applications of the plant-dairy protein mixtures.

In chapter 4, the focus is on the screening the suitable plant protein sources and the possible methods to improve the functionalities of dairy-plant protein. Plant proteins were isolated from four New-Zealand-grown crops, and hemp was selected as the plant protein material because of its relatively simple protein composition and scientific novelty. The salt-extracted and freeze-dried hemp globulins (HG) fraction was characterised and its phase diagram was examined. Interaction between HG and amphiphilic molecules (caseins and surfactant) was introduced by homogenisation and the change in solubility of HG was measured. Heat-induced aggregation between HG and dairy whey proteins was also investigated. The results of this chapter gave us the main research theme of the following chapters – water solubility/colloidal stability and heat stability of HG-casein blends.

Chapter 5 reports investigations on the chaperone-like effect of caseins on the heat-induced aggregation of HG. Solubility, colloidal stability and aggregation kinetics of HG or HG-casein blends were measured during heat treatment (90 °C, 0.5 M ionic strength for up to 15 min). The effect of caseins on the aggregate size of HG was explained by the change of aggregation regime. The molecular interactions between HG and caseins was characterised and a new high through-put method was developed to quantify the hydrophobic interactions in real-time.

Another method, pH-cycling, is reported in Chapter 6 to introduce interactions between HG and caseins. During pH-cycling, the pH of HG dispersion was adjusted to 12 before neutralisation to pH 7. Colloidally stable casein-hemp protein nanoparticles were made after the pH-cycling process. These nanoparticles were characterised, and the improvement of HG solubility was measured. In addition, the heat stability and the molecular interactions (covalent or non-covalent) of these protein nanoparticles were studied.

Concentrated Pickering emulsions stabilised by casein-hemp protein nanoparticles made in chapter 6 was investigated in chapter 7. The stability and rheological properties of these Pickering emulsions were monitored during storage. The rheological properties of emulsions stabilised by casein-hemp protein particles can be tuned by adjusting HG/casein ratio. The structure of emulsions was elucidated by the data of rheological experiments and confocal laser scanning microscopy.

2. LITERATURE REVIEW

2.1. Plant seed storage proteins

Plant seed proteins can be classified by a classic Osborne fractionation method according to their solubility in different solvents with a sequential fractionation (Osborne, 1924). The first solvent used is water and the soluble fraction is called albumins. After the water extraction, the fractionation is followed by a dilute salt solution to obtain the globulin fraction, dilute alkali solution for the glutelin fraction and an alcohol/water mixture for the prolamin fraction. This type of sequential solvent extraction process has become a common and easy method to extract and classify plant seed protein. The Osborne fractionation series provides information about the relative distribution across these broad plant protein classes. However, each solubility class is a complex mixture of proteins, and there can be significant overlap between the four Osborne fractions (Day, 2013).

Plant proteins can also be classified by function: storage proteins are the major proteins in seeds that store energy for the seeds' germination. Because the Osborne series may not actually fractionate the storage protein, modern classification of seed storage proteins is based on their sedimentation coefficients in water at 20 °C ($S_{20,w}$): globulins have $S_{20,w}$ values of around 7 (vicilin-type) or 11 (legumin-type) protein; while albumins have a $S_{20,w}$ value of about 2. Therefore, legume storage proteins are classified as globulins (7S and 11S) and albumins (2S). Hemp storage protein is mainly 11S globulins. Cereals, apart from oats and rice, contain mainly prolamins as storage protein (Table 1).

Table 1 Distribution of storage protein types in seed of selected crops. Adapted from Shewry and Casey (1999).

	2S Albumins	7S Globulins	11S Globulins	Prolamins
Major components	Legumes	Legumes	Legumes	Cereals
	Castor bean	Cottonseed	Oats and Rice	
	Cottonseed	Palms	Hemp	
	Brazil nut	Cocoa	Brazil nut	
Minor components		Cereals	French bean	Oats
				Rice

2.1.1. *Storage proteins of soy, pea and hemp*

Globulins are the major seed storage proteins in legumes and hemp (Table 1). About 90% of soy storage protein is globulin, and the levels of globulins in pea and hemp are 50-60 % and 60-80 % respectively (Day, 2013; Park, Seo, & Lee, 2012). However, the ratios of 11S to 7S globulins are different among these plants and might result in different protein functionalities. The protein functionalities are specific functional properties that protein could perform in the food systems, such as forming the colloidal structures that serve as building blocks of the food matrix (Foegeding & Davis, 2011; Kristo & Corredig, 2014), being emulsifier or inactive filler that does not increase the solubility, etc.

Table 2 Major seed globulins from selected crops. Adapted from Casey (1999), X.-S. Wang, Tang, Yang, and Gao (2008) and Duranti, Consonni, Magni, Sessa, and Scarafoni (2008).

Protein	Species	MW (kDa)	Polypeptide MW (kDa)	
7S				
Vicilin	*Pisum sativum* (pea)	150-190	12, 13, 16, 19, 25, 30, 33, 34, 50	
	Vicia faba (broad bean)	150		
Convicilin	*Pisum sativum* (pea)	220-290		
	Vicia faba (broad bean)			
β-conglycinin	*Glycine max* (soybean)	150-210	45-52, 57-83	
Conglutin *β*	*Lupinus spp.* (Iupins)	143-260	17-20, 24-46, 53-64	
11S				
			Acidic subunits	Basic subunits
Legumin	*Pisum sativum* (pea)	330-450	24.5-43	20.7-21.9
	Vicia faba (broad bean)	320-400	23-58	19-23.8
Glycinin	*Glycine max* (soybean)	320-375	10.6, 30, 31.6, 37, 42	19-20.7
Edestin	*Cannabis sativa* (hemp)	300	34	18, 20
Conglutin *α*	*Lupinus spp.* (lupin)	315		
Helianthinin	*Helianthus annuus* (sunflower)	300-350		
Cruciferin	*Brassica napus* (oilseed rape)	300		

The storage proteins of plant seeds are homologous, and Table 2 shows the basic information of globulins in selected crops. The 11S globulins of soy (glycinin), pea (legumin) and hemp (edestin) have conserved amino acid sequences (Figure 2-1); the similar composition of secondary structure and the tertiary structures of seed globulins are also believed to be conserved (Marcone, Kakuda, & Yada, 1998a). The current structural models consider the 7S proteins to be trimeric and the 11S proteins to be hexameric, with the monomers held together by non-covalent interactions. The 7S trimer consists of three subunits of MW 50-70 kDa; whereas the 11S hexamers consist of six subunits of MW 60-80 kDa. Each subunit of 11S globulins is itself a dimer of one acidic polypeptide and one basic polypeptide linked by disulfide bonds (Table 2), and the positions of cysteine residues are highly conserved among 11S globulins from different plant seeds as indicated by the black arrows in Figure 2-1.

Since the seed globulins are similar in structure and molecular weights, they also share some similar attributes. For example, the denaturation temperatures of plant seed globulins are much higher than those of dairy whey proteins, e.g. denaturation temperature of soy, pea and hemp globulins are 95.4, 83.8 and 95.8 °C respectively (Marcone, Kakuda, & Yada, 1998b), compared with 78 °C for β-lactoglobulin and 62 °C for α-lactalbumin from bovine milk (Brodkorb, Croguennec, Bouhallab, & Kehoe, 2016). The higher denaturation temperature may hinder the heat-induced cross-linking between plant globulins and whey proteins via disulfide linkages. The post-translational modifications (e.g. glycosylation) and proteolysis are common among globulins, which might provide structural diversity and complexity in these storage proteins (Casey, 1999). Another difference between globulins from different plants is the ratio of 11S to 7S globulins, which might result in different

protein functionalities among these plant seeds. There is much more 11S protein in hemp, with the 11S/7S ratio being higher than 6.3 in salt-extracted HG according to the intensities of protein bands in the SDS-PAGE gel (Hadnađev et al., 2017; Tang, Ten, Wang, & Yang, 2006), whereas the average ratio is around 1.29 in soy protein isolates (Arrese, Sorgentini, Wagner, & Anon, 1991) and 0.57 – 0.81 in pea protein isolates (Barac et al., 2010). It has been reported that the 7S globulins of soy (β-conglycinin) could limit the heat-induced aggregation of its 11S globulin (glycinin) (J. Guo et al., 2012), so the high 11S/7S ratio of HG composition might result in lower heat stability because of the extremely low content of 7S globulins.

2.1.1. *Hemp seed protein*

Hemp seed protein is used as a source of plant protein. Industrial hemp (*Cannabis sativa* L.) has a low level of tetrahydrocannabinol, the psychoactive compound, and it can be grown in a variety of soil types without fungicides, herbicides and pesticides (Aluko, 2016). In addition to its traditional use for the fibre from the stalk, the hemp oil and hemp protein are also attracting attention because of their nutritional values. New Zealand government legalised the other parts of hemp seed, in addition to hemp seed oil, as food in 2018 because of its nutritional value and the expected revenue of $10-20 million NZD (O'Connor, 2018). Hemp seed typically contains more than 30% of oil and around 25% protein. Hemp seed oil has more than 80% polyunsaturated oil and has an exceptionally high amount of two essential fatty acids – linoleic acid and *alpha*-linolenic acid (Callaway, 2004).

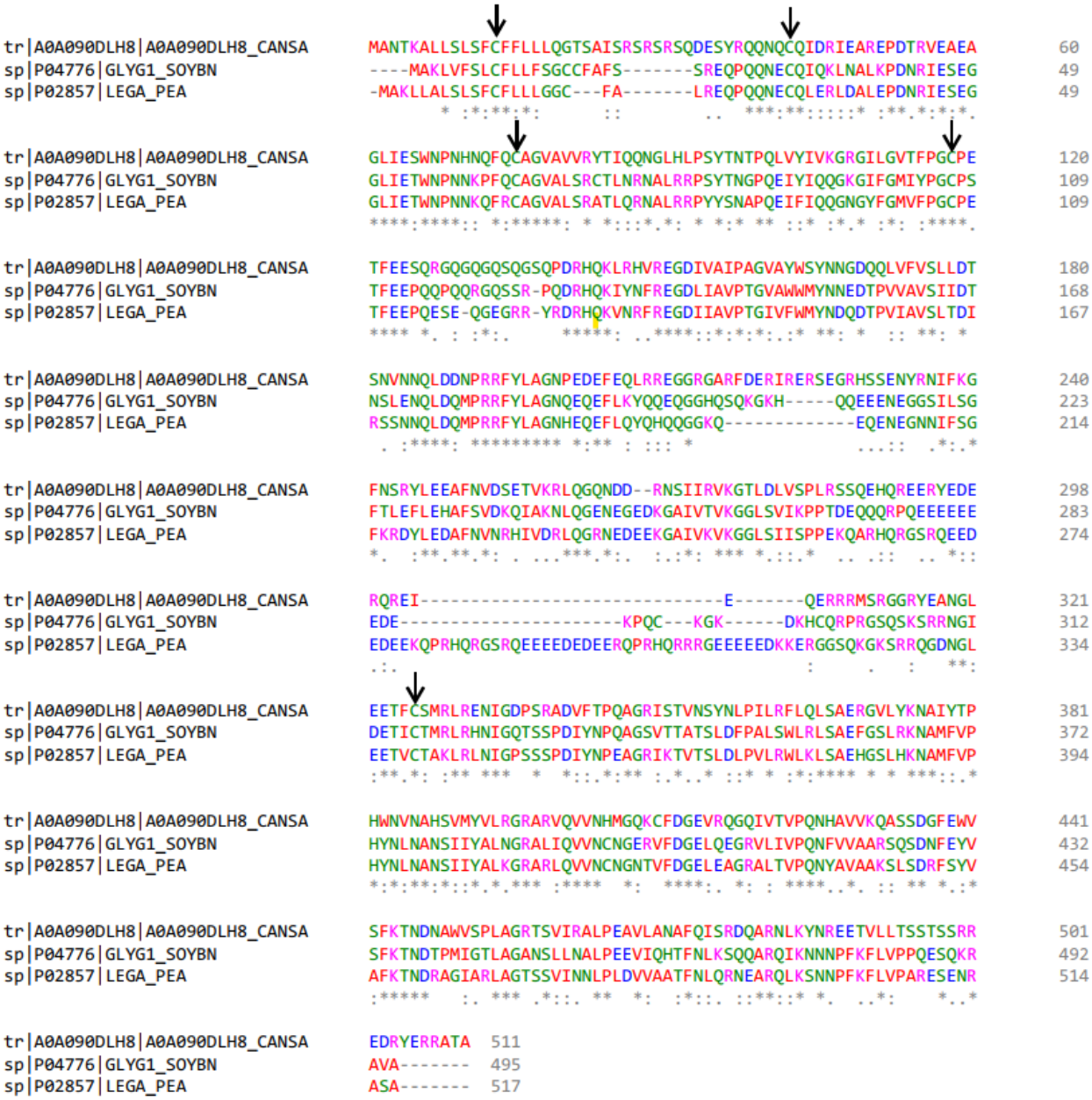

Figure 2-1 Sequence alignment of 11S globulins of soy Glycinin (UniProt accession number: P04776), pea Legumin (P02857) and hemp Edestin (A0A090DLH8). Aligned with the claustral omega tool https://www.ebi.ac.uk/Tools/msa/clustalo/ (Madeira et al., 2019). The symbol "*" indicates positions that have a single and fully conserved residue; the symbol ":" indicates conservation between groups of strongly similar properties; the symbol "." indicates conservation between groups of weakly similar properties.

Hemp seed protein is comprised of around 60 – 80% edestin (the 11S globulin, salt soluble) and 20 – 30% albumin which is water-soluble (J.-J. Kim & Lee, 2011). Edestin is believed to be hexamer as mentioned in the previous section. The basic unit of the hexamer has a molecular weight of around 50 kDa, which is composed of a basic domain (≈ 33 kDa) and an acidic domain (≈ 20 kDa) that are linked via disulfide bonds (Tang et al., 2006). The cleavage site of acid and basic domains is between residue G320 and L321 – the N-terminal being the basic subunit and the C-terminal being the acidic subunit. The two domains are linked via a disulfide bond between residue C118 and C326; while C42 and C75 form a intrachain disulfide bond (Docimo, Caruso, Ponzoni, Mattana, & Galasso, 2014). Edestins stack to form polygonal-shaped crystalloids which have a diameter of around 8 nm. The 8-nm crystalloids would further stack into large crystalloids that are micron-sized and form the protein body in hemp seeds (St. Angelo, Yatsu, & Altschul, 1968).

Hemp seed protein has high digestibility of 88 – 91%, which is much higher than the 71% digestibility of soy protein isolate (X.-S. Wang et al., 2008). However, hemp protein is not nutritionally complete and its protein digestibility-corrected amino acid score (PDCAAS) was around 0.5 – 0.6, which is limited by the first essential amino acid lysine (House, Neufeld, & Leson, 2010). The PDCAAS value of hemp protein is even lower than other common plant protein sources such as soy (1.02 – 1.09) and pea (0.84) (Mathai et al., 2017). On the other hand, the PDCAAS of milk proteins products are higher than much higher, e.g. the milk protein concentrate have the value of 1.42 for the > 3-year-old population (Mathai et al., 2017). Therefore, combining hemp and dairy proteins would improve the efficiency of utilisation of the poor-quality hemp protein, which fulfils the definition of "protein complementation" (Bressani, 1988).

2.1.1. *Functionalities of hemp seed protein*

Solubility is an important functionality as proteins are frequently solubilised or hydrated before use. Generally, proteins are soluble when the sum of repulsive forces (electrostatic) is larger than the sum of attractive forces (electrostatic, hydrophobic, hydrogen bonding, etc.). Therefore, protein solubility is dependent on intrinsic properties of the protein (sequence and composition of amino acids) and environmental properties (e.g., temperature, pH and ionic strength) (Shridhar, 2012). The solubility of hemp seed protein reaches the minimum value at pH 4 – 6 and the protein becomes more soluble at lower or higher pH (Tang et al., 2006). Hemp seed protein became highly soluble (> 80% soluble) when the pH is higher than 8 (Hadnađev et al., 2017; Tang et al., 2006). Hemp seed protein extracted by the isoelectric method still has low solubility in water at pH 7: around 5 – 35% of the protein was soluble out of 1% protein dispersion, which means the solutions have only 0.05 – 0.35% soluble protein (Hadnađev et al., 2017; Tang et al., 2006; Yin et al., 2008). However, hemp protein extracted by the micellisation method, i.e. extract the protein with salt solution then dialyse to remove salt, had higher solubility, probably because this method results in less denaturation than extraction at alkaline pH (Hadnađev et al., 2017). The water holding capacity of hemp seed protein was low due to its low solubility in water (Tang et al., 2006).

Gelation is another important functionality because many foods are protein gels, e.g. tofu, yogurt, pudding. It could also be an undesirable property in some foods systems such as beverages. There are two steps of the protein gelation process: (1) denaturation of protein and (2) association or aggregation of the partially denatured protein molecules (Matsumura & Mori, 1996). There are many methods to induce protein gelation, e.g. heating, acidifying

and enzymatic cross-linking, and only the heat-induced gelation had been studied in hemp seed protein. Malomo, He, and Aluko (2014) reported that at least 22% protein was needed for the gelation at 95 °C for hemp seed protein isolated by the isoelectric method. Since the solubility of hemp protein was extremely low (< 0.35% soluble protein), the 22% protein dispersion might already have a paste-like texture just like 30% hemp protein dispersion (Dapčević-Hadnađev, Hadnađev, Lazaridou, Moschakis, & Biliaderis, 2018), which could already be partially self-supporting.

Foam can be stabilised by protein when protein is solubilised in the solvent and then transported, adsorbed and reorganised onto the air/water interface on the thin film of bubbles. (Wilde & Clark, 1996). Malomo et al. (2014) showed that hemp protein isolate (20 mg/mL) had higher foam capacity (≈ 500% volume expansion when homogenised) at pH 3 than at pH 5 – 9, possibly due to greater protein flexibility, so proteins could be reorganised on the air/water interface.

Emulsification is another functionality regarding interfacial properties. An emulsion is a dispersion or a suspension of two immiscible liquids (Hill, 1996). Protein can also be transported, adsorbed and reorganised on the liquid/liquid interface on the surface droplets just like the foam system, and thus stabilises the emulsion. The emulsifying properties (emulsifying activity and stability) of hemp protein isolate are significantly lower than that of soy protein isolate at pH 3 – 8 (Tang et al., 2006). The authors also found that the profile of emulsifying activity versus pH was similar to the profile of protein solubility between pH 3 – 6, suggesting that the emulsifying property was correlated to the solubility of hemp protein at the acidic environment. However, the higher protein solubility at pH 7 and 8 did not result in a higher emulsifying activity, so other parameters such as aggregation state

and surface hydrophobicity might also contribute to the emulsifying properties of hemp protein. Nevertheless, emulsions stabilised by hemp protein isolate have high emulsion stability of almost 100% in most conditions (protein concentration: 1 – 5 % w/v, pH 3 – 9) when tested by Malomo et al. (2014).

In summary, it seems that the inferior solubility of hemp seed protein is a limiting functionality that would affect other functionalities such as water holding capacity and emulsifying properties. Therefore, it might be beneficial to tackle the problem of the low solubility of hemp proteins first.

2.2. Dairy proteins

Protein constitutes around 3.3 % of bovine milk and dairy proteins can be fractionated into caseins and whey proteins according to their solubility at pH 4.6 at 20 °C – caseins would precipitate and native whey protein is still soluble under these conditions (Fox & Kelly, 2004). Caseins make up around 80 % of total milk protein and the whey proteins make up around 20 %.

Caseins are phosphoproteins, which are amphiphilic with highly hydrophobic regions interspersed with hydrophilic regions, and associate with each other in casein micelles in raw milk (Pritchard & Kailasapathy, 2011). The dry matter of casein micelles is made up with around 95% of caseins and around 5% minerals, which are collectively referred to as colloidal calcium phosphate (CCP). Casein micelles are highly hydrated, containing 3 – 3.5 g water for one g of dry matter. Casein micelles are spherical and have a radius of around 50 – 150 nm (Huppertz, 2013; McMahon & Oommen, 2013). There are four major caseins – α_{s1}-, α_{s2}-, β- and κ-casein, which have weight ratios of around 40:10:40:10 and

their molecular weights are around 19-25 kDa (Augustin, Oliver, & Hemar, 2011). α_{s1}-, α_{s2}- and β-caseins are referred to as calcium-sensitive caseins because they lose solubility when ionic calcium is present. The negatively-charged side chains of these calcium-sensitive caseins, e.g. phosphorylated serine, can interact with the positively charged divalent ions (e.g. Ca^{2+}) and the decreased net charge on protein results in lower solubility. On the other hand, the solubility of κ-casein is insensitive to positively charged ions (Huppertz, Fox, & Kelly, 2018).

There are many models for the structure of casein micelles, and one possible structure was described as the nanocluster model (de Kruif, Huppertz, Urban, & Petukhov, 2012). In this model, the nanocluster made of CCP is dispersed and the calcium-sensitive caseins are believed to interact and cover the CCP nanoclusters. The tails of these caseins of the casein-CCP aggregates associated via collective weak interaction and form a porous protein matrix. The association of casein-CCP aggregates is believed to be terminated by κ-casein on the surface of casein micelles. Another model is the dual binding model (Horne, 1998), which involves the hydrophobic interactions and electrostatic neutralisation. The hydrophobic parts of α- and β-caseins associate together and form a bonded cluster, and the growth of these clusters is inhibited by the electrostatic repulsions between caseins. The CCP could bind and neutralise the negatively charged phosphoserine residues on caseins to reduce the electrostatic repulsions and facilitate the further association of α- and β-caseins, as one CCP is considered to be able to bind up to four or more phosphoserine clusters from different casein molecules. On the other hand, κ-casein would terminate the further growth of casein micelle because it has no phosphoserine residues and so does not associate with CCP. κ-casein has only one hydrophobic region which will be occupied

already when interact with other hydrophobic regions of caseins so cannot extend the hydrophobic interactions. However, these models did not explain the porous structure of casein micelles observed under electron microscope. Dalgleish (2011) improve the models by introducing the concepts of water channels and mobile β-casein. The caseins and CCP-associated nanoclusters and the spaces between them are penetrated by water. Some β-caseins can act as surfactant and stabilise the surface of the water channels inside the casein micelles due to its amphiphilic nature.

During milk processing, caseins can be coagulated through acidification or rennet addition and are readily separated from the whey. Caseinates are made by neutralising precipitated acid casein with alkali with different metal counter ions. For example, sodium caseinate (SC) is made by (1) acidifing skim milk to pH 4.6 to solubilise CCP and precipitate the casein, (2) washing to remove whey proteins from the casein curd and (3) neutralising the acid casein with sodium hydroxide back to pH 6.7 (O'Kennedy, Mounsey, Murphy, Duggan, & Kelly, 2006; O'Regan & Mulvihill, 2011). The native casein micelle structure is disrupted during the acidification and neutralisation process, while the individual molecules are believed to associate again and are reported to form star-like structures (radius ≈ 11 nm) in high ionic strength (> 0.1 M) (HadjSadok, Pitkowski, Nicolai, Benyahia, & Moulai-Mostefa, 2008). As for the making of rennet casein, the enzymes in rennet, particularly chymosin, hydrolyse κ-casein on the surface of casein micelles, removing a hydrophilic peptide that stabilises the micelles. As a result, the micelles aggregate and coagulate via hydrophobic interactions and calcium bridging to form a gel (Aguilera & Rademacher, 2004).

Whey proteins, which include β-lactoglobulin (β-lg), α-lactalbumin (α-la), bovine serum albumin (BSA), immunoglobulins and polypeptides protease peptones can be recovered from acid whey when the pH was adjusted to 4.6 at 20 °C. Whey proteins denature above around 60 °C at neutral pH – the initial denaturation temperature of β-lg, α-la and BSA is at 78, 62 and 64 °C respectively (Brodkorb et al., 2016). There are two intramolecular disulfide bonds and one free thiol group at Cys 121 in β-lg. The free thiol group can be cross-linked to the disulfide bonds of other proteins via thiol-disulfide exchange reactions during heating. α-la is a small protein stabilised by four disulfide bonds but has no free thiol groups, so it is quite heat-stable in the absence of other milk proteins. When whey proteins are recovered from the renneting process, the product is called sweet whey. The sweet whey contains caseinomacropeptide, which appears when κ-casein was cleaved by the enzymes in rennet. Caseinomacropeptide is absent in acid whey (Boland, 2011).

2.2.1. *Functionalities of milk protein products*

In this study, the dairy protein source was predominantly SC, with some work using whey protein isolate (WPI), so the functionalities of these two dairy protein products will be reviewed. Singh (2011) summarised some of the functionalities of milk protein products (Table 3), and it can be seen that the SC has excellent functionalities in solubility, interfacial properties (emulsification and foaming), water binding, providing viscosity and heat stability. On the other hand, WPI has excellent acid stability and solubility, and good interfacial properties.

SC is very soluble in water: 89 – 97% of solubility had been reported (Bastier, Dumay, & Cheftel, 1993), and the high solubility of caseinates is one of the reasons for their high

emulsifying and foaming properties. Another reason for the high interfacial functionalities is that the major components of caseinate (α_{S1}- and β-casein) are flexible and strongly amphiphilic, and these properties could rapidly lower the interfacial tension during emulsification. The adsorbed caseins provide good stability because of electrostatic and steric repulsions (Dickinson & Golding, 1997). Therefore, SC is the most used protein when it comes to the stabilisation of food emulsions (Hill, 1996).

Table 3. Functionalities of milk protein products. From Singh (2011).

	Caseinates		Whey protein products		
	Sodium	Calcium	WPC	WPI	Milk protein concentrates
Solubility	xxx	x	xxx	xxx	xx
Emulsification	xxx	x	xx	xx	x
Foaming	xxx	x	xx	xx	x
Water binding	xxx	x	x	x	x
Viscosity	xxx	x	x	x	x
Gelation			xxx	x	
Heat stability	xxx	x	x	x	x
Acid stability	x	x	xxx	xxx	x
Freeze–thaw stability	xxx	x	x	x	x

x, poor; xx, good; xxx, excellent.

SC is also commonly used to increase the viscosity and provide desirable textures in foods such as soups and sauces (Singh, 2011). The viscosity of SC increased with SC concentration and decreased with temperature. Pitkowski, Durand, and Nicolai (2008)

showed that the viscosity increased sharply above a critical concentration of around 13% SC at 20 °C, due to the jamming of the SC aggregates.

SC is quite heat-stable, as they do not denature and aggregate during heat treatment when compared to whey proteins. SC is still almost soluble when heated at 132 °C for 60 min at pH 7 (M. R. Guo, Fox, Flynn, & Kindstedt, 1996). The first reason for its heat stability is that caseins are not globular proteins and they are relatively unstructured, i.e. they are already more or less unfolded. Besides, the majority of caseins (α_{s1}- and β-casein) has no cysteine residues, so no heat-induced thiol/disulfide exchange would happen. In addition, none of the caseins has free Cys residues. The minor fraction of α_{S2}- and κ-casein have two cysteine residues, which form intermolecular disulfide bonds (O'Mahony & Fox, 2013). Native α_{S2}-casein appears mainly as dimer and κ-casein is linked with internal disulfide bonds, and could be monomer to oligomers which comprises with more than 8 κ-caseins (Huppertz, 2013).

In terms of gelation, caseinate can form gels when acid is added. On acidification of casein micelles to pH close to their pI of pH 4.6, the net charges of casein molecules are close to zero, hydrophobic interactions become dominant, and so-called acid-induced casein gels can form (Lucey, 2017).

WPI is also highly soluble in water, with > 80 % solubility below 40 °C between pH 3.5 – 7.8, and the lowest solubility of 82% appears at pH 4.5 (Pelegrine & Gasparetto, 2005). However, the heat stability of WPI is not as high as SC due to the denaturation of whey proteins, which generally leads to the loss of solubility (Bonnaillie & Tomasula, 2009). For example, β-lg can aggregate via heat-induced thiol/disulfide exchange above around 65 °C,

resulting in lower solubility (Sava, Van der Plancken, Claeys, & Hendrickx, 2005). Heat-induced aggregates may cross-link into a 3-dimensional and self-supporting network when the protein concentration exceeds the critical concentration (Mahmoudi, Mehalebi, Nicolai, Durand, & Riaublanc, 2007).

2.3. Comparison of functionalities between soy and milk proteins

The functionality of plant protein is different from than that of dairy protein. Webb, Naeem, and Schmidt (2002) compared several functionalities of soy protein isolate (SPI), whey protein isolate (WPI) and SC. SPI is the most common plant seed protein product in the market, so it can be seen as the benchmark for the plant protein functionalities. The results show that the solubility, foam capacity and foam stability of SPI is much lower than that of dairy proteins. On the other hand, SPI is a more potent protein when it comes to making O/W emulsion by having higher emulsifying properties (emulsion activity, stability and higher amount of adsorbed protein on the interface).

2.4. Protein-protein interactions

There are many types of molecular interactions between polypeptide chains (Figure 2-2). The sum of these interactions determines the structure of a native protein and its functionalities. Interactions between proteins take place during food processing due to the change of environment (temperature, pH, shearing force, etc.), and thus the functionalities and the structure and texture of the food change accordingly.

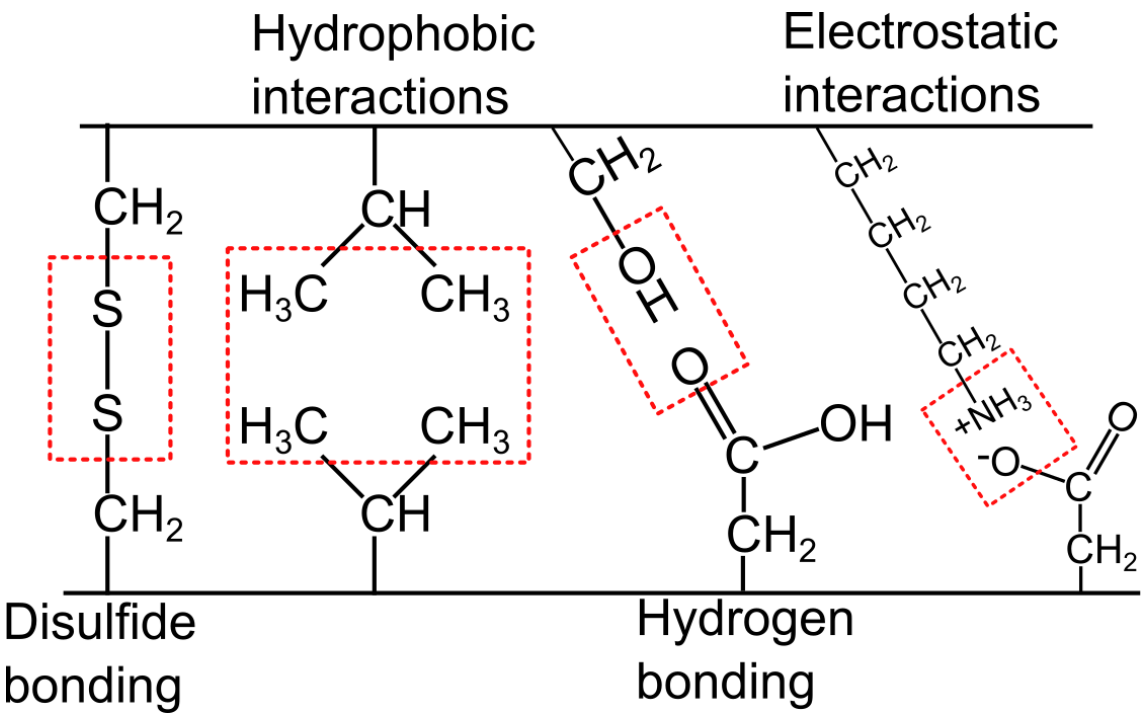

Figure 2-2 Schematic figure of possible protein-protein interactions between side chains of amino acids.

2.4.1. *Covalent interactions*

Disulfide bonding is the most common covalent linkage between side chains of amino acids in the protein. It is a strong bond formed between two thiol groups of cysteine, with the heat of formation of about 50 kcal/mol (Howell, 1992).

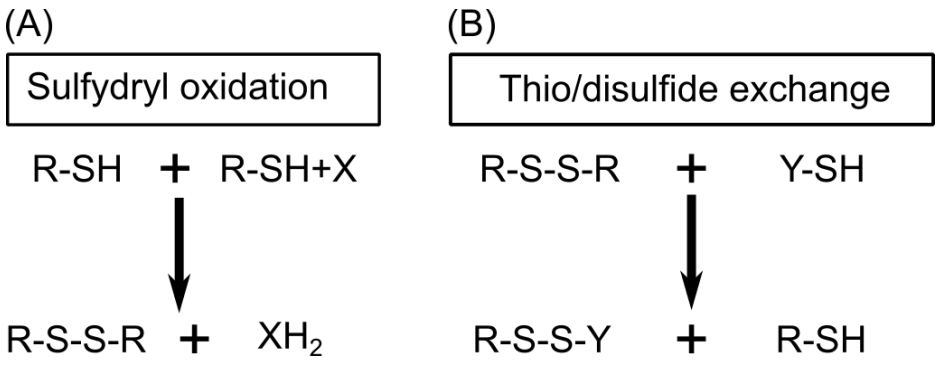

Figure 2-3 Formation of disulfide linkages.

The formation of disulfide bonds can be induced by heating or by moderate to high pH in the presence of oxidising agents. During heating, proteins unfold and the buried thiol groups of native protein become exposed and are readily reactive when the condition is right, such as high pH. The pKa of sulfhydryl group of free Cys is around 8.3, above which there will be more reactive deprotonated thiolate groups (S^-) than the non-reactive thiol group (SH). Then the higher amount of reactive thiolate group would have higher chance to form disulfide bonds with another cysteine (Figure 2-3A); the oxidised thiolate group could also interact with another disulfide bond, so the old disulfide bond breaks and a new disulfide bond forms, which is called thiol-disulfide exchange reaction (Figure 2-3B) (Visschers & De Jongh, 2005). In short, the higher the pH, the higher reaction rate of sulfhydryl oxidation and thiol/disulfide exchange. Nevertheless, the formation of new disulfide bonds between dairy proteins still occurs at the neutral pH of milk of pH 6.7 or even at more acidic pH, especially when heated (de la Fuente, Singh, & Hemar, 2002).

Protein aggregation may result from the formation of disulfide bonds between proteins. In a system with dairy protein and plant seed storage proteins, there are two disulfide bonds and one free thiol group in β-lg, and many disulfide bonds and one free thiol group in plant globulins (Shewry, Napier, & Tatham, 1995). Therefore, heat-induced aggregation between β-lg and plant globulins via thiol-disulfide exchange reactions could be expected. Other covalent bonding might be formed between proteins, e.g. via Maillard reaction, via the pathway of dehydroprotein and the subsequent formation of lysinoalanine and lanthionine. However, most research on these covalent linkages focused on their impact on the protein digestibility and not much has been done on their influences on the protein functionalities (Gerrard, 2002).

2.4.2. *Non-covalent interactions*

Hydrophobic interactions are attractive forces between non-polar groups separated by water. Non-polar groups, such as the non-polar side chains of valine and amino acids with aromatic groups (Figure 2-2), may interact with their neighbours via van der Waals interactions, and water molecules are rearranged around non-polar groups via hydrogen bonding to reach a thermodynamically stable state. The strength of hydrophobic interactions increases with temperature up to 60-70 °C (Scheraga, Nemethy, & Steinberg, 1962). Hydrophobic interactions are important in the stabilisation of emulsions. Emulsifiers must be amphiphilic, i.e. parts of the molecules are hydrophobic and parts of the molecules are hydrophilic. When making an emulsion, different parts of the protein adsorb on the O/W interface and may align and reorganise into the oil phase or the water phase according to their hydrophobicity (Hill, 1996).

Hydrogen bonds are weak electrostatic bonds. A hydrogen atom covalently bound to an electronegative atom (e.g. oxygen and nitrogen) is partially positive (δ^+), and the proton of this hydrogen can be shared with other partially negative (δ^-) groups. Hydrogen bonds are important in maintaining the structure of proteins, e.g. the secondary structures α-helix and β-sheet (Li-Chan, 2004). Hydrogen bonds became weaker at a higher temperature during processing and the proteins are therefore became partially unfolded, exposing the hydrophobic core and cysteine/disulfide bonds.

Electrostatic interactions occur when two proteins have opposite charges (attractive) or when they have like charges (repulsive). The charge of protein depends on the pI of the protein and the pH of the environment. A protein is negatively charged when the pH is

higher than its pI, and vice versa. When the pH is far away from pI, the repulsive electrostatic forces would prevent the protein precipitation and the protein is solubilised. On the other hand, protein molecules have no net surface charge at the pI and thus are precipitated. The food industry uses this property to extract or fractionate proteins, e.g. to separate caseins and whey proteins by adjusting the pH to the pI of casein (pH 4.6). Ions in the solution can shield the charge of protein (Debye layer) and decrease the effect of electrostatic interactions, and thus control the solubility of protein. For globulins and some albumins, the protein solubility increases with the concentration of neutral salt (salting-in, generally in the magnitude of 0.1 – 1 M ionic strength). The solubility would reach a maximum and then decrease with further increase in salt concentration, and this phenomenon is called salting-out (Vojdani, 1996).

Van der Waals interaction results from transient shift of electron density, which induces a transient charge that could interact with nearby molecules either by attraction or repulsion. They are weak attractive forces over a short distance which could also lead to the aggregation of proteins (Boulet, Britten, & Lamarche, 2000).

Steric hindrance results from extremely strong repulsion forces between overlapping electron clouds of two molecules when they are close to each other, i.e. two molecules cannot occupy the same space. Steric hindrance define the size, shape and the conformation of the protein in the solution (Bryant & McClements, 1998). The steric hindrance is heavily used in the food industry to stabilise emulsions or foams, e.g. caseins adsorb as a monolayer on the O/W interface on the dispersed oil droplet, which generates a strong repulsive barrier that prevents the aggregation with other casein-coated droplets (Dickinson, 2013).

2.5. The functionality of dairy-plant protein blends

Soy and pea are the two most popular plant protein sources because they both have stable commercial supplies and are already widely used in various food products – around 50% of active patents of plant-based foods are made with soy or pea (Srivastava, 2020). The research on the dairy-plant protein interactions has mostly utilised soy as well some with pea protein. This section will review some of the relevant studies on the interactions between dairy and soy or pea proteins.

2.5.1. *Functionalities of dairy-soy protein blends*

Some of the published studies of dairy-soy protein blends are shown in Table 4. The aggregation and gelation behaviour (heat-induced or acid-induced) of dairy-soy blends are popular research topics, while other model systems are less studied.

Table 4 Published studies of dairy-soy protein blends in model systems. The functional synergy indicates that higher functionalities were observed in the protein blends than in the individual proteins.

Protein fraction	System	Functional Synergy?	Interactions	Reference
Cheese whey, soy flour	Solution	Y	–	(Guy, Vettel, & Pallansch, 1969)
MPC, SPI	Gel (cold-set)	N	–	(Chronakis & Kasapis, 1993)
WPI, SPI	Gel (heat)	N	–	(Comfort & Howell, 2002)
Skim milk powder, SPC	Gel (acid)	Y	–	(Roesch et al., 2004)
WPI, SPC	Solution,	Y	disulfide bond	(Roesch & Corredig, 2005)

	gel (heat)			
casein micelle, SPI, whey	Gel (acid)	N	–	(Roesch & Corredig, 2006)
WPI, Soy 11S, Soy 7S	Emulsion	N	–	(Manion & Corredig, 2006)
β-lg, Soy 11S, Sesame 11S	Emulsion, foam, solution	N	disulfide bond hydrophobic	(Anuradha & Prakash, 2009)
Whey powder, defatted soy flour	Co-precipitates gel (heat)	–	non-covalent interactions	(Alu'datt, Alli, & Nagadi, 2012)
Skim milk, soymilk	Gel (acid) gel (rennet)	N	–	(Grygorczyk, Alexander, & Corredig, 2013)
Micellar casein, SPI	Gel (heat) solution	N	No chemical interactions	(Beliciu & Moraru, 2013)
WPI, Ca caseinate, SPI	Incipient gel	N	disulfide bond hydrogen bond hydrophobic	(Onwulata, Thomas-Gahring, & Phillips, 2014)
WPI, Ca caseinate, SPI	Incipient gel	–	–	(Onwulata, Tunick, & Mukhopadhyay, 2014)
WPI, SPI	Gel (heat), solution	Y	–	(Jose et al., 2016)
Na caseinate, SPI	Gel (acid) gel (heat, acid), solution	N	–	(Martin, De Los Reyes Jiménez, & Pouvreau, 2016)

Skim milk powder, SPI	Ice cream	–	–	(Cheng et al., 2016)
Micellar casein, MPC, SPI, PPI	Gel (heat)	N	–	(Silva, Cochereau, Schmitt, Chassenieux, & Nicolai, 2018)
Micellar casein, MPC, SPI, PPI	Gel (heat)	N	–	(Silva, Balakrishnan, Schmitt, Chassenieux, & Nicolai, 2018)
WPI, Na caseinate, SPI, PPI	Emulsion	Y and N	–	(Ho, Schroën, San Martín-González, & Berton-Carabin, 2018)
WPI, SPI	Gel (heat)	N	–	(McCann, Guyon, Fischer, & Day, 2018)
Micellar casein, WPI, SPI, PPI	Emulsion gel	N	–	(Silva et al., 2019)

SPI: soy protein isolate; SPC: soy protein concentrate; WPI: whey protein isolate; MPC: milk protein concentrate; PPI: pea protein isolate.

Dairy-soy protein blends may have slightly better solubility after processing under certain conditions. In an early study, whey protein from cheese whey and soy flour were pasteurised, homogenised in a two-stage high-pressure homogeniser, concentrated and spray-dried to produce a free-flowing powder (Guy et al., 1969). Such processing increased the colloidal stability of the soy flour. The homogenised whey-soy blend had improved physical stability as there was no visible settling of particles, while precipitation of soy flour could be observed in the unhomogenised sample. There was no mechanism suggested for the changes in dispersibility and solubility on homogenisation and after spray-drying.

Whey proteins and soy proteins may form disulfide linkages during heating. Roesch and Corredig (2005) found that whey proteins and all subunits of soy proteins were present in

the soluble aggregates after heat treatments (90 °C for 10-60 min), indicating disulfide bonds form between whey and soy proteins. The contribution of disulfide bonds was verified by the addition of the disulfide blocking reagent n-ethylmaleimide (NEM), which inhibited the formation of large soluble complexes. After the proteins were treated with NEM, the amount of soluble complexes reduced significantly and a precipitate formed.

When the protein concentration is increased above a certain value, the aggregates may cross-link into a network and thus a gel is formed. Most heat-induced gelation studies have used whey (WPC or WPI) as the dairy protein source. Because commercial soy protein ingredients may have different degrees of protein denaturation, which will affect functionality and capacity to interact, it is difficult to compare published results directly and the results are not consistent. During heating of soy protein, Chronakis and Kasapis (1993) and Comfort and Howell (2002) both observed large aggregates in the dispersion and phase inversion or separation was also observed. The aggregates that result from denaturation in commercial soy protein might be the reason for phase separation. Roesch and Corredig (2005) avoided the phase separation by using an SPI with a relatively mild processing history and by pre-treating the SPI using centrifugation to discard large aggregates prior to heating. Whey protein is believed to be the main component of the heat-induced gel network, while the soy protein aggregates interacted with and filled within the whey protein backbones (McCann et al., 2018; Roesch & Corredig, 2005). This phase separation of whey and soy protein could result from their different nature – whey proteins are soluble in water and denature above around 60 °C; while soy 11S globulins are less soluble in water and denature at around 95 °C.

Acid-induced gelation of dairy-soy blends was also studied and stronger gels could be achieved even when part of the dairy protein was substituted by soy protein. Roesch et al. (2004) used glucono-δ-lactone (GDL) to lower the pH and induced gelation in the blends of skim milk powder and soy protein concentrate (12% total solids). There was no phase separation as in the heat-induced whey-soy blends. Incorporating soy protein into milk increased the pore size of the gel. The storage modulus (G'), which is a rheological measure of the solid-like behaviour of viscoelastic materials, increased when the skim milk powder was partially substituted (dairy: soy = 70:30), but further increases in the soy ratio above 50% did not increase the G' further, i.e. samples with dairy: soy ratios of 50:50 and 30:70 had higher G' than 70:30 samples, but they are not significantly different. However, it was not possible to see if the skim milk powder – soy blends could make stronger gels than individual protein because soy protein along cannot form a homogeneous gel.

Grygorczyk et al. (2013) blended soymilk and milk (4.5% total protein) and induced gelation by GDL and/or rennet. Soy protein started to aggregate and form gel below pH 6, which is the pI of soy proteins, but skim milk did not aggregate within the tested pH range of 6.5 – 5.6. So when only GDL was added, the formation of the milk-soy gel was only due to the aggregation of soy protein particles and the casein micelles act as a non-interacting filler. In another experiment, GDL and rennet were used together to introduce the gelation, which was shown to be able to form a milk gel. However, the milk-soy gel had much lower G' than the milk or soy only control samples, indicating less optimal packing of the aggregates in the milk-soy system. Both the milk protein and soy protein participated in the formation of the gel network in milk-soy blends when GDL and rennet were added together, and the gel structure could be modulated by changing the ratio of

milk and soy protein: pure milk gel had the structure of large pores and interconnected strands, the soy gel network is made of densely packed protein aggregates, and the milk-soy gel has the structure in between that of milk alone or soy alone.

Martin et al. (2016) used SC as the casein source and lowered the final pH to 4.8, so the acid-induced caseinate gel can be made. When it comes to SC-soy blends, they found that pre-heating (95 °C for 1 hr at pH 6.5) was necessary to increase the gel strength, e.g. acid gel of unheated SC-soy blends (SC: soy = 7:3) had lower G' at the final pH of 4.8 than that of 100% SC acid gel, while the same blends exhibited higher G' if they were pre-heated. Another finding is that the heat treatment resulted in the formation of soy protein aggregates, which raised the onset pH during gelation because these soy protein aggregates are more susceptible to acid induced gelation. The result was consistent with the casein micelle – soy protein system (Roesch & Corredig, 2006). To sum up, the aggregation of SC was influenced by aggregated soy protein during the pre-heating stage, which in turn influenced the rheological properties of the acid gel.

When it comes to heat-induced interactions between caseins and soy protein, heat treatments at 95 °C did not induce any covalent bonds between casein micelles and soy proteins (Beliciu & Moraru, 2013), as there was no new bands observed in non-reducing polyacrylamide gel electrophoresis. The formation of disulfide bonds was most likely only between soy 11S proteins themselves. Silva, Cochereau, et al. (2018) reported heat-induced gelation of micellar casein with pea or soy protein. A gel was formed, and soy protein and micellar casein formed networks independently as in the heat-induced whey-soy protein gels, indicating no interactions between them. Interestingly, adding soy or pea protein may even hinder the gelation of micellar casein due to the chelation of calcium ions by plant

proteins, so a higher gelling temperature was necessary for the dairy-plant protein blends. The final G' values of the micellar casein-plant protein gels (1 h at 90 °C) were close to that of the individual gel which was the dominant protein, e.g. a 70% micellar casein - 30% soy protein gel had similar G' as the 70% micellar casein gel, so the soy protein did not reinforce the gel network. These findings suggested that the dominant protein forms the gel network and the minor protein just acted as a filler, i.e. the micellar casein and plant proteins did not co-aggregate.

In summary, soy protein and dairy proteins were incompatible when it comes to gelation, i.e. they do not form homogeneous networks. Heat treatment may induce disulfide cross-linking between whey protein and some soy protein. However, the cross-linking was primarily between whey proteins, so the whey proteins are the main component of the heat-induced whey-soy protein gel while soy proteins act mainly as filler. Caseins and soy protein did not react primarily via disulfide cross-linking during heat treatment because most caseins (α_{S1}- and β- casein) have no cysteine residue. The acid-induced gelation of soy and milk/casein is possible because the soy proteins and caseins can both precipitate under acidic conditions. However, pre-treatment such as heating was necessary prior to acidification to achieve similar gel properties as pure casein gels.

2.5.2. *Functionalities of dairy-pea protein blends*

The other plant protein with commercial importance is pea protein, and Table 5 lists examples of dairy-pea studies.

Heat treatment seems to be able to influence the functionality of dairy-pea proteins mixtures. P. R. Patel, Youngs, and Grant (1981) reported higher water and oil holding

capacity, emulsification and foaming properties when cheese whey protein concentrate and pea protein concentrate were heated at 63 °C, which is much lower than the denaturation temperature of pea proteins so there should be no formation of covalent bonds between pea and whey proteins. Jackman and Yada (1989a) studied blends of acid whey protein concentrate with pea proteins without heat-treatment. They tested functionalities of whey-pea protein blends (solubility, heat stability, emulsifying properties, and foaming capacity), measured under conditions of varying pH and varying ratios of dairy/pea protein to generate response surfaces. The result showed that whey-pea protein blends all displayed intermediate functionalities between the individual whey and pea proteins, so there was no functional synergy in these protein blends. In addition, the functionalities improved with the ratio of whey protein, i.e. the more pea protein, the less functional the whey-pea protein blend is.

Heat-induced aggregation was reported in dairy-pea protein blends. Chihi, Mession, Sok, and Saurel (2016) showed that β-lg and pea globulins aggregate via disulfide bonds and non-covalent interactions. These aggregates were dense, with higher molecular weights and smaller particle sizes than aggregates from native pea globulins. The rheological properties and water holding capacity of acid-induced gel made of these β-lg-pea protein aggregates are intermediate between that made of pure β-lg and pea globulins as in the unheated whey-pea protein blends.

Table 5 Published studies of dairy-pea protein blends in model systems.

Protein fraction	System	Functional Synergy?	Interactions	Reference
cheese whey, PPC	bread	Y	–	(P. R. Patel et al., 1981)
cheese whey, PPI pea globulins, pea albumins	solution	–	Electrostatic, possible hydrophobic	(P. R. Patel & Grant, 1982)
whey	Emulsion, foam, solution	N	–	(Jackman & Yada, 1989a)
whey	Emulsion, foam, solution	N	Hydrophobic	(Jackman & Yada, 1989b)
whey	Solution	N	Hydrophobic	(Jackman & Yada, 1989c)
whey	Gel (heat)	Y	–	(D. Wong et al., 2013)
whey	gel (acid), gel (rennet), solution	Y	–	(Boursier et al., 2013)
casein micelle, pea protein, pea 11S-rich, pea 7S-rich	solution	–	disulfide bond, non-covalent	(Mession, Roustel, & Saurel, 2015)
β-lg, pea globulins	solution	–	disulfide bond, electrostatic, hydrophobic	(Chihi et al., 2016)
caseinate, PPI	emulsion solution	Y	hydrophobic	(Yerramilli et al., 2017)
casein micelle, pea protein, pea 11S-rich, pea 7S-rich	Gel (acid)	Y and N	Non-covalent	(Mession, Roustel, & Saurel, 2017)

skim milk powder, PPI	Gel (heat), gel (acid), gel (enzyme) Emulsion gel	N	–	(Ben-Harb et al., 2018)
micellar casein, PPI, SPI, WPI	Gel (heat)	N	–	(Silva, Cochereau, et al., 2018)
β-lg, Pea globulins	Solution, gel (acid)	N	–	(Chihi, Sok, & Saurel, 2018)
Micellar casein, WPI, SPI, PPI	Emulsion gel	N	–	(Silva et al., 2019)
WPI, SC, PPI	Emulsion	Y	–	(Hinderink et al., 2019)

PPC: pea protein concentrate; PPI: pea protein isolate

2.5.3. *Functional synergy of dairy-plant protein blends*

Intermediate functionalities of dairy-plant protein blends were observed in most studies. However, functional synergy in gelation properties has been found in some studies under specific conditions. Synergy in gelling properties is the most common observation (Table 4 and Table 5). Higher G' was reported in an acid-induced gel made of soy protein and skim milk powder (Roesch et al., 2004) or SC (Martin et al., 2016). When it comes to heat-induced gels, it seems that the whey-soy gels with higher G', compared to that of whey or soy gel alone, is achievable when 20 – 50% of the dairy protein was substituted by plant protein and when the ionic strength was around 0.1 M (Jose et al., 2016; Roesch & Corredig, 2005). In the heat-induced whey-pea protein gel, the synergy in the gelling properties also occurs in a tiny window – 10% total protein, whey/pea ratio = 8:2, pH 6 and ionic strength of around 0.43 M (D. Wong et al., 2013). In the heat-induced dairy-plant

protein gel system, the whey proteins are believed to be the building blocks of the network structure, while the plant protein increases the gel strength by acting as filler. However, too much plant protein will result in insufficient whey protein network and thus a weaker gel.

To sum up, synergy in gelling properties of dairy-plant protein blends is possible when a number of parameters are optimal, including the degree of protein denaturation, the protein concentration, the ratio of dairy to plant protein, pH and ionic strength.

There are few studies of dairy-plant protein blends reporting on the synergy in other ingredient functionalities, such as solubility, colloidal stability and emulsifying properties. As mentioned earlier, better physical stability of soy flour could be achieved by homogenising blends of whey and soy flour (Guy et al., 1969). A similar increase in the stability/dispersibility of plant protein was reported in a patent (Boursier et al., 2013), who showed higher solubility of pea proteins when pea protein and casein micelles were blended and homogenised together. The solubility of pea protein was increased by 12% after such treatment. Since many protein functionalities, such as emulsifying and foaming properties, are highly dependent on the protein solubility (Jackman & Yada, 1989b) and plant storage proteins are generally less soluble in water, it is tempting to try to explore more ways to improve the solubility of plant protein by mixing and introducing interactions between caseins and plant proteins.

Another less-studied synergy of functionality is emulsifying properties. Blends of dairy and pea proteins may provide better emulsion stability. Yerramilli et al. (2017) found that nanoemulsions can be stabilised by a blend of SC and pea protein isolate at a caseinate/pea protein ratio of 50/50. SC alone resulted in creaming, due to depletion flocculation, while

PPI alone could not produce a flowable nanoemulsion. It was proposed that after homogenisation the hydrophobic residues at the centre of undenatured proteins were exposed, the flexible casein molecules were able to stabilise pea protein via hydrophobic interactions because the values of surface hydrophobicity increased in the blends high-pressure homogenisation. The authors also postulated it was possible that disulfide bonds were disrupted by homogenisation but did not show proof of this. Hinderink et al. (2019) found that both caseinate-pea blends and WPI-pea blends can have a synergistic effect on emulsion stability. However, Ho et al. (2018) reported that caseinate-pea blends cannot be used to produce stable emulsion. The inconsistency may result from the different pea protein material and/or different protein concentration.

2.6. Research gaps

The literature shows that most studies of dairy-plant protein blends focused on the heat-induced aggregation and gelation (heat- or acid-induced). Therefore, there are more protein functionalities to be explored, e.g. heat stability, solubility and emulsifying properties. It has been shown that higher solubility could be achieved in whey protein-soy protein or casein-pea protein blends via homogenisation (Boursier et al., 2013; Guy et al., 1969), but there were no further studies. Since solubility is a key functionality for many food applications, it is worth trying to improve the solubility of plant seed proteins by introducing interactions with dairy proteins. In addition to heat-treatment and acidification, there are other possible methods such as pH-cycling (Jiang, Xiong, & Chen, 2010).

Another important but overlooked functionality is heat stability. It has been known that caseins have chaperone-like effects for protecting the globular whey proteins against heat-

induced aggregation and precipitation (Morgan, Treweek, Lindner, Price, & Carver, 2005; Yong & Foegeding, 2010). Since plant storage proteins are also globular proteins, it is possible that caseins might also have chaperone-like effect with these plant protein

Most studies of dairy-plant protein blends utilise soy and pea because they are commercially available in large quantities. However, other novel plant proteins are also interesting and attracting attention. In this study, several crops grown in New Zealand (hemp, chia, flaxseed and pea) will be used for protein extraction and one suitable plant protein will be used to study dairy-plant protein blends and its functionalities.

3. MATERIAL AND METHODS

3.1. Materials

Hemp seed cake flour, which is a by-product after cold-pressed hemp oil extraction, was kindly provided by Midlands Seed Limited (Ashburton, New Zealand). Temperature was kept below 40 °C during oil extraction, and exposure to oxygen and light were minimised. Hemp seed oil cake flour has approximately 34% protein, 38% carbohydrate and 13% oil according to the product specification. Sodium caseinate (Alanate 180) was supplied by Fonterra Cooperative Ltd (Auckland, New Zealand). SC contains 94.5% protein, 6.0% moisture and 4.0% ash according to the specification sheet. All chemicals were purchased from Sigma-Aldrich (St. Louis, Missouri, USA): polyvinylpolypyrrolidone (PVPP) beads (~110 µm particle size), sodium azide, sodium metabisulfite, sodium chloride, sodium hydroxide, hydrochloric acid, bicinchoninic acid working reagent, 1,4-dithiothreitol (DTT), SYPRO orange.

3.2. Finalised HG extraction

A salt-extraction method based on that of Malomo and Aluko (2015a) was used to extract HG. The extraction buffer contained 0.1 M sodium phosphate (pH 7), 0.5 M NaCl and 0.02% sodium azide. PVPP (1.5% w/w) and sodium metabisulfite (0.1%) were added to inhibit protein-phenolic compounds crosslinking during extraction (Martin, Nieuwland, & De Jong, 2014). PVPP is a synthetic, high-molecular-weight clarifying agent which is commonly used as a polyphenol adsorbent in wine and beer industry. Two hundred grams of hemp seed cake flour were dispersed and stirred in 1.6 L of extraction buffer solution at

25 °C for 90 min. The supernatant was collected after centrifugation (4000 × g, 25 °C, 30 min); the pellet was re-dispersed, and the extraction was repeated twice with extraction buffer, to give a final ratio of hemp seed cake flour to buffer at 1:24 (w/w). The supernatant was clarified through grade 1 filter paper (GE Healthcare, Buckinghamshire, UK) and concentrated with an ultrafiltration module with 10 kDa molecular weight cut off membrane (Millipore, Burlington, MA, USA). The concentrate was dialysed against RO water at 4 °C for three days in 12 kDa MWCO dialysis tubing (Sigma-Aldrich, St. Louis, MO, USA), and the water was changed twice per day. The content of the dialysis tubing was centrifuged (20000 × g at 4 °C for 30 min) and the pellet containing the globulins was re-dispersed in water, freeze-dried and stored at -20 °C. The freeze-dried HG contained 89.6% protein, which was determined by the Dumas combustion method with a nitrogen-to-protein conversion factor of 5.7 that is suitable for seed storage proteins (Berghout, Venema, Boom, & van der Goot, 2015).

3.3. Protein quantification

The protein content was measured by bicinchoninic acid (BCA) protein assay (Noble & Bailey, 2009). The standard curve was made by bovine serum albumin (BSA) stock solutions with the range of 200-1000 µg/mL. To quantify the protein, 50 parts of reagent A (BCA solution, Sigma-Aldrich, Cat. No. B9436) and 1 part reagent B (4% $CuSO_4$ solution) and protein solution were first mixed to make BCA working solution, which is stable for up to a week at room temperature. The BCA working solution is highly alkaline (pH 11.25), so the aggregated proteins will generally be dissolved so the absorbance are not affected by the turbidity. The BCA working solution (200 µL) put into 96-well microplate and mixed with BSA standards (25 µL) or protein samples (25 µL). The

microplate was covered with lid to prevent evaporation and incubated for 30 min at 37 °C. Protein content of samples was determined by measuring the absorbance at a wavelength of 562 nm and compared against the BSA standard curve.

3.4. Turbidity

Aliquots (90 µL) of protein solution were transferred into a clear flat-bottomed 96-well microplate. Absorbance was determined by measuring at 540 nm using a UV-visible spectrometer SPECTROstar Nano (BMG LABTECH, Ortenberg, Germany). Turbidity was transformed from the absorbance with the formula: $\text{Turbidity} = 2.303 \times Absorbance \times \frac{1}{L}$, where L is the optical path length.

3.5. Dynamic light scattering

Particle size was measured by dynamic light scattering (DLS) with a Zetasizer ZS (Malvern Panalytical Ltd, Worcestershire, UK). The measurement was carried out after equilibrating at 25 °C for 60 s. The measurement angle was 173°. The refractive index of protein particles was set at 1.45, and the viscosity and refractive index of dispersant were calculated with the built-in solvent builder program. Three measurements were taken with automatic settings of measurement duration, measuring position and attenuation level. The particle size used in this study is the average diameter based on volume-based particle size distributions.

3.6. Sodium dodecyl sulfate polyacrylamide gel electrophoresis

Tricine sodium dodecyl sulfate polyacrylamide gel electrophoresis (SDS-PAGE) was used following the method of Schägger (2006). Protein samples were mixed with nonreducing

sample buffer and kept at 37 °C for 45 min, and the final SDS concentration was 1%. Gels (4% stacking gel and 10% separating gel) were cast, and electrophoresis was performed with a Mini-PROTEAN electrophoresis system (Bio-Rad, Hercules, CA, USA). The initial voltage was kept at 20 V for one hour, raised to 90 V for another hour then adjusted to 120 V and maintained at that voltage until the tracking dye front was just out of the gel. The gel was stained with colloidal Coomassie blue and destained according to Dyballa and Metzger (2009). The gel was scanned with a Gel Doc XR+ Gel Documentation System (Bio-Rad, Hercules, CA, USA) and the density of protein bands was quantified by Image Lab software (Bio-Rad, Hercules, CA, USA).

3.7. Two-dimensional SDS-PAGE (2D-PAGE)

Two-dimensional SDS-PAGE followed the method by Dave et al. (2013) with some modifications. The protein blend was heated in the PCR thermocycler iCycler (Bio-Rad, Hercules, CA, USA) at 90 °C for 30 min, and the heated protein solution was incubated with 1% SDS at 37 °C for 45 min. The protein solution was separated by glycine SDS-PAGE (Laemmli, 1970), with 4.5% stacking gel and 16% separating gel. One strip of gel (approximately 7 mm in width) was excised from the nonreducing gel, immersed in 2.5 mL 0.2 M DTT solution and heated at 56 °C for 20 min to reduce disulfide bonds. The gel strip was then placed horizontally between glass gel-casting plates in the stacking gel area. Resolving gel solution was poured to approximately 1 cm below the gel strip, then a layer of water was added to flatten the top of the gel. After the resolving gel was set, the water was poured out and stacking gel solution was poured on top of the resolving gel and around the gel strip to fill the gel-casting plates. The gel was run with the voltage initially at 100 V until proteins had entered the stacking gel and raised to 200 V. The gel run was

terminated when the tracking dye left the gel. The gel was stained and destained as described in section 3.6.

3.8. Determination of oil droplet size

The droplet size distribution was measured by laser diffraction (Mastersizer 2000, Malvern Instruments Ltd., Malvern, Worcestershire, UK). The refractive index was set at 1.47 for oil and 1.33 for water. The absorbance of the droplets was set as 0.001. The calculation of oil droplet size distribution results was based on the general purpose model distribution assuming spherical particle shape. The results were presented as D[4,3], the volume moment mean.

4. EXTRACTION AND CHARACTERISATION OF HEMP GLOBULINS

4.1. Introduction

The first step of this study is to extract and find a suitable plant protein source. Four plant materials (hemp seed cake flour, flaxseed cake flour, chia flour and yellow pea flour) were kindly donated by Midland Seeds Limited (Ashburton, New Zealand). Two extraction methods, the classic Osborne fractionation and a conventional salt extraction, were applied, and an appropriate method was chosen. The extracted hemp protein was characterised for its protein composition, solubility, and aggregation behaviours at different pH, ionic strength and protein concentrations. Different methods were also tried to introduce interactions between hemp protein and dairy proteins (fraction of whey or casein). The change of functionalities of the interacted dairy-plant protein blends was observed, which gave the research ideas for the following chapters.

4.2. Material and methods

4.2.1. *Osborne fractionation of proteins*

A classical Osborne fractionation of protein was trialled first to analyse the proteins in the plant ingredients. Flaxseed cake was omitted because the polysaccharides resulted in a thick and gel-like mucilage that made it hard to extract and filter the dispersions. Therefore, only yellow pea flour, hemp seed cake flour and chia flour were used. Hemp seed cake flour and chia flour were ground (Ultra centrifugal mill ZM 200, Retsch, Haan, Germany, with 0.25 mm ring sieve) and, after grinding, all materials were defatted by hexane with

solid to solvent ratio of 1:4. The defatted flours were air dried in a fume hood for one night. Defatted samples were extracted two times with each solvent sequentially (Figure 4-1, modified from Ju, Hettiarachchy, and Rath (2001)), which were water, salt solution (5% NaCl solution), alkali solution (0.02 M NaOH, pH ≈ 11), then 70% alcohol to obtain the albumin, globulin, glutelin and prolamin fractions respectively. After each extraction, the dispersion was centrifuged (4500 ×g, 30 min) to separate the supernatant from the pellet. The pellet was then extracted with the next solvent. The supernatants were dialysed against 4 °C RO water for globulin and glutelin fractions with dialysis tubing (6 kDa MWCO) or vacuum-evaporated for prolamin fractions.

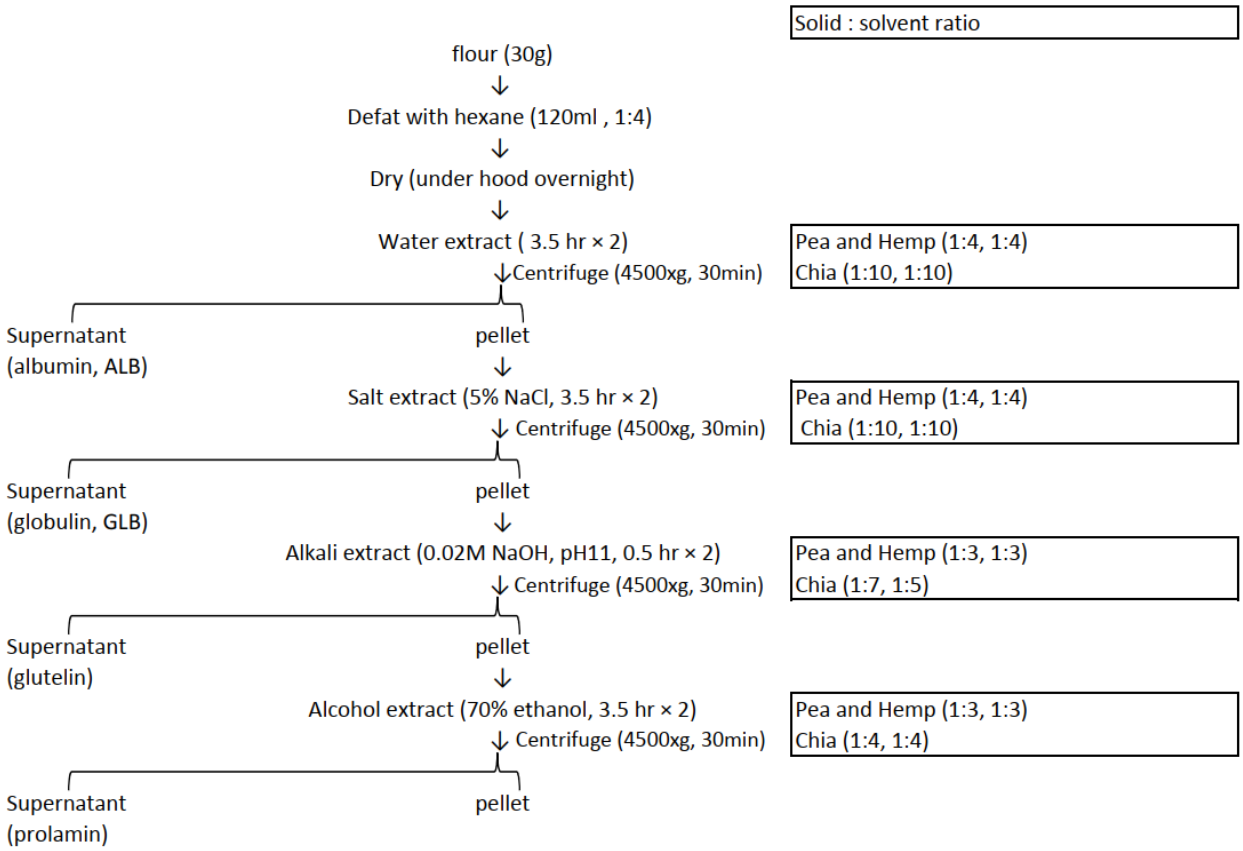

Figure 4-1. Flowchart of Osborne fractionation.

4.2.2. *Salt extraction of HG*

A common salt-extraction method followed by a desalting step was used to extract hemp seed cake flour (Gueguen & Barbot, 1988). Two extractions were tested (SE1 and SE2 in Figure 4-2). The extractant in these two extractions contained 0.25 M of Na_2SO_4. Three or four washes during salt extraction were performed in order to recover more protein, and the solid-to-solvent ratios were both 1:24 in total. More solvent (1:24) was used in salt extraction than in the Osborne fractionation extraction (1:16 in the water and salt extraction steps for hemp) in the hope to achieve higher protein recovery. The protein extracts were concentrated using a stirred cell device (Millipore Amicon: Model 402, working volume = 400 mL) in SE1 or a tangential flow filtration (TFF) device (Millipore Spiral-Wound UF Modules:TFF-1) in SE2. Concentrated protein extracts were desalted with dialysis tubing (SE1) or diafiltration (SE2). The extracted proteins were dried by freeze-drying.

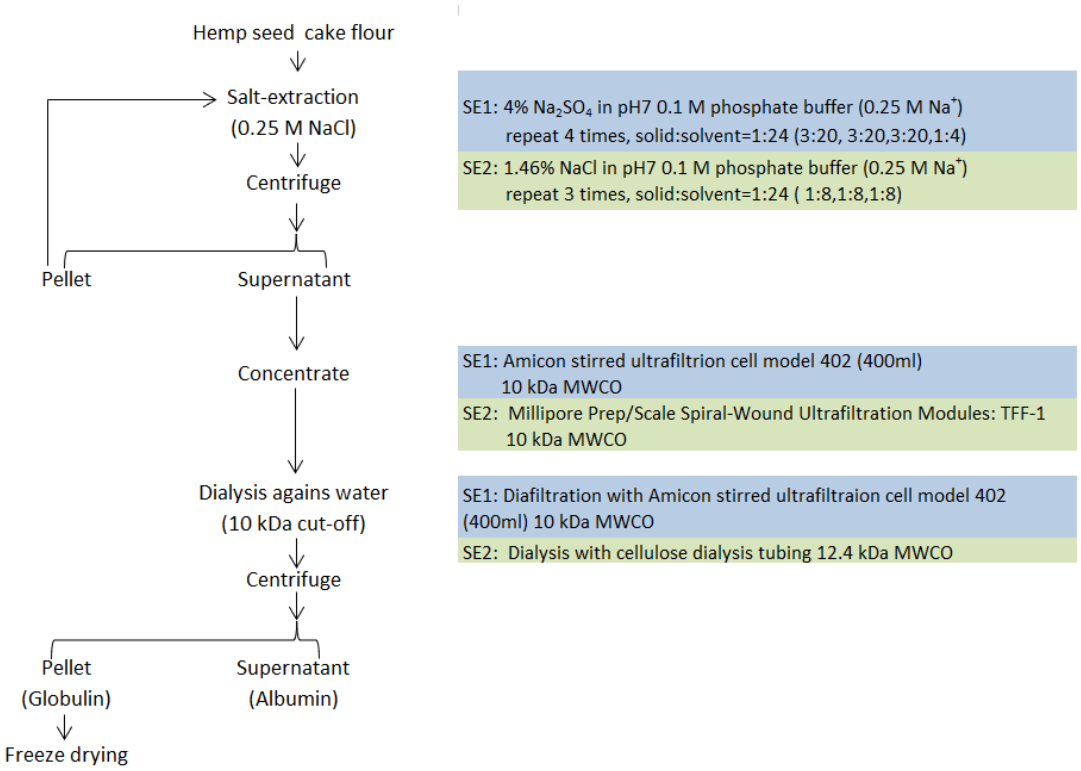

Figure 4-2 Flowchart of salt extraction of proteins.

4.2.3. *Protein solubility at different pH and ionic strength*

The solubility of HG was determined between pH 3.75 – 8 at two ionic strengths. Phosphate buffer was used to cover the pH between 5.75 – 8 and acetate buffer was used to cover the pH between 3.75 – 5.5. The ionic strengths of the buffer solutions were calculated and adjusted at 25.0 °C, according to Beynon and Easterby (2003), and topped up with sodium chloride to values of ionic strength of 0.5 M or 0.086 M. HG (5 mg) was dispersed with the buffer solutions and shaken overnight in an incubator at 25 °C. Sodium azide (0.02%) was added to prevent microbial growth. The protein dispersions were centrifuged (10000 ×g, 20 min, 25 °C) and the protein concentration in the supernatant and the whole protein dispersion was determined by the BCA method. The protein solubility was expressed as percentage ratio of protein content in the supernatant to that in the whole protein dispersion.

4.2.4. *Solubility of HG in different dissociating reagents*

HG (0.5%, w/v) was dispersed in water and stirred overnight at room temperature. Sodium azide (0.04%) was added to stop microbial growth. Aliquots of HG dispersion were mixed in a 1:1 ratio (v/v) with four dissociating solutions containing different combinations of dissociating reagents, and mixtures were stirred for 1 hour at room temperature. The dissociating solutions were (A) 50 mM dithiothreitol (DTT) and 2% Triton X-100, (B) 8 M urea and 2% Triton X-100, (C) 8 M urea and 50 mM DTT and (D) 8 M urea, 50 mM DTT and 2% Triton X-100. The mixtures of protein dispersion and dissociating solution were centrifuged (5000×g, 10 min, 20 °C). The protein content in the supernatants was quantified by BCA method.

4.3. Results and discussion

4.3.1. *Protein extraction*

4.3.1.1. Osborne fractionation of proteins

The amount of glutenin and prolamin fractions in hemp, pea and chia turned out to be negligible (Table 6), so only the albumin (water-soluble) and globulin (salt soluble) fractions will be examined and only the first two extraction steps are necessary. The protein yield of the Osborne fractionation was low, only 25-40 % of total protein in the starting material could be extracted.

Table 6. Amount, protein content of each Osborne fraction and protein yield from 30 g of starting material.

		Pea	Hemp	Chia
Albumin	Weight (g)	3.82	1.72	2.92
	Protein content (%)	42.58	26.52	33.53
Globulin	Weight (g)	0.50	0.77	1.41
	Protein content (%)	80.83	82.11	58.43
Glutelin	Weight (g)	0.02	-	-
	Protein content (%)	-	-	-
Prolamin	Weight (g)	-	-	-
	Protein content (%)	-	-	-
	Protein yield (%)	25.00	40.20	35.80

The albumin and globulin fractions in pea and chia are not fully separated according to the result of reducing SDS-PAGE (Figure 4-3), as many proteins were present in both fractions. This indicated that some proteins in pea and chia were soluble in both water and salt solution. The major protein, edestin, in hemp (≈ 52 kDa) dissociates into basic and acidic subunits (≈ 34 and 20 kDa respectively, lane 4 in Figure 4-3) after reduction (Malomo & Aluko, 2015a), and the 34 kDa basic subunit was mostly shown in the globulin fraction, indicating that the fractionation is more effective in hemp. There was another minor hemp protein which was around 50 kDa even after reduction and this protein could belong to the subunit of 7S protein of hemp (Docimo, Caruso, Ponzoni, Mattana, & Galasso, 2014; Tang et al., 2006).

Hemp was chosen as the source of plant protein for further investigation because of the simple composition of the hemp protein (compared to pea) and its effective fractionation by water or salt extraction. The simple composition should make it easier to analyse their interactions with dairy proteins.

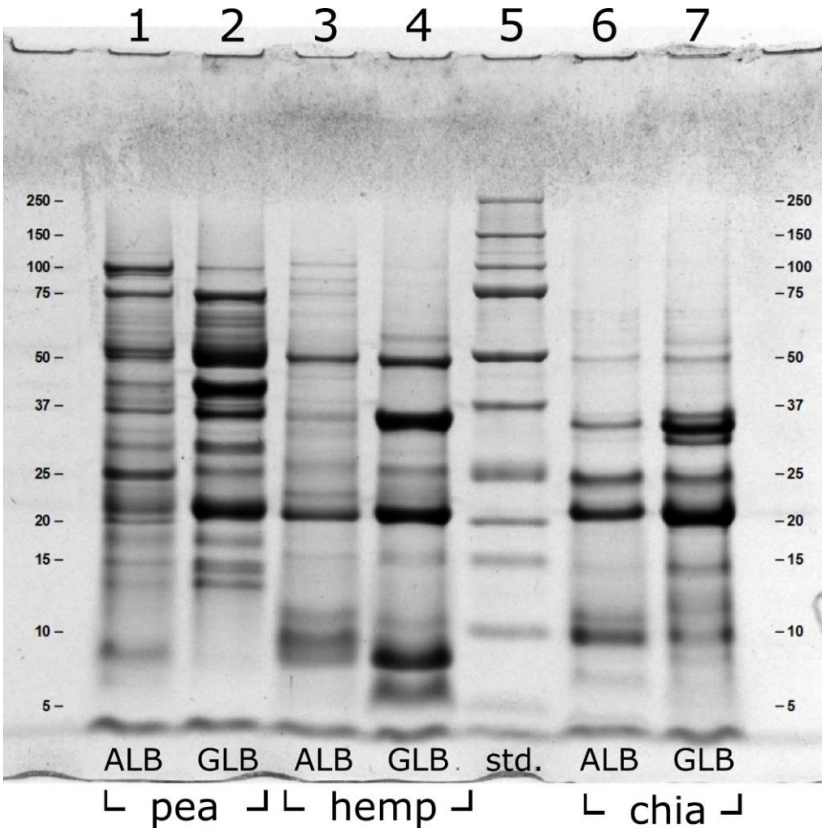

Figure 4-3. SDS-PAGE of albumin (ALB) and globulin (GLB) fractions by Osborne fractionation under reducing conditions.

4.3.1.2. Salt extraction of proteins

As the whole Osborne fractionation process was not necessary to extract the protein in pea and hemp, only the salt extraction, followed by dialysis/diafiltration to remove the salt was needed to extract hemp proteins. Within the two salt extraction experiments (Figure 4-2), SE2 is the more efficient extraction method in terms of time consumption. The TFF device was 3 to 8 times faster than the stirred cell when it comes to concentrating the protein solutions. In addition, albumins and globulins of hemp were well separated by dialysis tubing in SE2, as shown by a significant difference in the protein amount band patterns

(Figure 4-4). Diafiltration used in SE1 with five volumes was not enough to separate pea albumins and globulins, as shown by bands with the same molecular weight in the albumin and globulin fractions and the high amount of residual protein in the albumin fraction (Figure 4-4).

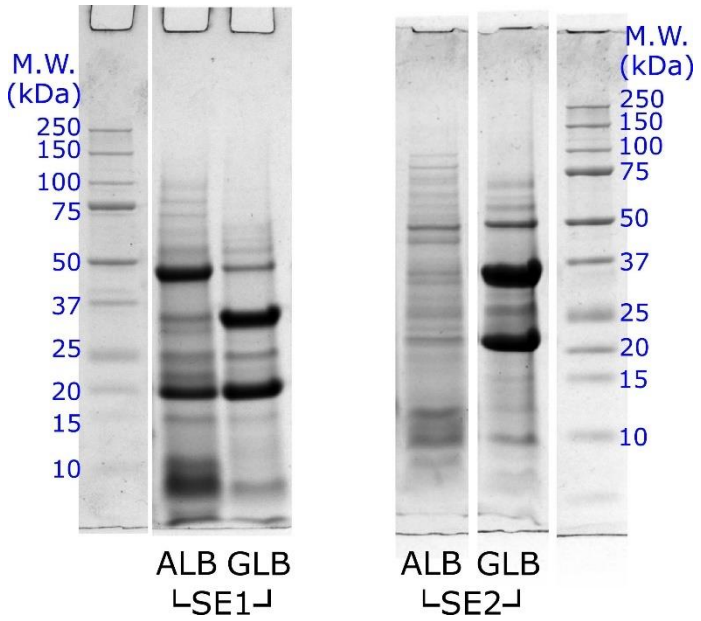

Figure 4-4. Results of separation of hemp proteins by the two salt-extractions SE1 and SE2 with reducing SDS-PAGE.

The protein content obtained by SE2 was determined by the Dumas method with a nitrogen-to-protein factor of 5.7 (Berghout et al., 2015), and the protein content of extracted HG was high (88.9 ± 0.7 %). However, the protein yield of these two salt extractions were both low, which was 18.2% for SE1 and 14.8% for SE2.

In summary, it is more time-efficient to extract HG with SE2 process, i.e. concentrate with the TFF device and dialyse with dialysis tubing to extract HG, and the extracted protein is relatively pure.

4.3.2. *Characterisation of HG*

The composition of salt-extracted HG is rather pure and simple. There was only one major protein in the non-reducing condition, which is edestin that has a molecular weight of around 55 kDa (Figure 4-5). After reduction, edestin is dissociated into basic subunits (≈ 33 kDa) and acidic subunits (≈ 20 kDa). The composition of HG is consistent with previous studies (J.-J. Kim & Lee, 2011; X.-S. Wang et al., 2008).

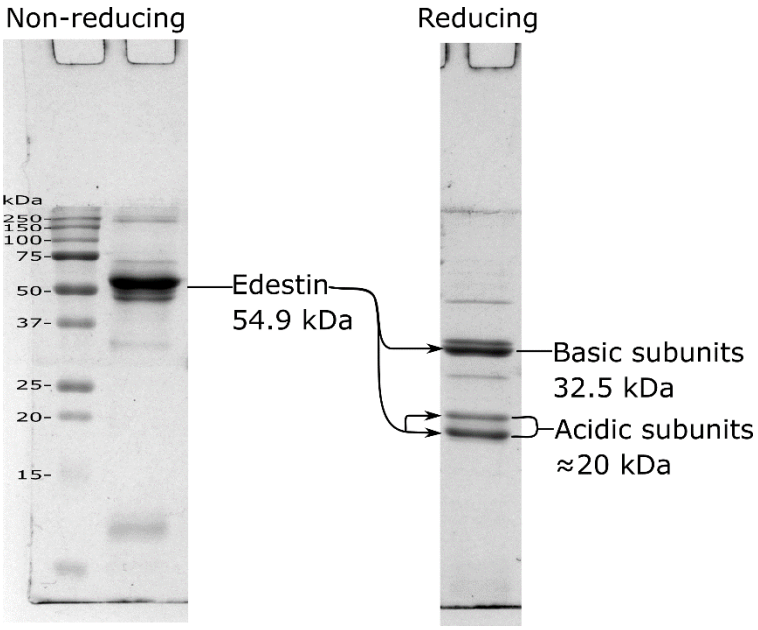

Figure 4-5. Composition of salt-extracted HG.

4.3.2.1. HG solubility in water at different pH and ionic strength

The solubility of HG at two ionic strength (0.086 M and 0.5 M) and different pH (3.75 – 8) is shown in Figure 4-6. At 0.086 M of ionic strength, which was close to that of the milk system (Gaucheron, 2005), the solubility of HG was low (≈ 25% at pH 7) and its minimum solubility occurred between pH 5 – 6, which is the pI of HG (Hadnađev et al., 2017; Q.

Wang & Xiong, 2019). The solubility of HG increased at higher ionic strength (0.5 M), which could be expected because HG was extracted with salt solution and precipitated by dialysis to remove the salt. The solubility of HG increased with pH and was about 70% above pH 7 at 0.5 M ionic strength.

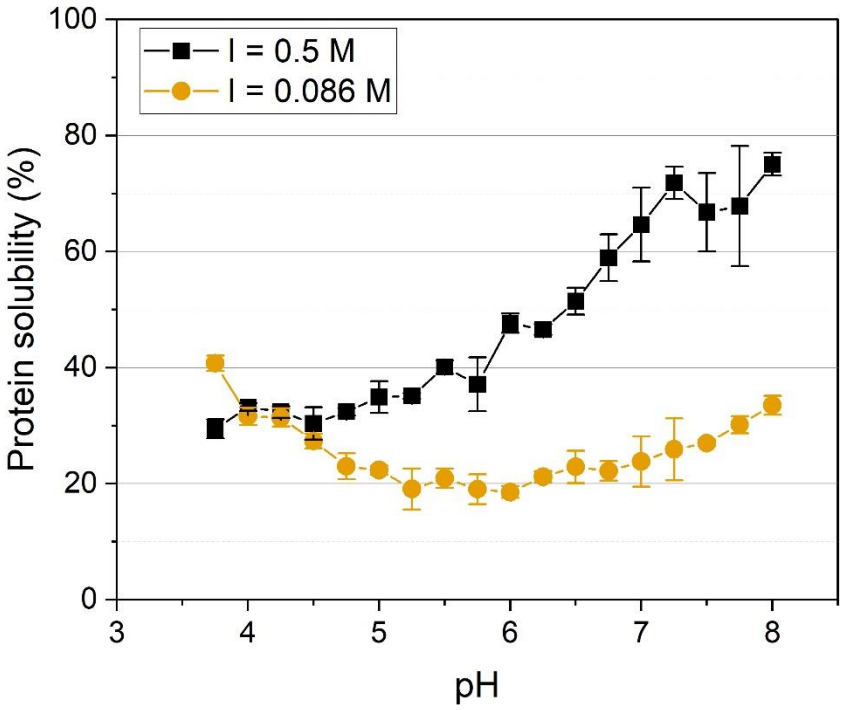

Figure 4-6. Solubility of HG at different pH under 2 ionic strengths, 100% protein solubility equals to 8.96 mg/mL soluble protein.

Solubility might be controlled by the structural reorganisation within hemp edestin. Lakemond, de Jongh, Hessing, Gruppen, and Voragen (2000) studied the effect of ionic strength and pH on the solubility of glycinin, which has highly conserved amino acid sequence and similar protein structure as hemp edestin. The solubility profile of soy glycinin was very similar to that of HG, i.e. lowest solubility observed between pH 5 to 6 at 0.03 mM ionic strength, and higher solubility at 0.5 M ionic strength that also increased

with pH (pH 3 to 7). They found that the tertiary or quaternary structure of soy glycinin was modulated by ionic strength and pH, and it might also be the case for hemp edestin.

The solubility of HG suggests that it will be challenging to use it in many food systems that require the solubilisation of proteins because most food systems are in neutral or low acid environment and with low salt concentrations.

4.3.2.2. Solubility in different reagents

Types of protein-protein interactions could be determined and semi-quantified by their solubility in different dissociation reagents (Hammann & Schmid, 2014; Liu & Hsieh, 2008), and the results were shown in Figure 4-7. The highest solubility of HG (≈ 60%) was observed when the dissociating solution containing all the reagents (urea, DTT and Triton X-100), which could be expected because the combination of all the reagents should dissociate most protein-protein interactions.

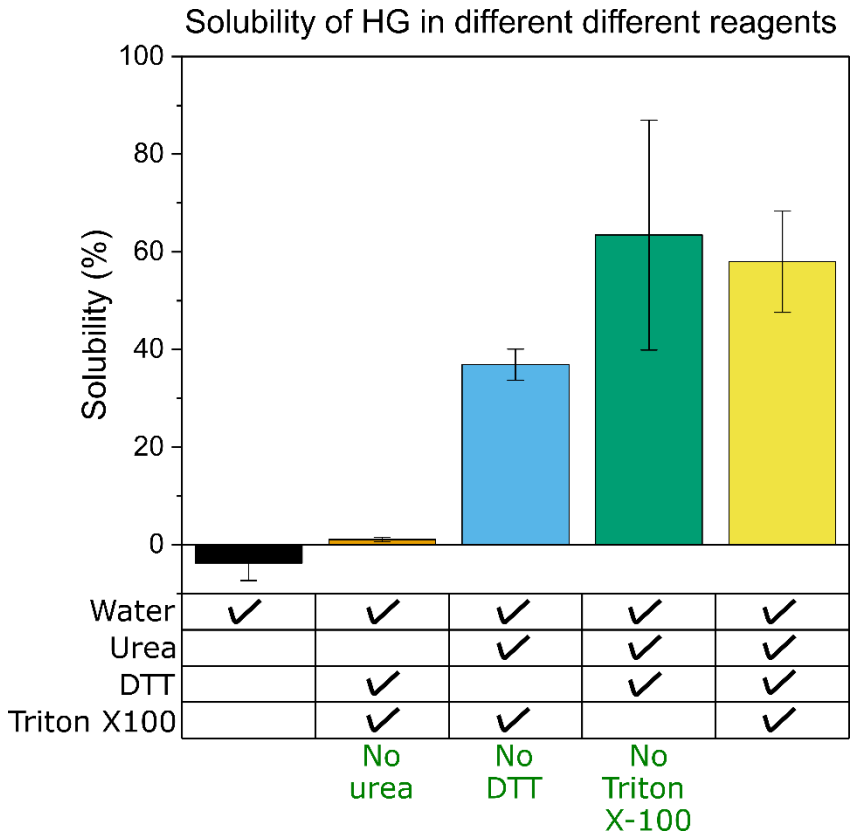

Figure 4-7. The solubility of HG in different dissociation reagents and water. HG was dispersed in water and the dissociation reagents were added into the dispersion directly. 100% protein solubility equals to 8.96 mg/mL soluble protein.

The omission of Triton X-100, a non-ionic surfactant that is capable of disrupting hydrophobic interactions, did not lower the solubility of HG when compared with the solution containing all the reagents, suggesting that hydrophobic interaction was less important in the low solubility and aggregation of HG.

The solubility decreased to ≈ 37% when there was no DTT in the solution, indicating that disulfide bonds were partially responsible for the low solubility of HG. Since there was no heat treatment during the extraction and drying processes, there should be no formation of

new disulfide bonds via thiol-disulfide exchange. The major hemp seed protein edestin is known to have one intrachain disulfide bond in its acidic subunit and one interchain disulfide bond linking the acidic and basic subunits (Docimo et al., 2014). The reduction by DTT may partially break these disulfide bonds and dissociate the protein subunits, which in turn increased the solubility of HG. Since DTT could only reduce the disulfide bonds that are close to the protein surface (Derbyshire, Wright, & Boulter, 1976), it is possible therefore that are some surface disulfide bonds which may react with other free thiol groups to start the thiol-disulfide interchange reactions at a higher temperature and/or pH.

The omission of urea resulted in totally insoluble HG (Figure 4-7). Urea is a very effective reagent to disrupt non-covalent interactions such as hydrogen bonding and hydrophobic interactions (Liu & Hsieh, 2007; Stumpe & Grubmüller, 2007). Therefore, the origin of the low solubility of HG in water is mainly non-covalent interactions between HG proteins. These results suggest that disrupting these intra- and inter-molecular hydrogen bonding and/or hydrophobic interactions could be a method to increase the solubility of HG.

4.3.3. *Phase behaviour of HG*

The low solubility at low ionic strength resulted from protein aggregation because the particle size of HG increased significantly when the ionic strength was below 0.3 M (Figure 4-8A). The particle size of 0.16% HG was around 10 – 20 nm when the ionic strength was higher than 0.3 M. However, the particle size of HG increased abruptly to a few hundred nm when the ionic strength was lowered from 0.3 to 0.25 M, the larger particle size resulted

in a translucent protein dispersion at 0.25 M ionic strength (Figure 4-8B). When the ionic strength was further lowered to 0.2 and 0.15 M, the particle sizes were larger than 1 µm, and the protein dispersions were opaque.

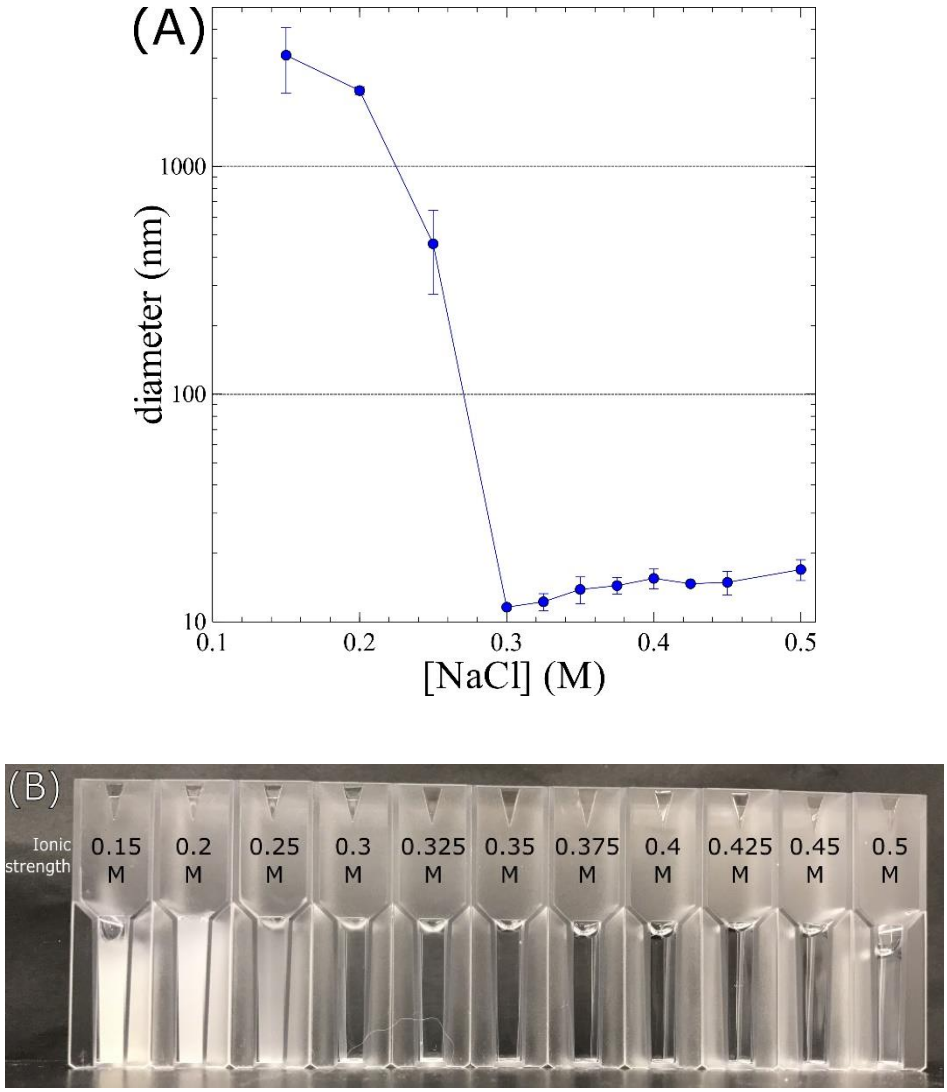

Figure 4-8. (A) Particle size of HG at different ionic strengths and (B) appearance of 0.16 % HG under different ionic strength at pH 7.

The ζ-potential of HG was around -4 to -6 mV at an ionic strength of 0.5, 0.3 and 0.25 M (Table 7), which are not significantly different, indicating that the surface charge and

electrostatic interactions are not the reason for the change of solubility of HG at different ionic strengths. The ζ-potential of -4 to -6 mV was rather low and should induce strong agglomeration and precipitation (Salopek, Krasić, & Filipović, 1992), but HG was soluble at 0.5 M because of its transparent appearance and small particle size (≈ 17 nm). The increase in the solubility may occur due to the salting-in effect, which describes that the solubility of globulins increases with the concentration of neutral salts (Vojdani, 1996).

Table 7. ζ-potential of HG at different ionic strength (n=3).

Ionic strength (M)	ζ-potential (mV)
0.5	-4.6 ± 1.0
0.3	-4.1 ± 2.1
0.25	-6.3 ± 3.5

The protein aggregates formed at lower ionic strength and/or low pH were mainly made of edestin. Figure 4-9 shows the protein composition in the supernatant of protein dispersions, and the decrease of edestin could be clearly observed when the ionic strength was lowered from 0.5 to 0.25 M in lane 1 – 6. In addition to edestin, there seems to be a protein fraction with high molecular weight (> 100 kDa) also precipitated at lower ionic strength. At pH 3, all the edestin was precipitated and did not stay in the supernatant even at a high ionic strength of 0.5 M (lanes 7 – 12 in Figure 4-9). At pH 9, edestin was soluble (lanes 13 – 18 in Figure 4-9).

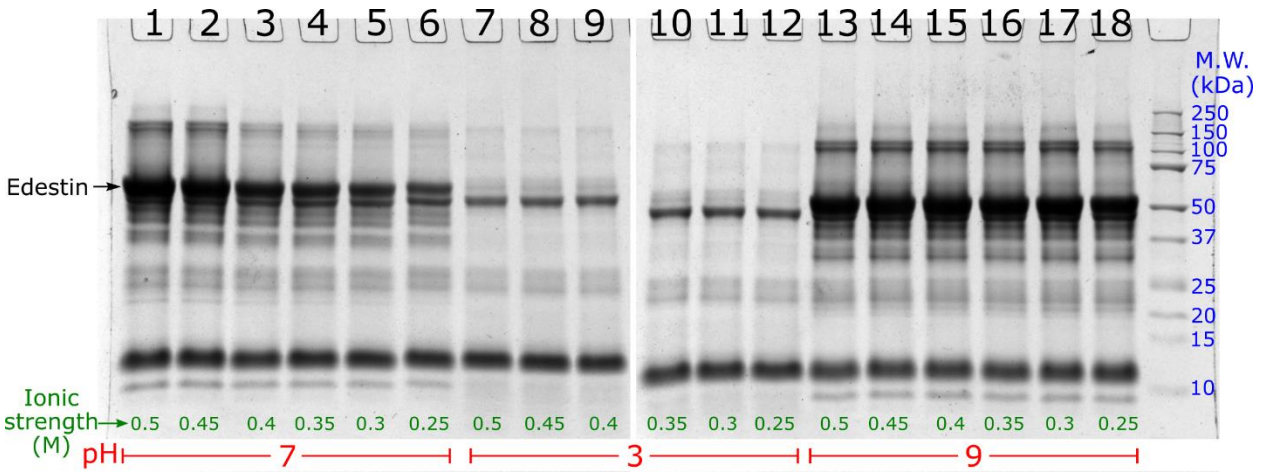

Figure 4-9. Non-reducing SDS-PAGE result of the protein composition in the supernatant at different ionic strengths and 3 pH.

4.3.3.1. Phase diagram of HG

The colloidal stability of HG could be controlled by ionic strength and protein concentration. To know HG better and find the conditions of soluble phase, a standard cloud point method was first tried to make the phase diagram (Kaul, 2000), but this method was not easily applicable to HG. Figure 4-10 shows the process of the cloud point method. In the beginning, the 0.52 % HG solution was clear at 0.5 M ionic strength. The HG concentration and ionic strength were lowered by diluting the HG solution with 0.05 M pH 7 phosphate buffer until the abrupt development of turbidity, which happened at 0.28% HG and 0.27 M ionic strength. Next, the HG concentration was lowered and ionic strength was increased by adding 0.5 M NaCl.

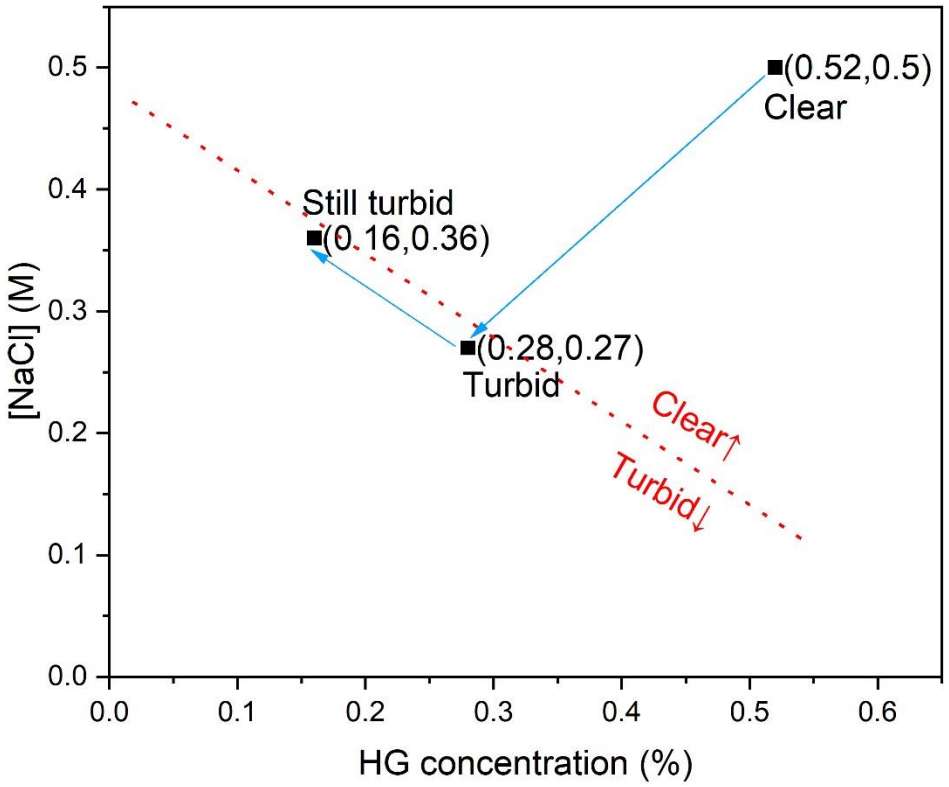

Figure 4-10. Trial of cloud point method to determine the phase behaviour of HG.

However, the HG dispersion did not become clear again even at 0.16% HG and 0.36 M ionic strength, and after 30 minutes after preparation. The solution was expected to be clear because of its small particle size of around 15 nm (Figure 4-8A). It could be that the newly formed aggregates (0.28% HG at 0.27 M ionic strength) need a much longer time to be dissolved again after dilution (0.16% HG at 0.36 M ionic strength).

The morphology and aggregate size of HG could be controlled by ionic strength. Figure 4-11 shows the edestin aggregates (0.16% HG) after 3-day storage at different ionic strengths. At 0.3 M, the few aggregates are large (≈ 10 – 20 μm) and looked like large crystals. However, the average particle size of the sample was very small just after

preparation (≈ 12 nm, Figure 4-8A). It could be that the most edestin was still dissolved, while a fraction of edestin was supersaturated and crystallised into large crystals.

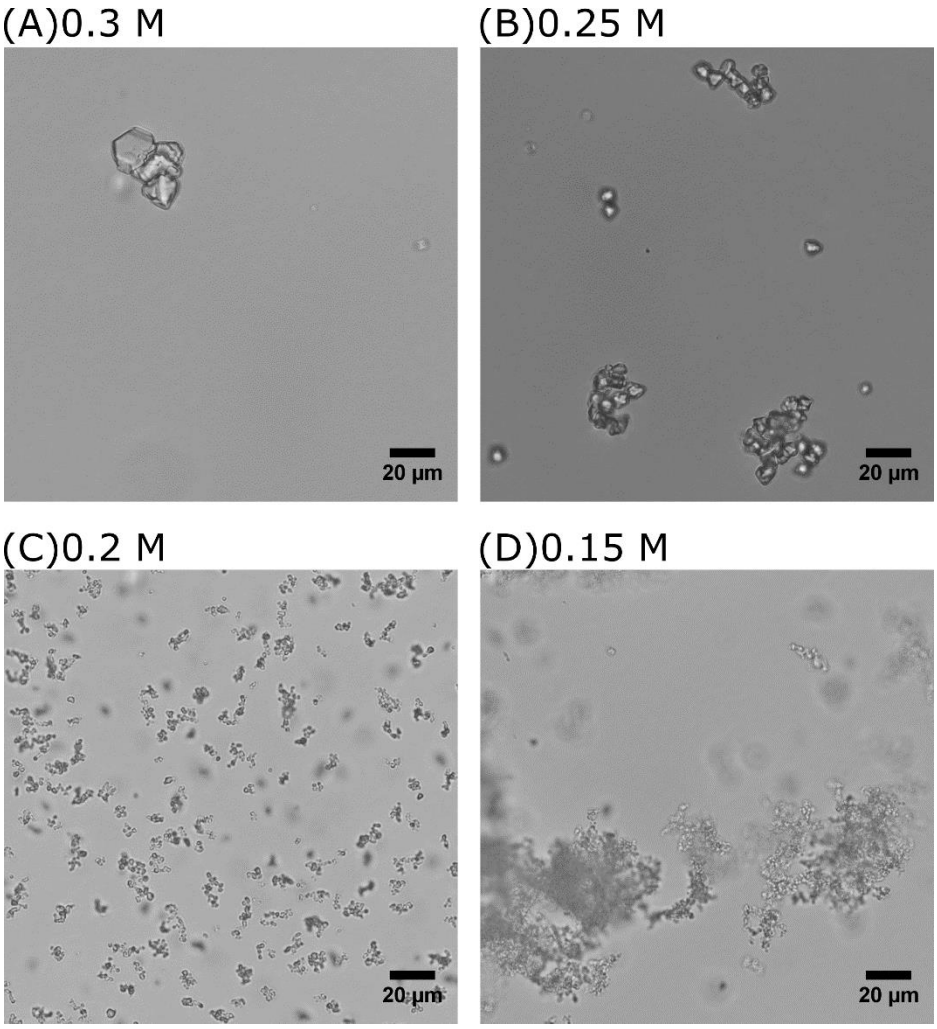

Figure 4-11. Light micrographs of 0.16% HG at different ionic strength after 3 days.

When the ionic strength was lowered to 0.25 and 0.2 M, the size of these crystal-like aggregates decreased and their number increased (Figure 4-11B and 15C). The individual aggregates were clustered into larger clusters of aggregates when the ionic strength was further lowered 0.15 M (Figure 4-11D), which looked like amorphous aggregates of soy

glycinin (Lui, Litster, & White, 2007). The amorphous aggregates indicate that the increase of particle size at lower ionic strength was not originated from liquid-liquid phase separation, where two liquid phases would form (high or low protein content) and one liquid phase dispersed as spherical droplets in another liquid phase.

The aggregation process of HG was not immediately reversible once it had occurred, so the cloud point method was not convenient. Another method was applied to determine the phase diagram by monitoring the turbidity of HG for 12 hours at different protein concentrations and ionic strengths at 25 °C. The development of turbidity of 0.078% HG with time was shown in Figure 4-12, the one at 0.3 M ionic strength remained clear during the 12-hour storage. When the ionic strength was lower than 0.225 M, the development of turbidity followed a similar pattern – a lag phase followed by an exponential phase and a plateau phase. At 0.075 M, the turbidity reached the plateau within 2 hours, while it took more than 5 hours to reach the plateau value at 0.225 M. Therefore, the aggregation rate was correlated to HG concentration, indicating that delayed aggregation might result from the collision between HG.

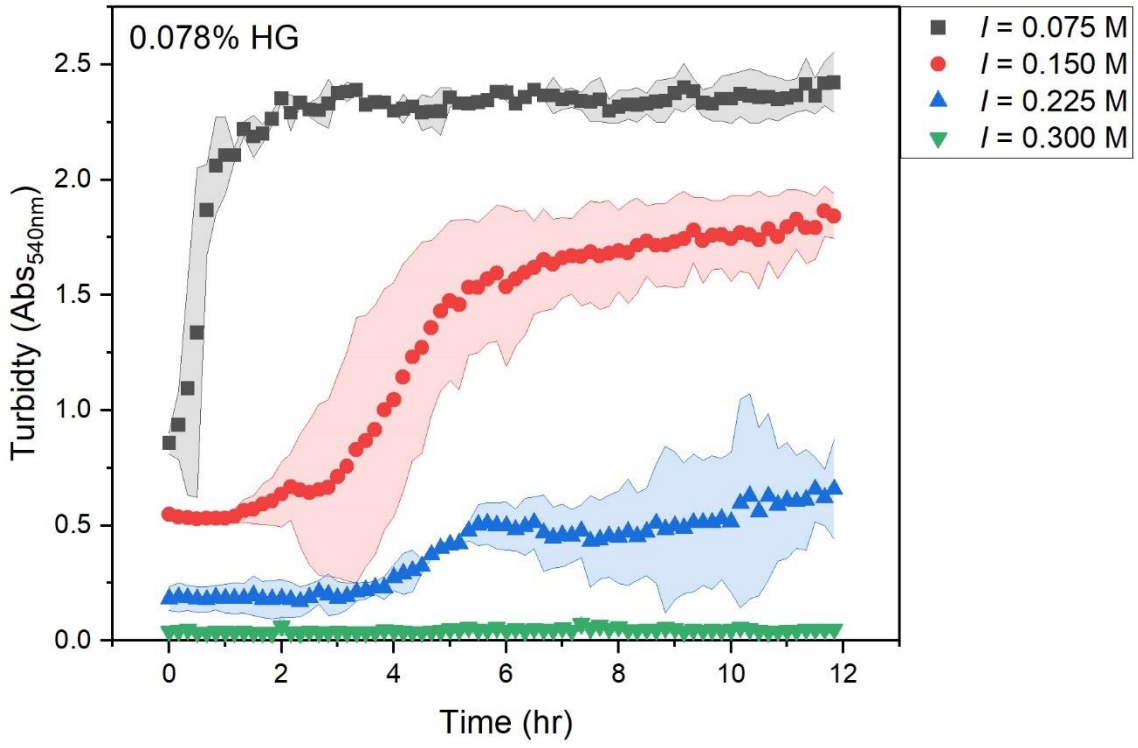

Figure 4-12 Development of turbidity of 0.078% HG at different ionic strengths, the shaded area represents one standard deviation, n=3.

Figure 4-13A shows the turbidity of HG solution/dispersion just after the protein concentration and ionic strength were adjusted to the target value – the x-axis being the HG concentration (0.26 – 4.42%) and y-axis being the ionic strength (0.025 – 0.5 M). The value and the colour intensity of each data point represent its turbidity.

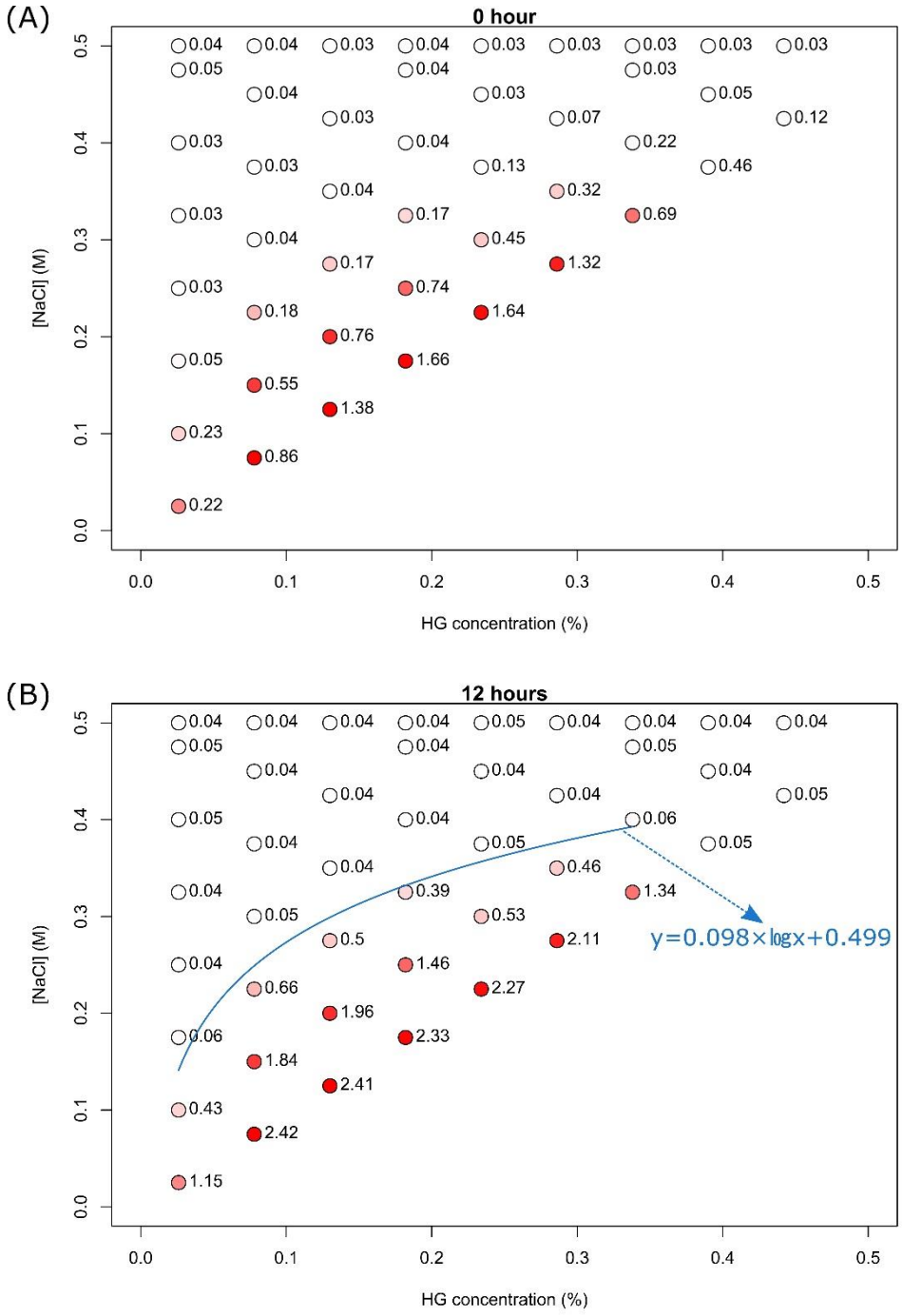

Figure 4-13. Phase diagram (turbidity vs. NaCl and HG concentration) of HG at (A) 0 hour and (B) 12 hours after preparation.

The turbidity of freshly prepared HG solutions/dispersions increased with increased protein concentration and decreased with increased ionic strength. After 12 hours, the clear HG solutions remained clear, while the turbid ones became more turbid, indicating slow aggregation processes happened within the 12 hours (Figure 4-13B).

In summary, the phase diagram of HG was obtained and can be used to make soluble HG solutions. An empirical phase boundary was calculated by fitting a logarithm formula with the interpolated data point that had turbidity of 0.3. The boundary shown in Figure 4-13B will give an empirical prediction for the phase behaviour/solubility of HG, and the equation being $y = 0.098 \times \log x + 0.499$ covering the HG concentration of 0.026 to 0.34%.

4.4. Heat aggregation of the mixture of hemp protein and whey protein

In order to introduce interactions between hemp and dairy proteins, HG and WPI were mixed and heated together. The aggregation behaviour of HG and WPI were monitored by turbidity after heat treatment. HG (0.15%) and mixture of HG and WPI (0.075%: 0.075%) were heated at 85.8, 89.6 and 92.4 °C (pH 7, ionic strength = 0.5 M) for specific times. Figure 4-14A shows that when there was only 0.15% HG, the solution became turbid slowly at 85.8 °C, and no visible precipitation was observed after 1200 seconds of heat treatment. When the temperature was raised to 89.6 and 92.4 °C, the increase of turbidity was faster and visible aggregates were formed after 600 and 300 seconds respectively.

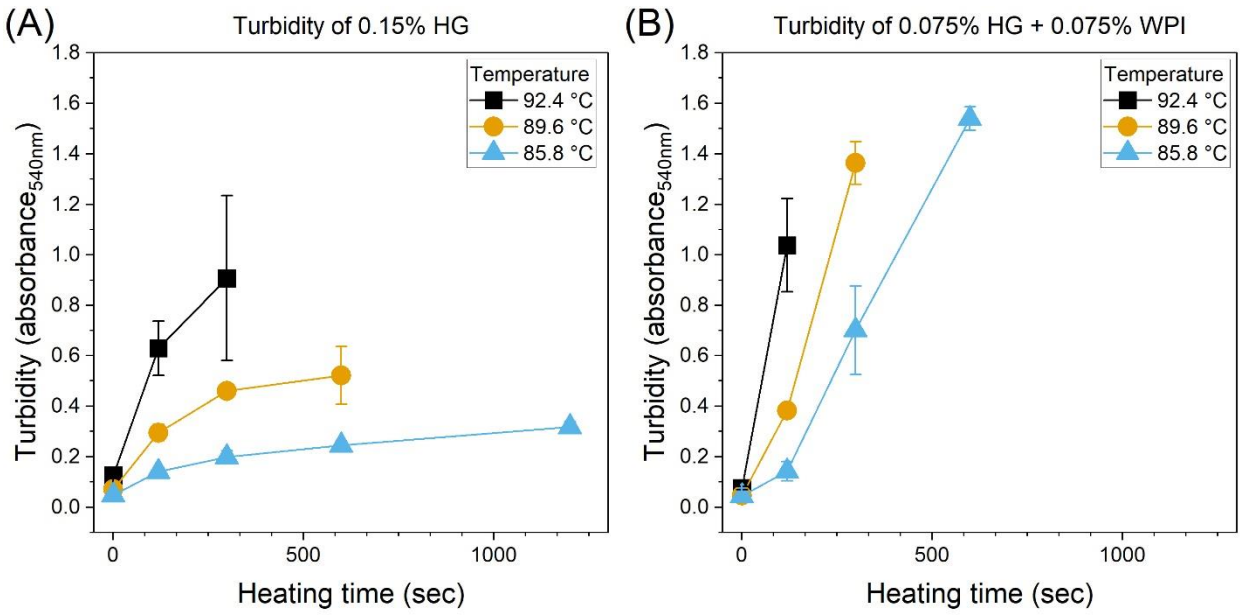

Figure 4-14. Turbidity of heated (A) 0.15% HG solution and (B) blend of 0.075% HG and 0.075% WPI at different heating time and temperature (n=3).

The difference of turbidity development of HG at different temperature could be expected because the DSC thermogram shows that the onset temperature and melting temperature of HG were 81.69 °C and 91.41 °C respectively (Figure 4-15). Therefore, the higher heating temperature will result in a higher degree of unfolding of HG, exposing more buried free thiol groups and disulfide bonds. The higher temperature would also provide higher reaction rate of the thiol-disulfide interchange (Visschers & De Jongh, 2005). These two factors contributed to the higher rate of development of turbidity of heated HG at a higher temperature. The difference could also be seen in the results of SDS-PAGE, as native-like edestin, which have the molecular weight of ~50 kDa, decreased with heating time at 90.4 °C (lane 6 – 9 in Figure 4-16A). On the other hand, the decrease of native edestin was not so significant at 85.5 °C (lane 2 and 5 in Figure 4-16A).

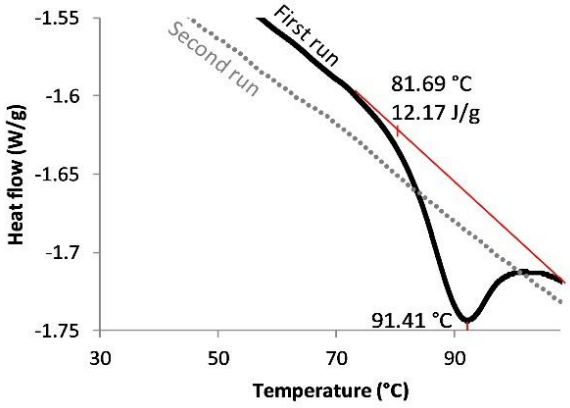

Figure 4-15. DSC thermogram of HG.

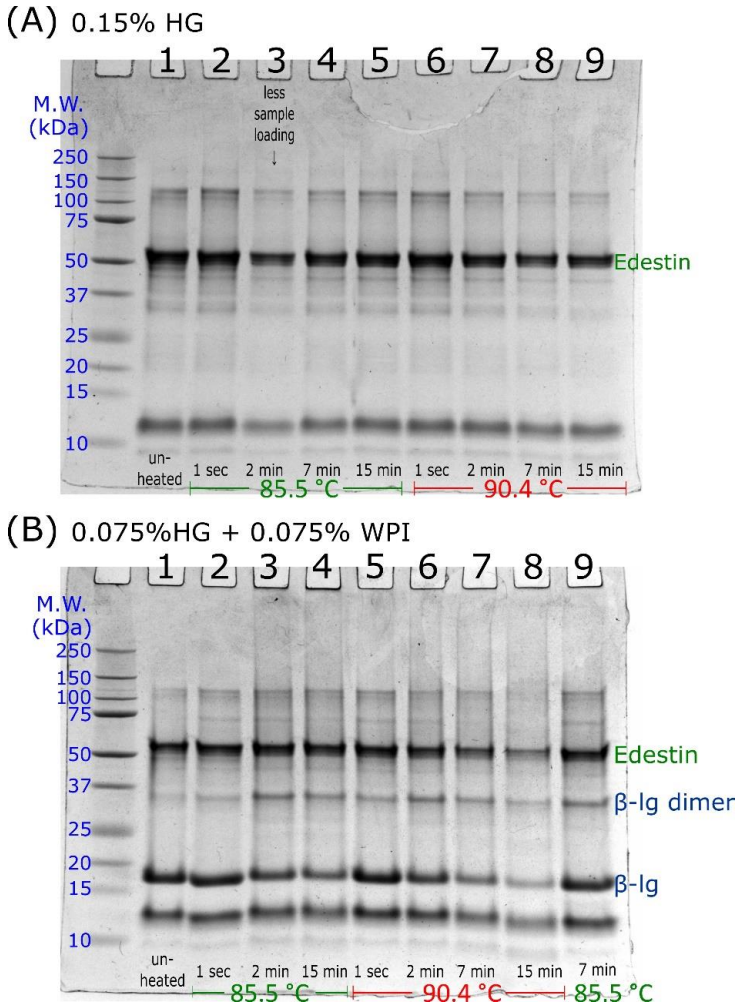

Figure 4-16. Results of non-reducing SDS-PAGE of heated (A) 0.15% HG and (B) mixture of 0.075% HG and 0.075% WPI at 0.5 M ionic strength.

The rate of turbidity development was higher in the mixture of HG and WPI (0.75%: 0.075%) because the turbidity of HG-WPI mixture (Figure 4-14B) was always higher than that of pure HG (Figure 4-14A). It could result from WPI-WPI aggregation. HG and WPI might aggregate with each other at around 90 °C because both the bands of edestin and β-lg in WPI diminished with increasing heating time (lane 5 – 8 in Figure 4-16B). In addition, 2D SDS-PAGE results showed that the aggregates presented as a smear with a high molecular weight in the gel were made of the basic subunits, acidic subunit of edestin and β-lg (Figure 4-17). On the other hand, only β-lg aggregated while edestin was mostly native when heated at 85.5 °C (lane 2 – 4 in Figure 4-16B). This result may be explained by the fact that the denaturation temperature of HG and β-lg were different. The melting point of HG was around 91 °C, so the temperature of 85.5 °C could not fully unfold/denature HG. In contrast, WPI would be fully denatured and aggregate because the denaturation temperature of the proteins in WPI was around 78.3 °C at 0.5 M ionic strength (Hussain, Gaiani, Jeandel, Ghanbaja, & Scher, 2012).

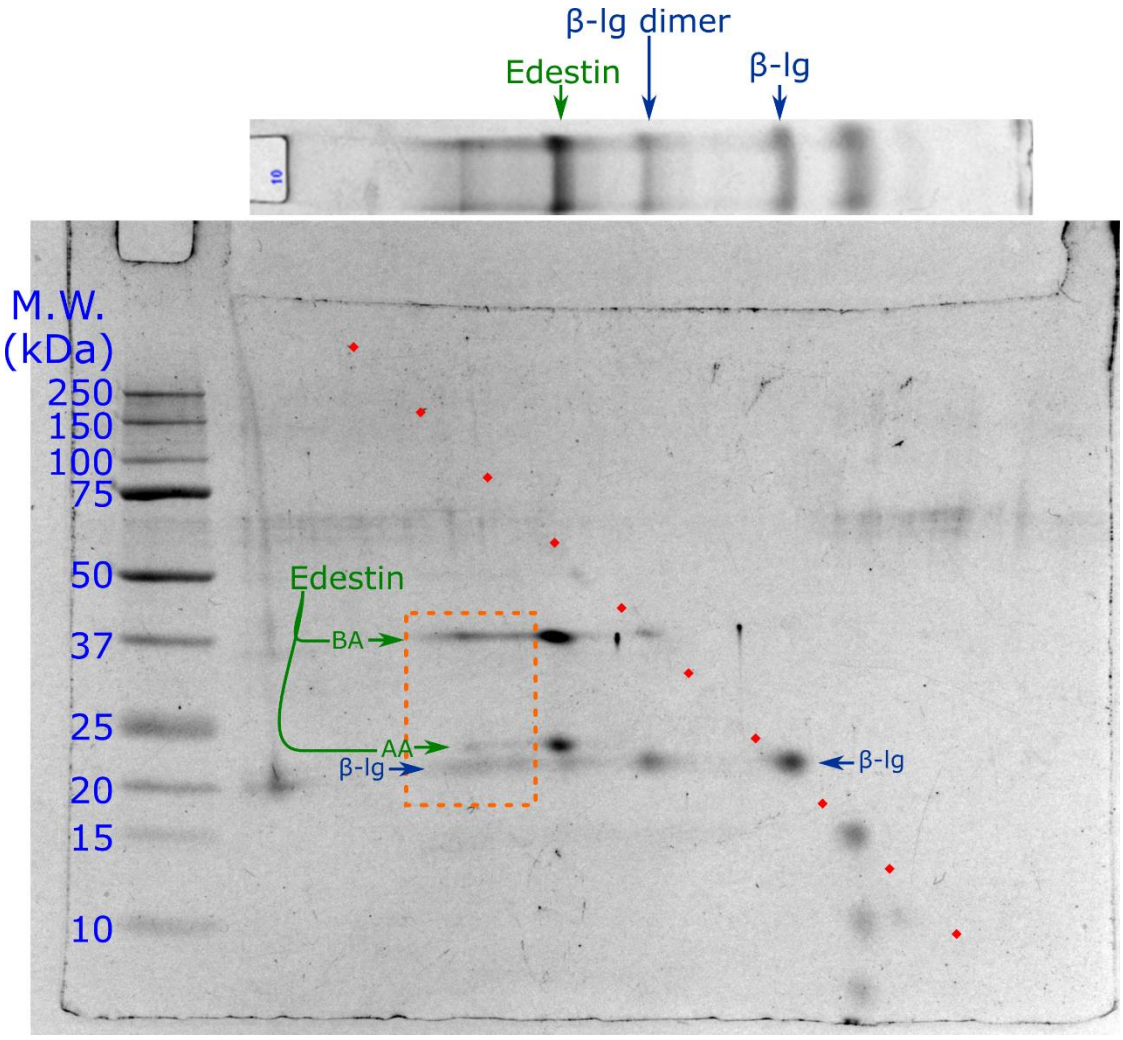

Figure 4-17. Result of 2D SDS-PAGE of heated mixture of HG and WPI heated at 89.6 °C for 10 minutes. BA: basic subunits of edestin; AA: acidic subunits of edestin.

Figure 4-18A presents the turbidity of HG-WPI mixture heated at different temperature (59.4 – 82.5 °C) for 1 second or 15 minutes. For the brief 1-second heating, the turbidity of HG-WPI mixtures was not different across different temperatures. The turbidity started to be different after 15 minutes of heating when the temperature was higher than 72.5 °C which is close to the denautration temperature of β-lg of 78.3 °C, indicating that the

denaturation and protein aggregation was initiated by the WPI. To further confirm the role of disulfide bonds in the heat-induced aggregation of HG and WPI, DTT (10 mM) was added into the protein solutions. Figure 4-18B shows that when disulfide bonds were reduced with DTT, the HG-WPI mixture stays clear even after heated at 82.5 °C for 15 minutes, which further support the importance of disulfide bond formation between HG and WPI.

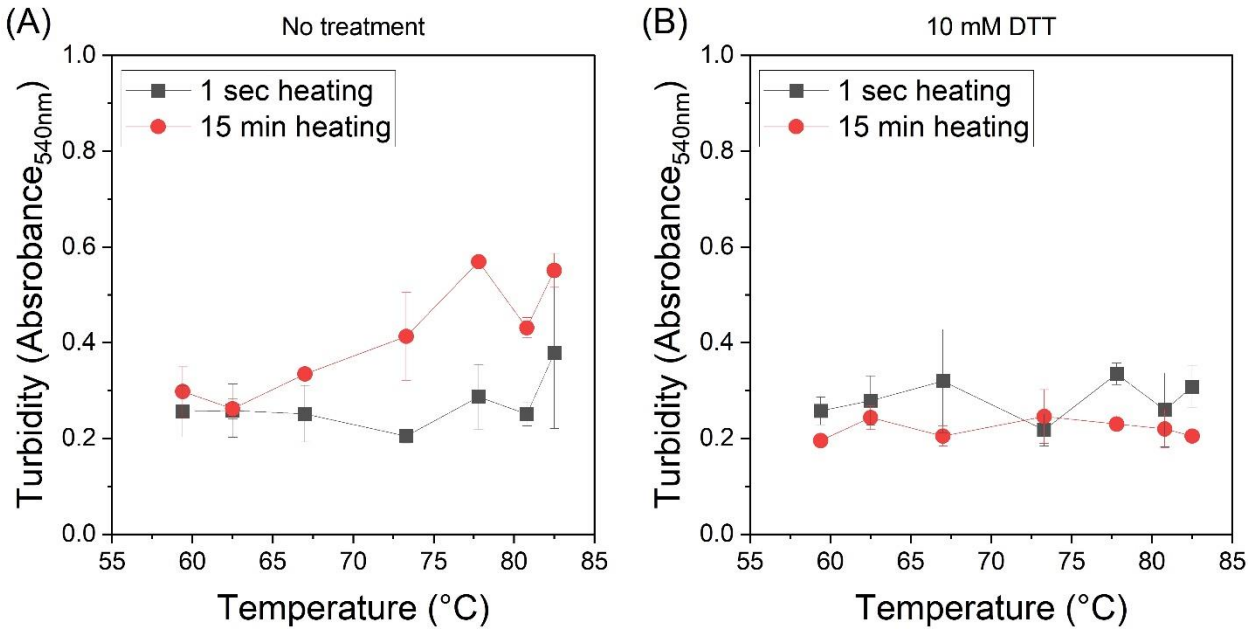

Figure 4-18. Turbidity of mixture of HG (0.135%) and WPI (0.18%) at different target temperature and different heating time. (A) no treatment and (B) the protein solution contained 10 mM DTT.

In summary, HG and WPI do not interact with each other until the temperature was close to the melting point of HG (91.41 °C), below which only WPI aggregated with itself. But when the temperature was close or higher than 91.41 °C, WPI would trigger extensive and

fast aggregation between HG and WPI via thiol-disulfide interchange and results in higher turbidity and are more likely to precipitate than when there was only HG.

4.5. Improvement of protein solubility by homogenisation of hemp protein with SC or surfactant

The other major dairy protein fraction is the caseins, and it had been reported that a mixture of plant protein and caseins could improve the solubility of the plant protein after high-pressure homogenisation (Boursier et al., 2013). To test this method, the mixture of HG and SC with constant 40 mg/mL protein and different SC/HG ratios (100/0, 75/25, 50/50, 25/75 or 0/100) were homogenised with rotor-stator homogeniser (Model D130, LabServ) at 33000 rpm for 1 min at room temperature. The homogenised dispersions were centrifuged and the soluble protein content in the supernatant was measured. The soluble protein content of each combination is the solid red line in Figure 4-19; the blue dotted line is the simple addition of the solubility of HG and SC. The improved solubility was statistically significant when the ratio of SC/HG ratio was 25/75. At this ratio, the solubility was increased from 7.19 to 8.65 mg/mL (20 % increase). The results indicate that interactions between HG and SC occurred during homogenisation, which results in higher solubility of HG.

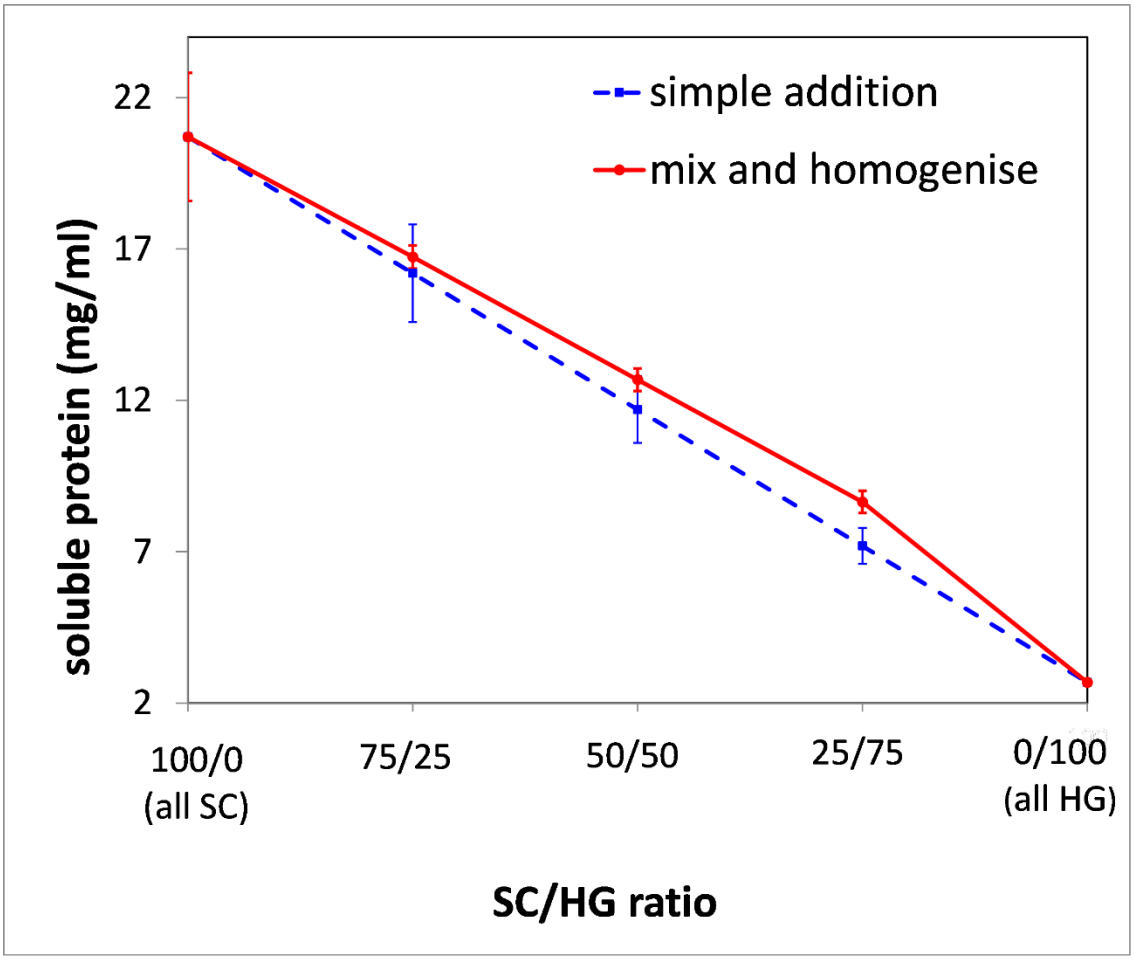

Figure 4-19. Solubility of homogenised HG-SC blends.

Caseins are amphiphilic molecules and have excellent surface-active properties (Augustin et al., 2011). The effect of improving plant protein solubility by homogenising with surface-active surfactant had been reported by Nakai, Ho, Tung, and Quinn (1980), and it is possible that the improvement of plant protein solubility by adding casein and then homogenising follows a similar principle. The author tested several surfactants on rapeseed protein and found that the solubility can only be raised by anionic surfactant such as SDS, and it was proposed that SDS could interact with the hydrophobic groups of the plant

protein after homogenisation and the negative charge on the anionic tail provides repulsive forces between proteins. Therefore, the protein solubility increased. However, caseins have a similar charge to HG because their pI are close. The pI of SC is between pH 4 – 5 (H. Ma et al., 2009) and the pI of HG is between pH 5 – 6 (Figure 4-6), so both HG and caseins should not carry strong charge at pH 7.

The improvement of HG solubility by mixing with SC and subsequently homogenising indicates that the SC might act as surfactant to solubilise HG. To make sure that non-ionic surfactant could be used to solubilise HG, Tween 60 was mixed and homogenised with HG. Figure 4-20 showed the homogenised mixture of HG and Tween 60 do have a higher protein solubility than un-homogenised and homogenised HG, and the increase of HG solubility when homogenised with Tween 60 (≈ 50%) was more significant than with SC (≈ 20%). Therefore, SC may be a less potent surfactant than Tween 60, but it could still interact with HG and increase its solubility. There are other processing methods that are harsher than the homogenisation with the rotor-stator homogeniser, such as heat treatment, pH adjustment or high-pressure homogenisation, and these processing methods may introduce more interactions between HG and SC and improve the colloidal stability and/or solubility of HG.

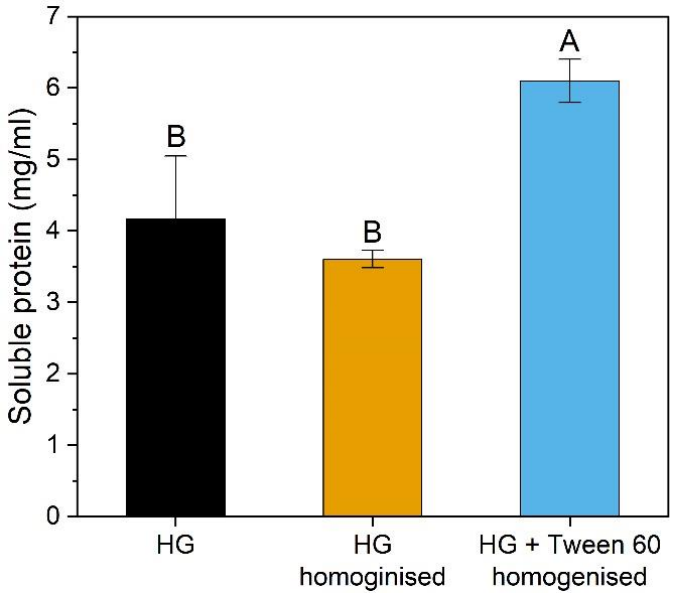

Figure 4-20. Solubility of HG, homogenised HG and homogenised mixture of HG and tween-60. Bars with different letter(s) are significantly different from each other and presented as means ± SD ($p < 0.05$).

4.6. Conclusion

Several plant protein sources were screened, and hemp protein was selected as the plant protein material to use in subsequent experiments. HG was extracted with a simple salt extraction method and the extracted HG had around 90% protein. There was only one major dimeric protein, edestin, which would make the future analysis of protein-protein interactions between HG and dairy proteins easier. HG had low solubility at low ionic strength, especially between pH 5 – 6. The low water solubility of HG made it challenging to use in many food systems, which do not usually have high ionic strength or high pH. A phase diagram of the turbidity of HG at different ionic strength and protein concentration was made so the solubility of HG could be easily referred. The origin of the low solubility might be strong non-covalent interactions between hemp edestin as urea is the most potent

dissociating reagent. To solubilise HG in the first place, these non-covalent bonds should be disrupted and dairy proteins may play a part in interacting with and stabilising them.

Caseins could be a more promising dairy protein fraction than the whey proteins when it comes to solubility. HG aggregates easily via disulfide bond formation when the temperature is close to its melting temperature of around 91 °C. On the other hand, WPI denatured and initiated thiol-disulfide reactions above 72.5 °C. The heat-induced aggregation between HG and WPI resulted in disulfide-linked large aggregates that could not enter the resolving gel during electrophoresis. Homogenising HG and SC increased the solubility of SC, suggesting the non-covalent interactions between HG and SC is a possible method to increase the solubility and other functionalities of HG.

However, homogenisation of mixtures of SC and HG only increases HG by around 20%. Therefore, interactions between HG and SC would be introduced with other processing methods to increase the colloidal stability and/or solubility at lower ionic strength in the next chapters, and some other functionalities will also be discussed.

5. HEMP GLOBULIN HEAT AGGREGATION IS INHIBITED BY THE CHAPERONE-LIKE ACTION OF CASEINS

The contents of this chapter have been published in a peer-reviewed journal article

Chuang, C.-C., Wegrzyn, T. F., Anema, S. G., & Loveday, S. M. (2019). Hemp globulin heat aggregation is inhibited by the chaperone-like action of caseins. *Food Hydrocolloids*, *93*, 46-55.

5.1. Introduction

Hemp edestin has extremely low solubility in water at neutral or acidic pH and is soluble only at high ionic strength or alkaline pH (Malomo & Aluko, 2015a). Many protein functionalities such as surface-active properties are correlated with protein solubility (Jackman & Yada, 1989b), and poor water solubility of HG is believed to result in its poor emulsifying and water holding properties when compared with soy protein isolate (Tang et al., 2006). It may be possible to achieve better functionalities of hemp protein by improving its solubility and/or colloidal stability – protein may form true solutions and the maximum concentration of soluble protein is its solubility; protein could also be insoluble, but be dispersed in the continuous liquid phase to form a stable colloidal suspension.

Caseins have no well-defined secondary and tertiary structures and can reversibly self-associate into aggregates at high ionic strength and high temperature (HadjSadok et al., 2008). The structure and amino acid sequence of caseins gives them chaperone-like ability, i.e. the ability to inhibit globular protein aggregation under stressed environments, and this interesting phenomenon has attracted much attention, especially in the last two decades

(Akbari, Bamdad, & Wu, 2018; Yong & Foegeding, 2010). Most research into the chaperone-like activity of caseins has focused on the milk protein system, i.e. the chaperone-like effect of individual or combined caseins on whey proteins. α_S- (α_{S1}- and α_{S2}-), β-, κ-Casein and caseinate all have been shown to have chaperone-like activity against heat-induced aggregation (Bhattacharyya & Das, 1999; Guyomarc'h, Nono, Nicolai, & Durand, 2009; Liyanaarachchi, Ramchandran, & Vasiljevic, 2015; Morgan et al., 2005; O'Kennedy & Mounsey, 2006; Yong & Foegeding, 2008; Zhang et al., 2005). For example, heated whey protein isolate solution (80 °C, 24 h) showed lower turbidity and smaller aggregates when SC was added (Guyomarc'h et al., 2009).

The activity of specific caseins might differ under different stresses and environments because of their distinctive structures. α_{S1}- and β-casein are believed to possess chaperone-like effects because they are flexible, relatively unstructured and amphiphilic. Their hydrophobic regions may associate with the hydrophobic regions of partially unfolded globular protein, and the phosphoserine-rich, negatively-charged regions may act as surfactants to solubilise the protein, e.g. as reported for α_{S1}- and β-casein (Koudelka, Hoffmann, & Carver, 2009). Since α_{S1}- and β-casein have no cysteine residues, aggregation between them and other substrate globular proteins via disulfide bonds is not possible. κ-casein may also stabilise heated globular protein via hydrophobic interactions, and it can also form covalent bonding with the substrate protein because there are two cysteine residues in it (Gaspard, Auty, Kelly, O'Mahony, & Brodkorb, 2017). Since the majority of plant storage proteins are also globular proteins, we hypothesise that the chaperone-like effect of caseins is also applicable to plant seed globulins.

In the previous chapter, SC had been shown to increase the solubility of HG after homogenisation, and the interaction could be non-covalent interactions. This chapter investigated the ability of SC to alter the aggregation behaviours of HG during heating at high ionic strength. Higher temperatures may introduce thiol-disulfide exchange between HG and κ-casein and strengthen hydrophobic interactions between HG and amphiphilic caseins. The heat-induced aggregates were characterised, and hydrophobic interactions and disulfide bonding between HG and SC were analysed. This chapter aimed to produce a more stable HG solution/dispersion after heat-treatment and dilution to low ionic strength, to enable the use of HG in beverages or protein-stabilised emulsions.

5.2. Material and methods

HG was obtained by a salt-extraction method and freeze-dried as described in section 3.2. The protein content was 89.6% (w/w) based on the Dumas combustion method with a nitrogen-to-protein conversion factor of 5.7. HG was further defatted with hexane. HG was stirred with hexane (1:7, w/w) for 1 h, then centrifuged (3000 × g, 10 min) to remove the hexane. The oil extraction step was repeated for two more times and residual hexane was evaporated by placing the HG in the fume hood for one night.

5.2.1. *Sample Preparation and Heat Treatment of Protein Solutions*

HG (1% w/v) and SC (3% w/v) were dispersed overnight at room temperature in the dispersion buffer, which contained 50 mM sodium phosphate (pH 7) and 0.02% sodium azide. The ionic strength was adjusted by adding 0.385 M NaCl to 0.5 M, which was calculated according to Beynon and Easterby (2003). Protein dispersions were centrifuged (10,000 × g, 25 °C, 30 min) and the supernatants were passed through a 0.45 μm

polyvinylidene fluoride filter (Millipore, Burlington, MA, USA) to obtain the soluble protein fraction. The major protein, edestin, remained dominant after the centrifugation and filtration steps (Figure 5-1). Protein content in soluble fraction was determined with the bicinchoninic acid assay (Noble & Bailey, 2009). HG solution (0.1% w/v) was prepared and blended with 0 – 0.2% w/v SC in dispersion buffer. To simplify the nomenclature, the '%' sign is omitted and the '|' sign is used for blends, e.g. the blend of 0.10% HG and 0.1% SC is presented as 0.10HG|0.10SC. The weight ratio of 1:1 (HG:SC) is estimated to be 1:2.2 (HG:SC) in molar ratio based on the composition and molecular weights of caseins in SC. Aliquots (100 µL) with known protein concentrations were transferred into 300 µL polymerase chain reaction (PCR) tubes and heated from 25 ˚C to 90 °C in approximately 51 s in a PCR thermocycler iCycler (Bio-Rad, Hercules, CA, USA), held at 90 °C for different holding times, then cooled to 25 °C in approximately 60 s.

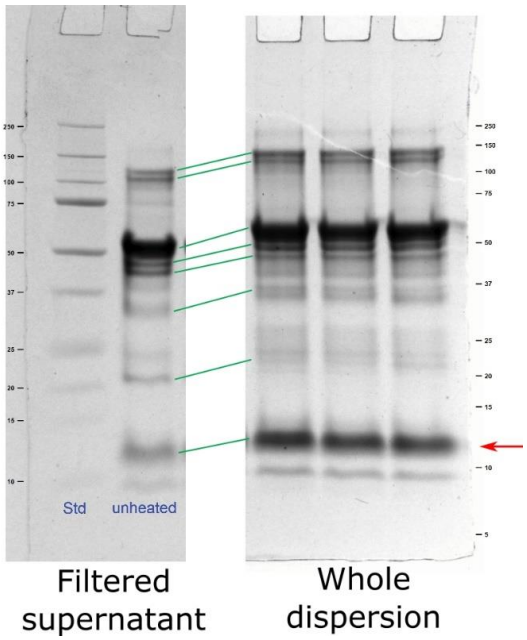

Figure 5-1 Non-reducing SDS-PAGE of HG before or after centrifugation and filtration. Only the protein labelled by the red arrow was significantly less after centrifugation and filtration.

5.2.2. *Kinetics of protein aggregation*

The kinetics of protein aggregation were studied by tricine SDS-PAGE. Protein solutions (0.1HG or 0.1HG|0.2SC) were heated in the PCR thermocycler as described in the sample preparation section. The quantity of remaining edestin after different heating times was fitted with the following formula to obtain the apparent reaction rate k_{app} and the reaction order n : $\frac{C}{C_0} = [(n-1)k_{app}t + 1]^{\frac{1}{1-n}}$, in which C_0 is the band intensity in unheated samples, and C is the band intensity at a given heating time, t. The nonlinear regression was done with Origin 2017 (OriginLab Corporation, Northampton, MA, USA).

5.2.3. *Transmission electron microscopy (TEM)*

Negative staining and sample preparation were performed using the method of Vinceković, Ćurlin, and Jurašin (2014), and the samples were examined with a Philips CM10 electron microscope (Eindhoven, The Netherlands). The image was analysed by the Fiji image processing package (Schindelin et al., 2012) and the fractal dimension was calculated by the box count method with the FracLac plugin (Karperien, 2013).

5.2.4. *SYPRO orange binding fluorescence*

Fluorescent dye SYPRO orange (SO) was used to determine the surface hydrophobicity in the protein solutions. The method was based on standard differential scanning fluorimetry (Niesen, Berglund, & Vedadi, 2007), but isothermal holding at 90 °C was used instead of temperature ramping to mimic the heating profile in the turbidity experiments. Protein solutions and SO were diluted with dispersion buffer to assigned concentrations with a

final volume of 20 µL in a white 96-well PCR plate, which was sealed before putting into a real-time PCR machine LightCycler 480 II (Roche Molecular Systems Inc., Pleasanton, CA, USA). Samples were heated from 20 °C to 90 °C in approximately 20 s, held at 90 °C for 10 or 30 min and cooled to 20 °C in approximately 60 s. The excitation wavelength was 465 nm and the detection wavelength was 580 nm.

5.3. Results and discussion

5.3.1. *Turbidity at 0.5 M or 0.17 M ionic strength*

SC delayed or even inhibited the development of turbidity of HG solution after heat treatment (Figure 5-2A). The turbidity of 0.1% HG rose after a short lag phase of 15 s and reached a plateau after 5 min. Incorporating 0.05% SC with 0.1% HG extended the lag phase to 1 min before reaching a similar plateau turbidity as with 0.1HG alone. Increasing SC concentration to 0.1% delayed the lag phase further to 3 min, with the plateau in turbidity lower by more than 50% than that of 0.1HG and 0.1HG|0.05SC. The development of turbidity could be inhibited entirely when ≥ 0.15% of SC was blended with 0.1% HG. The reduction of turbidity after heat treatment by incorporating SC was consistent with previous studies using other globular proteins, such as bovine whey proteins (Guyomarc'h et al., 2009; Mounsey & O'Kennedy, 2010).

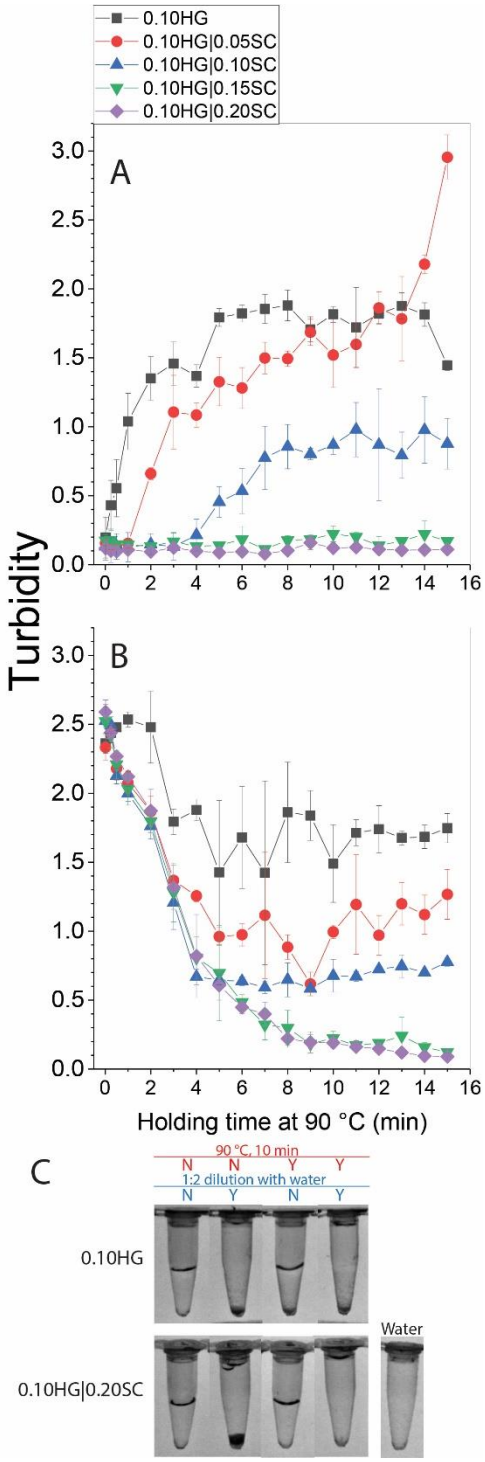

Figure 5-2 (A) Turbidity of protein solutions after being heated and held at 90 °C, (B) Turbidity of heated protein solutions after 3× water dilution and (C) photos of the protein solutions taken 21 hours after preparation. Error bars represent one standard deviation, n=3.

Heat-treated HG|SC blends had surprisingly high colloidal stability, even when diluted to lower ionic strength. After heating and cooling, one volume of heated protein solution was diluted with two volumes of water to produce a final HG concentration of 0.03% and an ionic strength of 0.17 M. Samples held at 90 °C for only 1 s became turbid (Figure 5-2B). HG in these briefly-heated samples should not denature completely and would still aggregate at lower ionic strength as shown in Figure 4-13. The precipitation of HG after dilution with water was expected because plant globulins are salt-soluble by definition and precipitate at low ionic strength (Hadnađev et al., 2017; Stone, Karalash, Tyler, Warkentin, & Nickerson, 2015). The extracted HG was shown to be predominately in the native form at an ionic strength of 0.5 M because an endothermic peak can be found in DSC traces at approximately 90 °C (Figure 5-9).

The turbidity of diluted HG solutions was much lower when blended and heated with SC, and this effect became more prominent with increasing SC concentration and longer holding time. HG|SC blends were transparent when ≥ 0.15% SC was incorporated and heated at 90 °C for more than 9 min. It can be concluded that HG interacted with SC during heating, which resulted in inhibition of HG aggregation during heat treatment, and after dilution to lower ionic strength.

The development of turbidity resulted in the formation of a precipitate in the bottom of tubes, as seen in Figure 5-2C, which shows tubes 21 hours after preparation (storage at ambient temperature). Precipitation was observed in 0.1HG after heat treatment and

dilution to low ionic strength; 0.1HG|0.2SC had no visual precipitation after both treatments.

5.4. Solubility of HG in heated HG|SC complexes

Mixing and heating SC and HG together not only improved the colloidal stability but also increased the solubility of HG. Protein solutions, which had constant protein content (0.5%) and different HG/SC ratio (100:0, 75:25, 50:50, 25:75 and 0:100), were centrifuged (10, 000 × g, 20 min, 25 °C) after the heat treatment to see the change of the amount of soluble protein in the supernatant. Figure 5-3A shows the amount of soluble protein of heated protein solution with different holding time at 90 °C. When there was 100% HG, the solubility of HG became significantly lower after 3 minutes of holding time at 90 °C and further decreased with longer holding time. When 25% of HG was substituted with SC (HG : SC = 75 : 25), the holding time extended to 5 minutes before the solubility decreased significantly. When there were more than 50% of HG in the mixture (HG : SC = 50 : 50 or 25 : 75), the protein solubility did not decrease even after 10 minutes at 90 °C. The solubility of 100% SC did not change after 10 minutes of holding at 90 °C as well, indicating that the loss of solubility when there was less than 25% of SC in the mixture originated from aggregated HG.

The heated protein mixtures were also diluted with two volumes of water to lower the ionic strength to 0.17 M as in the turbidity experiments. Mixing SC with HG resulted in similar protein solubility in the heated solutions, as the amount of soluble protein did not differ significantly to that of unheated protein solutions even after 10 minutes of heating at 90 °C when there were more than 25% of HG was substituted with SC (Figure 5-3B). On the

other hand, the protein solubility of pure HG decreased with increasing holding time at 90 °C. The HG|SC protein mixtures may even provide higher protein solubility after heating and diluting with water in certain conditions. For example, when the HG : SC ratio was 50 : 50 and the holding time was between 1 – 5 minutes, the heated and diluted samples had a slightly higher amount of soluble protein than the unheated one (Figure 5-3B).

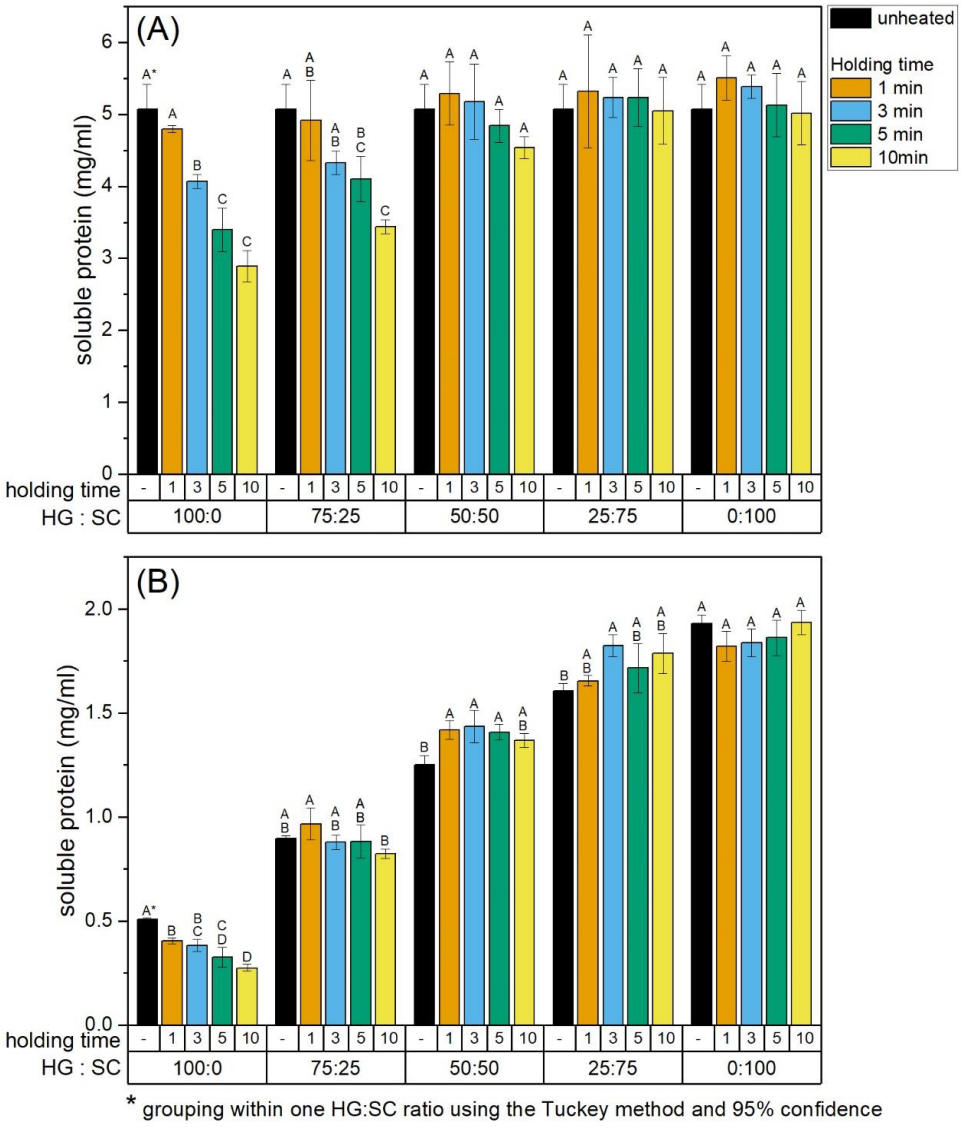

Figure 5-3 Protein solubility of (A) heated and (B) heated and diluted with 3× water (ionic strength: 0.167 M) at different HG/SC ratio and heating time. Error bars represent one standard deviation, n=3.

5.5. Size distribution and morphology of heat-induced aggregates

Unheated HG and SC solutions had bimodal particle size distribution (PSD, Figure 5-4A), indicating possible self-assembly before heating. There were two peaks in 0.1% HG according to the intensity particle size distribution (Figure 5-4A), with a major 17-nm peak and a minor 248-nm peak. This contrasts with the findings of Teh, Bekhit, Carne, and Birch (2016) who only saw one population with a large particle size (177 nm) in the water-soluble fraction of hemp protein isolate (ionic strength = 0). Since globulins are soluble in salt solutions by definition, the 0.5 M ionic strength used in these experiments could readily dissociate large globulin complexes and give rise to smaller particles. The major population with 17-nm diameter may be edestin hexamer (S. Patel, Cudney, & McPherson, 1994), similar to DLS observations of soy glycinin (Pizones Ruiz-Henestrosa, Martinez, Patino, & Pilosof, 2012). When the intensity PSD was converted into volume PSD by the Zetasizer software using the Mie theory, the population with a smaller diameter (13.5 nm) predominated (Figure 5-4B).

Two peaks were also observed in the intensity PSD of 0.2% SC (Figure 5-4A). This result was consistent with earlier studies (HadjSadok et al., 2008), with the 25-nm population attributable to small SC aggregates which arise from screened electrostatic interactions at high ionic strength, while the sizeable 235 nm population may be protein-fat or protein-protein complexes (HadjSadok et al., 2008; Lucey, Srinivasan, Singh, & Munro, 2000). The volumetric PSD (Figure 5-4B) showed that the small SC aggregates had a single peak at 13.5 nm, which occupied more than 95% of the volume, whereas the larger complexes were marginal and polydisperse.

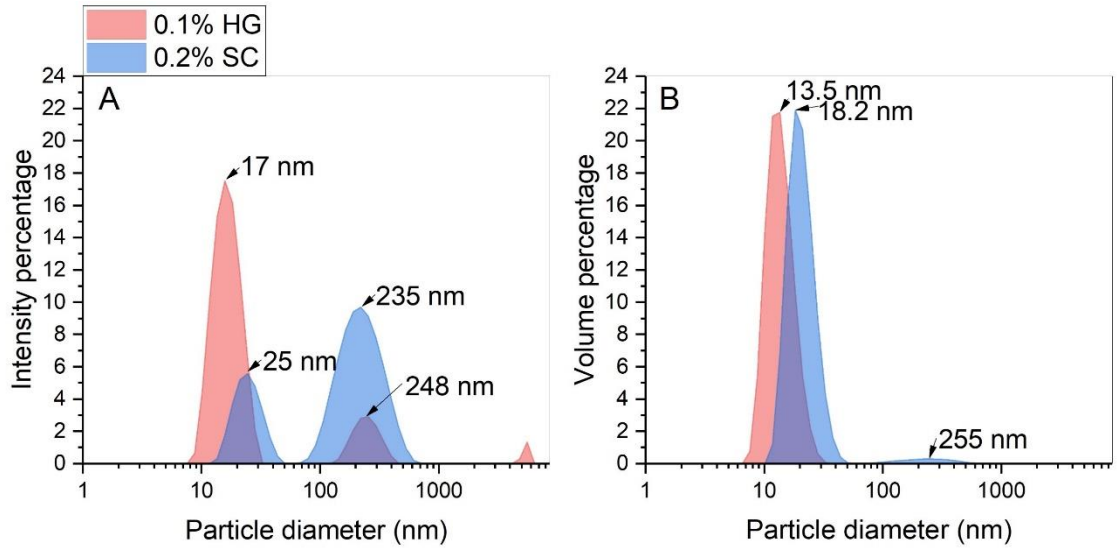

Figure 5-4 PSD of unheated 0.1% HG and 0.2% SC solution at I=0.5 M, based on (A) intensity percentage or (B) volume percentage.

The derived count rate (DCR) indicates the total amount of scattering; an increase in DCR is an indicator of increasing particle size and/or number (Loveday, Ye, Anema, & Singh, 2013). DCR of 0.1HG increased after holding at 90 °C for 30 s (Figure 5-5), and then decreased because of the formation of large aggregates that settled rapidly (fewer particles in the light path). The increase in DCR occurred at later times as SC concentration was increased, i.e. the aggregation rate was lowered by the addition of SC. The DCR peak was absent in heated 0.1HG|0.20SC solution, suggesting that aggregates were not large enough to precipitate in this case.

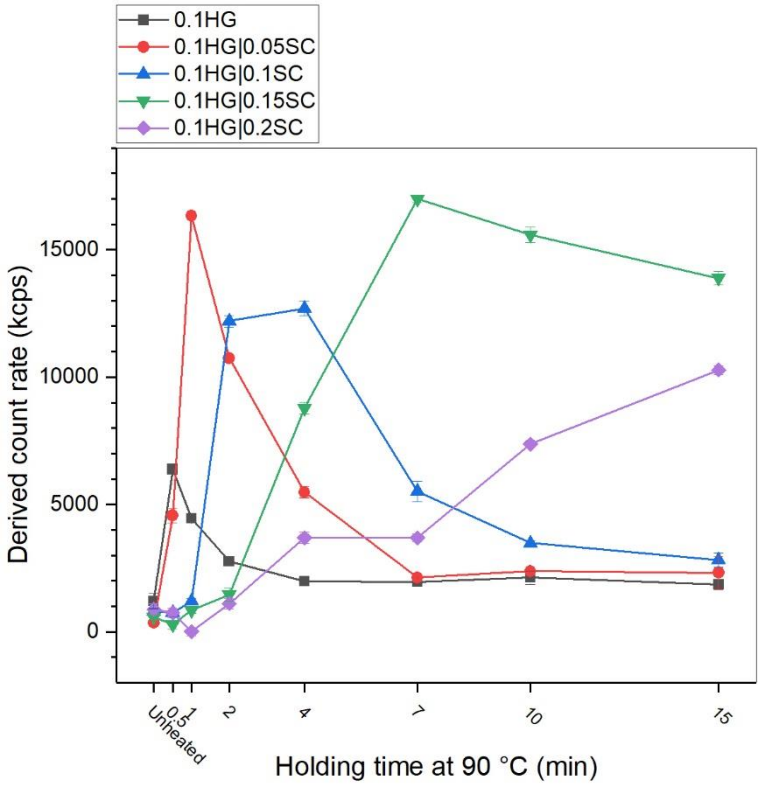

Figure 5-5 Derived count rate (DCR) of unheated and of heated protein solutions with different holding time at 90 °C.

Blending SC with HG delayed the formation of large aggregates by lowering the rate of protein aggregation. Figure 5-6A shows the volumetric PSD of 0.1HG. Large particles a few μm in diameter were formed after 0.5 min at 90 °C and subsequent cooling, and these aggregates were visible and prone to precipitation. When 0.05% SC was blended with 0.1% HG solution (Figure 5-6B), a transient intermediate population 70-800 nm in diameter appeared with 0.5 min and 1 min holding times. After that only particles with diameters of a few μm were observed. Increasing SC concentration further delayed the appearance of intermediate-sized aggregates and large visible aggregates (Figure 5-6C and 11D). When the SC concentration increased to 0.2 %, only a small polydisperse population of intermediate aggregates (up to 400 nm) was detected, and the formation of large aggregates

was completely inhibited (Figure 5-6E). The effect of SC was to delay aggregate formation and decrease aggregate size, which indicates that SC altered the kinetics of aggregation and/or limited the size of aggregates. The disappearance of edestin and casein populations (10 – 30 nm) after heat treatment suggested that HG|SC complexes were stable (top of Figure 5-6B). The change in aggregation rate in HG|SC suggests the aggregation regime is altered. There are two regimes of protein aggregation – diffusion-limited cluster aggregation (DLCA) and reaction-limited cluster aggregation (RLCA) (Vreeker, Hoekstra, den Boer, & Agterof, 1992). There is no repulsive barrier between particles in the DLCA regime. Therefore the aggregation is rapid and only limited by the diffusion of aggregate particles, and every collision between proteins results in sticking and aggregation. On the other hand, aggregation in the RLCA regime is much slower because there is an energy barrier between particles. Hence the sticking probability between proteins is decreased, and more collisions have to occur before the aggregates stick together. Incorporating SC with HG seems to change the aggregation regime from DLCA to RLCA because the aggregation rate is lower in the HG|SC blends.

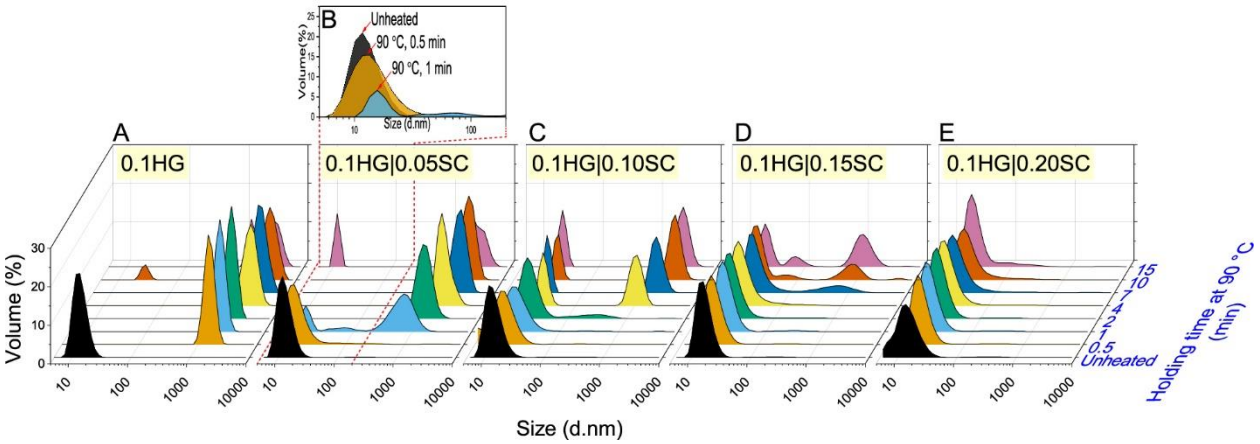

Figure 5-6 Volumetric PSD of HG and HG|SC blends heated at 90 °C with different holding times. Protein solutions were cooled to 25 °C before measurement.

Another indication of an altered aggregation regime is the presence of intermediate aggregates in HG|SC blends. The monomodal size distribution of 0.1HG aggregates and the absence of intermediate aggregates (Figure 5-6A) implied that the HG aggregation proceeded in the DLCA regime (Markossian, Yudin, & Kurganov, 2009), in which the first step of protein aggregation is the formation of starting aggregates, followed by the association of starting aggregates, so that no intermediate aggregates form. On the other hand, a bimodal distribution of the aggregates can be observed in 0.1HG|0.15SC (Figure 5-6D) when the holding time was 10 or 15 min. This splitting of the protein aggregate population was consistent with systems which were known to be following the RLCA regime (Golub, Markossian, Sholukh, Muranov, & Kurganov, 2009; Khanova et al., 2005). Markossian et al. (2009) interpreted a bimodal aggregate size distribution as an indication that some substrate proteins retained more aggregation sites, so their probability to aggregate was higher and aggregation produced larger particles, whereas other substrate proteins had fewer available aggregation sites and therefore aggregated into smaller particles.

The particle sizes measured by DLS are supported by TEM micrographs. Particles with a diameter of 15-20 nm were observed in unheated HG (Figure 5-7A). Heat treatment at 90 °C for 10 min (Figure 5-7B) produced large amorphous aggregates, which may become the building blocks for gel formation when protein concentration is higher (Dapčević-Hadnađev et al., 2018). After the ionic strength was lowered to 0.17 M by water dilution, these heat-induced aggregates had an open and network-like structure (Figure 5-7C), possibly due to stronger electrostatic repulsion at lower ionic strength. It could also be

inferred that the aggregates were cross-linked via covalent bonds (disulfide linkages), as the structure was strong enough to withstand repulsion forces at lower ionic strength. In the unheated and heated 0.1HG|0.2SC, the solution was crowded with SC particles (Figure 5-7D and 12E). Polydisperse amorphous aggregates with particle sizes up to a few μm formed after dilution with water (Figure 5-7F) and the formation of the network-like structure was inhibited.

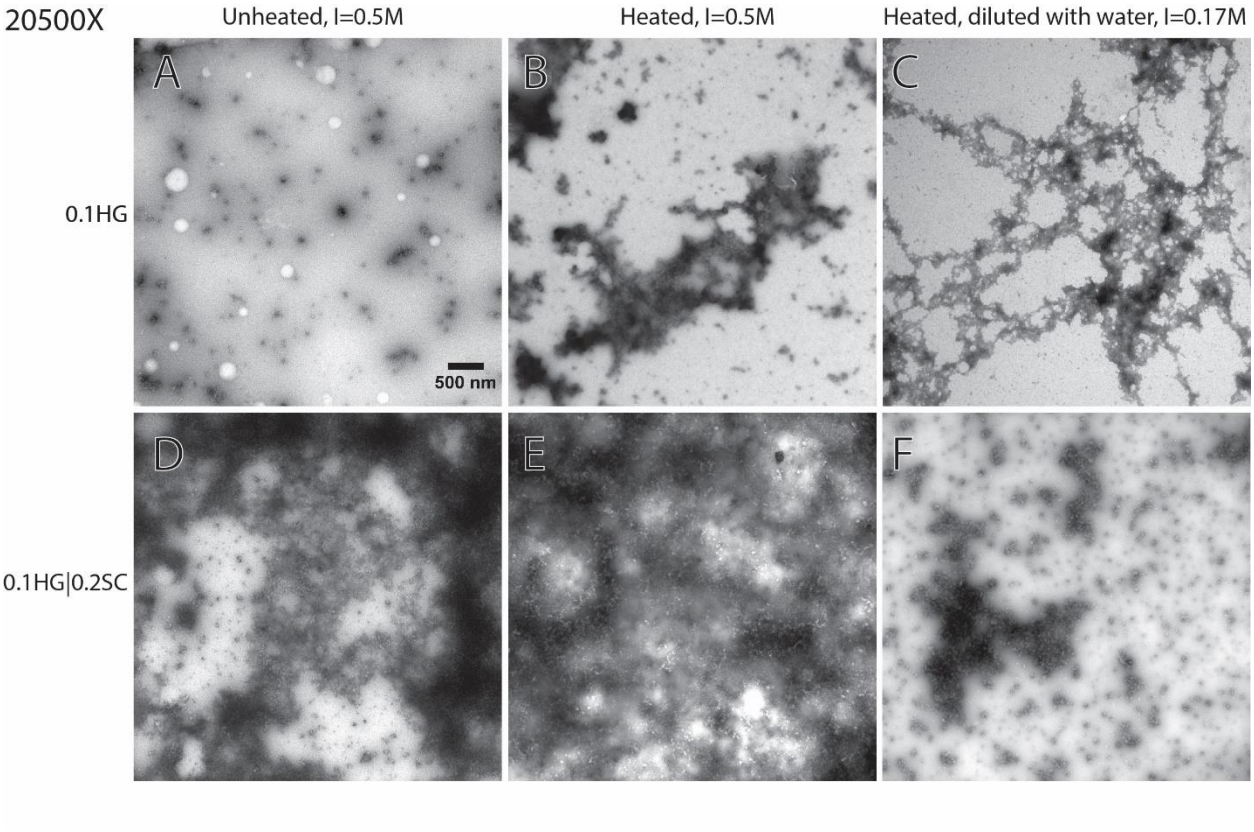

Figure 5-7 Transmission electron micrograph of 0.1HG and 0.1HG|0.2SC with different treatments. (A)-(C) 0.1 HG; (D)-(F) 0.1 HG|0.2SC.

These TEM micrographs provide further evidence for the change of aggregation regime from DLCA to RLCA. The heated and diluted aggregates of 0.1HG in Figure 5-7C seem

to be stable after sample treatment, and no overlapping between aggregates is observed, so the fractal dimension can be estimated by image analysis. The fractal dimension of HG aggregates was calculated to be 1.72 ± 0.03 by the box count method, and the value is within the range expected for DLCA at 1.7 – 1.8 (Ikeda, Foegeding, & Hagiwara, 1999). There seems to be overlapping between aggregates in 0.1H|0.2SC (Figure 5-7F), which made it impossible to obtain the original sizes and shapes of the aggregates, so image analysis was not applicable for these aggregates. Nevertheless, the compact aggregates of 0.1H|0.2SC may already suggest an RLCA regime, because more compact structures are formed in RLCA while open structures are found in the DLCA regime (Lazzari, Nicoud, Jaquet, Lattuada, & Morbidelli, 2016).

5.6. Analysis of the kinetics of disulfide-linked aggregation by SDS-PAGE

Whole protein dispersions were analysed by non-reducing SDS-PAGE to quantify residual native edestin after heat treatment. Incorporating SC did not change the rate of HG denaturation and aggregation via disulfide bonds because the n and k_{app} were not significantly different after adding 0.2% SC according to Tukey's post-hoc test (Figure 5-8). DSC results (Figure 5-9) showed that the melting temperature and denaturation enthalpy of 0.1% HG were unchanged in the presence of SC, providing further evidence that the effect of SC was not due to a change in HG denaturation behaviour. These results are in line with β-casein|whey protein blends, in which no significant change in the denaturation kinetics and denaturation temperature was observed (Kehoe & Foegeding, 2011).

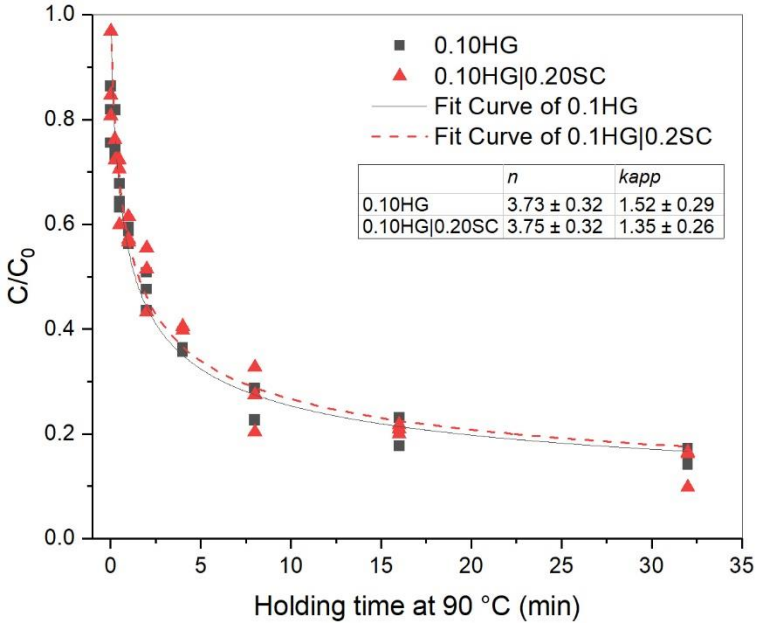

Figure 5-8 Fractional concentration of native edestin after heating at 90 °C for 1 second to 32 minutes, calculated from densitometry data from SDS-PAGE.

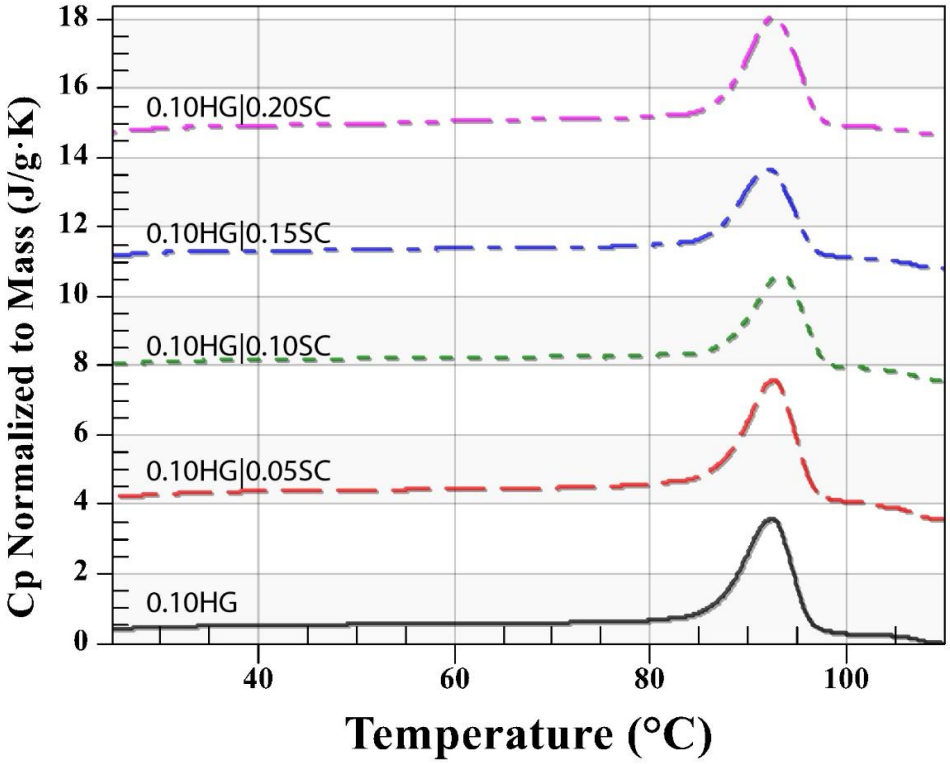

Figure 5-9 DSC result of 0.1HG blended with different amount of SC. All specific heat capacity (Cp) values were normalised to mass (J/g · K).

5.7. Analysis of aggregate composition by 2D PAGE

In HG|SC, κ-casein was the only casein complexed with HG after heat treatment, according to results of 2D SDS-PAGE. The designation of the bands is given on the gel in Figure 5-10. Continuous lines of the two caseins can be observed (Figure 5-10B), which existed because the resolving gel did not gel well so the protein samples flowed out and dispersed all over the gel as presented in Figure 5-10C. The amount of flowed protein solution was not much, so only the most abundant proteins (αS1- and β-casein) could be visualized after staining.

(A)

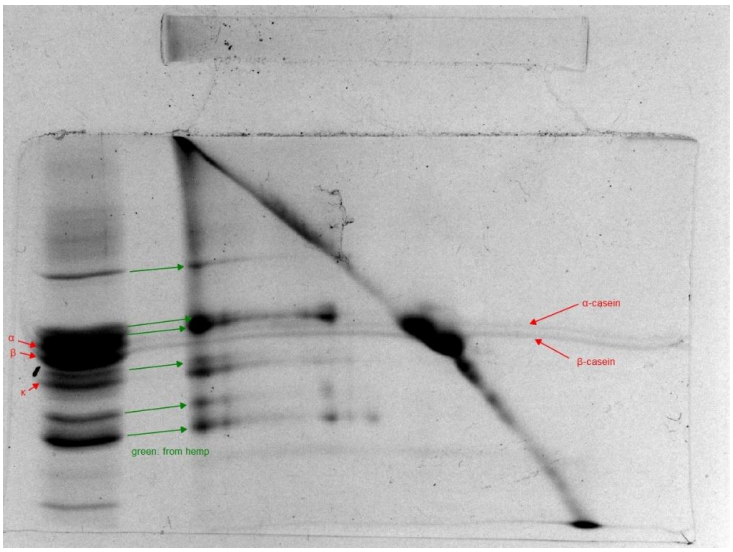

(B)

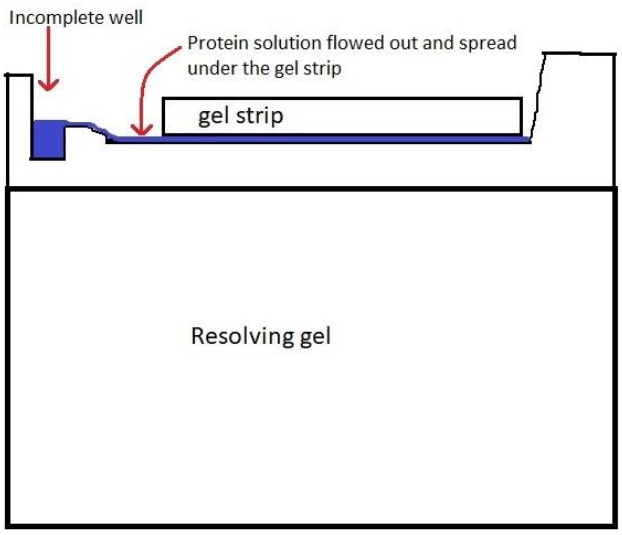

Figure 5-10 (A) Photo and (B) schematic diagram of a 2D SDS-PAGE gel, that confirm the position of αS1- and β- casein bands, which are the continuous lines that existed because the resolving gel did not set properly so the protein samples flowed out and dispersed all over the gel.

Figure 5-11 shows that a smear with high molecular weight in the first dimension (non-reducing, treated with 1% SDS), indicated polydisperse aggregates formed via disulfide linkages. In the second dimension (reduced), the aggregates were separated into κ-casein (band 7 in Figure 5-11), edestin acidic subunits (bands 2 and 3), edestin basic subunits (bands 8 and 9) (Tang et al., 2006), plus other minor HG proteins (bands 2 and 6). On the

other hand, α_{S1}-casein and β-casein were not detected in the aggregates – as there is no cysteine in these caseins they cannot interact through thiol-disulfide exchange reactions, and therefore cannot form intermolecular disulfide bonds.

Since α_{S1}-casein and β-casein were also complexed with HG according to DLS results, it could be concluded that these two caseins complex with HG via non-covalent interactions, which were disrupted by the SDS.

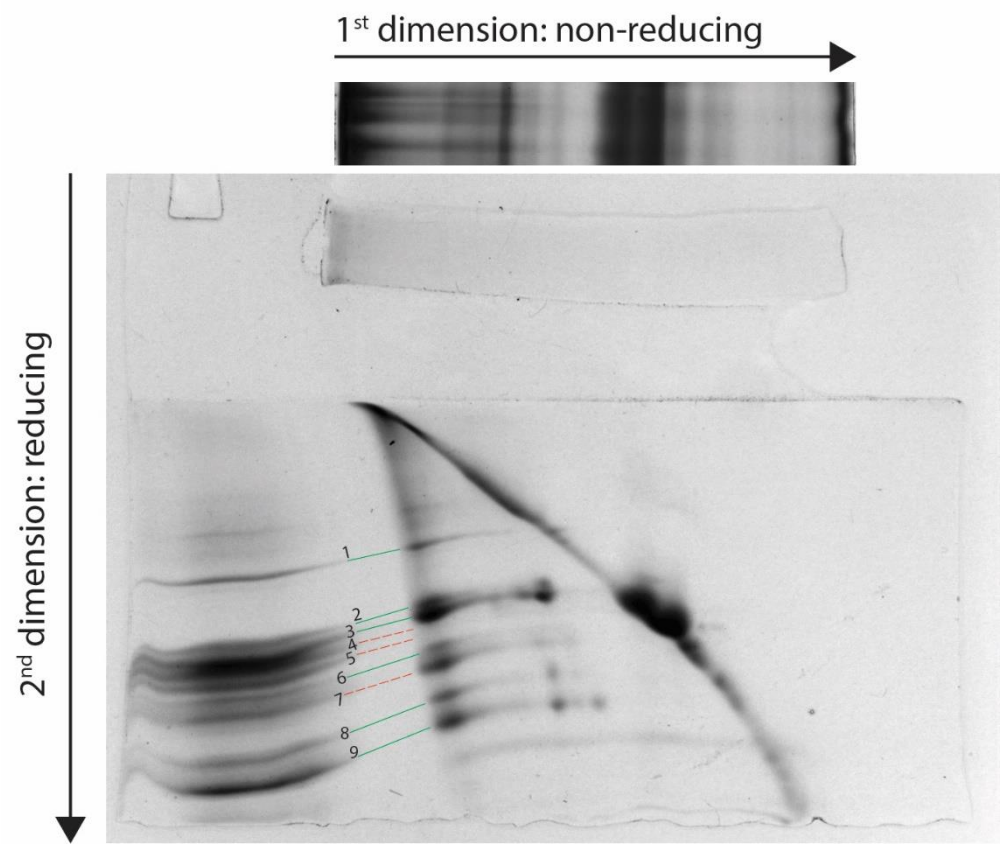

Figure 5-11 2D-PAGE of the heated 0.1HG|0.2SC aggregate, which was held at 90 °C for 30 minutes. The first-dimension gel stripe is shown at the top. Bands 1, 2, 3, 6, 8 and 9 were assigned to HG; bands 2 and 3 were the acidic subunit, and bands 8 and 9 were the basic subunits of edestin. Band 4, 5 and 7 were α_{S1}-, β- and κ-casein respectively.

5.8. Surface hydrophobicity measured by SYPRO Orange fluorescence

Surface hydrophobicity was determined by using SO as the extrinsic fluorescent probe, which becomes highly fluorescent when the environment is non-polar, e.g. when SO binds to the exposed hydrophobic regions of an unfolded protein. Differential scanning fluorimetry (DSF) uses this feature of SO to detect the melting temperature of proteins by monitoring the increase in SO fluorescence signal during a temperature scan. It is also possible to quantify ligand-protein or protein-protein interactions from the change of melting temperature when the protein is blended with another protein or a ligand (Layton & Hellinga, 2011; Niesen et al., 2007).

Table 8 Turbidity (Absorbance$_{600nm}$) of heated 0.1% HG with (30× or 60× dilution) or without SO. Different letters in one column represent significant differences at $p < 0.05$.

SO concentration	Heating time at 90 °C	
	1 min	2 min
No SO	0.29 ± 0.02[a]	0.41 ± 0.02[a]
30×	0.49 ± 0.31[a]	0.47 ± 0.24[a]
60×	0.32 ± 0.04[a]	0.51 ± 0.04[a]

However, it was found to be problematic to quantify protein-protein interactions between HG and SC by DSF, because SC itself had high surface hydrophobicity and SO fluorescence was temperature-dependent. Figure 5-12 shows the SO fluorescence of 0.05% HG and 1-butanol, an organic solvent that provides SO fluorescence (Lakowicz, 2006), both decreased with temperature (20 – 90 °C) during the temperature ramping stage. Therefore, an isothermal heating profile similar to those used in the turbidity experiments

was applied. SO fluorescence was measured either in situ during holding at 90 ˚C, or after heating, holding and cooling to 20 ˚C. Adding SO did not change the turbidity of heated 0.1HG significantly (Table 8), indicating that aggregation was not suppressed by SO. Unheated 0.1% HG had low SO fluorescence at 20 °C, while the 20-fold increase in fluorescence after holding at 90 °C for 10 min (Figure 5-13) may be explained by the exposure of hydrophobic regions after HG denaturation and aggregation. The increase in fluorescence in heat-induced protein aggregates was consistent with previous results using SO or another common fluorescence dye, Bis-ANS (Alizadeh-Pasdar & Li-Chan, 2000; Oshinbolu et al., 2018). The SO fluorescence of unheated SC increased when SC concentration was raised from 0.05% to 0.1%, but SO fluorescence did not increase further at higher concentrations. This phenomenon could be due to the self-assembly of caseins at high ionic strength (HadjSadok et al., 2008; O'Connell, Grinberg, & de Kruif, 2003), which would reduce the exposed hydrophobic regions.

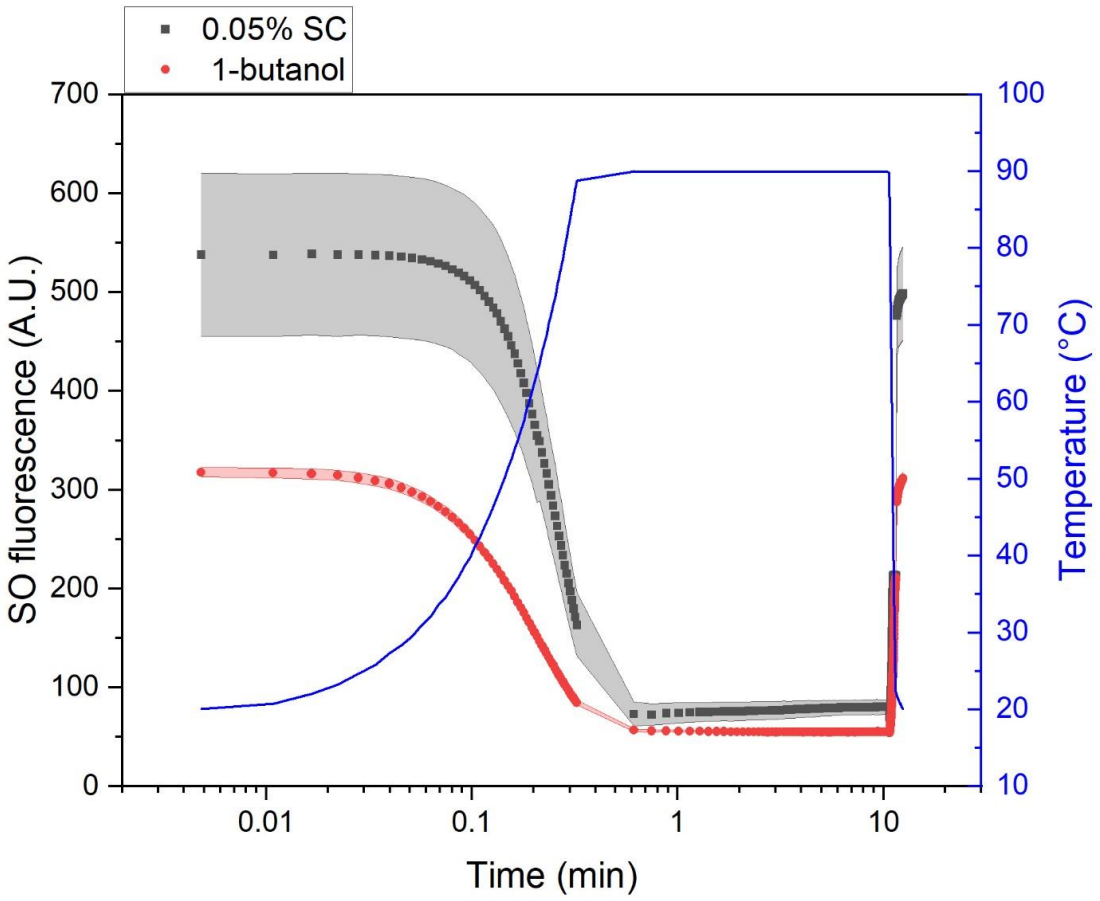

Figure 5-12 SO fluorescence of 0.05% SC and 1-butanol during the heating program in the real-time PCR machine. The left y axis is the intensity of SO fluorescence, and the right y axis is the temperature profile of the heating program. The shaded area represents one standard deviation, n=3.

The caseins in SC may interact with each other during heating, but complexes seem to be unstable and dissociated again after cooling down. Caseins in SC are known to aggregate with each other and form micellar structures during heating (0.3% caseinate, 0.25 M NaCl, 20 – 70 °C), but the aggregation was reversible when temperature was lowered (HadjSadok, Pitkowski, Nicolai, Benyahia, & Moulai-Mostefa, 2008). During the micellar structure formation, the surface hydrophobicity determined by extrinsic fluorescence dye was lowered (O'Connell, Grinberg, & de Kruif, 2003). The fluorescence data of pure SC

were similar after heating (Figure 5-13), suggesting that the complexation between SC-SC complexes was reversible. Surface hydrophobicity of SC solutions did not change significantly after heat treatment due to the random coil structure of caseins.

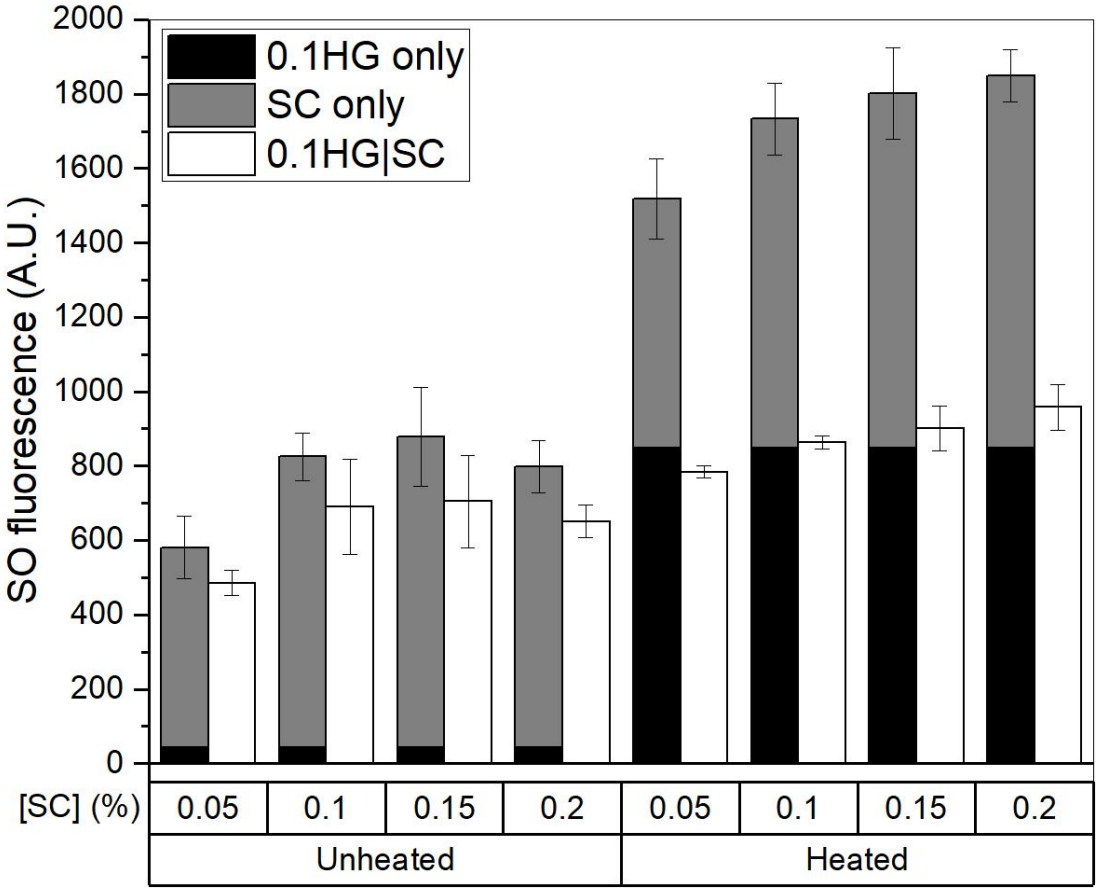

Figure 5-13 The calculated sum of SO fluorescence signal from HG (black bar) and SC (grey bar), or the SO fluorescence of HG|SC blends (white bar) before and after heat treatment (90 °C, 10 minutes). Measurement was performed at 20 °C. Error bars represent one standard deviation, n=3.

There appeared to be hydrophobic interactions between HG and SC after heat treatment. The SO fluorescence of HG|SC was subtracted from the summed values of unblended HG and SC to get the value of ΔSO fluorescence – this value should be close to zero if there

were no interactions, as can be observed in the unheated samples in Figure 5-13. By contrast, ΔSO fluorescence of heated HG|SC samples has high positive values, which may result from the adsorption of SC and desorption of SO from the newly exposed hydrophobic regions of HG during the unfolding process. In other words, SO and SC compete for the available hydrophobic regions of denatured HG. Interactions between SC and the hydrophobic regions of HG seem to be stable, as the ΔSO fluorescence of the blends did not change significantly after 21 h storage at room temperature (Table 9).

Using SO as the fluorescent dye and detecting the signal with a real-time PCR machine made it possible to monitor the change of fluorescence signal during heat treatment in real time. SO fluorescence of 0.1HG increased continuously during 30 min holding at 90 °C (Figure 5-14A), indicating the unfolding of HG and the exposure of the hydrophobic regions. SO fluorescence of SC (0.05% or 0.2%) did not increase significantly at 90 °C. The difference in SO fluorescence between 0.05% and 0.2% SC at 90 °C was more significant than that measured at 20 °C (Figure 5-13), suggesting that SC self-assembly behaviour was different at a higher temperature. Blending SC with HG resulted in positive ΔSO fluorescence, and the value increased with holding time at 90°C. The positive and increasing ΔSO fluorescence indicated adsorption of SC to hydrophobic regions of HG. ΔSO fluorescence was proportional to the SC concentration, suggesting that SC and SO compete for the exposed hydrophobic regions of HG. Incorporating 0.05% SC into 0.1% HG resulted in ΔSO fluorescence that increased over the first 15 min and plateaued at around 80 AU. It may be possible that 0.05 % SC was not enough to interact with all the exposed hydrophobic regions of HG. On the other hand, the ΔSO fluorescence of 0.1HG|0.2SC sample continued to increase with holding time to around 170 AU.

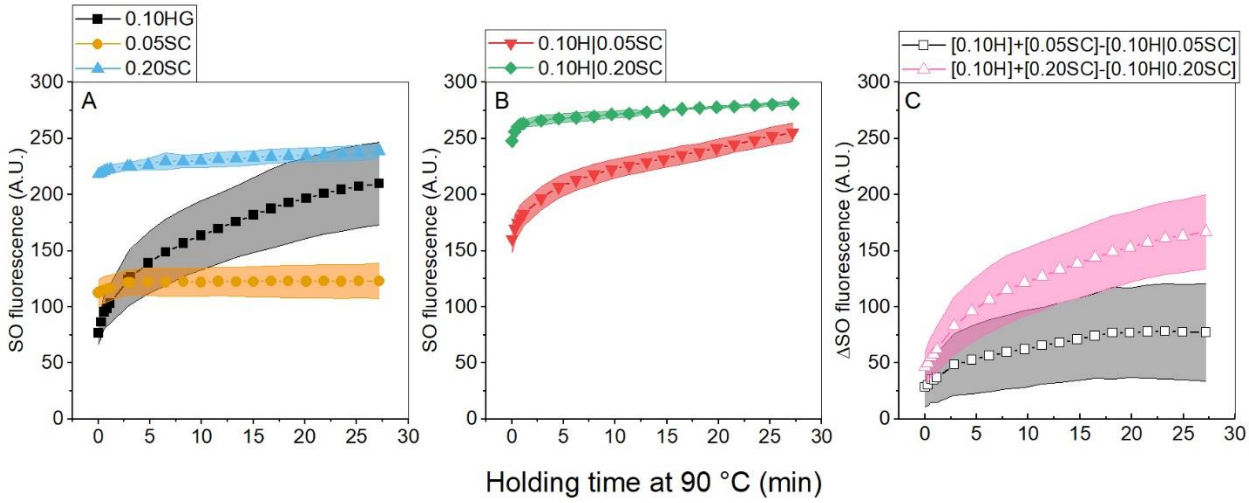

Figure 5-14 SO fluorescence during the holding stage of (A) individual protein solutions, (B) HG|SC blends, and (C) ΔSO value after substracting signal of HG|SC blend from the additive value of HG and SC alone. The shaded area represents one standard deviation, n=3.

Sharifizadeh, Saboury, Moosavi-Movahedi, Salami, and Yousefi (2012) reported similar results of lower fluorescence in the heated blends of bovine carbonic anhydrase and β-casein by measuring the intrinsic fluorescence signal of tryptophan. However, Kehoe and Foegeding (2014) found no apparent difference in the ANS fluorescence signal in heated blends of β-LG and β-casein, i.e. no significant decrease in ΔANS fluorescence after heat treatment. The authors were not sure whether β-casein and β-LG formed a stable complex after cooling (Kehoe & Foegeding, 2011), while the result of ANS fluorescence analysis may have suggested the dissociation of β-LG|β-casein complexes. The positive ΔSO fluorescence at 20 ˚C after heating remained stable over 21 h after heating (Table 9), indicating that HG|SC complexation was persistent. This result is in agreement with the DLS study.

Table 9. Δ SO fluorescence of 0.1% HG with different amount of HG before and after heating at 90 °C for 10 minutes. The Δ SO fluorescence values of heated protein solutions were monitored after 1 and 21 hours of storage. Different letters in one row represent significant differences at $p < 0.05$.

SC concentration for 0.1% HG (%)	Δ SO fluorescence			
	unheated	Heated and after different time of storage		
		0-h	1-h	21-h
0.05	100 ± 50[b]	730 ± 110[a]	730 ± 1230[a]	530 ±310[ab]
0.10	140 ± 150[b]	870 ± 90[a]	950 ± 85[a]	650 ± 190[a]
0.15	170 ± 180[b]	900 ± 80[a]	990 ± 60[a]	850 ± 200[a]
0.20	150 ± 100[b]	890 ± 30[a]	990± 10[a]	900 ± 60[a]

These experiments showed that SC significantly reduced the particle size of heated HG, which was similar to previous studies on SC|whey protein systems (Guyomarc'h et al., 2009; Mounsey & O'Kennedy, 2010). However, the ionic strength used here (0.5 M) was much higher than in these previous studies. High ionic strength is known to weaken the chaperone-like effect of caseins on whey proteins (Kehoe & Foegeding, 2011; Mounsey & O'Kennedy, 2010; O'Kennedy & Mounsey, 2006).

Two hypotheses have been proposed to explain the influence of ionic strength. The first hypothesis is that high ionic strength intensifies the intramolecular interactions in β-lg while weakening the non-covalent interactions between β-lg and caseins, possibly due to the charge screening effect of the salt (Kehoe & Foegeding, 2011). The other hypothesis is that α_{S2}-, β- and κ-casein have reduced solubility in high ionic strength, so there are fewer caseins available to stabilise heated globular protein (Mounsey & O'Kennedy, 2010). The fact that SC can still stabilise HG at such a high ionic strength may be explained by the solubility hypothesis. To make the chaperone-like effect possible, both the substrate globular protein and the caseins must be soluble in the first place. Otherwise, the non-soluble globular proteins would precipitate and aggregate with each other via disulfide bonds during heat treatment. HG aggregates precipitated even when the concentration was as low as 0.033% in 0.17 M ionic strength solutions (Figure 5-2B and 7C), possibly due to structural rearrangement of edestin, as described for soy glycinin (Lakemond et al., 2000). Therefore, it was necessary to raise the ionic strength to solubilise HG first. There was also no problem of insoluble SC because only the soluble SC was taken after centrifugation and filtration.

Under the conditions used here, electrostatic interactions would be reduced by charge-screening effects, both before dilution (ionic strength 0.5 M) and after dilution (0.17 M); hydrogen bonding would also be weak at high temperature of 90 °C. Therefore, thiol/disulfide exchange and hydrophobic interactions should be the main driving forces for the chaperone-like effect between HG and SC. These two interactions may be competitive as proposed by Kehoe and Foegeding (2011) – proteins which contain one or more cysteine residues (edestin, some other HG and κ-casein) aggregate with each other

via thiol/disulfide exchange, while the exposed hydrophobic regions on denatured edestin may interact with amphiphilic α_{S1}-casein and β-casein.

HG was solubilised at ionic strength of 0.5 M, and disulfide-linked primary aggregates formed when the temperature was raised to 90 °C (see the schematic mechanism in Figure 5-15A). Electrostatic repulsive forces between HG primary aggregates would be weak at high ionic strengths, so the further aggregation between the primary aggregates followed the DLCA regime, resulting in large and open amorphous aggregates. When SC was blended with HG, α_{S1}-casein and β-casein would potentially have strong hydrophobic interaction with the denatured HG at 90 °C, because these interactions increase with temperature (Scheraga et al., 1962). This interpretation is supported by the SO fluorescence experiments. HG could form primary aggregates with α_{S1}- and β-caseins, and these caseins brought about steric hindrance between the primary aggregates (Figure 5-15B). Therefore, the steric hindrance lowered the possibility to form new disulfide bonds between primary aggregates, which encouraged a RLCA regime, giving rise to smaller and compact aggregates.

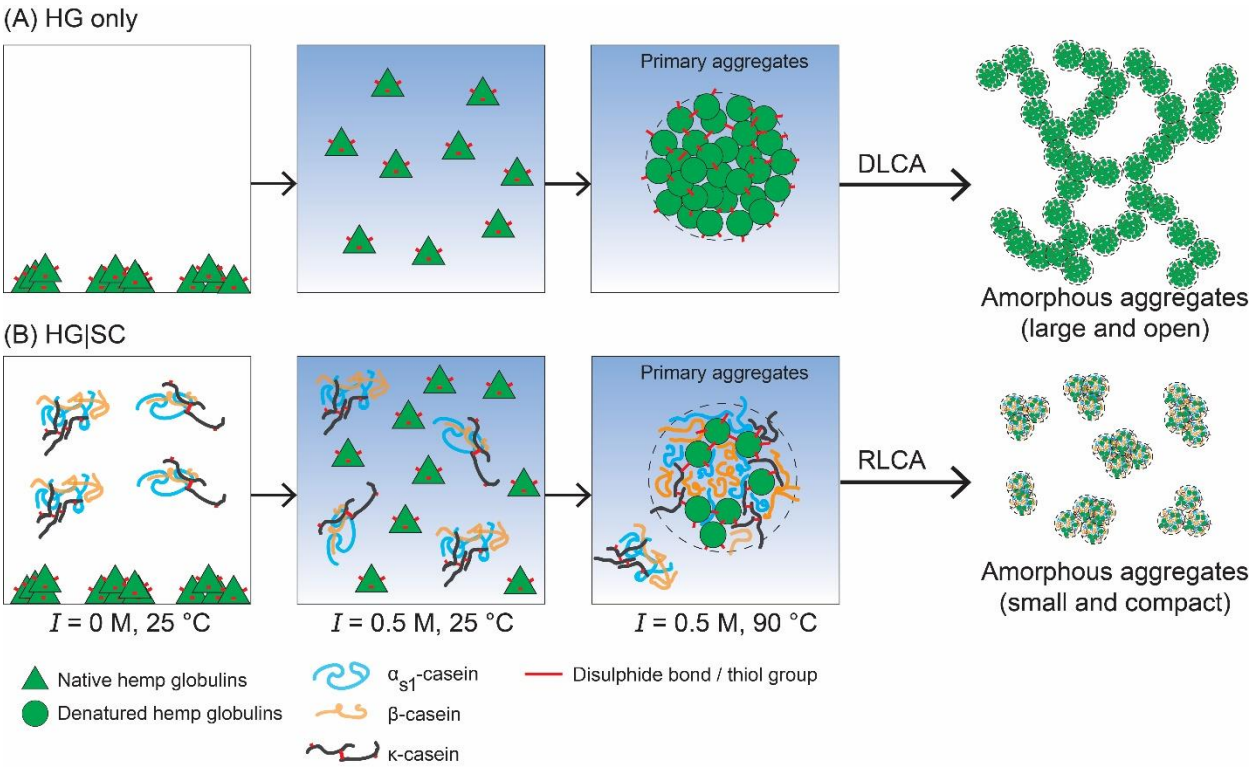

Figure 5-15 Schematic mechanism of heat-induced aggregation of HG (A) without or (B) with the presence of SC

The two cysteine residues in κ-casein can undergo complicated disulfide bonding rearrangement with other κ-caseins, resulting in oligomers consisting up to 10 or more κ-casein monomers (Farrell, Wickham, & Groves, 1998). In 2D PAGE results, the dissociation of high molecular weight aggregates into κ-casein and HG under reducing conditions (Figure 5-11) suggests co-aggregation. These disulfide-cross-linked κ-casein oligomers may co-aggregate with HG via disulfide exchange reactions according to 2D PAGE results (Figure 5-11). Guyomarc'h et al. (2009) suggested a detergent-like role for the glycated hydrophilic portion of κ-casein, encouraging solubilisation in SC|whey blends, and it may play a similar role in the HG|SC blends.

In summary, when HG was blended with SC and heated, caseins self-assembled under elevated temperature and high ionic strength. HG denatured and unfolded when the temperature reached 90 °C, resulting in the exposure of hydrophobic regions and increasing the possibility of thiol/disulfide exchange between HG and κ-casein. At the same time, the exposed hydrophobic regions could interact with α_S- and β- casein via hydrophobic interactions. The caseins provided a steric barrier, decreasing the possibility of thiol/disulfide exchange between HG–HG and HG–κ-casein. Therefore, the aggregation regime shifted from DLCA to RLCA, which produced smaller and more compact aggregates. However, SC did not change the kinetics of HG denaturation. After cooling, the aggregates remained stable.

5.9. Conclusion

This chapter shows that the chaperone-like effect of casein on whey protein stabilisation is also applicable to plant storage proteins. Casein proteins inhibited heat-induced aggregation of HG at high ionic strength by lowering the aggregation rate and changing the aggregation regime from DLCA to RLCA. The reacted HG|SC complexes were smaller and more compact, retaining better colloidal stability even when the ionic strength was lowered. The maximum protein concentration used in this work was 0.3%, which may be applicable to make Pickering emulsions; however, further investigations should be made at higher protein concentrations. It might be possible to raise the concentration of HG|SC complexes by drying or filtration to increase the applicability for the food industry. It is also feasible to apply this method to other plant storage proteins to make protein blends with improved solubility and functionalities.

The results in this chapter may also allow a rational design approach to further experiments. (1) HG must be solubilised first. Possible methods include raising the temperature (below the melting temperature of edestin) and ionic strength as in this chapter. Other methods could be pH adjustment to alkali pH, incorporating surfactants, reducing agent or chaotropic agents. (2) HG has to be denatured. This can be accomplished by adding chemical denaturants. Note that many reagents may cause solubilisation and denaturation simultaneously. Physical methods can also be considered, e.g. heating, mechanical shearing, and high pressure treatment. (3) Induce interactions between HG and SC. Thiol/disulfide exchange can be controlled by temperature and pH. Non-covalent interaction such as hydrophobic, electrostatic interactions can be controlled by temperature, ionic strength and pH. It may be possible to produce HG|SC blends with better functionality by carefully choosing processing methods according to the three requirements.

6. HEMP GLOBULIN FORMS COLLOIDAL NANOCOMPLEXES WITH SODIUM CASEINATE DURING PH-CYCLING

The contents of this chapter have been submitted to a peer-reviewed journal

Chuang, C.-C., Anema, S. G., Ye, A., & Loveday, S. M. (2020). Submitted: Hemp globulin forms colloidal nanocomplexes with sodium caseinate during pH-cycling. Food Research International.

6.1. Introduction

Industrial Hemp (*Cannabis sativa L.*) is a sustainable protein source, which grows well in diverse climates and soil types without herbicides and pesticides (Aluko, 2016). In addition to the classic use of hemp fibre and hemp oil, there is still around 25% protein in the whole hemp seeds and around 34% protein in the hemp seed meal (Callaway, 2004). Hemp seed storage protein contains around 67 – 75 % globulins (7S and 11S) and around 25 – 37% albumins (Aluko, 2016). Hemp protein is easily digested (X.-S. Wang et al., 2008). However, the functionalities of hemp protein are limited due to the low solubility. The solubility in water was less than 10% at pH 7 (Hadnađev et al., 2017), which is lower than other plant proteins such as soy (Tang et al., 2006).

The low solubility is a common problem of plant storage proteins, possibly due to their strong intramolecular interactions, and methods to increase the solubility of these proteins generally involves the destruction of the compact protein structure. Chemical or biological methods such as pH-cycling to partially unfold the protein at alkali or acidic pH (Jiang et al., 2010) and partial enzymatic hydrolysis of protein (Achouri et al., 1998) were successful

in raising the solubility of soy protein. However, these methods alone were not so effective for some other plant proteins with lower solubility, and some harsh processing methods must be used simultaneously. For example, rice protein achieved higher solubility when pH-cycling and freeze-milling were both applied (T. Wang et al., 2015). For hemp protein, it seems that pH-cycling must be combined with heat treatment to increase the solubility of hemp protein, i.e. hemp protein must be heated at alkali pH before neutralisation (Alavi, Emam-Djomeh, & Chen, 2020; Q. Wang, Jin, & Xiong, 2018). The heating step with alkali treatment could result in the toxic product of lysinoalanine. Therefore, the parameters of heat treatment at alkali condition (temperature and time) must be minimised and the highest achievable solubility was around 60% when the lysinoalanine content is controlled within the acceptable level of 1000 ppm.

Another method to solubilise plant protein is to incorporate other stabilisers that interact with the partially unfolded protein and caseinate is an ideal material (Pan & Zhong, 2016). SC is purified by precipitation of milk at its pI (pH 4.6) to separate the insoluble casein fraction from the whey fraction, followed by re-solubilisation of the casein fraction by adjusting the pH to around 7 with sodium hydroxide. The caseins (α_{S1}-, β-, κ- and α_{S2}-casein) in SC have a flexible structure and are rearranged into clusters when reconstituted in water (Haratifar & Guri, 2017). The flexible and amphiphilic nature of caseins are known to show chaperone-like activity to the heat aggregation behaviour of globular proteins such as β-lg (Kehoe & Foegeding, 2014). The chaperone-like effect of caseins was also applicable to hemp protein and the colloidal stability of casein-hemp protein heat aggregates was increased as shown in Chapter 5. In addition to heat treatment, there are other methods to partially unfold plant storage proteins such as using organic solvents (anti-

solvent method), followed by interaction with caseinate before removing the organic solvent by evaporation (A. R. Patel, Bouwens, & Velikov, 2010). Another method is pH-cycling, which had been used together with caseinate to improve the colloidal stability of zein (Pan & Zhong, 2016; Sun, Gao, & Zhong, 2018a, 2018b; L. Wang, Xue, & Zhang, 2019; L. Wang & Zhang, 2017) and rice protein (Tao Wang, Yue, Xu, Wang, & Chen, 2018) by making the zein-casein or rice protein-casein nanoparticles. Zein and rice protein belong to the prolamin and glutelin fractions respectively.

The majority of hemp seed protein belongs to the globulin fraction and no previous study focused on the solubilisation of plant globulin by introducing interactions with caseinate. In this chapter, a simple method was applied to increase the solubility of HG by interacting with SC through a pH-cycling method without heat treatment. The molecular interactions between HG and caseins were analysed.

6.2. Material and methods

6.2.1. *pH-cycling*

HG (1% w/v) and SC (0 – 2% w/v) were dispersed and stirred in deionised water overnight at ambient temperature, with 0.02% sodium azide (w/v) added to inhibit microbial growth. To simplify the nomenclature, the '%' sign is omitted and the '|' sign is used for blends, e.g. the blend of 1.0% HG and 1.0% SC is presented as 1.0HG|1.0SC. It should be noted that such nomenclature only indicates the ratio of the raw protein materials of HG and SC, and the actual quantities of protein can be adjusted by the protein content, e.g. the 1.0HG|1.0SC actually contained 0.90% HG and 0.94% SC. The water, HG and SC dispersions were combined according to designated ratios, and the pH was slowly adjusted

to 12.0 with 1 M NaOH. Preliminary experiments showed that at least 30 min was necessary for the interactions between HG and SC at pH 12.0, so the reaction time was kept at 1 hour. After 1 hour, the pH of protein dispersions was adjusted back to 7.0 with 1 M HCl, and the ionic strength was topped up to 35 mM with 1 M NaCl. The pH-cycled protein dispersions were centrifuged (100, 000 × g, 25 °C, 10 min), and the supernatant and pellet were collected.

6.2.2. *Pre-treatment of HG with NEM*

HG (1% w/v) was stirred and dispersed in water with 0.02% (w/v) sodium azide overnight at ambient temperature. The dispersions were treated with N-ethylmaleimide (NEM, NEM: protein = 9:4 w/w) to block the free thiol groups. The reaction was allowed to react for 2 hours at room temperature. Excess NEM was then removed with dialysis kits (Pur-A-Lyzer Maxi Dialysis Kit, MWCO 12 – 14 kDa, Sigma-Aldrich Co., St. Louis, USA).

6.2.3. *SDS-PAGE*

The composition and amount of proteins were studied by tris-glycine sodium dodecyl sulfate polyacrylamide gel electrophoresis (SDS-PAGE) with precast gels (12% Criterion TGX gels, Bio-Rad, Hercules, CA, USA). The whole portion or the supernatant of HG|SC dispersions was diluted with water and analysed directly, while the insoluble pellet was reconstituted and solubilised with 0.02 M NaOH prior to the SDS-PAGE analysis.

6.2.4. *Dynamic light scattering and ζ-potential measurement*

Particle sizes in the supernatant were measured by DLS using a Zetasizer Nano ZS (Malvern Panalytical Ltd, Worcestershire, UK). PSD measurements were performed at 25

°C, and the measurement angle was fixed at 173°. The refractive index of protein was set at 1.45. Results were represented as volume percentage versus particle size diameter (nm). In situ heating was realised with the built-in temperature control unit of the Zetasizer. The temperature was set between 20 – 90 °C, with seven temperatures steps in between (10.8 °C for each step). The time to reach each target temperature was between 3 to 5 min. Equilibration time of 2 min was applied before each of the 3 measurements after reaching the target temperature. The samples were held at each target temperature for around 7.5 min, including the equilibrium time.

The ζ-potential was measured by laser Doppler electrophoresis in the folded capillary cell DTS1070 with Zetasizer ZS (Malvern Panalytical Ltd, Worcestershire, UK) at 25 °C and with the forward scattering at an angle of 13°. The ζ-potential in this chapter will be referred to as the amount of charge, i.e. higher means more charge/further away from zero and lower means less charge/closer to zero regardless the negative or positive sign.

6.2.5. *Stability against dissociation reagents*

To study the interactions responsible for the formation of HG|SC nanoparticles, various dissociation reagents (1 M NaOH to adjust pH to 12, 20 mM DTT, 8M Urea or 4% Triton X-100) were added to the solutions and stirred for 2 hours at room temperature. Particle sizes were then determined by DLS as described above.

6.2.6. *Intrinsic fluorescence*

Intrinsic fluorescence signal of 0.05%HG, 0.05%SC or 0.05%HG|0.05%SC pH-cycled nanoparticles were measured by Jasco fluorometer FP-6200 (Tokyo, Japan). The excitation

was length was set at 387.0 nm and the emission wavelength was 479 nm. The bandwidth of excitation and emission were 5 nm and 10 nm respectively.

6.3. Results and discussion

6.3.1. *Increased solubility of HG, SDS-PAGE*

The solubility of HG was much higher when HG was mixed with SC and subjected to pH-cycling, during which the pH was raised from 7.0 to 12.0 and reacted for 1 hour, followed by neutralisation back to pH 7.0. Figure 6-1 shows the protein composition of the whole dispersion, supernatant and pellet of the pH-cycled protein dispersions. When there was only HG, almost all proteins were found in the pellet after centrifugation (lane 3, Figure 6-1B). Only a small amount of protein with low molecular weight (< 15 kDa) remained in the supernatant (lane 2, Figure 6-1B). The amount of insoluble protein in the pellet phase decreased with increasing SC content. SC concentration of 0.5% resulted in a translucent supernatant after pH-cycling (Figure 6-2), indicating the formation of small, soluble and colloidally-stable protein particles.

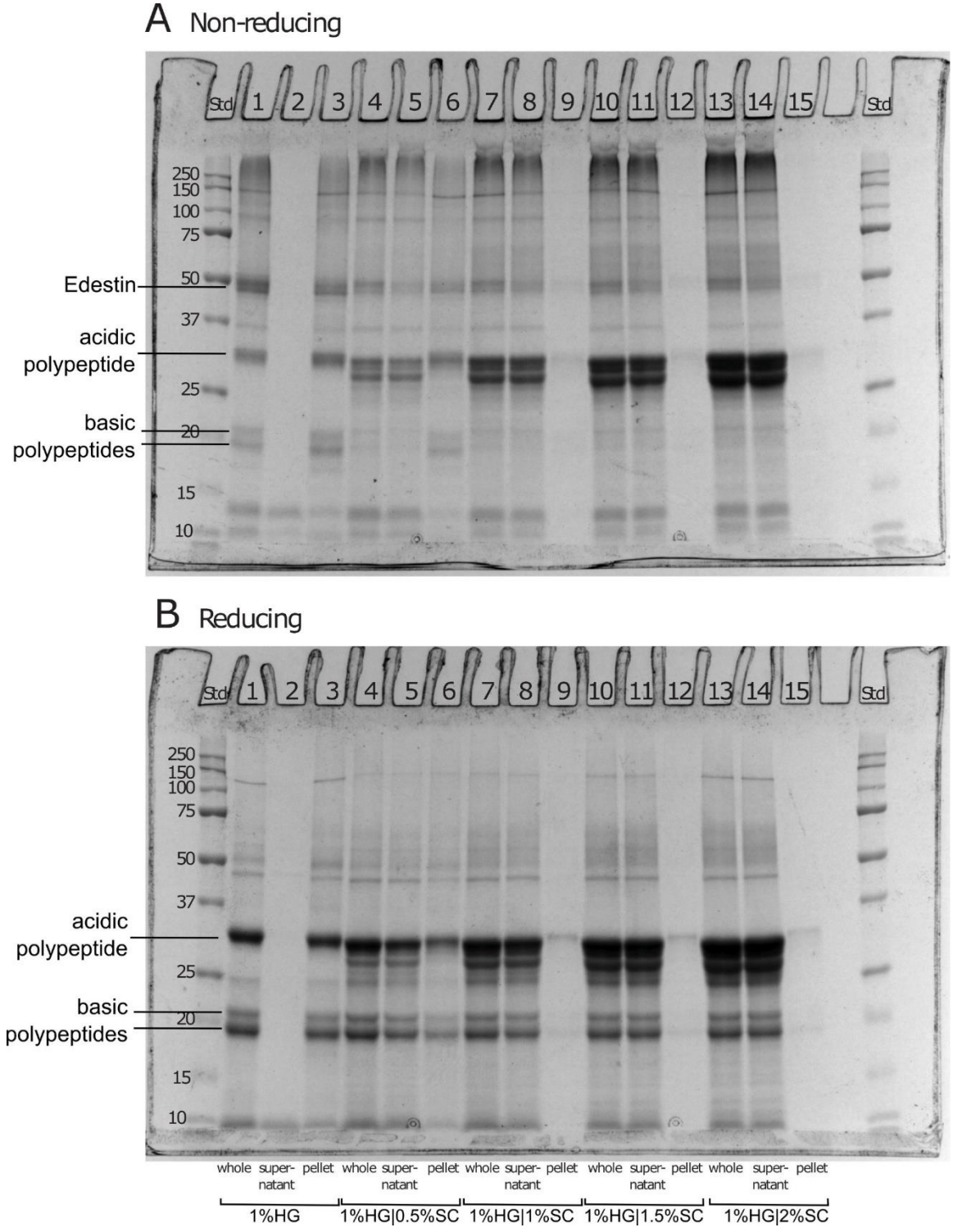

Figure 6-1. SDS-PAGE results of the whole dispersion, supernatant or the pellet (precipitate) after pH-cycling, 1% of HG was reacted alone or with 0.5 – 2% SC. A: non-reducing conditions, B: reducing conditions.

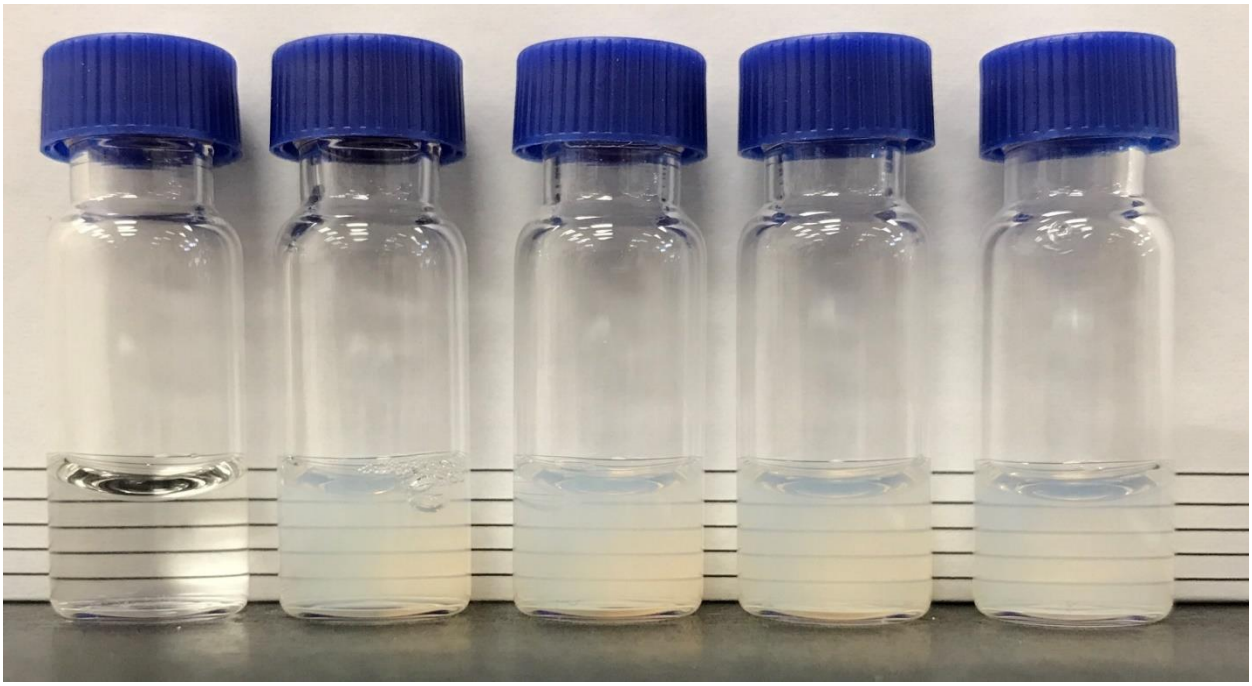

Figure 6-2. Photo of supernatants of HG|SC dispersions after pH-cycling with different SC ratio, from left to right: 0% SC, 0.5% SC, 1.0% SC, 1.5% SC and 2% SC.

The increase in the solubility of HG depended on the amount of SC, and a 1 to 1 ratio between HG and SC achieved optimal solubility of HG, whereas SC was very soluble. What stands out in the SDS-PAGE results is that the protein in the pellet after centrifugation mostly belonged to HG. Therefore, the amount of insoluble HG in the precipitate was measured by the BCA method and compared with the original HG content to calculate the solubility of HG after pH cycling. Pure HG became totally insoluble after pH-cycling (Figure 6-3), which was even less than the 20% solubility of untreated salt-extracted HG (Figure 4-6), indicating some HG-HG interactions were occurring during pH-cycling, which will be discussed in the following sections. The solubility of HG after pH-cycling was also inferior to previously reported results, which showed HG was still around 15% soluble after pH-cycling (Q. Wang et al., 2018). The difference may be due to

different protein extraction method. HG in this project was extracted by a salt solution, while the previous study used an isoelectric precipitation method.

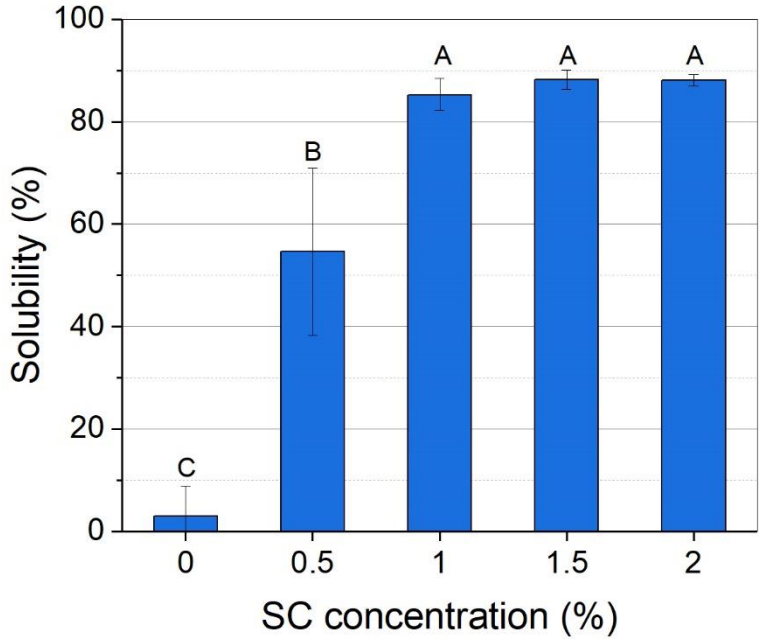

Figure 6-3. The solubility of HG when the different concentration of SC was incorporated and underwent pH-cycling (n = 3). The 100% solubility equals to 8.96 mg/mL of HG. The error bars represent one standard deviation and different letters in the graph indicate significant difference between groups ($p < 0.05$).

Figure 6-3 also shows that > 80% of HG could be solubilised after the pH-cycling process when there was ≥ 1% SC and adding more SC did not increase the solubility further. Although SC had been shown to increase the solubility of insoluble plant storage proteins with a pH-cycling process, only one study measured the improvement of solubility of plant proteins (T. Wang, M. Yue, et al., 2018) and the authors reported that 1% rice protein (glutelins fraction, which is alkali-soluble) need only 0.01% of SC to achieve 90% solubility after pH-cycling. The results indicate that although the effect of increasing solubility when incorporating SC and pH-cycling may be universal for plant storage

protein, the amount of SC needed depends on the nature of the target plant protein, possibly due to different amino acid composition and different extents of intra-molecular interactions.

Preliminary results showed that at least 30 min of reaction time was necessary to make soluble HG|SC nanoparticles (Figure 6-4A – D). It could be that HG needs time to dissolve or the reaction between HG and SC needs time. Unlike rice protein (R. Wang, Xu, Chen, Zhou, & Wang, 2019), HG does not form soluble aggregates with WPI (Figure 6-4E). HG either does not interact with WPI or interacts extensively via thiol-disulfide exchange reactions, leading to the formation of large insoluble aggregates. On the other hand, HG and pure β-casein interacted and formed soluble aggregates after pH-cycling (Figure 6-4F). Since there are no cysteine residues in β-casein, the formation of disulfide bonds is not expected. Instead, non-covalent interactions contribute to the stabilising effect of SC and β-casein to HG after pH-cycling.

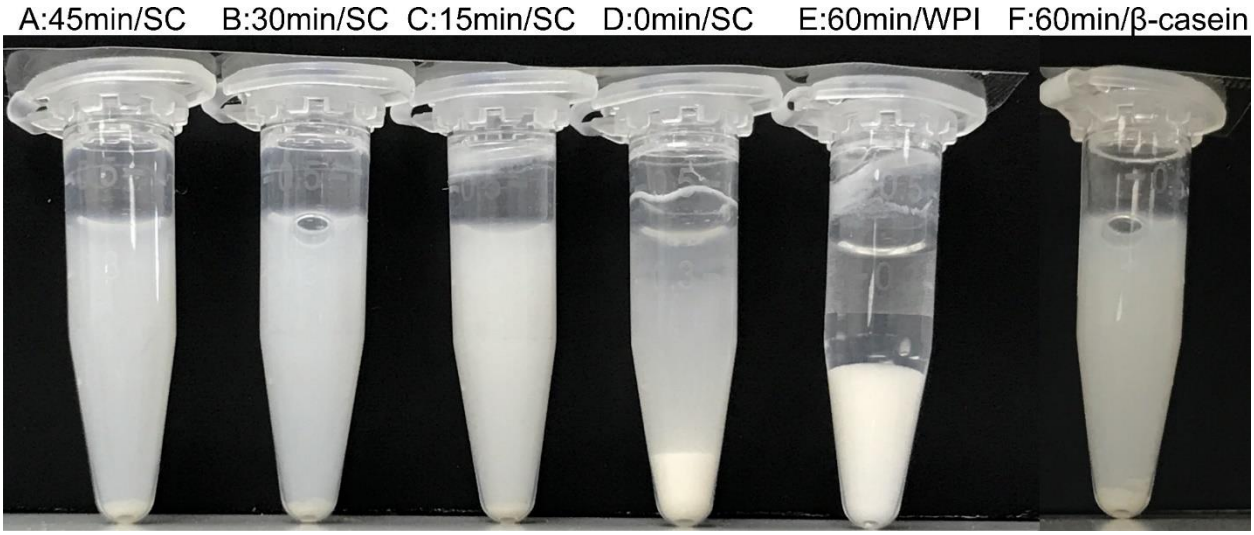

Figure 6-4. (A – D) pH-cycled dispersions of HG|SC with different reaction times at pH 12, and HG reacted with (E) WPI or (F) β-casein at pH 12 for 60 min.

6.3.2. *Characterisation of the HG|SC nanoparticles by DLS*

Soluble HG|SC nanoparticles were formed when there was more than 1% of SC for 1% of HG, and these HG|SC nanoparticles had similar characteristics. Similar particles size (z-average ≈ 130 nm), DCR, polydispersity index (PDI < 0.17) and ζ-potential (≈ -17 mV) were observed, as shown in Table 10.

Table 10. DLS results of non-pH-cycled SC and pH-cycled HG|SC nanoparticles with different ratio of SC (n=7,* except n=4 for 1.0HG|0.5SC complex). Values with different letters are significantly different ($p < 0.05$).

	z-average (nm)	DCR (kcps)	PDI	ζ-potential (mV)
2% SC (no pH cycling)	210 ± 35^{a}	$(0.10 \pm 0.05) \times 10^{5\,b}$	0.56 ± 0.09^{a}	NA
1.0HG|0.5SC*	210 ± 190^{a}	$(1.2 \pm 0.7) \times 10^{5\,a}$	0.22 ± 0.22^{b}	-7.9 ± 3.6^{a}
1.0HG|1.0SC	132 ± 29^{a}	$(1.0 \pm 0.4) \times 10^{5\,a}$	0.12 ± 0.03^{c}	-17.4 ± 2.5^{b}
1.0HG|1.5SC	128 ± 18^{a}	$(1.1 \pm 0.2) \times 10^{5\,a}$	0.14 ± 0.05^{bc}	-17.5 ± 0.8^{b}
1.0HG|2.0SC	133 ± 11^{a}	$(1.0 \pm 0.4) \times 10^{5\,a}$	0.16 ± 0.07^{bc}	-16.7 ± 1.1^{b}

The ζ-potential of pure SC was reported to be -28 mV at pH 7 (Ye, Flanagan, & Singh, 2006). The ζ-potential of 1.0HG|0.5SC nanoparticles at pH 7 (≈ -8 mV) was lower than that of HG|SC nanoparticles with more than 1% of SC (≈ -17 mV). The lower ζ-potential indicates lower surface charge, which may be the reason for its lower solubility (Figure 6-3) and the higher amount of residual edestin in the pellet phase (lane 6 in Figure 6-1B).

It was not possible to measure ζ-potential in pH-cycled HG-only solutions due to extremely low solubility. However, a more dilute solutions of HG (0.16% w/v) revealed ζ-potential of only -4 to -6 mV (Table 7), which is insufficient to counteract intermolecular attraction

due to hydrophobic interactions and van der Waals forces. A possible explanation for results seen with 1.0HG|0.5SC is that 0.5% of SC was not enough to interact with the partially unfolded HG at pH 12, so the HG without enough SC complexation remained insoluble when the pH was adjusted back to 7. The lower surface charge of 1HG|0.5SC nanoparticles also suggested the negatively charged part of SC was on the surface of these nanoparticles. When SC was increased from 0.5% to above 1% the magnitude of ζ-potential increased and provided electrostatic repulsion that solubilises the protein particles. Nevertheless, the ζ-potential of around -17 mV was lower than the surface charge (< -30 mV) of other nanoparticles produced by a pH-cycling method made with other plant storage protein (zein or rice protein) and caseins (Pan & Zhong, 2016; Sun et al., 2018a; T. Wang, M. Yue, et al., 2018). It is believed that at least -30 mV was necessary to give medium stability (Salopek et al., 1992), while these HG|SC nanoparticles with only ≈ -17 mV surface charge were still stable, indicating other stabilising mechanisms exist. SC may provide not only electrostatic repulsions but also gave extra steric hindrance that contributes to the stability of HG|SC nanoparticles.

Since HG refolded into totally insoluble aggregates after the pH-cycling and the SC micelles (association of flexible caseins) dissociated and re-associated after pH-cycling (Figure 6-5), it could be inferred that the pH-cycled HG|SC nanoparticles are composed of rigid HG aggregates and flexible caseins. The HG|SC nanoparticles (1.0HG|1.0SC, 1.0HG|1.5SC and 1.0HG|2.0SC) had similar z-average sizes, DCR (Table 10) and constant HG concentration of 1%, suggesting that each HG|SC nanoparticle have the same amount of HG and different amounts of SC. The insensitivity on the z-average of HG|SC nanoparticles to the SC content from 1.0 - 2.0% SC may suggest that all interaction sites

on HG are saturated with SC, and the excess SC remained free in the solution. And any effect of free SC on Zetasizer measurements is apparently swamped by 10-fold greater scattering from HG|SC particles.

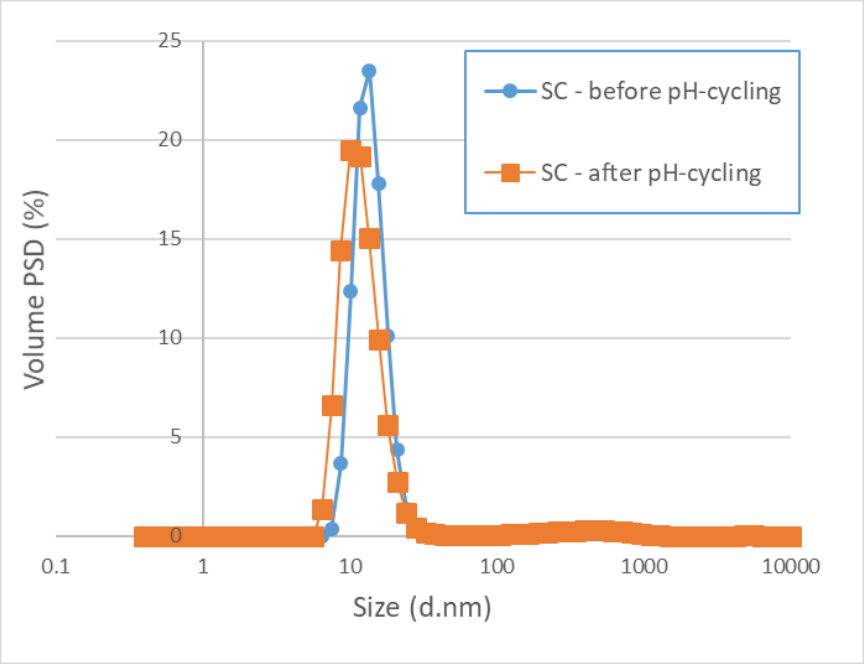

Figure 6-5. Volumetric PSD of SC before or after pH-cycling.

HG|SC nanoparticles do not precipitate at alkaline pH. HG|SC nanoparticles still had ζ-potential s of around -17 mV when the pH was > 5, reached 0 mV between 4.0 and 4.5 and became positive when below pH 4 (Figure 6-6A). However, the visible precipitate can already be observed at pH 6 (Figure 6-6B), and the precipitation became more significant when the pH was further adjusted down. The particles were entirely precipitated at pH 4 and 4.5 because the supernatant was clear, and the particles could be partially solubilised again below pH 3. The full precipitation between pH 4 and 4.5 was expected because HG

and SC both had a pI and lowest solubility at around pH 4 (Jahaniaval, Kakuda, Abraham, & Marcone, 2000; Malomo et al., 2014).

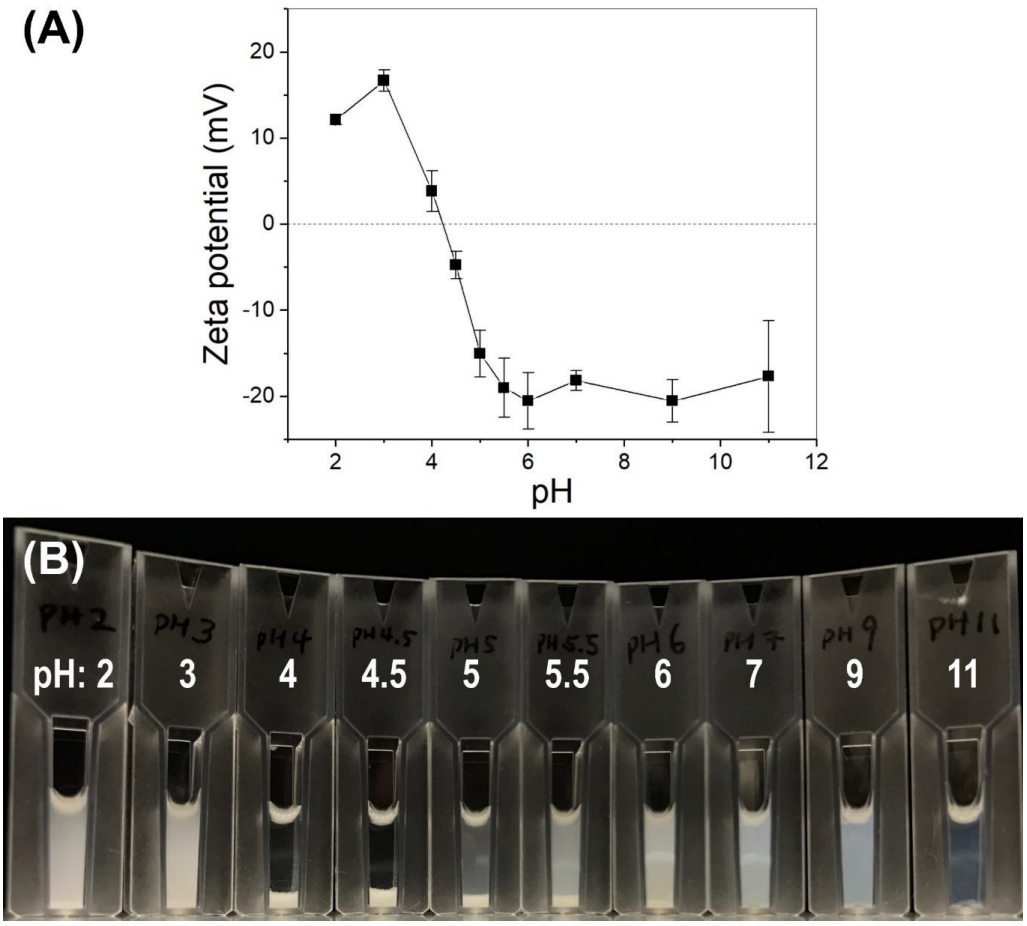

Figure 6-6. (A) Z-potential of 1HG|1SC nanoparticles at different pH (n = 3). The error bars represent one standard deviation. (B) the appearance of 1HG|1SC nanoparticles at different pH.

6.3.3. *In situ heating during DLS*

The size and aggregation behaviour of HG|SC particles changed with temperature. Figure 6-7 shows that the z-average size throughout the in-situ heating during DLS measurement (ionic strength = 35 mM, pH 7). Another parameter, DCR is shown in Figure 6-7B. DCR reflect the scattering intensity, which represents the particle number and/or size (Loveday et al., 2013). Hoverer, DCR obtained at one fixed angle in DLS can only be used as a

sensitive indicator of aggregation or dissociation, because it is susceptible to many factors such as the change in size and refractive index, which alter the scattering angle distribution and thus the count rate will also change (Kurzhals, Zirbs, & Reimhult, 2015).

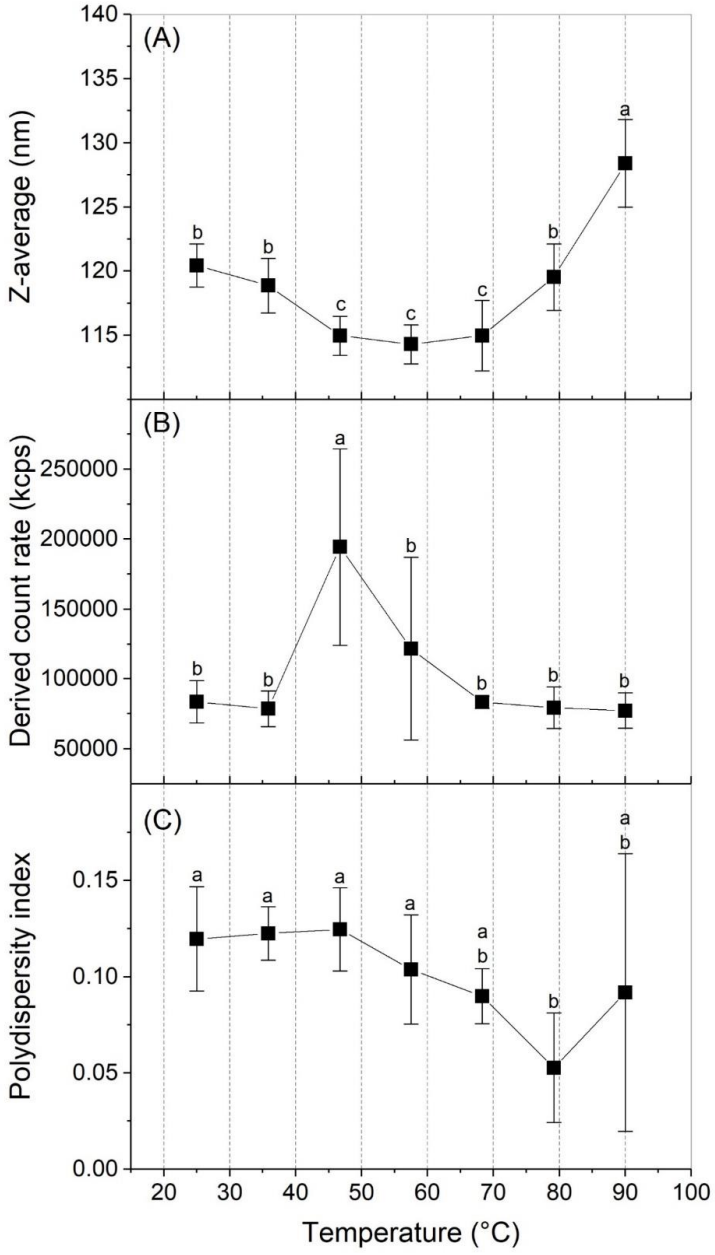

Figure 6-7. (A) z-average size, (B) DCR and (C) polydispersity index of 1HG|1SC particles during in-situ heating at different temperature (n=3). The error bars represent one standard deviation and different letters in each graph indicate significant difference between groups ($p < 0.05$).

The most interesting aspect of Figure 6-7 is that DCR and z-average changed concurrently with increasing temperature, and three temperature regions can be identified. At ambient/low temperature (20 – 40 °C), a constant value of DCR (≈ 80000 kcps) and z-average (≈ 120 nm) were observed. When the temperature was increased to 40 – 60 °C, the DCR increased significantly, indicating aggregation or dissociation happened, and it could be dissociation because the z-average decreased slightly and the polydispersity index hardly changed. The dissociation resulted in the formation of smaller aggregates as the average size decreased. DCR changed again when the temperature was raised further to 60 – 90 °C, suggesting aggregation of HG|SC particles because the z-average kept increasing with increasing temperature. The polydispersity index was significantly lower at 79.2 °C than at other temperatures (Figure 6-7C), indicating a more monodisperse population of the aggregates.

During the heat treatment, hydrogen bonds and disulfide bonds are all responsible for the aggregation/dissociation of the HG|SC nanoparticles. The dissociation of HG|SC nanoparticles between 40 – 60 °C shows that the complexation between HG and SC was non-covalent in nature, and hydrogen bonds could be the dominant force stabilising the HG|SC complex. Hydrogen bonding is one of the non-covalent attractive interactions that has reduced strength at the higher temperature (Bryant & McClements, 1998; Cordier & Grzesiek, 2002). Another possible attractive force had higher strength at higher temperature is electrostatic interactions. However, the complexation is not originated from electrostatic interactions because HG and SC both had a similar pI at around pH 4, as mentioned before, so they should both possess negative charge at pH 7 and therefore no

electrostatic attractions between them. The attractive hydrophobic interactions, which increased with temperature up to around 140 °C (Schellman, 1997; Scheraga et al., 1962), was weak and cannot compensate the disruption of hydrogen bonds to stop the dissociation of HG|SC nanoparticles. The dissociated protein particles aggregated again above 60 °C because the DCR changed, and z-average started to increase. The heat-induced aggregation involved in strong attractive forces because the aggregation was not reversible when the temperature was lowered again (data not shown), and it could be covalent linkages or extensive non-covalent interactions. The permanent aggregation could result from the formation of disulfide bonds, as thiol-disulfide exchange at elevated temperature is prevalent in food proteins (Visschers & De Jongh, 2005). In spite of the non-reversible heat-induced aggregation, these protein particles are quite heat-stable. In another experiment, HG|SC particles were heated at 90 °C for 30 min and the z-average increased from 120 nm to 229 nm (Figure 6-8A), while HG alone aggregated and precipitated in less than one minute at 90 °C even when they were solubilised at an ionic strength of 0.5 M (Figure 5-2A). In other words, HG|SC particles underwent limited heat-induced aggregation (increase in particle size), but aggregation was not sufficient to diminish colloidal stability, indicating that these protein particles are relatively heat-stable.

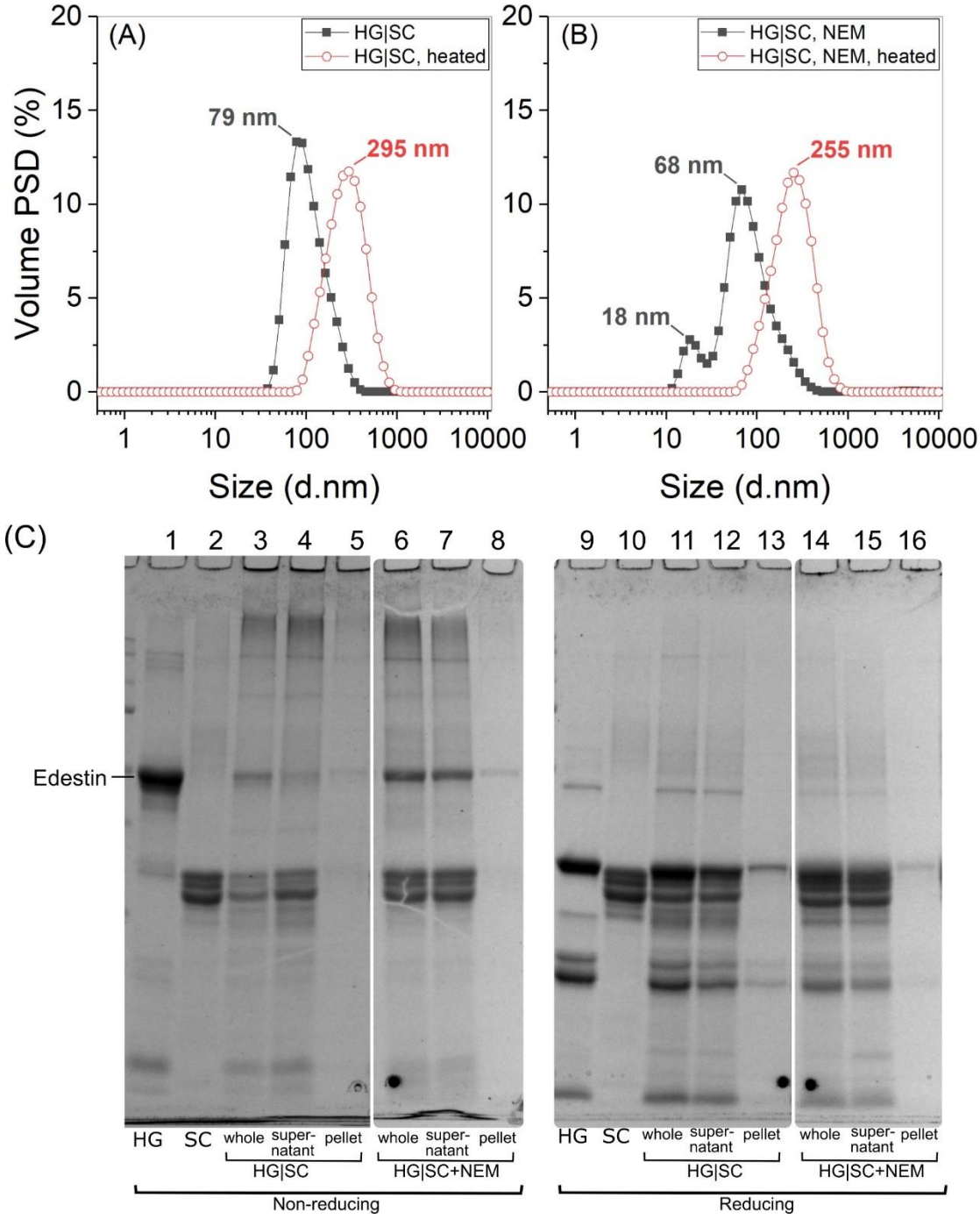

Figure 6-8. (A) Volumetric PSD of unheated and heated HG|SC nanoparticles and (B) PSD when HG was pre-treated with NEM. (C) SDS-PAGE results of the two samples.

Another interesting finding is that the change of z-average with temperature was not as marked as the change of DCR. DCR increased by around 3 times when the temperature was increased from 40 – 60 °C, an indication of extensive aggregation or dissociation, while the z-average decreased by only around 3%. The insensitivity might again suggest that HG|SC nanoparticles are not solid, so the dissociation did not change the hydrodynamic radius of the aggregates. They may have a hairy or star-like structure, as mentioned in the DLS results. The extra steric hindrance between particles may explain the high stability of these nanoparticles at 90 °C.

6.3.4. *Stability of HG|SC nanoparticles against different dissociation reagents*

In order to identify intra-particle interactions during the formation of protein particles, different dissociation reagents were applied to the HG|SC nanoparticle dispersion. The change in particle size was also determined by DLS.

The complexation between HG and SC during the second step of pH-cycling (from pH 12 to 7) was partially reversible. HG|SC dispersion became clear after adjusting the pH back to 12 with NaOH (Figure 6-9A), indicating the partial dissociation of HG|SC particles. The dissociation can be confirmed by the change of volumetric PSD (Figure 6-9B), the 122-nm population (HG|SC nanoparticle) split into two peaks – a dissociated 28-nm population and a 342-nm population that cannot be dissociated by alkali. At pH 12, both HG and SC possess negative charges, and it could be that the electrostatic repulsions became strong enough to break the non-covalent attractive interactions that hold the structure of HG|SC complexes. Therefore, the HG|SC complex was dissociated, and a population with a size around 28 nm was formed. On the other hand, the 342-nm population may present some

protein complexes that were held by strong attractive forces (either non-covalent or covalent) and could withstand the strong electrostatic repulsive forces at pH 12.

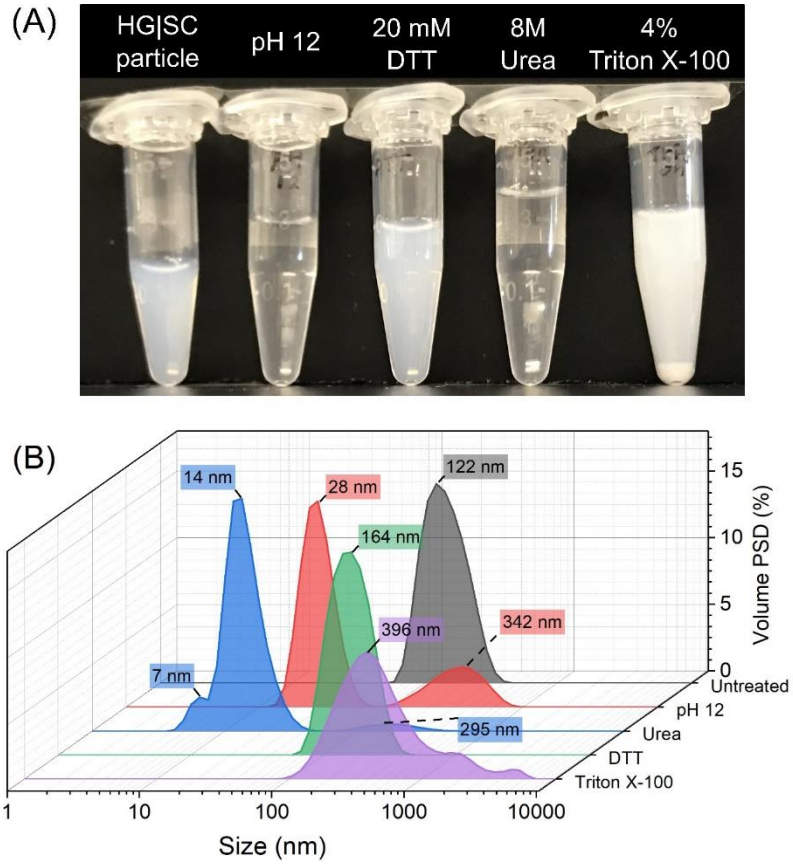

Figure 6-9 (A) Photo of HG|SC nanoparticle dispersions treated with different dissociation reagents and (B) their volumetric PSD in diameter determined by DLS.

The interaction that holds the structure of HG|SC complexes is most likely hydrogen bonds. Urea is a strong hydrogen bond breaker, which resulted in clear HG|SC dispersion as well (Figure 6-9A). The DLS results show that 8 M urea was more potent to dissociate HG|SC complexes than the pH 12 alkali treatment. The major populations with the size of 7 nm and 14 nm are smaller than the particles in alkali-treated samples. Despite the strong dissociation effect, there was still a small fraction of large particles (20 – 70 nm and ≈ 295 nm), which are larger than the size of native HG and SC. These aggregates may be

complexes held by covalent bonds as discussed in the next section. The importance of hydrogen bond observed here was consistent literature reports on rice – soy protein nanoparticles which were also made by pH-cycling, and showed that the formation of composite particles was inhibited when urea was added during the pH 12 treatment (Tao Wang, Xu, Chen, & Wang, 2018; Tao Wang, Xu, Chen, Zhou, & Wang, 2018).

Disulfide bonds are not essential or not solvent-accessible because there was no significant difference in the visual appearance and volumetric PSD between the DTT-treated samples and HG|SC nanoparticles. Hydrophobic interaction is not critical to the formation of HG|SC nanoparticles because no dissociation was observed when reagents that disrupt hydrophobic bonding (Triton X-100) were added to the nanoparticles. Instead, Triton X-100 caused aggregation and precipitation, which can be observed in both the photo and DLS results (Figure 6-9). The aggregation might result from depletion flocculation caused by excess Triton X-100 micelles (Alexeev et al., 1996).

6.3.5. *Intrinsic fluorescence*

Plant storage proteins are known to be partially denatured and turned into the molten globular state during and after the alkaline treatment (Jiang et al., 2009), which results in the exposure of previously-buried hydrophobic side chains and the increase in intrinsic fluorescence signal from tryptophan residues. Figure 6-10 shows the experimental value of intrinsic fluorescence of the HG|SC nanoparticles and the theoretical value that was the sum of HG and SC signals. The experimental value was lower than the theoretical value at pH 12. At pH 12, HG turned into the molten globular state, and SC nano-aggregates are dissociated (Pan, Luo, Gan, Baek, & Zhong, 2014), so they can interact with each other via

non-covalent interactions. The interactions resulted in the quenching of the intrinsic fluorescence, indicating that the exposed tryptophan residues of HG were in close contact with SC, so the polarity around tryptophan residues increased. Such interactions were kept even after neutralisation, as the experimental value of intrinsic fluorescence was still lower than the theoretical value at pH 7. Another interesting point is that the fluorescence signal was higher when the pH was adjusted back to 7 than at pH 12, which may indicate the refolding of HG|SC complexes into higher-order conformations (T. Wang, P. Xu, Z. Chen, & R. Wang, 2018).

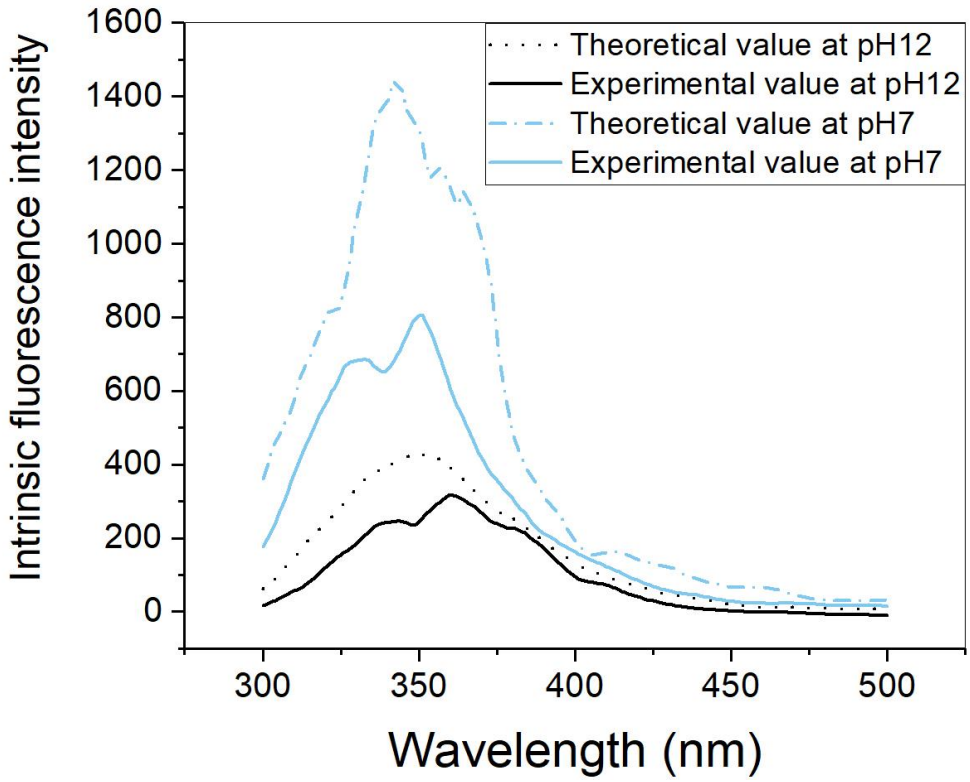

Figure 6-10. Intrinsic fluorescence of HG|SC complex or their additive value.

6.3.6. *Formation and breakage of disulphide bonds during pH-cycling*

The formation of disulfide bonds has been reported for pH-cycled plant storage proteins (Jiang et al., 2009), but it was overlooked in the previous studies when SC was incorporated with plant storage proteins during pH-cycling. To study the effect of disulfide bonds, HG was pre-treated with NEM to block the free thiol groups and thus prevent sulfhydryl oxidation or thiol-disulfide exchange.

NEM pre-treatment of HG reduced the size and amount of aggregates. The number of large aggregates that could not enter the stacking gel and stuck on the bottom of loading well had higher intensity in the sample without NEM treatment (lane 4 in Figure 6-8C) than the one pre-treated with NEM (lane 7 in Figure 6-8C). These large aggregates resulted from disulfide linkages between cysteine-containing proteins (mainly edestin and κ-casein), as they dissociated after reducing (lane 12 in in Figure 6-8C). Interestingly, there was much more intact edestin in the supernatant of the NEM-treated HG|SC nanoparticles (lane 7 in Figure 6-8C) than the non-treated one (lane 4 in Figure 6-8C). This result also shows that less edestin was aggregated via disulfide bonds.

The reduction of the size of disulfide-linked aggregates resulted in smaller HG|SC nanoparticles. Figure 6-8A shows that unheated HG|SC nanoparticles were monomodal and had a peak at 79 nm. The NEM-treated one was bimodal – one small peak centred at 18 nm and another peak at 68 nm (Figure 6-8B). The 18-nm population might be HG|SC nanoparticles because HG itself cannot be solubilised after pH-cycling (lane 2 in Figure 6-1A).

Alkali treatment of proteins is also known to cause the breakdown of disulfide bonds, which had been reported in the HG treated with dilute alkali solution at room temperature (Q. Wang et al., 2018). Part of HG did dissociate into acidic and basic polypeptides after the pH-cycling when there was no SC (lane 1 in Figure 6-1A). SC seems to be able to induce the thiol-disulfide exchange between these dissociated polypeptides, as no acidic polypeptide and only faint basic polypeptide bands can be observed when there was more than 0.5% SC in the whole dispersion (lane 4, 7, 10 and 13 in Figure 6-1A).

6.3.7. *The proposed mechanism on the formation of HG|SC nanoparticles*

With all the result shown above, a modified mechanism for the formation of HG|SC nanoparticles is proposed, involving the degradation and formation of disulfide bonds. HG is insoluble and precipitates when dispersed in water, while SC is known to form soluble micellar-like structures (Figure 6-11A). If HG alone is present, HG would dissolve at pH 12 and turn into the molten globular state (Figure 6-11B1). This HG undergoes two reactions: (1) dissociation of disulfide bonds of edestin into acidic (30 kDa) and basic (18 and 20 kDa) polypeptides and (2) thiol-disulfide interchange to form disulfide-linked aggregates. When the pH was adjusted back to 7, these aggregates (made mainly from edestin and its polypeptides) refolded into non-soluble precipitates due to strong hydrogen bonding (Figure 6-11B2), and these aggregates have lower solubility than the non-pH-cycled HG.

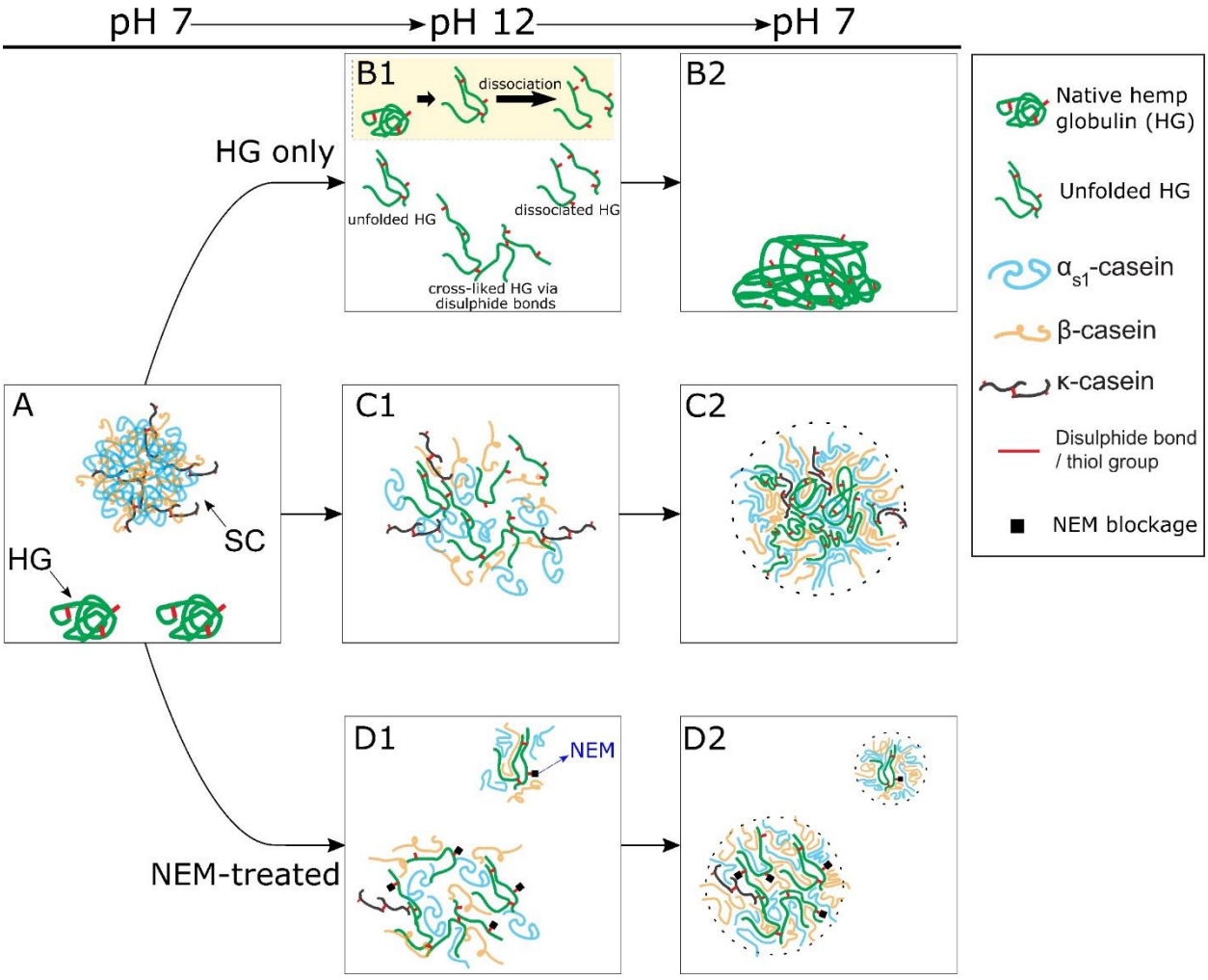

Figure 6-11. Proposed mechanism of HG, HG|SC and NEM pre-treated HG|SC after pH-cycling. (A) HG and SC dispersed in water at pH 7, and pH-cycling for (B1 – B2) solely HG, (C1 – C2) HG and SC, and (D1 – D2) HG pre-treated with NEM and SC.

When SC was mixed with HG at pH 12, the partial degradation of disulfide bonds in edestin and thiol-disulfide exchange takes place simultaneously. This enables the formation of disulfide-linked chains or aggregates between proteins with cysteine residues (edestin, its polypeptides and κ-casein). The covalently bound aggregates are stable even when treated with urea, and act as a template or backbone to interact with other caseins (α_{S1}- and β-

casein) via non-covalent interactions. The intrinsic fluorescence of unfolded HG was quenched due to these non-covalent interactions (Figure 6-11C1). When the pH was lowered to 7, the backbone made mainly of edestin refolds and SC was incorporated, due to the loss of repulsive charge and the strong, attractive forces from hydrogen bonding (Figure 6-11C2). Part of SC is exposed to the solvent after neutralisation, providing electrostatic repulsion and steric hindrance to stabilise the water-soluble particles. The HG|SC nanoparticles were monodisperse and stable.

When HG was pre-treated with NEM, most of the free thiol groups were blocked. Therefore, the thiol-disulfide exchange between HG and other proteins was reduced, resulting in smaller covalently-bound aggregates and much more individual edestin molecules. However, there are still some unblocked thiol groups that were not accessible to NEM, due to the compact globular structure of HG. Therefore, the thiol-disulfide exchange could still occur to some extent, and smaller disulfide-linked chains are formed due to the lower amount of free thiol groups. The polydispersity of the disulfide-linked chains resulted in the polydispersity of the HG|SC particles after pH-cycling. Some small particles even the had the same size as native soluble HG or SC micelle (Figure 6-11D2).

6.4. Conclusion

The solubility of HG increased to more than 80% when mixed with SC and after pH-cycling treatment due to the formation of the HG|SC nanoparticles. The HG|SC nanoparticles had z-average of around 130 nm and were monodisperse. These particles are composed of disulfide-linked protein chains/aggregates, which interact with SC mainly via non-covalent interaction at pH 12. During the neutralisation, HG|SC complexed and

refolded into nanoparticles due to diminished electrostatic repulsion and the strong attractive hydrogen bonding. The HG|SC nanoparticles were colloidally suspended in water, stable above pH 7 and had heat stability to some extent. . Further research is needed to establish how drying and rehydration affects the structure and properties of HG|SC nanoparticles. These protein nanoparticles could be used in beverages to increase the content of otherwise insoluble plant protein and have potential to encapsulate water-insoluble compounds. In other work we have shown that they can be used as emulsifiers to make tunable concentrated Pickering emulsions will be discussed in the next chapter.

7. CONCENTRATED PICKERING EMULSION STABILISED BY HEMP GLOBULIN – CASEIN NANOPARTICLES: TUNING THE RHEOLOGICAL PROPERTIES BY ADJUSTING HG/SC RATIO

The contents of this chapter have been published in a peer-reviewed journal article

Chuang, C.-C., Ye, A., Anema, S. G., & Loveday, S. M. (2020). Concentrated Pickering emulsions stabilised by hemp globulin–caseinate nanoparticles: tuning the rheological properties by adjusting the hemp globulin:caseinate ratio. Food & Function 10.1039/D0FO01745K

7.1. Introduction

The solubility of HG was increased from < 20% to > 80% by making hemp–casein protein nanoparticles through a pH-cycling process at ambient temperature in Chapter 6. In this chapter, we investigated the ability of these protein nanoparticles to stabilise Pickering emulsions. A Pickering emulsion is an emulsion stabilised by solid colloidal particles that will position at the oil–water interface. Pickering-stabilised emulsions require high energy to remove the colloidal particles adsorbed on the interface. In addition, the particles can act as a mechanical barrier to coalescence or shrinkage. Therefore, Pickering emulsions are highly stable against droplet coalescence and Ostwald ripening (Berton-Carabin & Schroën, 2015; Murray, 2019). Protein particles can be used to form Pickering emulsions because of their amphiphilic nature. However, many protein particles will dissociate and unfold after adsorption on the interface, which means that they can no longer be regarded as particles. Methods such as heat treatment and enzymatic cross-linking have been used

in attempts to strengthen the structure to make “solid-like” protein particles (Linke & Drusch, 2018). Even after these pre-treatments, emulsions stabilised by protein particles seem to be limited to systems with high viscosity, which can be produced by increasing the volume of the internal phase ($\varphi > 0.6$) or by gel formation with excess protein particles in the continuous phase (Linke & Drusch, 2018).

One of the interesting properties of emulsions is that they can have tuneable rheological properties that are dependent on the composition, e.g. emulsions can be tuned to have solid-like properties by increasing the volume fraction, which leads to jamming of the droplets (H. S. Kim & Mason, 2017). In addition, time-dependent rheological properties can also be tuned by the emulsifier, e.g. a SC-stabilised emulsion became incrementally more viscous during 14 days of storage (Dickinson & Golding, 1997). This time-dependent change in the rheological properties is important in food products because their sensory properties and physical stabilities are expected to be stable during their shelf life.

The anti-solvent process is the most common method for making colloidally stable particles from non-soluble plant seed proteins. This method involves dissolving the proteins in an organic solvent (de Folter, van Ruijven, & Velikov, 2012; Jiao, Shi, Wang, & Binks, 2018; L. Ma, Zou, McClements, & Liu, 2020; Xiao, Wang, Perez Gonzalez, & Huang, 2016; Zhu, Lu, Zhu, Zhang, & Yin, 2019; Zou et al., 2017). However, for food applications, an extra step to evaporate or remove the organic solvent is necessary. In addition to the anti-solvent method, plant seed protein–polysaccharide complexes have been used to modify or stabilise the protein particles before making a Pickering emulsion (L. Ma et al., 2020; Zhu et al., 2019) .

Another promising method for solubilising/stabilising insoluble plant seed proteins in water is pH-cycling. The protein dispersion is adjusted to higher or lower pH and then neutralised. No organic solvent is used in pH-cycling and the only residue is salts originating from the acid and base used to adjust the pH. The process of pH-cycling, especially through alkali treatment, increases the solubility and improves the emulsifying activity of soy protein at neutral pH (Jiang et al., 2009; Jiang et al., 2010). However, pH-cycling alone cannot solubilise/stabilise some plant seed proteins, especially those that have much lower solubility than soy protein, e.g. rice protein and zein protein from corn. Additional stabilisers such as caseinate are necessary; the combination of pH-cycling and caseinate addition, which leads to co-assembly of the caseinate with the plant protein, can produce colloidally stable nanoparticles for these proteins (Chuang, Anema, Ye, & Loveday, 2020; Pan & Zhong, 2016; Sun et al., 2018a, 2018b; L. Wang et al., 2019; L. Wang & Zhang, 2017; T. Wang, M. Yue, et al., 2018).

Little previous work has been done on the emulsifying properties of protein nanoparticles made through pH-cycling and complexation with caseinate. High-internal-phase Pickering emulsions have been made through a pH-cycling process using nanoparticles composed of zein, caseinate and propylene glycol alginate (Sun et al. (2018b)). However, propylene glycol alginate is a high-molecular-weight linear polysaccharide that has thickening and emulsifying properties itself. In the present study, pure protein particles were made from HG and caseinate through a pH-cycling process, which turned the insoluble hemp protein into soluble HG–SC nanoparticles. These protein nanoparticles were used to make a concentrated emulsion. The emulsifying properties of the HG–SC nanoparticles and the rheological properties of the emulsions during storage were examined.

7.2. Material and methods

7.2.1. *Formation of HG|SC protein particles.*

The HG-SC composite particles (HG|SC nanoparticles) were made through the pH-cycling method described in Chapter 6.

7.2.2. *Interfacial tension measurement*

The dynamic interfacial tension was measured using a pendant drop tensiometer (CAM 200, KSV Instruments Ltd, Helsinki, Finland). Solutions of HG|SC nanoparticles or SC were serially diluted with 35 mM NaCl solution to produce a final protein concentration of 0.005%. A drop of protein solution (around 9 µL) was extruded into soy oil, and the shape of the hanging drop was monitored over time by a camera. The interfacial tension at the oil–water interface was calculated using the equation $\gamma = \frac{\Delta\rho \times g \times R_0}{\beta}$, where γ is the interfacial tension, $\Delta\rho$ is the difference in density between the soy oil and the protein solution, R_0 is the radius of the drop curvature at the apex and β is the shape factor, which was calculated through the Young–Laplace equation with the instrument's built-in software (KSV Instruments Ltd).

7.2.3. *Emulsion preparation*

Soya oil and aqueous protein solution (1.8% w/w solution of SC or HG|SC nanoparticles) were mixed in a glass tube at a volume ratio of 70:30. The emulsion was prepared by homogenising the mixture with a rotor–stator homogeniser (Model D130, LabServ) with a 10-mm dispersing shaft at 12,000 rev/min for 1 min. During the homogenisation, the glass tube was put into a water bath at room temperature. The emulsion was transferred into a

glass vial with a screw cap to prevent drying during the 21 days of storage. The emulsion was an oil-in-water emulsion because the droplets dispersed when a drop of emulsion was put into water but not when put into soya oil.

7.2.4. *Confocal laser scanning microscopy (CLSM)*

The structures of the emulsions were analysed using a confocal laser scanning microscope (Leica DM6000 B, Heidelberg, Germany). The emulsion was mixed with Fast Green (1 mg/mL in Milli-Q water) and Nile Red (1 mg/mL in acetone) in a 10:1:1 ratio (v/v) to stain the protein phase and the oil phase respectively. The stained emulsion was placed on a concave microscope slide and covered with a coverslip. The excitation wavelengths for Fast Green and Nile Red were 633 nm and 561 nm respectively. At least 4 confocal images were taken from each sample at each magnification.

7.2.5. *Rheological characterisation*

The rheological properties of the emulsions were measured using an MCR 302 rheometer (Anton Paar, Graz, Austria) with a cone-and-plate geometry (CP10-4). The temperature was maintained at 20 °C. An emulsion sample was loaded onto the plate and the cone was lowered into position. Excess sample was carefully scraped out, and then a thin layer of mineral oil was used to cover the edge to prevent evaporation. All emulsions were pre-sheared initially (100 s^{-1}, 1 min). Then a series of measurements was conducted: (1) a time sweep test with constant strain amplitude (0.5%) and angular frequency (1 rad/s) was performed for 3 h to determine the recovery of the structure (rebodying); (2) after the time sweep test, a frequency sweep test was carried out at 0.5% strain with the angular frequency being increased from 0.1 to 100 rad/s; (3) a strain sweep test was performed at a constant

angular frequency of 1 rad/s and the strain was adjusted from 0.01 to 1000%. After these three oscillation tests, a continuous rotation with a shear rate of 100 s^{-1} was again applied for 1 min, followed by (4) steady shearing experiments: two continuous rotational shearing regimes were applied to determine the change in apparent viscosity. The shear rate was firstly increased from 0.01 to 100 s^{-1} and then decreased from 100 to 0.01 s^{-1} at the rate of six points/decade.

7.3. Results and discussion

7.3.1. *Interfacial tension of the HG|SC nanoparticles*

Plots of interfacial tension versus log time for soya oil with different protein solutions/dispersions are shown in Figure 7-1. The decrease in interfacial tension over time followed a common pattern of three distinct regimes (Beverung, Radke, & Blanch, 1999), which gave information about the adsorption behaviour of the protein on to the interface. In Regime I, all samples showed a similar initial induction time (from 1 to around 20 s) during which the interfacial tension was somewhat constant (Figure 7-1). This induction time was attributed to the limited diffusion and subsequent adsorption of the proteins on to the interface, i.e. the protein needed some time to diffuse, adsorb and unfold its side chains on to the oil–water interface to lower the interfacial tension. The similar induction times indicated that the diffusion rates and the initial adsorption rates were also similar among the three samples.

Above a certain concentration of adsorbed protein, all three plots moved into Regime II after around 70 s and there was a steep decline in interfacial tension in all samples. The continuing decline of the interfacial tension in Regime II has been attributed to two mechanisms (Beverung et al., 1999). The first mechanism is the continuing diffusion of new protein from the bulk water phase to the interface. Then another mechanism takes place – the protein conformation relaxes and/or unfolds on the interface, allowing new side chains inside the protein to orient themselves into the oil phase and provide more contact points between protein and the oil phase. Therefore, the interfacial tension declines steeply towards monolayer coverage of the pendant drop.

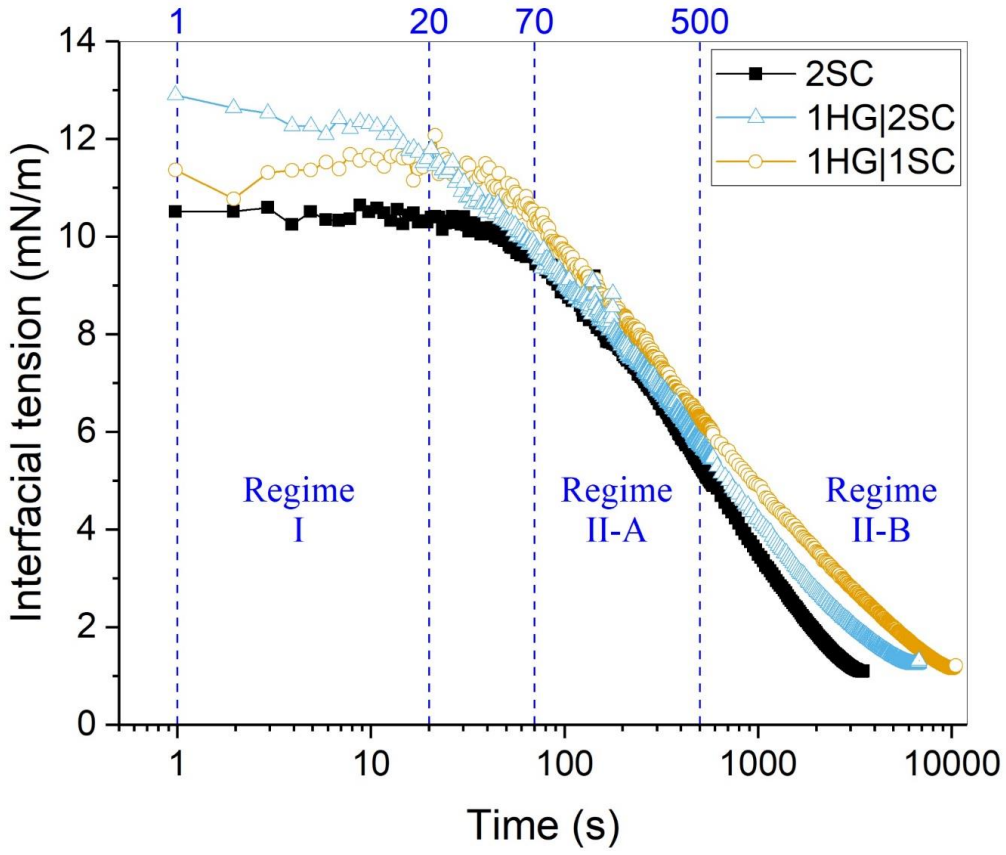

Figure 7-1. Interfacial tension between soya oil and 35 mM NaCl solution containing (■) 2SC, (△) 1HG|2SC nanoparticles or (◯) 1HG|1SC nanoparticles at 25 °C. The protein concentration was fixed at 0.005%.

Interestingly, Regime II could be split into two regions by comparing the slopes of the three samples – Regime II-A (70–500 s), in which all plots had a similar slope, and Regime II-B (> 500 s), in which the interfacial tensions started to diverge. These two regions in Regime II can be explained by the two aforementioned mechanisms – diffusion-limited adsorption on to the interface and reorientation of the protein adsorbed at the interface.

Both the similar induction times in Regime I and the same slopes in Regime II-A indicate a similar diffusion rate at the beginning of protein adsorption. In contrast, the different slopes in Regime II-B correlated with the ratio of HG. The 2SC solution had the steepest slope and reached about 1 mN/m at around 3000 s before the pendant drop fell from the syringe. The slope of the 1HG|1SC dispersion, which contained the highest amount of HG, did not reach the final interfacial tension of 1 mN/m until around 10,000 s; the 1HG|2SC dispersion reached the final interfacial tension at an intermediate time (around 6000 s, between those of 2SC and 1HG|1SC).

The difference in slope may reflect the different flexibilities of SC and HG. As caseins are known to have flexible conformations and amphiphilic properties (Holt, Carver, Ecroyd, & Thorn, 2013; Huppertz et al., 2018), it is possible for them to relax and rearrange on the interface more efficiently. Native HG is in the form of rigid crystalloids within the hemp seed (St. Angelo et al., 1968). The steeper slope when more SC was incorporated via pH-cycling suggests that the flexibility of HG|SC nanoparticles can be controlled by the HG:SC ratio, i.e. their emulsifying properties can be tuned by the HG:SC ratio.

Regime III, a slow and prolonged decline in the interfacial tension, as proposed by Beverung et al. (1999), was not observed. It could be that the protein concentration was high compared with the surface area of the pendant drop, so that the interfacial tension dropped quickly, and the pendant drop fell before the gradual decline; therefore, the equilibrium interfacial tension was not achieved. Nevertheless, this experiment still shows the different interfacial properties of SC and HG|SC nanoparticles, as indicated in Regime II-B.

7.3.2. *Appearance of emulsions*

All emulsions had good stability, and no creaming or phase separation was observed during the 21 days of storage at room temperature (Figure 7-2). The 1HG|2SC emulsion (the emulsion that was stabilised by 1HG|2SC nanoparticles) was viscous and stuck to the glass when the vial was inverted. The most interesting aspect was that only the 1HG|1SC emulsion was self-supporting, i.e. it did not flow when the vial was inverted. The gel-like property of the 1HG|1SC emulsion can also be seen in Figure 7-2B. This was the only emulsion that could hold its structure without spreading when transferred on to a flat glass plate, indicating the formation of a gel-like material with a yield stress.

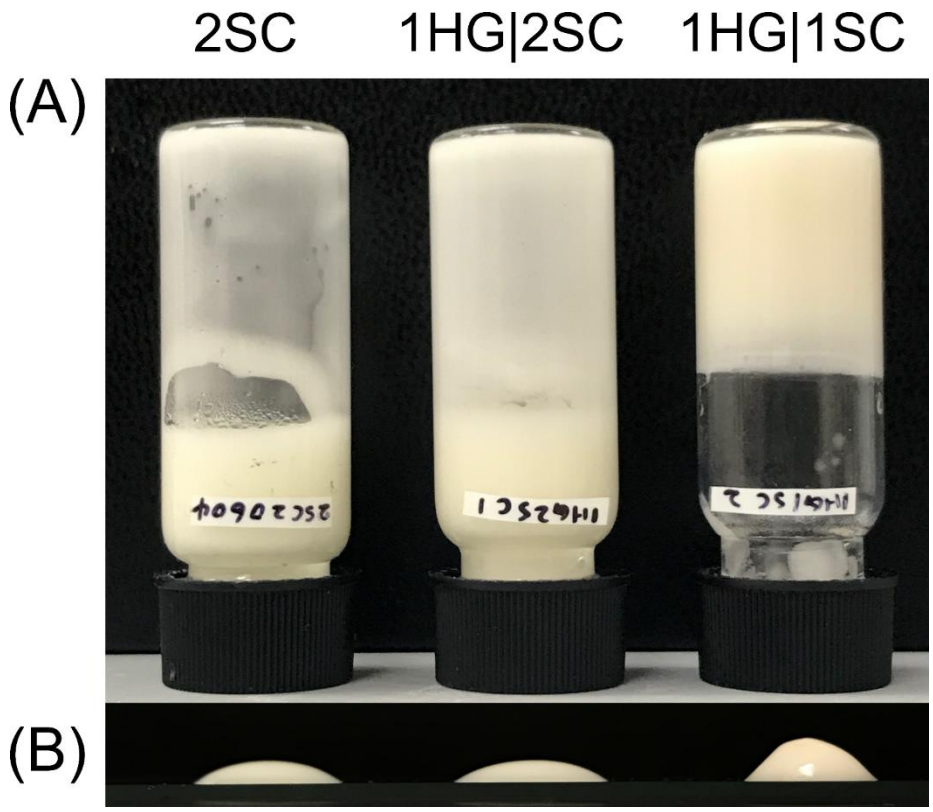

Figure 7-2. Photo of emulsions stabilised by 2SC or HG|SC protein particles with different HG|SC ratio, after 21-day storage. (A) the emulsions in inverted tubes (B) drop of emulsions placed on a flat glass plate.

7.3.3. *Rheological properties of emulsions during storage*

The gel-like properties of the HG|SC emulsions were further characterised by rheometry, as the rheological properties of concentrated emulsions can provide information about structure and the interactions between the droplets in the emulsion.

7.3.3.1. Time sweep test

The stronger gel-like properties in the 1HG|1SC emulsion were also observed in the time sweep test. After the pre-shearing (100 s^{-1}, 1 min), all emulsions were still gel-like, as G' was always greater than G'' (Figure 7-3A–C). G' increased steadily during the 3-h experiment, regardless of the emulsifier used (SC or HG|SC nanoparticles) or the storage

time. The increasing G’ during the time sweep test indicated the regeneration of structure, which resulted from the strengthening interactions between the droplets and/or the development of the internal structure during the 3 h.

The change in G’ during the 21-day storage period was different in aged SC and HG|SC emulsions. The G' value of the 2SC emulsions decreased with an increase in the storage time (from day 0 to day 21) (Figure 7-3A), indicating droplet–droplet interactions or that the internal structure of the emulsions stabilised only by SC became weaker during storage. In contrast, the G' values of both the 1HG|2SC emulsion and the 1HG|1SC emulsion increased throughout the 21-day storage period. In addition, the extent of increasing solid-like properties was more pronounced when the ratio of HG in the particles was higher (Figure 7-3B and C). Figure 7-3C shows that the G' value of the 1HG|1SC emulsion increased at the end of the 3-h test from 130 Pa at day 0 to 177 and 306 Pa at 7 and 21 days respectively. The same time-hardening phenomenon was also found in the emulsion stabilised by 1HG|2SC nanoparticles (Figure 7-3B), but the increase in G' was not as high as with the 1HG|1SC nanoparticles (Figure 7-3C).

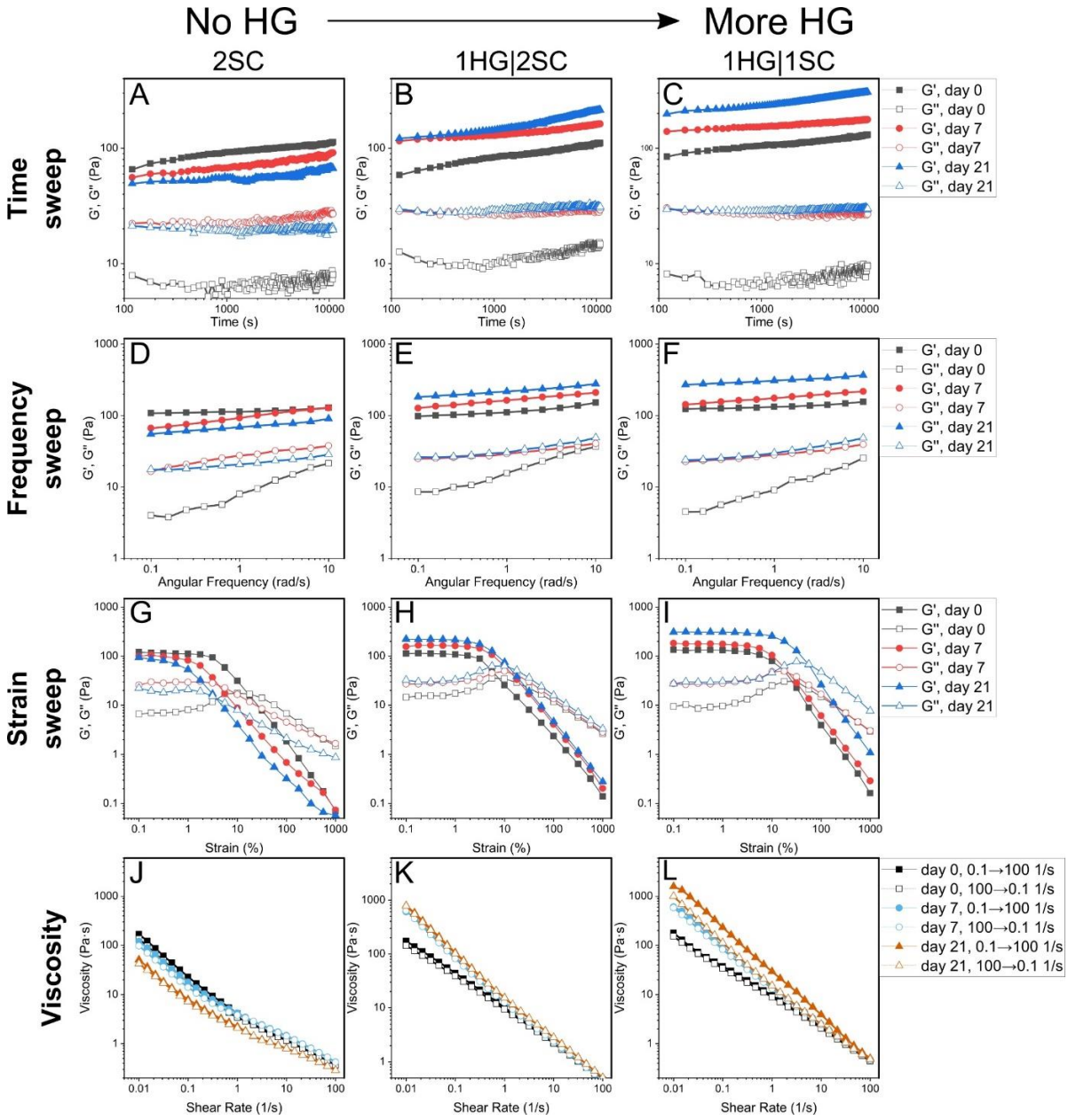

Figure 7-3. Rheological properties of emulsion stabilized by SC or HG|SC with different HG ratios during storage. (A – C) Time sweep tests; (D – F) strain sweep tests; (G – I) rate and (J – L) frequency sweep tests. n = 2.

7.3.3.2. Frequency sweep test

The rheological properties of the emulsions after structural regeneration during the time sweep test were further analysed with frequency sweep tests. Figure 7-3D–F show the dependence of G' on the frequency of the emulsions stabilised by 2SC solution and 1HG|2SC and 1HG|1SC nanoparticles respectively. Both G' and G'' were dependent on the frequency (although the dependence was weak for G'), which may be an indication of a highly flocculated structure (Chevalier & Bolzinger, 2013; Xiao et al., 2016), stabilised by non-covalent physical interactions (Tang & Liu, 2013). Solid-like behaviour (G' > G'') was still observed in all emulsions throughout the entire frequency range. With increasing oscillation frequency, G'' had a steeper slope than G' in all samples at day 0, suggesting that all emulsions could be described as concentrated solutions. The emulsions turned into weak gels after 7 days of storage because G'' became parallel to G' (S. K. Lee & Klostermeyer, 2001). The time-softening in the aged SC emulsions and the time-hardening in the aged HG|SC emulsions were consistent with the results from the time sweep tests.

The frequency sweep data can reveal more about the internal structure and interactions in the emulsion according to Bohlin's co-operative theory of flow (Bohlin, 1980) by fitting the data into the following formula:

$$G' = A\omega^{\frac{1}{z}}$$

In this formula, G' is the storage modulus (Pa) and ω is the frequency (rad/s was transformed into Hz). The parameters A ($Pa \cdot s^{1/z}$) and z (dimensionless) can be fitted and calculated. In Bohlin's model, the system is treated as a network of rheological units that

interact with each other to establish an internal structure. The parameter A is interpreted as the magnitude of interactions between the rheological flow units, which are collections of z relaxation elements (hypothetical flocs of emulsion droplets in this case) that act co-operatively in response to stresses, i.e. A is the magnitude of attractive forces between flow units. The parameter z is the coordination number for the co-operative flow units, which is a measure of the degree of co-operativity among flow elements (i.e. the size of the hypothetical flocs) interacting with each other in the internal three-dimensional (3D) structure, which can be interpreted as the spatial extent of interactions within the 3D network structure (Gabriele, de Cindio, & D'Antona, 2001; Manoi & Rizvi, 2009; Peressini, Sensidoni, & de Cindio, 1998; Zaidel, Chronakis, & Meyer, 2013).

Table 11. Parameters fitted with Bohlin's model and values obtained by strain sweep test (flow point and torque at flow point). Values were calculated or measured for emulsions stabilised by 2SC, 1HG|2SC particles or 1HG|1SC particles during storage (0, 7 or 21 days). Values are average of duplicates from the frequency sweep tests or strain sweep test.

		2SC			1HG|2SC			1HG|1SC		
	Storage time (day)	0	7	21	0	7	21	0	7	21
Bohlin's model	A ($Pa \cdot s^{1/z}$)	108.9	70.4	58.1	99.9	134.5	188.0	124.8	149.5	277.8
	z	41.7	6.6	10.4	16.9	9.3	12.4	33.4	11.3	17.6
	R^2	0.940	0.993	0.989	0.973	0.997	0.998	0.938	0.990	0.998
Strain sweep	Flow point (%)	16.1	4.3	4.6	7.7	13.1	11.5	23.5	21.3	45.6
	Torque at flow point (Pa)	4.0	1.5	0.8	3.9	9.1	10.5	11.2	14.1	53.2

The parameters calculated according to Bohlin's model are shown in Table 11. The time-softening property of the 2SC emulsions can also be seen in Bohlin's parameters. Parameter A was 108.9 $Pa \cdot s^{1/z}$ at day 0 and decreased during storage, indicating that the

strength of the interactions between flow units became weaker over time. Parameter z also decreased after day 7, suggesting that the size of the flow units diminished after 7 days. These findings indicate weaker interactions and a more localised (lower z) internal 3D structure in the aged SC emulsions. Low A and low z also indicate that the emulsions were less stable under mechanical stress.

The results in Table 11 demonstrate that both the 1HG|2SC emulsion and the 1HG|1SC emulsion behaved differently from the 2SC emulsion. Parameter A for the 1HG|1SC emulsion increased during storage – from 124.8 $Pa{\cdot}s^{1/z}$ at day 0 to 149.5 $Pa{\cdot}s^{1/z}$ at day 7 and to 277.8 Pa at day 21. The increase in parameter A indicates that the interactions between the HG|SC-nanoparticle-stabilised droplets strengthened during storage. In contrast, the change in parameter z was similar to that in the SC emulsion – having the highest value of 33.4 at day 0 and decreasing during storage (11.3 at day 7 and 17.6 at day 21). The decrease in parameter z suggested a less extended or more localised internal 3D structure in the aged 1HG|1SC emulsion. This most solid-like emulsion (the 1HG|1SC emulsion after 21 days of storage) had Bohlin's parameters that were comparable with those of yoghurt at 15 °C, a parameter A of 274.9 $Pa{\cdot}s^{1/z}$ and a parameter z of 7.92 (Gabriele et al., 2001). Given that the aged 1HG|1SC emulsion did not flow and the changes in parameters A and z during storage, it can be inferred that the stiffness of the aged 1HG|1SC emulsion resulted mainly from attractive interactions between localised groups of droplets, and less from the formation of extended 3D networks or flocs.

The time-hardening property can be controlled by the HG:SC ratio. Parameter A of the 1HG|2SC emulsion increased during storage, but the magnitude was lower for the

1HG|1SC emulsion. The intermediate parameter A indicates that the interactions between droplets became stronger, but not as strong as in the 1HG|1SC emulsion.

7.3.3.3. Strain sweep test

Differences between the SC-stabilised emulsion and the HG|SC-nanoparticle-stabilised emulsions were also observed in the strain sweep tests. Figure 7-3G shows the G' and G'' values of emulsions stabilised by SC alone during the 21 days of storage. At day 0, the SC emulsion had solid-like properties because G' was larger than G''. Interestingly, G'' exhibited a plateau before reaching a maximum value (G'' max) at around 10% strain and decreased at higher strain.

Previous work proposed a two-step mechanism for the destruction of the internal structure during strain sweep tests (Majesté, Carrot, Olalla, & Fulchiron, 2012), and this model fitted perfectly with the development of G'', i.e. G'' exhibited a plateau with a G'' max value, followed by a decline with increasing strain. The system was seen as the dispersed phase (oil droplets and protein particles in this case) agglomerated into local flocs with certain finite sizes, and these local flocs in turn constituted the emulsion. In the first step of structural destruction, protein particles and oil droplets moved against each other (re-organisation) within the local flocs under the shear force in the low strain region.

In other words, there was a change in the configuration of the network of particles and droplets inside the flocs. This internal re-organisation within the flocs resulted in deformation of the local flocs but the flocs had not yet ruptured, leading to energy dissipation; thus, a plateau in G'' was observed. G'' subsequently increased with an increase in the strain amplitude and reached a G'' max at around 10% strain, indicating the

larger extent of re-organisation within the local flocs so that the energy dissipation was higher. In the next step, G'' became greater than G' at a flow point of 16.1% strain (Table 11), suggesting the rupture of the flocs and the overall internal structure, so that the emulsion became liquid-like.

The internal structure of the 2SC emulsion became strikingly weaker after storage, as the emulsion yielded even at 0.1% strain after 21 days. As a G'' plateau remained after 7 and 21 days of storage, there was still re-organisation within the local flocs. Interestingly, the G'' plots of the 7- and 21-day samples showed no G'' max when the strain was increased after the G'' plateau region, indicating that the localised flocs were weaker and could not resist the greater extent of re-organisation observed at day 0. This is consistent with lower z values in the Bohlin model (Table 11), i.e. weaker intra-floc cohesion would lead to smaller flocs.

The weaker structure of the aged 2SC emulsions can also be seen in the change in the flow point, which decreased from 16.1% to 4.3 and 4.6% after 7 and 21 days respectively (Table 11). Although the flow point was similar at 7 and 21 days, much less torque was needed to make the emulsion flow after 21 days of storage, at which point the torque had decreased from 1.5 to 0.8 μN.m (Table 11).

In contrast, the HG|SC emulsions had a stronger internal structure that developed further during storage. Figure 7-3I shows the development of G' and G'' in the 1HG|1SC emulsion; G', G'', the yield point, the flow point and G'' max during the strain sweep test were similar to those of the 2SC emulsion at day 0. Interestingly, a strong internal structure was observed after storage: after 21 days, the value of the plateau G' in the linear

viscoelastic region increased from around 135 Pa at day 0 to 310 Pa at day 21, the yield point increased from 7.7 to 12.5% and the flow point increased from 23.5 to 45.6% (Table 11). The 1HG|2SC emulsion had a similar pattern to the 1HG|1SC emulsion, but the extent of time-hardening was less than in the 1HG|1SC emulsion.

7.3.3.4. Steady shearing experiments

All emulsions showed non-Newtonian (shear-thinning) behaviour between the tested shear rates of 0.01–100 s^{-1} (Figure 7-3J–L). Shear-thinning behaviour has been proposed to be the result of aggregation ↔ dissociation reactions (Campanella, Dorward, & Singh, 1995; Manoi & Rizvi, 2009). The droplets were close enough to interact with each other in the concentrated emulsions, enabling the formation of a network of connected droplets, which could still hold the internal structure when the shear rate was low. When the shear rate increased, the network of droplets dissociated into individual droplets and the continuous phase, previously trapped within the network, was released, resulting in a lower effective oil volume fraction and therefore a lower viscosity. Consequently, all emulsions had low viscosity (< 1 Pa·s) when at a shear rate of 100 s^{-1}.

Only the 21-day aged 1HG|1SC emulsion showed thixotropic behaviour (hysteresis) (Figure 7-3L), i.e. its viscosity did not recover immediately when the shear rate was lowered again. The reduction in viscosity indicated that the aggregation ↔ dissociation phenomenon was not immediately reversible; thus, the internal structure could not rapidly go back to its original structure after shearing in this emulsion. Therefore, this showed that the 21-day aged 1HG|1SC emulsion still had strong internal structure even after the continuous shearing (100 s^{-1}, 1 min). In contrast, non-thixotropic behaviour was observed

in all other emulsions, i.e. similar viscosity was retained, suggesting that the internal structure/droplet–droplet interactions did not change after the two shearing programmes.

7.3.4. *Microstructure*

The microstructures of the emulsions were analysed by CLSM; the oil and protein phases were stained with fluorescent dye and are represented by red and green respectively (Figure 7-4). The CLSM micrographs confirmed that the emulsions could be classified as concentrated emulsions, which covers a wide concentration of the dispersed phase between two boundaries of volume fraction (φ). The lower boundary is the dilute emulsion, in which there is negligible interaction between the droplets; the higher boundary is when the droplets are closely packed and even adding one more droplet will result in the deformation of other droplets ,(Derkach, 2009), which occurs when $\varphi > 74\%$ for the monodisperse system and the system can be regarded as a high-internal-phase emulsion (HIPE) (Binks, 1998).

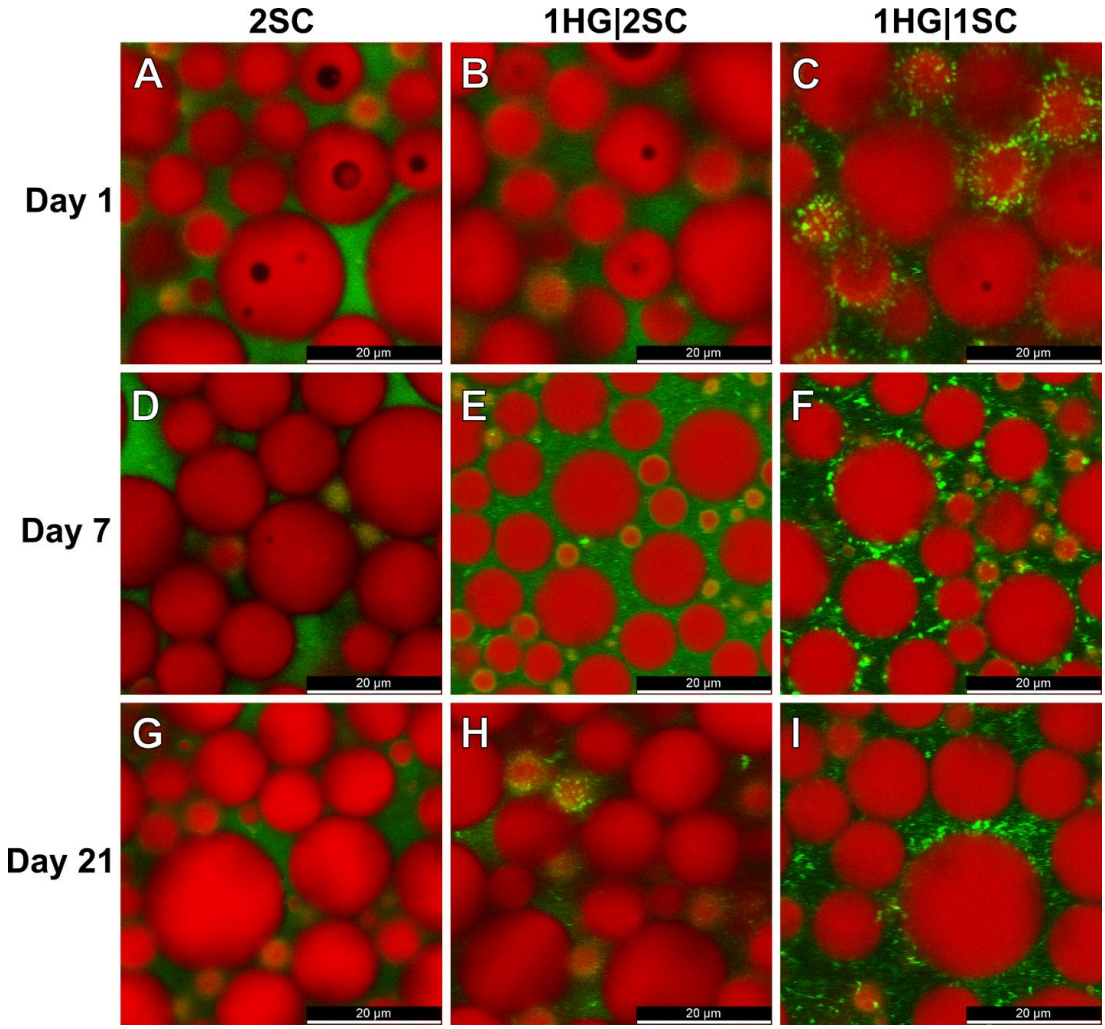

Figure 7-4. CLSM micrograph of the emulsion during storage stabilized by 2SC (A, D, G), 1HG|2SC protein complexes (B, E, G) or 1HG|1SC protein complexes (C, F, I).

As the oil droplets in the emulsions did not pack closely and no deformation into polyhedral shapes could be seen (Figure 7-4), this system was not an HIPE. The oil droplets still had round shapes and had few contact points with each other. Because of the few contact points between droplets, the high viscosity or stronger internal structure observed in HIPEs was not anticipated in our emulsions. Indeed, the G' values of the freshly prepared emulsions

during the frequency sweep tests were all lower than those of HIPEs stabilised by protein particles (Hu et al., 2016; Sun et al., 2018b; Zeng et al., 2017). Nevertheless, all emulsions were already solid-like on day 0, as shown in the rheological behaviour (Figure 7-3).

The size of particles on the interface and the surface coverage can be controlled by adjusting the HG:SC ratio. Protein particles were clearly observed on the surfaces of the oil droplets in the 1HG|1SC emulsions (Figure 7-4C, F and I). As these 1HG|1SC nanoparticles were rigid or solid-like and retained spherical conformations, the 1HG|1SC emulsions can be regarded as Pickering emulsions, which is also consistent with the conclusion drawn from the interfacial tension experiments. However, the interface was not fully covered by 1HG|1SC nanoparticles.

When more SC was incorporated with the HG (i.e. 1HG|2SC, Figure 7-4B, E and H), the size of the protein particles appeared to be smaller and the surface coverage was higher. No visible protein particles were observed on the interface in the 2SC emulsions because of the much smaller particle size and the flexible nature of caseins, but the interface appeared to be fully covered (Figure 7-4A, D and G). Micrographs of the droplets in diluted emulsions (5× dilution) were also obtained so that the protein on the interface could be clearly visualised (Figure 7-5). The same effect of the SC ratio on the interface coverage was reported for zein particles in which the surfaces were modified by SC via sonication (Feng & Lee, 2016). These authors proposed that the SC on the zein particles improved the interfacial properties and facilitated the particle adsorption by controlling the hydrophobicity on the surface of the protein particles with different zein:SC ratios.

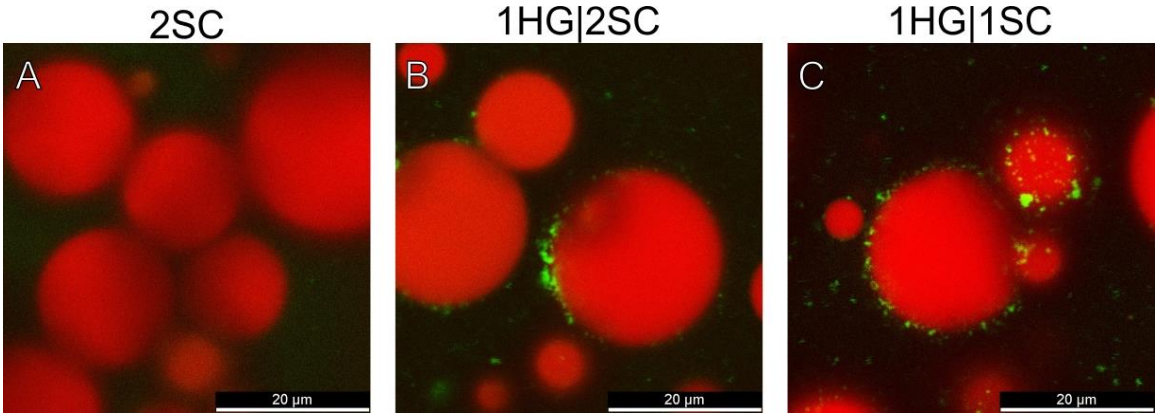

Figure 7-5 CLSM micrographs of diluted (5x) Pickering emulsions after 21 days of storage.

These CLSM micrographs also suggest that the HG|SC nanoparticles kept their integrity during the emulsification process, after adsorption and during the storage. Protein aggregates were visible on the surface (Figure 7-4C, 4F, 4H and 4I and Figure 7-5), indicating that the nanoparticles did not dissociate. This was because disulfide bonds, rather than hydrophobic interactions or other non-covalent interactions, were involved in the formation of the complex particles, so that dissociation and deformation occurring during and after adsorption on the surface was unlikely.

7.3.5. *Gel-like properties of emulsions and change of rheological properties during storage*

The gel-like or thickening properties during storage had three possible origins. The first possibility is the formation of a network of connected droplets in the concentrated emulsion because of the high volume fraction, as mentioned in the Section 3.3.4. The second is droplet flocculation that developed gradually during storage.(Dickinson, 2001) The third is the interactions between the excess particles in the continuous phase, which is common

in Pickering emulsions (Chevalier & Bolzinger, 2013). These three possibilities are discussed below.

7.3.5.1. Network of connected droplets

The appearance of yield points in all emulsions (Figure 7-3G, H and I) and the non-Newtonian flow curves (Figure 7-3J, K and L) indicated the formation of structures that were caused by droplet–droplet interactions even on day 0 (Derkach, 2010). The structure could have resulted from the network of connected droplets because of the high volume fraction of oil and the close proximity of the oil droplets. The oil droplets were dispersed and stacked homogeneously after emulsification because no phase separation was observed. The network of connected droplets could be seen in the CLSM images (Figure 7-4), as the droplets were not deformed and several contact points could be clearly seen in all emulsions. The results also show that all emulsions had similar droplet size distributions ($D[4,3] \approx 20$ μm) during the 21 days of storage (Figure 7-6), indicating that there was no coalescence of the droplets.

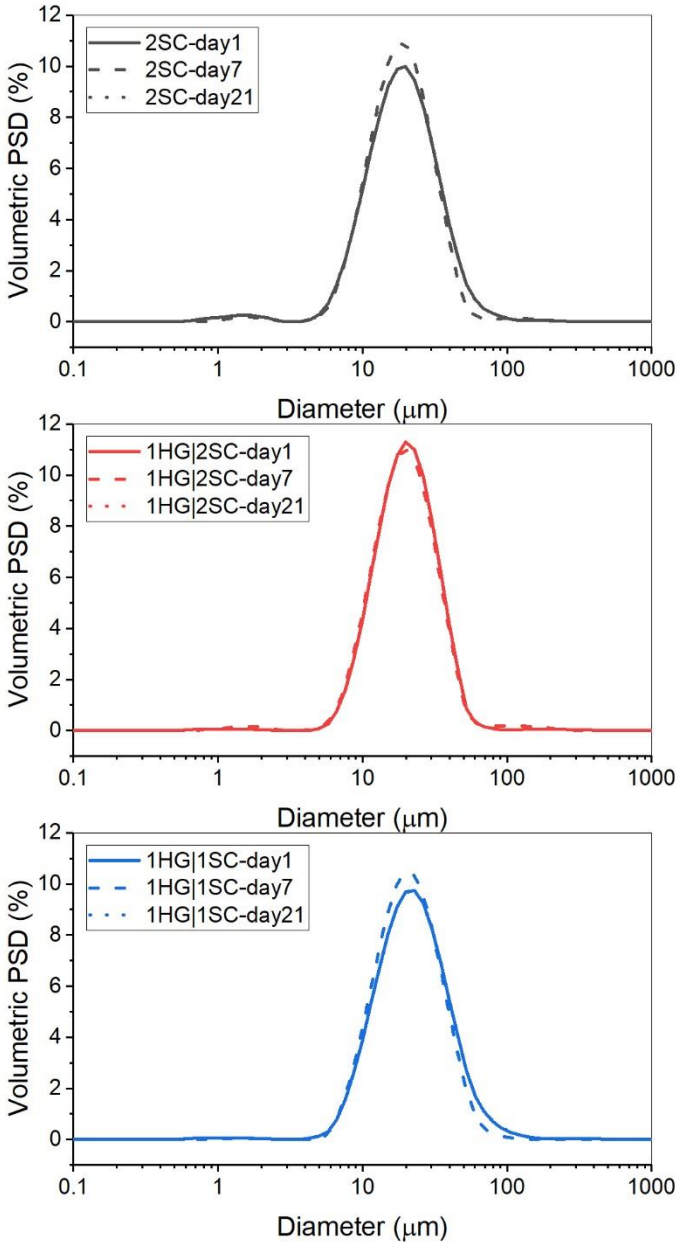

Figure 7-6 Droplet size distributions of the Pickering emulsions during storage.

7.3.5.2. Droplet flocculation during storage

The HG|SC emulsions became more solid-like during storage, which may have originated from droplet flocculation and the further development of internal structures. Dickinson and Golding (1997) reported the slow recovery of viscosity similar to the slowly increasing G' in the time sweep test (Figure 7-3A – C) and attributed the phenomenon to flocculation of droplets.

However, the results indicate that droplet flocculation was not the origin of the development of gel-like properties during storage. There are two types of flocculation induced by the polymer in the continuous phase: bridging flocculation and depletion flocculation. Bridging flocculation, which resulted from the protein particles interacting with two droplets at the same time, could be ruled out because bridging-flocculated droplets do not dissociate on dilution during laser diffraction analysis (Day, Xu, Hoobin, Burgar, & Augustin, 2007; Dickinson, Golding, & Povey, 1997). If strong bridging flocculation did happen, an increase in the effective droplet size would be observed in the laser diffraction data during the storage, and this was not seen (Figure 7-6).

As depletion flocculation is known to be reversible during dilution, it could not be monitored just by the change in droplet size. Nevertheless, it can be suggested that depletion flocculation did not occur in this emulsion system. Firstly, no creaming or phase separation was observed in any emulsion (Figure 7-2). As the creaming phenomenon is dominated by droplet flocculation (Robins, 2000), the stability of the emulsions might suggest that there was no severe flocculation. Secondly, depletion flocculation occurs when the gap between two droplets is smaller than the diameter of the unadsorbed polymer,

resulting in the exclusion of polymers from the inter-droplet space because of the difference in the osmotic pressure. The strong protein signals in the continuous phase of the CLSM micrographs suggested that there was indeed excess protein in the continuous phase. However, as according to the CLSM micrographs (Figure 7-4), the large droplets were already in contact with each other because of the high volume fraction of oil, there were no gaps between these large droplets for depletion flocculation to occur. Nevertheless, the smaller particles that could move in the space between large droplets might still undergo depletion flocculation.

Lastly, the potential for depletion flocculation was calculated by Radford and Dickinson (2004), and the depletion force reached its maximum under specific conditions, e.g. for a droplet size of 0.4 μm, the depletion force reached a maximum when the casein particles were around 20 nm in radius. The depletion force decreased when the protein particle was larger or smaller than 20 nm. If depletion flocculation was important to the regeneration of the internal structure of these emulsions, then there should have been a difference in the time sweep test because SC ($d \approx$ 15–20 nm) and the HG|SC nanoparticles ($d \approx$ 130 nm) had different particle sizes. However, a similar pattern of increasing G' was found during the 3-h time sweep test on day 0 (Figure 7-3A–C) regardless of the stabiliser used, which might indicate that either depletion flocculation was not crucial to the regeneration of the internal structure, or the particle size did not affect the depletion force.

Another interesting finding was the time-softening property of the 2SC emulsion; this was different from the SC-stabilised emulsions in a previous study, which became more viscous during storage (Dickinson & Golding, 1997). These authors explained the increase in viscosity by a slow bridging flocculation process. Bridging flocculation did not occur in

our study (as discussed earlier), possibly because of the difference in the droplet sizes. The droplet size here ($D[4,3] \approx 20$ μm) was much larger than that in the previous study ($D[3,2] \approx 0.4$ μm). Therefore, the protein coverage was much higher because of the much lower specific surface area of the droplets. The high protein coverage acted as a steric barrier to prevent bridging flocculation. These authors proposed a slow change of structure/composition of the casein layer on the oil–water interface during storage. Such a change in the interfacial casein layer may have been the reason for the time-softening properties of the 2SC emulsion.

7.3.5.3. Interactions between protein particles

The third possible origin of the solid-like properties of the emulsions is the interactions between particles in the continuous phase. Excess proteins in the continuous phase usually results in thickening or even gelling of this phase (Chevalier & Bolzinger, 2013). The protein particles may even aggregate into fractal-type gel-like structures in the continuous phase (Dickinson, 2017), which results in solid-like rheological properties and enhanced stability against creaming and serum separation (Dickinson, 2013).

The amphiphilic nature of the HG|SC nanoparticles made it possible for them to be used as good emulsifiers, as shown in the CLSM micrographs (Figure 7-4C). The hydrophobic parts of proteins can aggregate via hydrophobic interactions, and the aggregation in the continuous phase can result in gel-like properties, as reported for soy, sorghum and zein protein nanoparticles (Tang & Liu, 2013; Xiao et al., 2016; Zou et al., 2017). The importance of hydrophobic interactions between plant seed storage proteins was confirmed by tuning the stiffness of the emulsion through adjusting the ionic strength (Tang & Liu,

2013; Xiao et al., 2016), which screens the electrostatic forces and intensifies hydrophobic interactions.

HG is more hydrophobic than soy protein (Yin, Tang, Wen, & Yang, 2007) and was calculated to more hydrophobic than α_{S1}-casein (Bigelow, 1967), which is the most hydrophobic casein among all the caseins based on the retention times using hydrophobic interaction chromatography (Bramanti, Sortino, Onor, Beni, & Raspi, 2003). Therefore, it would be expected that increasing the HG content in the HG|SC nanoparticles would result in higher hydrophobicity. In addition to the hydrophobic nature of HG, other conditions in this study were in favour of hydrophobic interactions between particles and droplets. Excess protein particles can be seen in the continuous phase in the CLSM micrographs (Figure 7-4), and the ζ-potential of these particles was low (approximately –18 mV under 35 mM NaCl). The 1HG|1SC nanoparticles appeared to be larger in the aged emulsion (Figure 7-4I) than in the freshly prepared emulsion (Figure 7-4C), indicating short-range particle–particle interactions. The 1HG|1SC nanoparticles (Figure 7-4C, F and I) were also larger than the 1HG|2SC nanoparticles (Figure 7-4B, E and H), suggesting that the 1HG|1SC nanoparticles formed larger aggregates because of the higher attractive forces between them. In contrast, the extra caseins in the 1HG|2SC nanoparticles made them more hydrophilic and/or electrostatically repulsive, which resulted in smaller aggregates.

7.3.6. *Proposed mechanism of the aging of emulsions stabilised by SC or HG|SC particles*

One study has reported a similar development of gel-like properties in aged protein-stabilised Pickering emulsions (Zou et al., 2017). The authors proposed that both flocculation and the formation of particle networks in the continuous phase were the

reasons for the gel-like property. They found that the droplets were flocculated because of the larger droplet sizes, and that the flocculated droplets dissociated when sodium dodecyl sulfate was added. The formation of a protein particle network was indicated by the protein signals in the continuous phase observed using CLSM. However, in our case, the CLSM micrograph showed only an intense background protein signal in the continuous phase, and no microstructure could be observed.

The HG|SC emulsions shows a similar hardening phenomenon during storage. However, no droplet flocculation was observed in the CLSM results. In addition, a new method to tune the rheological properties of aged concentrated emulsions, by controlling the HG:SC ratio during the formation of protein nanoparticles with a constant and moderate ionic strength (35 mM) solution, has been developed (Chuang et al., 2020).

The difference in time-dependent changes of the rheological properties may result partly from the different rigidities of the proteins, as shown in the interfacial tension experiments. The rheological properties were similar in all emulsions at day 0, suggesting that the SC and the HG|SC nanoparticles had similar extents of particle–particle interaction in the freshly prepared emulsions. During storage, the aged SC emulsions became less solid-like and more flowable, indicating fewer and/or weaker interactions between SC particles and droplets.

This outcome is contrary to previous work by Dickinson and Golding (1997), who found that aged SC-stabilised emulsions became more viscous; this may be attributed to the differences in the particle size, droplet size and ionic strength between the two studies. Nevertheless, the change in viscosity suggests different strengths of the interactions

between protein particles and droplets, probably related to a delayed rearrangement of the casein structures.

The flexibility of the caseins in SC allows them to form micellar-like structures when dispersed in water (HadjSadok et al., 2008; Pitkowski et al., 2008) and to rearrange easily when adsorbed to the oil–water interface (B. T. Wong et al., 2012), turning the caseins into a soft elastic shell during storage (Bressy, Hébraud, Schmitt, & Bibette, 2003). The rearrangement of the proteins involves the exposure of hydrophilic parts to the water phase and the burial of hydrophobic parts toward the oil phase on the oil–water interface. Because of the rearrangement of the flexible caseins, it is possible that hydrophobic interactions between the dispersed phase and the interfacial caseins diminished, which resulted in a less solid-like emulsion after storage.

The rigidity and hydrophobicity of HG may explain the change in the rheological properties of the HG|SC emulsions during storage. Aged HG|SC emulsions became more solid-like, and the extent of hardening correlated with the amount of HG. Different HG:SC ratios resulted in different extents of rigidity (Figure 7-1) and different particle sizes (Figure 7-4B and C) of the HG|SC nanoparticles.

As the higher rigidity of the HG|SC nanoparticles resulted in a lower rate of protein rearrangement and unfolding on the oil–water interface, the hydrophilic moieties needed more time to orient themselves into the continuous phase and therefore there was a lower rate of decrease in the hydrophobicity, i.e. the surface of the droplets would be more hydrophobic when there was more HG in the HG|SC nanoparticles. The higher hydrophobicity would provide stronger attractive hydrophobic interactions (both particle–

particle and particle–droplet), which resulted in the localised flocs of droplets and the more solid-like texture after storage.

To summarise, there was a two-step formation of the internal structure in the emulsion with an immediate step and a delayed step. The immediate step originated from a physically connected network of droplets because of the high volume fraction and the large size of the oil droplets, which gave all freshly prepared emulsions a similar gel-like property. The delayed step originated from the change in particle–particle interactions between the protein particles in the continuous phase and on the surface of the droplets during storage. The rigidity and possibly the hydrophobicity of HG|SC nanoparticles can be tuned by controlling the HG:SC ratio, which in turn changes the protein–protein interactions and the rheological properties of HG|SC emulsions during storage. The increase in the short-range and attractive interactions between protein particles can be quantified by the higher parameter *A* according to Bohlin's model, whereas no extended internal 3D structure was formed, according to the CLSM micrographs and the decreasing parameter *z* of Bohlin's model.

7.4. Conclusion

A stable concentrated emulsion was made using HG|SC nanoparticles as an emulsifier; the emulsion became self-supporting and did not coalescence after 21 days of storage at room temperature. The extent of solid-like properties and the viscosity of aged HG|SC emulsions could be controlled using different HG:SC ratios during the pH-cycling process to tune the rigidity of the protein particles without adding a high level of salt. The internal structure of the emulsion was formed mainly by short-range interactions between HG|SC nanoparticles

in the continuous phase and at the oil–water interface, which resulted in localised flocs of droplets. Stable concentrated HG|SC emulsions have the potential to be used to deliver hydrophobic compounds or to modulate the texture of semi-solid foods.

8. SUMMARY AND OVERALL DISCUSSION

In this study, plant proteins were extracted by a salt extraction method and freeze-dried to ensure that the extracted plant proteins are native, which should minimise the inconsistency of the functionalities of commercial plant protein products due to different processing history such as heating and spray drying. When compared to the conventional isoelectric precipitation method, the salt extraction method makes the extracted hemp seed protein lighter in colour and leads to a lower degree of denaturation, because the alkali would result in partial denaturation and co-extraction of polyphenols (Hadnađev et al., 2017).

The protein composition of HG was dominated by one protein, edestin, which is practically insoluble in water at neutral pH and could only be solubilised in alkaline, acidic or salt solutions. A phase diagram (Figure 4-13) of colloidal stability of HG at different protein concentrations (0.26 – 4.42% w/v) and ionic strengths (0.025 – 0.5 M) was constructed by monitoring the turbidity of protein solutions/dispersions. The solubility of HG in different dissociation reagents shows that its insolubility originated mainly from strong non-covalent interactions between HG, leading to extensive aggregation, and disulfide bonds play a minor role.

8.1. Interactions between HG and whey proteins

Insoluble aggregates were formed between HG and whey proteins either during heat-treatment (Figure 4-14) or after pH-cycling (Figure 6-4). The aggregations resulted from the formation of disulfide bonds, which is favourable at high temperature and/or alkaline pH (Visschers & De Jongh, 2005). Therefore, it seems that it will be challenging to make

soluble aggregates between HG and whey proteins. Besides, it is also difficult to make homogeneous HG-whey protein dispersions or gels because of the differences in solubility in water, i.e. the insoluble HG precipitates on the bottom while whey proteins are solubilised.

8.2. Interactions between HG and caseins

8.2.1. *Chaperone-like activity of caseins on the heat-induced aggregation of HG*

In Chapter 5, soluble aggregates were made by inducing interactions between HG and SC through heating. HG was mixed with SC with high ionic strength (0.5 M) at pH 7 and heated at 90 °C for up to 15 minutes. Heating HG alone led to extensive aggregation and precipitation. SC dramatically reduced the turbidity of the heated hemp-caseinate protein solution, exhibiting a chaperone-like effect against heat stress. The HG solution remained non-turbid when there was more than 0.15% of SC for 0.1% HG after the heat treatment. The DLS result showed that SC aggregated with HG, and the presence of SC also delayed the formation of aggregates and reduced the size of aggregates. However, the kinetics of edestin denaturation and melting temperature was unaffected by SC addition.

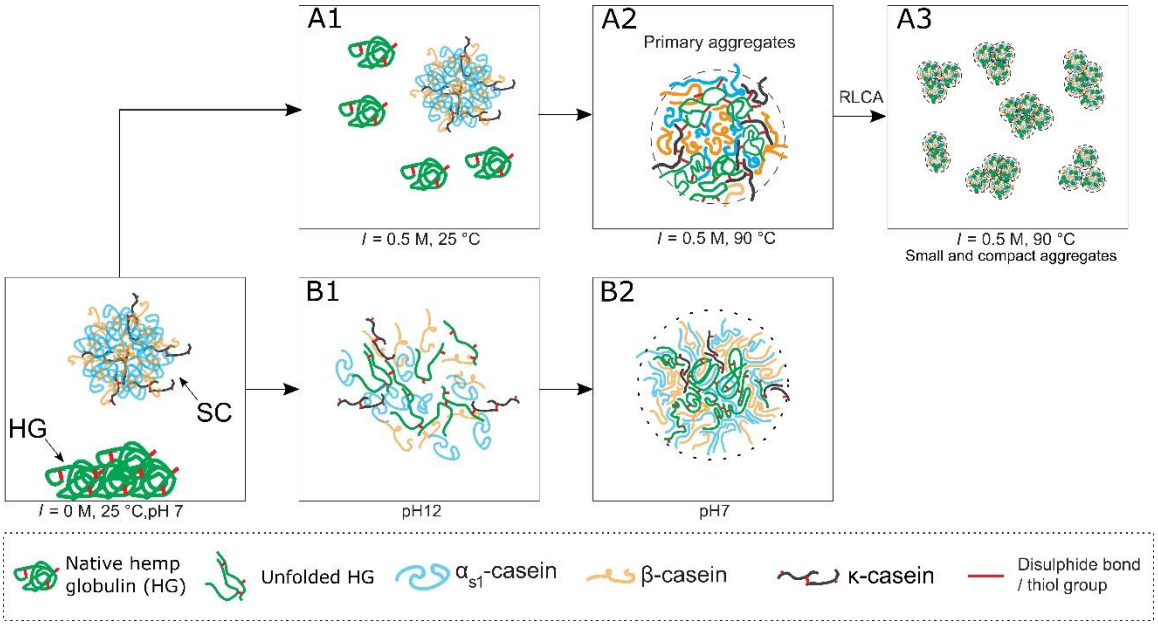

Figure 8-1 Proposed mechanism of interactions between HG and SC via (A1-A3) heat treatment at 0.5 M ionic strength and (B1-B2) pH-cycling process.

It was proposed that the addition of SC changed the aggregation regime from diffusion-limited cluster aggregation to reaction-limited cluster aggregation because more collisions were necessary for two particles to form stable aggregates. When HG and SC were heated together, proteins with cysteine residues (mainly edestin, other HG and κ-casein) would aggregate via the formation of disulfide bonds, while caseins interact with these disulfide-linked aggregates via hydrophobic interactions (Figure 8-1A). The adsorption of α_{S1}- and β-casein to the exposed hydrophobic regions of HG may thus provide steric hindrance so the probability of the reactive thiolate groups to react with other thiol groups or disulfide bonds became lower. Therefore, it needs more collisions to form disulfide-bonded aggregates, and this reaction-limited cluster regime and gives smaller and more compact aggregates.

A high-throughput and in-situ fluorescence method with a real-time PCR machine was developed to monitor the surface hydrophobicity in protein solutions. The results show that surface hydrophobicity of HG|SC blends was lower than the summed value of individual HG and SC after heat treatment, indicating that the exposed hydrophobic surface of HG do interact with the hydrophobic parts of SC. The HG|SC protein complexes remained colloidally stable when the ionic strength was lowered from 0.5 to 0.17 M, which broadens the possible applications in food systems.

8.2.2. *Formation of HG|SC nano particles by pH-shifting*

In chapter 6, the solubility of HG was improved by blending HG with SC and treating with a pH-cycling process. The pH-cycling involved adjusting the pH to 12 and reacting for 1 h, followed by neutralisation to pH 7. Compared to the results in Chapter 5, the HG concentration was raised from 0.1% to 1%, so the pH-cycled HG|SC nanoparticles should be more applicable in real food systems.

Nanoparticles composed of HG and SC (Z-average diameter ≈ 130 nm) were formed after the pH-cycling, and the solubility of HG increased from ~20% to > 80% when there was more than 1% of SC for 1% of HG. These HG|SC nanoparticles were monodisperse (PDI < 0.17) and the ζ-potential was ≈ -17 mV. Hydrogen bonding was one of the driving forces for assembly of HG|SC nanoparticles, because the nanoparticles were dissociated by heat treatment (up to 60 °C) or urea, which is an effective hydrogen bond breaker. HG|SC nanoparticles aggregated irreversibly above 60 °C, possibly due to thiol-disulfide exchange reactions. Albeit heat-induced aggregation happened, the nanoparticle was rather heat-stable as the z-average was only 229 nm after heating at 90 °C for 30 min. Disulfide bonds

were important for the formation of monodisperse HG|SC nanoparticles. N-ethylmaleimide blocked free thiol groups on HG and resulted in less disulfide-linked HG aggregates after pH-cycling, which in turn led to smaller HG|SC nanoparticles and a bimodal PSD. The soluble and heat-stable HG|SC nanoparticles were used to make concentrated emulsions in Chapter 7.

8.2.3. *Principles of the interactions between HG and SC*

This study characterised the salt-extracted HG and found one of its major limitation – low solubility in water and extensive aggregation when heated. The two methods in Chapter 5 and Chapter 6 were both effective to tackle these two functional problems by introducing the interactions between HG and SC. Moreover, these two methods follow similar principles:

a) HG must be solubilised in the first place.

The structure of HG aggregates formed during purification was held compactly by strong non-covalent forces such as hydrogen bonding and therefore they were not soluble in water at pH 7 (Figure 4-7). If HG was not solubilised first, it would keep being precipitated and thus impossible to introduce interactions between HG and the soluble dairy proteins. In Chapter 5, a high ionic strength (0.5 M) was used to solubilise HG (Figure 8-1A1), which may be due to the structural reorganisation of the major protein edestin in HG as in the soy glycinin, (Lakemond et al., 2000). However, the solubility of HG was still limited at ≈ 0.5% (w/v) even when the ionic strength was 0.5 M. In Chapter 6, HG was solubilised in

alkali (Figure 8-1B1), which is more effective than the high ionic strength as HG became > 80% soluble above pH 9 (Hadnađev et al., 2017; Tang et al., 2006).

b) HG must be partially unfolded/denatured.

Native HG are packed into crystalloids and the crystalline structure/aggregate exists even when ionic strength was 0.3M (Figure 4-11A). In order to introduce interactions between HG and dairy proteins, HG must be partially unfold/denature, which will expose the hydrophobic core and the buried cysteine/disulfide bonds for possible interactions. In Chapter 5, the unfolding of HG was realised by heat treatment at 90 °C, which is close to the melting temperature of edestin of 91.4 °C. The unfolding was confirmed by the increasing SO fluorescence with holding time at 90 °C (Figure 5-12A). In Chapter 6, the unfolding was achieved by alkali (pH 12), which is known to induced the molten globule-like conformation of plant seed storage protein (Jiang et al., 2009).

c) Interactions between HG and SC must be formed.

The results in this study show that casein could interact with HG to change the aggregation pattern of HG or form complexes with HG to form nanoparticles. The interactions are the sum of various forces and could be controlled by the chemical and physical conditions of the environment.

The reaction was at high temperatures (90 °C) and high ionic strengths (0.5 M) in Chapter 5. This heat treatment induced the sulfhydryl oxidation and thiol/disulfide exchange between the unfolded HG proteins themselves and κ-casein via disulfide linkages, which led to aggregation/complexation. Under these conditions, hydrogen bonds are weak due to

high temperatures and the electrostatic forces should be screened by the ions. On the other hand, hydrophobic interactions are stronger at elevated temperature and the hydrophobic parts of caseins interacted with the exposed hydrophobic regions of HG. This hydrophobic interaction changed the aggregation pattern of HG and resulted in smaller aggregates containing both HG and SC.

In Chapter 6, the alkaline pH (pH 12) unfolded and solubilised HG. The high pH resulted in high negative charge on HG and caseins, which both have pI at around pH 4 – 6. During the neutralisation back to pH 7, HG began to re-fold and caseins were incorporated via non-covalent interactions to form HG|SC nanoparticles. Disulfide-linked aggregates were also formed at pH 12 because the thiol groups became reactive due to oxidation. The disulfide linkages between HG resulted in the monodisperse HG|SC nanoparticles after the pH-cycling process.

8.2.4. *Other possible methods to introduce interactions between HG and SC*

After knowing these principles, other methods might be identified to introducing interactions between HG and SC.

Other methods to denature HG could also be used in addition to the heat- and alkali-treatment proposed in this study. Possible methods including shearing, adding organic solvents or other additives, which are applicable in food industry (Ustunol, 2014). Shear rates less than 10^3 s^{-1} could significantly alter the 3D structure of the protein and lead to the exposure of hydrophobic regions (Bekard, Asimakis, Bertolini, & Dunstan, 2011), which are known to interact with caseins as shown in this study. High pressure could be another method which unfolds proteins by weakening the hydrophobic interactions and

changing the protein structure (Grigera & McCarthy, 2010). Non-polar solvents influence polar and non-polar interactions and may also denature proteins at high concentration (Ustunol, 2014).

Among these methods for denaturation, shearing is the most common processing method in the food industry, which can be done by high pressure homogeniser. Actually, homogenisation had already been shown to increase the solubility of HG slightly when homogenised with SC or surfactant (Chapter 4) and in the pea-micellar casein system (Boursier et al., 2013). The study used only a rotor-stator homogeniser for shearing, and a more severe shearing method such as high-pressure homogeniser could be a more effective way to denature HG and provide further improvements in HG functionality. Extrusion is another promising tool to produce functional HG|SC blends, which involves high temperature, pressure and shearing at the same time.

8.3. Other potential proteins to interact with HG

In this study, caseins interacted with HG via hydrophobic interactions when heated together in salt solution, so the amphiphilicity and high hydrophobicity are important attributes for the chaperone-like activity of caseins. In addition to the hydrophobic property of caseins, the flexibility of caseins is also believed to be the reason for their chaperone-like activity (Bhattacharyya & Das, 1999; Morgan et al., 2005).

Therefore, it is possible to find other potential proteins to interact with HG according to their amphiphicity and flexibility. Protein hydrophobicity can be estimated by the primary structure of protein with bioinformatic tools such as ProtScale (Gasteiger et al., 2005).Figure 8-2 shows the calculated distribution of hydrophobicity of β-casein. It can be

seen that the β-casein has high score in the first 30 amino acid residues, i.e. this region is highly hydrophilic. On the other hand, the region between 120 – 209 residues are hydrophobic with minus scores (Huppertz, 2013).

Figure 8-2 Calculated hydrophobicity of β-casein along its primary sequence using ProtScale with the scale of Tanford (1962).

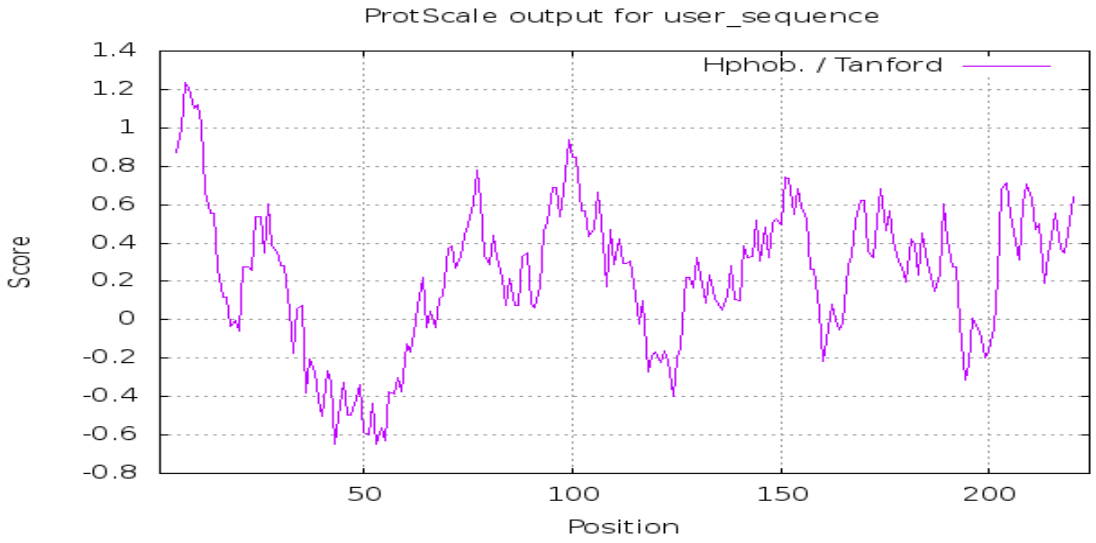

The flexibility of proteins can be obtained from a database (DisProt) for intrinsically disordered proteins (Hatos et al., 2020). For example, Table 12 shows the result of the bovine proteins that are 100% disordered and β-casein is among them (Perticaroli, Nickels, Ehlers, Mamontov, & Sokolov, 2014). By combining these bioinformatic tools and database, it is possible to screen for the potential proteins to interact with plant globulins.

Table 12 Bovine proteins that are 100% disordered retrieved from DisProt database (https://www.disprot.org/).

DisProt ID	UniProt Accession	Protein Name	Organism	Disorder content ↧
DP00329	P02666	Beta-casein	Bos taurus	100.00%
DP00047	P02687	Myelin basic protein	Bos taurus	100.00%
DP00118	P05059	Chromogranin-A	Bos taurus	100.00%
DP00814	P01252	Prothymosin alpha	Bos taurus	100.00%
DP00347	P04972	Retinal rod rhodopsin-sensitive cGMP 3',5'-cyclic phosphodiesterase subunit gamma	Bos taurus	100.00%
DP01801	P04985	Elastin	Bos taurus	100.00%
DP00795	P62326	Thymosin beta-4	Bos taurus	100.00%
DP00421	P07516	Protein phosphatase 1 regulatory subunit 1B	Bos taurus	100.00%
DP00955	P06836	Neuromodulin	Bos taurus	100.00%

8.4. The application of the HG|SC nanoparticles

Soluble nanoparticles were made from the HG and SC via a pH-cycling method and used to make O/W Pickering emulsions (Chapter 7). The emulsions were made with 70% oil phase and 30% water phase, which contained 2% protein (pure SC or HG-SC nanoparticles with HG/SC ratio of 1:2 or 1:1). All emulsions were stable during the 21-day storage, as there was no phase separation and the droplets did not coalescence or flocculate. At day 0, all emulsions were solid-like (G' > G'') regardless of the protein composition, while the rheological properties of emulsions during storage can be tuned by controlling HG/SC ratio in the HG|SC nanoparticles, i.e. emulsions became more solid-like when there was more HG in the HG-SC nanoparticles. On the other hand, emulsions stabilised by pure SC became more flowable during storage. The internal structure and interactions in the solid-like emulsions were evaluated by fitting the data obtained from frequency sweeping tests according to Bohlin's cooperative theory of flow (Bohlin, 1980). The results suggest that the solid-like emulsion resulted from stronger short-ranged interactions between flocs of oil droplets developed during storage when there were more HG in the HG-SC nanoparticles, while there was no extended structure three-dimensional network. The HG-

SC protein nanoparticles can be used to control the rheological properties of emulsion within its shelf life.

8.5. Recommendation for future work

In addition to the methods to introduce interactions between HC and SC such as high-pressure homogenisation and extrusion (Section 8.2.4), a number of potential areas are recommended for future work.

- Study the interactions between edestin and purified casein fractions

  The casein source in this study is SC. However, SC is a mixture of four caseins (α_{s1}-, α_{s2}-, β- and κ-casein), so it is hard to elucidate the detailed interactions between hemp edestin and these caseins. In order to get in-depth knowledge of the interactions between plant seed protein and caseins, it is better to purify the both the plant and dairy protein fractions, e.g. edestin and the individual caseins, and more accurate analytical methods could be used to study their interactions, such as isothermal calorimetry and surface plasmon resonance.

- Extend the chaperone-like effect of pH-cycling-induced complexation of caseins to other proteins.

  It has been shown that caseins could reduce the aggregate size of globular proteins, such as HG (chapter 5) and whey proteins (Yong & Foegeding, 2010). Since the globular 11S storage protein can be found in many other plants (Table 1), so the chaperone-like effect and the pH-cycling-induced complexation should be applicable

to other plant seed proteins as well. Other proteins with potential chaperone-like activity can also be tried as proposed in section 8.3.

- Nutritional synergy of hemp-casein protein blends.

Blending hemp protein and caseins fills the nutritional gap of insufficient indispensable amino acids by protein complementation. Moreover, it might also provide synergy in other nutritional values, such as sustained amino acid release and muscle growth as shown in dairy-soy protein blends (Reidy et al., 2013). An in-vitro digestion study could be the first step to see the release of amino acids and could give some information of the possible nutritional synergy.

- Production of HG-SC nanoparticles at pilot scale

The protein concentration (0.2 or 2% protein) used in this study was quite low when it comes to industrial scale, therefore it is useful to increase the protein concentration, e.g. 10 – 20 % protein, and try to make them at pilot scale. The pH-cycling method seems to be more promising for this application because of the simple procedure, higher protein concentrations and the good heat-stability of the products. It also worth trying to spray-dry the HG|SC nanoparticles and investigate their functionalities.

- The pH-cycled HG|SC nanoparticles could be used to encapsulate bioactive compounds.

pH-cycled soy protein or caseins have been made to encapsulate bioactive compounds such as curcumin and vitamin D_3 (H. Lee et al., 2016; Pan et al., 2014). This study showed that the characteristics of HG|SC nanoparticles could be tuned by changing HG/SC ratio. Therefore, it might be possible to improve the encapsulation efficiency

and loading capacity by tuning the HG/SC ratio according to the properties of the target bioactive compounds

REFERENCES

Achouri, A., Zhang, W., & Shiying, X. (1998). Enzymatic hydrolysis of soy protein isolate and effect of succinylation on the functional properties of resulting protein hydrolysates. *Food Research International, 31*(9), 617-623. doi:https://doi.org/10.1016/S0963-9969(98)00104-5

Aguilera, J. M., & Rademacher, B. (2004). Protein gels. In *Proteins in Food Processing* (pp. 468-482): Woodhead Publishing.

Akbari, A., Bamdad, F., & Wu, J. (2018). Chaperone-like food components: from basic concepts to food applications. *Food & Function*. doi:10.1039/C7FO01902E

Alavi, F., Emam-Djomeh, Z., & Chen, L. (2020). Acid-induced gelation of thermal co-aggregates from egg white and hempseed protein: Impact of microbial transglutaminase on mechanical and microstructural properties of gels. *Food Hydrocolloids, 107*, 105960. doi:https://doi.org/10.1016/j.foodhyd.2020.105960

Alexeev, V. L., Ilekti, P., Persello, J., Lambard, J., Gulik, T., & Cabane, B. (1996). Dispersions of Silica Particles in Surfactant Phases. *Langmuir, 12*(10), 2392-2401. doi:10.1021/la950707c

Alizadeh-Pasdar, N., & Li-Chan, E. C. Y. (2000). Comparison of Protein Surface Hydrophobicity Measured at Various pH Values Using Three Different Fluorescent Probes. *Journal of Agricultural and Food Chemistry, 48*(2), 328-334. doi:10.1021/jf990393p

Alu'datt, M. H., Alli, I., & Nagadi, M. (2012). Preparation, characterization and properties of whey-soy proteins co-precipitates. *Food Chemistry, 134*(1), 294-300. doi:http://dx.doi.org/10.1016/j.foodchem.2012.02.142

Aluko, R. E. (2016). Hemp Seed (Cannabis sativa L.) Proteins: Composition, Structure, Enzymatic Modification, and Functional or Bioactive Properties. In *Sustainable Protein Sources* (pp. 121-132).

Anuradha, S. N., & Prakash, V. (2009). Complexation of bovine β-lactoglobulin with 11S protein fractions of soybean (Glycine max) and sesame (Sesamum indicum). *International Journal of Food Sciences and Nutrition, 60*(SUPPL. 1), 27-42. doi:10.1080/09637480701877736

Arrese, E. L., Sorgentini, D. A., Wagner, J. R., & Anon, M. C. (1991). Electrophoretic, solubility and functional properties of commercial soy protein isolates. *Journal of Agricultural and Food Chemistry, 39*(6), 1029-1032. doi:10.1021/jf00006a004

Augustin, M. A., Oliver, C. M., & Hemar, Y. (2011). Casein, Caseinates, and Milk Protein Concentrates. In *Dairy Ingredients for Food Processing* (pp. 161-178): Wiley-Blackwell.

Barac, M., Cabrilo, S., Pesic, M., Stanojevic, S., Zilic, S., Macej, O., & Ristic, N. (2010). Profile and functional properties of seed proteins from six pea (Pisum sativum) genotypes. *International journal of molecular sciences, 11*(12), 4973-4990.

Bastier, P., Dumay, E., & Cheftel, J. C. (1993). Physico-chemical and Functional Properties of Commercial Caseinates. *LWT - Food Science and Technology, 26*(6), 529-537. doi:http://dx.doi.org/10.1006/fstl.1993.1104

Bekard, I. B., Asimakis, P., Bertolini, J., & Dunstan, D. E. (2011). The effects of shear flow on protein structure and function. *Biopolymers, 95*(11), 733-745. doi:10.1002/bip.21646

Beliciu, C. M., & Moraru, C. I. (2013). Physico-chemical changes in heat treated micellar casein - Soy protein mixtures. *LWT - Food Science and Technology, 54*(2), 469-476. doi:10.1016/j.lwt.2013.06.013

Ben-Harb, S., Panouillé, M., Huc-Mathis, D., Moulin, G., Saint-Eve, A., Irlinger, F., . . . Souchon, I. (2018). The rheological and microstructural properties of pea, milk, mixed pea/milk gels and gelled emulsions designed by thermal, acid, and enzyme treatments. *Food Hydrocolloids*. doi:https://doi.org/10.1016/j.foodhyd.2017.09.022

Berghout, J. A. M., Venema, P., Boom, R. M., & van der Goot, A. J. (2015). Comparing functional properties of concentrated protein isolates with freeze-dried protein isolates from lupin seeds. *Food Hydrocolloids, 51*, 346-354. doi:http://dx.doi.org/10.1016/j.foodhyd.2015.05.017

Berton-Carabin, C. C., & Schroën, K. (2015). Pickering Emulsions for Food Applications: Background, Trends, and Challenges. *Annual Review of Food Science and Technology, 6*(1), 263-297. doi:10.1146/annurev-food-081114-110822

Beverung, C. J., Radke, C. J., & Blanch, H. W. (1999). Protein adsorption at the oil/water interface: characterization of adsorption kinetics by dynamic interfacial tension measurements. *Biophysical Chemistry, 81*(1), 59-80. doi:https://doi.org/10.1016/S0301-4622(99)00082-4

Beynon, P. R., & Easterby, J. (2003). *Buffer Solutions*: Routledge.

Bhattacharyya, J., & Das, K. P. (1999). Molecular Chaperone-like Properties of an Unfolded Protein, αs-Casein. *Journal of Biological Chemistry, 274*(22), 15505-15509. doi:10.1074/jbc.274.22.15505

Bigelow, C. C. (1967). On the average hydrophobicity of proteins and the relation between it and protein structure. *Journal of Theoretical Biology, 16*(2), 187-211. doi:https://doi.org/10.1016/0022-5193(67)90004-5

Binks, B. P. (1998). *Modern aspects of emulsion science*. Cambridge, UK: Royal Society of Chemistry, Information Services.

Bohlin, L. (1980). A theory of flow as a cooperative phenomenon. *Journal of Colloid and Interface Science, 74*(2), 423-434. doi:https://doi.org/10.1016/0021-9797(80)90211-8

Boland, M. J. (2011). Whey proteins. In P. A. Williams (Ed.), *Handbook of Food Proteins* (pp. 30-55): Woodhead Publishing.

Boland, M. J., Rae, A. N., Vereijken, J. M., Meuwissen, M. P. M., Fischer, A. R. H., van Boekel, M. A. J. S., . . . Hendriks, W. H. (2013). The future supply of animal-derived protein for human consumption. *Trends in Food Science & Technology, 29*(1), 62-73. doi:http://dx.doi.org/10.1016/j.tifs.2012.07.002

Bonnaillie, L. M., & Tomasula, P. M. (2009). Whey Protein Fractionation. In *Whey Processing, Functionality and Health Benefits* (pp. 15-38): Wiley-Blackwell.

Boulet, M., Britten, M., & Lamarche, F. (2000). Aggregation of some food proteins in aqueous dispersions: effects of concentration, pH and ionic strength. *Food Hydrocolloids, 14*(2), 135-144. doi:http://dx.doi.org/10.1016/S0268-005X(99)00059-4

Boursier, B., Moretti, E., Ribadeau-Dumas, G., Belaid, S., Riaublanc, A., Gueguen, J., . . . Colin, I. (2013).

Bramanti, E., Sortino, C., Onor, M., Beni, F., & Raspi, G. (2003). Separation and determination of denatured αs1-, αs2-, β-and κ-caseins by hydrophobic interaction chromatography in cows', ewes' and goats' milk, milk mixtures and cheeses. *Journal of Chromatography A, 994*(1-2), 59-74.

Bressani, R. (1988). Protein Complementation of Foods. In E. Karmas & R. S. Harris (Eds.), *Nutritional Evaluation of Food Processing* (pp. 627-657). Dordrecht: Springer Netherlands.

Bressy, L., Hébraud, P., Schmitt, V., & Bibette, J. (2003). Rheology of Emulsions Stabilized by Solid Interfaces. *Langmuir, 19*(3), 598-604. doi:10.1021/la0264466

Brodkorb, A., Croguennec, T., Bouhallab, S., & Kehoe, J. J. (2016). Heat-induced denaturation, aggregation and gelation of whey proteins. In *Advanced Dairy Chemistry: Volume 1B: Proteins: Applied Aspects: Fourth Edition* (pp. 155-178).

Bryant, C. M., & McClements, D. J. (1998). Molecular basis of protein functionality with special consideration of cold-set gels derived from heat-denatured whey. *Trends in Food Science & Technology, 9*(4), 143-151. doi:http://dx.doi.org/10.1016/S0924-2244(98)00031-4

Callaway, J. C. (2004). Hempseed as a nutritional resource: An overview. *Euphytica, 140*(1-2), 65-72. doi:10.1007/s10681-004-4811-6

Campanella, O. H., Dorward, N. M., & Singh, H. (1995). A study of the rheological properties of concentrated food emulsions. *Journal of Food Engineering, 25*(3), 427-440. doi:https://doi.org/10.1016/0260-8774(94)00000-Y

Casey, R. (1999). Distribution and Some Properties of Seed Globulins. In P. R. Shewry & R. Casey (Eds.), *Seed Proteins* (pp. 159-169). Dordrecht: Springer Netherlands.

Cheng, J., Cui, J., Ma, Y., Yan, T., Wang, L., Li, H., & Li, X. (2016). Effects of soy-to-milk protein ratio and sucrose fatty acid ester addition on the stability of ice cream emulsions. *Food Hydrocolloids, 60*, 425-436. doi:10.1016/j.foodhyd.2016.04.002

Chevalier, Y., & Bolzinger, M.-A. (2013). Emulsions stabilized with solid nanoparticles: Pickering emulsions. *Colloids and Surfaces A: Physicochemical and Engineering Aspects, 439*, 23-34. doi:https://doi.org/10.1016/j.colsurfa.2013.02.054

Chihi, M. L., Mession, J. L., Sok, N., & Saurel, R. (2016). Heat-Induced Soluble Protein Aggregates from Mixed Pea Globulins and β-Lactoglobulin. *Journal of Agricultural and Food Chemistry, 64*(13), 2780-2791. doi:10.1021/acs.jafc.6b00087

Chihi, M. L., Sok, N., & Saurel, R. (2018). Acid gelation of mixed thermal aggregates of pea globulins and β-lactoglobulin. *Food Hydrocolloids, 85*, 120-128. doi:https://doi.org/10.1016/j.foodhyd.2018.07.006

Chronakis, I. S., & Kasapis, S. (1993). Structural properties of single and mixed milk/soya protein systems. *Food Hydrocolloids, 7*(6), 459-478. doi:http://dx.doi.org/10.1016/S0268-005X(09)80242-7

Chuang, C.-C., Anema, S. G., Ye, A., & Loveday, S. M. (2020). Submitted: Hemp globulin forms colloidal nanocomplexes with sodium caseinate during pH-cycling. *Food Research International*.

Comfort, S., & Howell, N. K. (2002). Gelation properties of soya and whey protein isolate mixtures. *Food Hydrocolloids, 16*(6), 661-672. doi:10.1016/s0268-005x(02)00033-4

Cordier, F., & Grzesiek, S. (2002). Temperature-dependence of protein hydrogen bond properties as studied by high-resolution NMR11Edited by P. E. Wright. *Journal of Molecular Biology, 317*(5), 739-752. doi:https://doi.org/10.1006/jmbi.2002.5446

Dalgleish, D. G. (2011). On the structural models of bovine casein micelles—review and possible improvements. *Soft Matter, 7*(6), 2265-2272. doi:10.1039/C0SM00806K

Dapčević-Hadnađev, T., Hadnađev, M., Lazaridou, A., Moschakis, T., & Biliaderis, C. G. (2018). Hempseed meal protein isolates prepared by different isolation techniques. Part II. gelation properties at different ionic strengths. *Food Hydrocolloids, 81*, 481-489. doi:https://doi.org/10.1016/j.foodhyd.2018.03.022

Dave, A. C., Loveday, S. M., Anema, S. G., Loo, T. S., Norris, G. E., Jameson, G. B., & Singh, H. (2013). β-Lactoglobulin Self-Assembly: Structural Changes in Early Stages and Disulfide Bonding in Fibrils. *Journal of Agricultural and Food Chemistry, 61*(32), 7817-7828. doi:10.1021/jf401084f

Day, L. (2013). Proteins from land plants – Potential resources for human nutrition and food security. *Trends in Food Science & Technology, 32*(1), 25-42. doi:http://dx.doi.org/10.1016/j.tifs.2013.05.005

Day, L., Xu, M., Hoobin, P., Burgar, I., & Augustin, M. A. (2007). Characterisation of fish oil emulsions stabilised by sodium caseinate. *Food Chemistry, 105*(2), 469-479. doi:https://doi.org/10.1016/j.foodchem.2007.04.013

de Folter, J. W. J., van Ruijven, M. W. M., & Velikov, K. P. (2012). Oil-in-water Pickering emulsions stabilized by colloidal particles from the water-insoluble protein zein. *Soft Matter, 8*(25), 6807-6815. doi:10.1039/C2SM07417F

de Kruif, C. G., Huppertz, T., Urban, V. S., & Petukhov, A. V. (2012). Casein micelles and their internal structure. *Advances in Colloid and Interface Science, 171-172*, 36-52. doi:https://doi.org/10.1016/j.cis.2012.01.002

de la Fuente, M. A., Singh, H., & Hemar, Y. (2002). Recent advances in the characterisation of heat-induced aggregates and intermediates of whey proteins. *Trends in Food Science & Technology, 13*(8), 262-274. doi:https://doi.org/10.1016/S0924-2244(02)00133-4

Derbyshire, E., Wright, D. J., & Boulter, D. (1976). Legumin and vicilin, storage proteins of legume seeds. *Phytochemistry, 15*(1), 3-24. doi:10.1016/S0031-9422(00)89046-9

Derkach, S. R. (2009). Rheology of emulsions. *Advances in Colloid and Interface Science, 151*(1), 1-23. doi:https://doi.org/10.1016/j.cis.2009.07.001

Derkach, S. R. (2010). Rheology on the way from dilute to concentrated emulsions. *International Review of Chemical Engineering, 2*(3), 465-472.

Dickinson, E. (2001). Milk protein interfacial layers and the relationship to emulsion stability and rheology. *Colloids and Surfaces B: Biointerfaces, 20*(3), 197-210. doi:https://doi.org/10.1016/S0927-7765(00)00204-6

Dickinson, E. (2013). Stabilising emulsion-based colloidal structures with mixed food ingredients. *Journal of the Science of Food and Agriculture, 93*(4), 710-721. doi:10.1002/jsfa.6013

Dickinson, E. (2017). Biopolymer-based particles as stabilizing agents for emulsions and foams. *Food Hydrocolloids, 68*, 219-231. doi:https://doi.org/10.1016/j.foodhyd.2016.06.024

Dickinson, E., & Golding, M. (1997). Rheology of Sodium Caseinate Stabilized Oil-in-Water Emulsions. *Journal of Colloid and Interface Science, 191*(1), 166-176. doi:https://doi.org/10.1006/jcis.1997.4939

Dickinson, E., Golding, M., & Povey, M. J. W. (1997). Creaming and Flocculation of Oil-in-Water Emulsions Containing Sodium Caseinate. *Journal of Colloid and Interface Science, 185*(2), 515-529. doi:https://doi.org/10.1006/jcis.1996.4605

Docimo, T., Caruso, I., Ponzoni, E., Mattana, M., & Galasso, I. (2014). Molecular characterization of edestin gene family in Cannabis sativa L. *Plant Physiology and Biochemistry, 84*, 142-148. doi:10.1016/j.plaphy.2014.09.011

Dong, X., Zhao, M., Yang, B., Yang, X., Shi, J., & Jiang, Y. (2011). EFFECT OF HIGH-PRESSURE HOMOGENIZATION ON THE FUNCTIONAL PROPERTY OF PEANUT PROTEIN. *Journal of Food Process Engineering, 34*(6), 2191-2204. doi:10.1111/j.1745-4530.2009.00546.x

Duranti, M., Consonni, A., Magni, C., Sessa, F., & Scarafoni, A. (2008). The major proteins of lupin seed: Characterisation and molecular properties for use as functional and nutraceutical ingredients. *Trends in Food Science & Technology, 19*(12), 624-633. doi:http://dx.doi.org/10.1016/j.tifs.2008.07.002

Dyballa, N., & Metzger, S. (2009). Fast and Sensitive Colloidal Coomassie G-250 Staining for Proteins in Polyacrylamide Gels. *Journal of Visualized Experiments : JoVE*(30), 1431. doi:10.3791/1431

Farrell, H. M., Wickham, E. D., & Groves, M. L. (1998). Environmental Influences on Purified κ-Casein: Disulfide Interactions1. *Journal of Dairy Science, 81*(11), 2974-2984. doi:https://doi.org/10.3168/jds.S0022-0302(98)75861-8

Feng, Y., & Lee, Y. (2016). Surface modification of zein colloidal particles with sodium caseinate to stabilize oil-in-water pickering emulsion. *Food Hydrocolloids, 56*, 292-302. doi:https://doi.org/10.1016/j.foodhyd.2015.12.030

Foegeding, E. A., & Davis, J. P. (2011). Food protein functionality: A comprehensive approach. *Food Hydrocolloids, 25*(8), 1853-1864. doi:https://doi.org/10.1016/j.foodhyd.2011.05.008

Fox, P. F., & Kelly, A. L. (2004). The caseins. In *Proteins in Food Processing* (pp. 29-71): Woodhead Publishing.

Gabriele, D., de Cindio, B., & D'Antona, P. (2001). A weak gel model for foods. *Rheologica Acta, 40*(2), 120-127. doi:10.1007/s003970000139

Gaspard, S. J., Auty, M. A. E., Kelly, A. L., O'Mahony, J. A., & Brodkorb, A. (2017). Isolation and characterisation of κ-casein/whey protein particles from heated milk protein concentrate and role of κ-casein in whey protein aggregation. *International Dairy Journal, 73*, 98-108. doi:https://doi.org/10.1016/j.idairyj.2017.05.012

Gasteiger, E., Hoogland, C., Gattiker, A., Duvaud, S. e., Wilkins, M. R., Appel, R. D., & Bairoch, A. (2005). Protein Identification and Analysis Tools on the ExPASy Server. In J. M. Walker (Ed.), *The Proteomics Protocols Handbook* (pp. 571-607). Totowa, NJ: Humana Press.

Gaucheron, F. (2005). The minerals of milk. *Reproduction Nutrition Development, 45*(4), 473-483.

Gerrard, J. A. (2002). Protein–protein crosslinking in food: methods, consequences, applications. *Trends in Food Science & Technology, 13*(12), 391-399. doi:http://dx.doi.org/10.1016/S0924-2244(02)00257-1

Golub, N. V., Markossian, K. A., Sholukh, M. V., Muranov, K. O., & Kurganov, B. I. (2009). Study of kinetics of thermal aggregation of mitochondrial aspartate aminotransferase by dynamic light scattering: protective effect of α-crystallin. *European Biophysics Journal, 38*(5), 547-556. doi:10.1007/s00249-009-0403-7

Grigera, J. R., & McCarthy, A. N. (2010). The Behavior of the Hydrophobic Effect under Pressure and Protein Denaturation. *Biophysical Journal, 98*(8), 1626-1631. doi:https://doi.org/10.1016/j.bpj.2009.12.4298

Grygorczyk, A., Alexander, M., & Corredig, M. (2013). Combined acid- and rennet-induced gelation of a mixed soya milk-cow's milk system. *International Journal of Food Science and Technology, 48*(11), 2306-2314. doi:10.1111/ijfs.12218

Gueguen, J., & Barbot, J. (1988). Quantitative and qualitative variability of pea (Pisum sativum L.) protein composition. *Journal of the Science of Food and Agriculture, 42*(3), 209-224. doi:10.1002/jsfa.2740420304

Guo, J., Yang, X.-Q., He, X.-T., Wu, N.-N., Wang, J.-M., Gu, W., & Zhang, Y.-Y. (2012). Limited Aggregation Behavior of β-Conglycinin and Its Terminating Effect on Glycinin Aggregation during Heating at pH 7.0. *Journal of Agricultural and Food Chemistry, 60*(14), 3782-3791. doi:10.1021/jf300409y

Guo, M. R., Fox, P. F., Flynn, A., & Kindstedt, P. S. (1996). Heat-induced modifications of the functional properties of sodium caseinate. *International Dairy Journal, 6*(5), 473-483. doi:https://doi.org/10.1016/0958-6946(95)00018-6

Guy, E. J., Vettel, H. E., & Pallansch, M. J. (1969). Spray-Dried Cheese Whey-Soy Flour Mixtures. *Journal of Dairy Science, 52*(4), 432-438. doi:10.3168/jds.S0022-0302(69)86583-5

Guyomarc'h, F., Nono, M., Nicolai, T., & Durand, D. (2009). Heat-induced aggregation of whey proteins in the presence of κ-casein or sodium caseinate. *Food Hydrocolloids, 23*(4), 1103-1110. doi:http://dx.doi.org/10.1016/j.foodhyd.2008.07.001

HadjSadok, A., Pitkowski, A., Nicolai, T., Benyahia, L., & Moulai-Mostefa, N. (2008). Characterisation of sodium caseinate as a function of ionic strength, pH and temperature using static and dynamic light scattering. *Food Hydrocolloids, 22*(8), 1460-1466. doi:http://dx.doi.org/10.1016/j.foodhyd.2007.09.002

Hadnađev, M., Dapčević-Hadnađev, T., Lazaridou, A., Moschakis, T., Michaelidou, A. M., Popović, S., & Biliaderis, C. G. (2017). Hempseed meal protein isolates prepared by different isolation techniques. Part I. physicochemical properties. *Food Hydrocolloids*. doi:https://doi.org/10.1016/j.foodhyd.2017.12.015

Hamada, J. S. (1994). Deamidation of food proteins to improve functionality. *Critical Reviews in Food Science and Nutrition, 34*(3), 283-292. doi:10.1080/10408399409527664

Hammann, F., & Schmid, M. (2014). Determination and quantification of molecular interactions in protein films: A review. *Materials, 7*(12), 7975-7996. doi:10.3390/ma7127975

Haratifar, S., & Guri, A. (2017). Nanocapsule formation by caseins. In S. M. Jafari (Ed.), *Nanoencapsulation Technologies for the Food and Nutraceutical Industries* (pp. 140-164): Academic Press.

Hatos, A., Hajdu-Soltész, B., Monzon, A. M., Palopoli, N., Álvarez, L., Aykac-Fas, B., . . . Piovesan, D. (2020). DisProt: intrinsic protein disorder annotation in 2020. *Nucleic Acids Research, 48*(D1), D269-d276. doi:10.1093/nar/gkz975

Hill, S. E. (1996). Emulsions. In G. M. Hall (Ed.), *Methods of testing protein functionality* (pp. 153-185). London.

Hinderink, E. B. A., Münch, K., Sagis, L., Schroën, K., & Berton-Carabin, C. C. (2019). Synergistic stabilisation of emulsions by blends of dairy and soluble pea proteins: Contribution of the interfacial composition. *Food Hydrocolloids, 97*, 105206. doi:https://doi.org/10.1016/j.foodhyd.2019.105206

Ho, K. K. H. Y., Schroën, K., San Martín-González, M. F., & Berton-Carabin, C. C. (2018). Synergistic and antagonistic effects of plant and dairy protein blends on the physicochemical stability of lycopene-loaded emulsions. *Food Hydrocolloids, 81*, 180-190. doi:https://doi.org/10.1016/j.foodhyd.2018.02.033

Holt, C., Carver, J. A., Ecroyd, H., & Thorn, D. C. (2013). Invited review: Caseins and the casein micelle: Their biological functions, structures, and behavior in foods. *Journal of Dairy Science, 96*(10), 6127-6146. doi:https://doi.org/10.3168/jds.2013-6831

Horne, D. S. (1998). Casein Interactions: Casting Light on the Black Boxes, the Structure in Dairy Products. *International Dairy Journal, 8*(3), 171-177. doi:https://doi.org/10.1016/S0958-6946(98)00040-5

House, J. D., Neufeld, J., & Leson, G. (2010). Evaluating the Quality of Protein from Hemp Seed (Cannabis sativa L.) Products Through the use of the Protein Digestibility-Corrected Amino Acid Score Method. *Journal of Agricultural and Food Chemistry, 58*(22), 11801-11807. doi:10.1021/jf102636b

Howell, N. K. (1992). Protein-protein interactions. In *Biochemistry of food proteins* (pp. 35-74): Springer.

Hu, Y.-Q., Yin, S.-W., Zhu, J.-H., Qi, J.-R., Guo, J., Wu, L.-Y., . . . Yang, X.-Q. (2016). Fabrication and characterization of novel Pickering emulsions and Pickering high internal emulsions stabilized by gliadin colloidal particles. *Food Hydrocolloids, 61*, 300-310. doi:https://doi.org/10.1016/j.foodhyd.2016.05.028

Huppertz, T. (2013). Chemistry of the Caseins. In P. L. H. McSweeney & P. F. Fox (Eds.), *Advanced Dairy Chemistry: Proteins: Basic Aspects* (4 ed., Vol. 1A, pp. 135-160). Boston, MA: Springer US.

Huppertz, T., Fox, P. F., & Kelly, A. L. (2018). The caseins: Structure, stability, and functionality. In *Proteins in Food Processing (Second Edition)* (pp. 49-92): Woodhead Publishing.

Hussain, R., Gaiani, C., Jeandel, C., Ghanbaja, J., & Scher, J. (2012). Combined effect of heat treatment and ionic strength on the functionality of whey proteins. *Journal of Dairy Science, 95*(11), 6260-6273. doi:http://dx.doi.org/10.3168/jds.2012-5416

Ikeda, S., Foegeding, E. A., & Hagiwara, T. (1999). Rheological Study on the Fractal Nature of the Protein Gel Structure. *Langmuir, 15*(25), 8584-8589. doi:10.1021/la9817415

Ipsen, R. (2017). Microparticulated whey proteins for improving dairy product texture. *International Dairy Journal, 67*, 73-79. doi:https://doi.org/10.1016/j.idairyj.2016.08.009

Jackman, R. L., & Yada, R. Y. (1989a). Functional Properties of Whey-Pea Protein Composite Blends in a Model System. *Journal of Food Science, 54*(5), 1287-1292. doi:10.1111/j.1365-2621.1989.tb05975.x

Jackman, R. L., & Yada, R. Y. (1989b). Multivariate Analysis of Functional and Structure-Related Properties of Whey-Vegetable Protein Composites. *Canadian Institute of Food Science and Technology Journal, 22*(3), 260-269. doi:http://dx.doi.org/10.1016/S0315-5463(89)70393-X

Jackman, R. L., & Yada, R. Y. (1989c). Ultraviolet Absorption and Fluorescence Properties of Whey-Potato and Whey-Pea Protein Composites. *Canadian Institute of Food Science and Technology Journal, 22*(3), 252-259. doi:http://dx.doi.org/10.1016/S0315-5463(89)70392-8

Jahaniaval, F., Kakuda, Y., Abraham, V., & Marcone, M. F. (2000). Soluble protein fractions from pH and heat treated sodium caseinate: physicochemical and functional properties. *Food Research International, 33*(8), 637-647. doi:http://dx.doi.org/10.1016/S0963-9969(00)00108-3

Jiang, J., Chen, J., & Xiong, Y. L. (2009). Structural and Emulsifying Properties of Soy Protein Isolate Subjected to Acid and Alkaline pH-Shifting Processes. *Journal of Agricultural and Food Chemistry, 57*(16), 7576-7583. doi:10.1021/jf901585n

Jiang, J., Xiong, Y. L., & Chen, J. (2010). pH Shifting Alters Solubility Characteristics and Thermal Stability of Soy Protein Isolate and Its Globulin Fractions in Different pH, Salt Concentration, and Temperature Conditions. *Journal of Agricultural and Food Chemistry, 58*(13), 8035-8042. doi:10.1021/jf101045b

Jiao, B., Shi, A., Wang, Q., & Binks, B. P. (2018). High-Internal-Phase Pickering Emulsions Stabilized Solely by Peanut-Protein-Isolate Microgel Particles with Multiple Potential Applications. *Angewandte Chemie International Edition, 57*(30), 9274-9278. doi:10.1002/anie.201801350

Jose, J., Pouvreau, L., & Martin, A. H. (2016). Mixing whey and soy proteins: Consequences for the gel mechanical response and water holding. *Food Hydrocolloids, 60*, 216-224. doi:http://dx.doi.org/10.1016/j.foodhyd.2016.03.031

Ju, Z. Y., Hettiarachchy, N. S., & Rath, N. (2001). Extraction, denaturation and hydrophobic Properties of Rice Flour Proteins. *Journal of Food Science, 66*(2), 229-232. doi:10.1111/j.1365-2621.2001.tb11322.x

Karperien, A. (2013). FracLac for ImageJ. doi:https://imagej.nih.gov/ij/plugins/fraclac/FLHelp/Introduction.htm

Kaul, A. (2000). The Phase Diagram. In R. Hatti-Kaul (Ed.), *Aqueous Two-Phase Systems: Methods and Protocols: Methods and Protocols* (pp. 11-21). Totowa, NJ: Humana Press.

Kehoe, J. J., & Foegeding, E. (2014). The characteristics of heat-induced aggregates formed by mixtures of β-lactoglobulin and β-casein. *Food Hydrocolloids, 39*, 264-271.

Kehoe, J. J., & Foegeding, E. A. (2011). Interaction between β-Casein and Whey Proteins As a Function of pH and Salt Concentration. *Journal of Agricultural and Food Chemistry, 59*(1), 349-355. doi:10.1021/jf103371g

Khanova, H. A., Markossian, K. A., Kurganov, B. I., Samoilov, A. M., Kleimenov, S. Y., Levitsky, D. I., . . . Ostrovsky, M. A. (2005). Mechanism of Chaperone-like

Activity. Suppression of Thermal Aggregation of βL-Crystallin by α-Crystallin. *Biochemistry, 44*(47), 15480-15487. doi:10.1021/bi051175u

Kim, H. S., & Mason, T. G. (2017). Advances and challenges in the rheology of concentrated emulsions and nanoemulsions. *Advances in Colloid and Interface Science, 247*, 397-412. doi:https://doi.org/10.1016/j.cis.2017.07.002

Kim, J.-J., & Lee, M.-Y. (2011). Isolation and characterization of edestin from Cheungsam hempseed. *Journal of Applied Biological Chemistry, 54*(2), 84-88.

Koudelka, T., Hoffmann, P., & Carver, J. A. (2009). Dephosphorylation of αs- and β-Caseins and Its Effect on Chaperone Activity: A Structural and Functional Investigation. *Journal of Agricultural and Food Chemistry, 57*(13), 5956-5964. doi:10.1021/jf9008372

Kristo, E., & Corredig, M. (2014). Functional Properties of Food Proteins. In *Applied Food Protein Chemistry* (pp. 47-73): John Wiley & Sons, Ltd.

Kurzhals, S., Zirbs, R., & Reimhult, E. (2015). Synthesis and Magneto-Thermal Actuation of Iron Oxide Core-PNIPAM Shell Nanoparticles. *ACS Applied Materials & Interfaces, 7*(34), 19342-19352. doi:10.1021/acsami.5b05459

Laemmli, U. K. (1970). Cleavage of Structural Proteins during the Assembly of the Head of Bacteriophage T4. *Nature, 227*, 680. doi:10.1038/227680a0

Lakemond, C. M. M., de Jongh, H. H. J., Hessing, M., Gruppen, H., & Voragen, A. G. J. (2000). Soy Glycinin: Influence of pH and Ionic Strength on Solubility and Molecular Structure at Ambient Temperatures. *Journal of Agricultural and Food Chemistry, 48*(6), 1985-1990. doi:10.1021/jf9908695

Lakowicz, J. R. (2006). *Principles of Fluorescence Spectroscopy* (3 ed.): Springer US.

Layton, C. J., & Hellinga, H. W. (2011). Quantitation of protein–protein interactions by thermal stability shift analysis. *Protein Science : A Publication of the Protein Society, 20*(8), 1439-1450. doi:10.1002/pro.674

Lazzari, S., Nicoud, L., Jaquet, B., Lattuada, M., & Morbidelli, M. (2016). Fractal-like structures in colloid science. *Advances in Colloid and Interface Science, 235*, 1-13. doi:https://doi.org/10.1016/j.cis.2016.05.002

Lee, H., Yildiz, G., dos Santos, L. C., Jiang, S., Andrade, J. E., Engeseth, N. J., & Feng, H. (2016). Soy protein nano-aggregates with improved functional properties prepared by sequential pH treatment and ultrasonication. *Food Hydrocolloids, 55*, 200-209. doi:10.1016/j.foodhyd.2015.11.022

Lee, S. K., & Klostermeyer, H. (2001). The Effect of pH on the Rheological Properties of Reduced-fat Model Processed Cheese Spreads. *LWT - Food Science and Technology, 34*(5), 288-292. doi:https://doi.org/10.1006/fstl.2001.0761

Li-Chan, E. C. Y. (2004). Properties of proteins in food systems: an introduction. In *Proteins in Food Processing* (pp. 2-26): Woodhead Publishing.

Linke, C., & Drusch, S. (2018). Pickering emulsions in foods - opportunities and limitations. *Critical Reviews in Food Science and Nutrition, 58*(12), 1971-1985. doi:10.1080/10408398.2017.1290578

Liu, K. S., & Hsieh, F.-H. (2007). Protein–Protein Interactions in High Moisture-Extruded Meat Analogs and Heat-Induced Soy Protein Gels. *Journal of the American Oil Chemists' Society, 84*(8), 741-748. doi:10.1007/s11746-007-1095-8

Liu, K. S., & Hsieh, F.-H. (2008). Protein–Protein Interactions during High-Moisture Extrusion for Fibrous Meat Analogues and Comparison of Protein Solubility

Methods Using Different Solvent Systems. *Journal of Agricultural and Food Chemistry, 56*(8), 2681-2687. doi:10.1021/jf073343q

Liyanaarachchi, W. S., Ramchandran, L., & Vasiljevic, T. (2015). Controlling heat induced aggregation of whey proteins by casein inclusion in concentrated protein dispersions. *International Dairy Journal, 44*, 21-30. doi:https://doi.org/10.1016/j.idairyj.2014.12.010

Loveday, S. M., Ye, A., Anema, S. G., & Singh, H. (2013). Heat-induced colloidal interactions of whey proteins, sodium caseinate and gum arabic in binary and ternary mixtures. *Food Research International, 54*(1), 111-117. doi:http://doi.org/10.1016/j.foodres.2013.06.013

Lucey, J. A. (2017). Formation, Structural Properties, and Rheology of Acid-Coagulated Milk Gels. In P. L. H. McSweeney, P. F. Fox, P. D. Cotter, & D. W. Everett (Eds.), *Cheese (Fourth Edition)* (pp. 179-197). San Diego: Academic Press.

Lucey, J. A., Srinivasan, M., Singh, H., & Munro, P. A. (2000). Characterization of Commercial and Experimental Sodium Caseinates by Multiangle Laser Light Scattering and Size-Exclusion Chromatography. *Journal of Agricultural and Food Chemistry, 48*(5), 1610-1616. doi:10.1021/jf990769z

Lui, D. Y. M., Litster, J. D., & White, E. T. (2007). Precipitation of soy proteins: Particle formation and protein separation. *AIChE Journal, 53*(2), 514-522. doi:10.1002/aic.11070

Ma, H., Forssell, P., Partanen, R., Seppänen, R., Buchert, J., & Boer, H. (2009). Sodium Caseinates with an Altered Isoelectric Point As Emulsifiers in Oil/Water Systems. *Journal of Agricultural and Food Chemistry, 57*(9), 3800-3807. doi:10.1021/jf803104s

Ma, L., Zou, L., McClements, D. J., & Liu, W. (2020). One-step preparation of high internal phase emulsions using natural edible Pickering stabilizers: Gliadin nanoparticles/gum Arabic. *Food Hydrocolloids, 100*, 105381. doi:https://doi.org/10.1016/j.foodhyd.2019.105381

Madeira, F., Park, Y. M., Lee, J., Buso, N., Gur, T., Madhusoodanan, N., . . . Lopez, R. (2019). The EMBL-EBI search and sequence analysis tools APIs in 2019. *Nucleic Acids Research, 47*(W1), W636-W641. doi:10.1093/nar/gkz268

Mahmoudi, N., Mehalebi, S., Nicolai, T., Durand, D., & Riaublanc, A. (2007). Light-Scattering Study of the Structure of Aggregates and Gels Formed by Heat-Denatured Whey Protein Isolate and β-Lactoglobulin at Neutral pH. *Journal of Agricultural and Food Chemistry, 55*(8), 3104-3111. doi:10.1021/jf063029g

Majesté, J.-C., Carrot, C., Olalla, B., & Fulchiron, R. (2012). Internal Reorganization of Agglomerates as an Explanation of Energy Dissipation at Very Low Strain for Heterogeneous Polymer Systems. *Macromolecular Theory and Simulations, 21*(2), 113-119. doi:10.1002/mats.201100063

Malomo, S. A., & Aluko, R. E. (2015a). A comparative study of the structural and functional properties of isolated hemp seed (Cannabis sativa L.) albumin and globulin fractions. *Food Hydrocolloids, 43*, 743-752. doi:http://dx.doi.org/10.1016/j.foodhyd.2014.08.001

Malomo, S. A., & Aluko, R. E. (2015b). Conversion of a low protein hemp seed meal into a functional protein concentrate through enzymatic digestion of fibre coupled with

membrane ultrafiltration. *Innovative Food Science & Emerging Technologies, 31*, 151-159. doi:http://dx.doi.org/10.1016/j.ifset.2015.08.004

Malomo, S. A., He, R., & Aluko, R. E. (2014). Structural and Functional Properties of Hemp Seed Protein Products. *Journal of Food Science, 79*(8), C1512-C1521. doi:10.1111/1750-3841.12537

Manion, B., & Corredig, M. (2006). Interactionns between whey protein isolate and soy protein fractions at oil-water interfaces: Effects of heat and concentration of protein in the aqueous phase. *Journal of Food Science, 71*(8), E343-E349. doi:10.1111/j.1750-3841.2006.00160.x

Manoi, K., & Rizvi, S. S. H. (2009). Emulsification mechanisms and characterizations of cold, gel-like emulsions produced from texturized whey protein concentrate. *Food Hydrocolloids, 23*(7), 1837-1847. doi:https://doi.org/10.1016/j.foodhyd.2009.02.011

Marcone, M. F., Kakuda, Y., & Yada, R. Y. (1998a). Salt-soluble seed globulins of dicotyledonous and monocotyledonous plants II. Structural characterization. *Food Chemistry, 63*(2), 265-274. doi:http://dx.doi.org/10.1016/S0308-8146(97)00159-3

Marcone, M. F., Kakuda, Y., & Yada, R. Y. (1998b). Salt-soluble seed globulins of various dicotyledonous and monocotyledonous plants—I. Isolation/purification and characterization. *Food Chemistry, 62*(1), 27-47. doi:http://dx.doi.org/10.1016/S0308-8146(97)00158-1

Markossian, K., Yudin, I., & Kurganov, B. (2009). Mechanism of Suppression of Protein Aggregation by α-Crystallin. *International journal of molecular sciences, 10*(3), 1314.

Martin, A. H., De Los Reyes Jiménez, M. L., & Pouvreau, L. (2016). Modulating the aggregation behaviour to restore the mechanical response of acid induced mixed gels of sodium caseinate and soy proteins. *Food Hydrocolloids, 58*, 215-223. doi:10.1016/j.foodhyd.2016.02.029

Martin, A. H., Nieuwland, M., & De Jong, G. A. H. (2014). Characterization of heat-set gels from RuBisCO in comparison to those from other proteins. *Journal of Agricultural and Food Chemistry, 62*(44), 10783-10791. doi:10.1021/jf502905g

Mathai, J. K., Liu, Y., & Stein, H. H. (2017). Values for digestible indispensable amino acid scores (DIAAS) for some dairy and plant proteins may better describe protein quality than values calculated using the concept for protein digestibility-corrected amino acid scores (PDCAAS). *British Journal of Nutrition, 117*(4), 490-499. doi:10.1017/S0007114517000125

Matsumura, Y., & Mori, T. (1996). Gelation. In G. M. Hall (Ed.), *Methods of testing protein functionality* (pp. 76-109). London: Blackie Academic & Professional.

McCann, T. H., Guyon, L., Fischer, P., & Day, L. (2018). Rheological properties and microstructure of soy-whey protein. *Food Hydrocolloids, 82*, 434-441. doi:https://doi.org/10.1016/j.foodhyd.2018.04.023

McMahon, D. J., & Oommen, B. S. (2013). Casein Micelle Structure, Functions, and Interactions. In P. L. H. McSweeney & P. F. Fox (Eds.), *Advanced Dairy Chemistry: Volume 1A: Proteins: Basic Aspects, 4th Edition* (pp. 185-209). Boston, MA: Springer US.

Message, J.-L., Roustel, S., & Saurel, R. (2015). Interactions in casein micelle – Pea protein system (part I): Heat-induced denaturation and aggregation. *Food Hydrocolloids*. doi:http://dx.doi.org/10.1016/j.foodhyd.2015.12.015

Message, J.-L., Roustel, S., & Saurel, R. (2017). Interactions in casein micelle - pea protein system (Part II): mixture acid gelation with glucono-δ-lactone. *Food Hydrocolloids*. doi:https://doi.org/10.1016/j.foodhyd.2017.06.029

Morgan, P. E., Treweek, T. M., Lindner, R. A., Price, W. E., & Carver, J. A. (2005). Casein Proteins as Molecular Chaperones. *Journal of Agricultural and Food Chemistry, 53*(7), 2670-2683. doi:10.1021/jf048329h

Mounsey, J. S., & O'Kennedy, B. T. (2010). Heat-stabilisation of β-lactoglobulin through interaction with sodium caseinate. *Milchwissenschaft, 65*(1), 79-83.

Murray, B. S. (2019). Pickering emulsions for food and drinks. *Current Opinion in Food Science, 27*, 57-63. doi:https://doi.org/10.1016/j.cofs.2019.05.004

Nakai, S., Ho, L., Tung, M. A., & Quinn, J. R. (1980). Solubilization of Rapeseed, Soy and Sunflower Protein Isolates by Surfactant and Proteinase Treatments. *Canadian Institute of Food Science and Technology Journal, 13*(1), 14-22. doi:http://dx.doi.org/10.1016/S0315-5463(80)73296-0

Niesen, F. H., Berglund, H., & Vedadi, M. (2007). The use of differential scanning fluorimetry to detect ligand interactions that promote protein stability. *Nature protocols, 2*, 2212. doi:10.1038/nprot.2007.321

Noble, J. E., & Bailey, M. J. A. (2009). Quantitation of Protein. In R. B. Richard & P. D. Murray (Eds.), *Methods in Enzymology* (Vol. Volume 463, pp. 73-95): Academic Press.

O'Connell, J. E., Grinberg, V. Y., & de Kruif, C. G. (2003). Association behavior of β-casein. *Journal of Colloid and Interface Science, 258*(1), 33-39. doi:https://doi.org/10.1016/S0021-9797(02)00066-8

O'Kennedy, B. T., & Mounsey, J. S. (2006). Control of Heat-Induced Aggregation of Whey Proteins Using Casein. *Journal of Agricultural and Food Chemistry, 54*(15), 5637-5642. doi:10.1021/jf0607866

O'Connor, D. (2018). Hemp seed can now be sold as food [Press release]. Retrieved from https://www.beehive.govt.nz/release/hemp-seed-can-now-be-sold-food

O'Kennedy, B. T., Mounsey, J. S., Murphy, F., Duggan, E., & Kelly, P. M. (2006). Factors affecting the acid gelation of sodium caseinate. *International Dairy Journal, 16*(10), 1132-1141. doi:https://doi.org/10.1016/j.idairyj.2005.11.003

O'Mahony, J. A., & Fox, P. F. (2013). Milk Proteins: Introduction and Historical Aspects. In P. L. H. McSweeney & P. F. Fox (Eds.), *Advanced Dairy Chemistry: Volume 1A: Proteins: Basic Aspects, 4th Edition* (pp. 43-85). Boston, MA: Springer US.

O'Regan, J., & Mulvihill, D. M. (2011). Caseins and Caseinates, Industrial Production, Compositional Standards, Specifications, and Regulatory Aspects. In *Encyclopedia of Dairy Sciences* (2 ed., pp. 855-863). San Diego: Academic Press.

Onwulata, C. I., Thomas-Gahring, A. E., & Phillips, J. G. (2014). Physical properties of mixed dairy food proteins. *International Journal of Food Properties, 17*(10), 2241-2262. doi:10.1080/10942912.2013.791836

Onwulata, C. I., Tunick, M. H., & Mukhopadhyay, S. (2014). Flow behavior of mixed-protein incipient gels. *International Journal of Food Properties, 17*(6), 1283-1302. doi:10.1080/10942912.2012.709208

Osborne, T. B. (1924). *The vegetable proteins* (2nd ed. ed.). London: Longmans Green and Co.

Oshinbolu, S., Shah, R., Finka, G., Molloy, M., Uden, M., & Bracewell, D. G. (2018). Evaluation of fluorescent dyes to measure protein aggregation within mammalian cell culture supernatants. *Journal of chemical technology and biotechnology (Oxford, Oxfordshire : 1986), 93*(3), 909-917. doi:10.1002/jctb.5519

Pan, K., Luo, Y., Gan, Y., Baek, S. J., & Zhong, Q. (2014). pH-driven encapsulation of curcumin in self-assembled casein nanoparticles for enhanced dispersibility and bioactivity. *Soft Matter, 10*(35), 6820-6830. doi:10.1039/c4sm00239c

Pan, K., & Zhong, Q. (2016). Low energy, organic solvent-free co-assembly of zein and caseinate to prepare stable dispersions. *Food Hydrocolloids, 52*, 600-606. doi:https://doi.org/10.1016/j.foodhyd.2015.08.014

Park, S.-K., Seo, J.-B., & Lee, M.-Y. (2012). Proteomic profiling of hempseed proteins from Cheungsam. *Biochimica et Biophysica Acta (BBA) - Proteins and Proteomics, 1824*(2), 374-382. doi:http://dx.doi.org/10.1016/j.bbapap.2011.10.005

Patel, A. R., Bouwens, E. C. M., & Velikov, K. P. (2010). Sodium Caseinate Stabilized Zein Colloidal Particles. *Journal of Agricultural and Food Chemistry, 58*(23), 12497-12503. doi:10.1021/jf102959b

Patel, P. R., & Grant, D. R. (1982). Protein Interactions of Cheese Whey-Pea Flour Blends. *Canadian Institute of Food Science and Technology Journal, 15*(1), 24-28. doi:http://dx.doi.org/10.1016/S0315-5463(82)72309-0

Patel, P. R., Youngs, C. G., & Grant, D. R. (1981). Preparation and properties of spray-dried pea protein concentrate-cheese whey blends. *Cereal Chemistry, 58*(4), 249-255.

Patel, S., Cudney, R., & McPherson, A. (1994). Crystallographic characterization and molecular symmetry of edestin, a legumin from hemp. *Journal of Molecular Biology, 235*(1), 361-363. doi:http://dx.doi.org/10.1016/S0022-2836(05)80040-3

Pelegrine, D. H. G., & Gasparetto, C. A. (2005). Whey proteins solubility as function of temperature and pH. *LWT - Food Science and Technology, 38*(1), 77-80. doi:http://dx.doi.org/10.1016/j.lwt.2004.03.013

Peressini, D., Sensidoni, A., & de Cindio, B. (1998). Rheological characterization of traditional and light mayonnaises. *Journal of Food Engineering, 35*(4), 409-417. doi:https://doi.org/10.1016/S0260-8774(98)00032-6

Perticaroli, S., Nickels, J. D., Ehlers, G., Mamontov, E., & Sokolov, A. P. (2014). Dynamics and Rigidity in an Intrinsically Disordered Protein, β-Casein. *The Journal of Physical Chemistry B, 118*(26), 7317-7326. doi:10.1021/jp503788r

Pitkowski, A., Durand, D., & Nicolai, T. (2008). Structure and dynamical mechanical properties of suspensions of sodium caseinate. *Journal of Colloid and Interface Science, 326*(1), 96-102. doi:https://doi.org/10.1016/j.jcis.2008.07.003

Pizones Ruiz-Henestrosa, V. M., Martinez, M. J., Patino, J. M. R., & Pilosof, A. M. R. (2012). A Dynamic Light Scattering Study on the Complex Assembly of Glycinin Soy Globulin in Aqueous Solutions. *Journal of the American Oil Chemists' Society, 89*(7), 1183-1191. doi:10.1007/s11746-012-2029-7

Poore, J., & Nemecek, T. (2018). Reducing food's environmental impacts through producers and consumers. *Science, 360*(6392), 987-992. doi:10.1126/science.aaq0216

Pritchard, S. R., & Kailasapathy, K. (2011). Chemical, Physical, and Functional Characteristics of Dairy Ingredients. In *Dairy Ingredients for Food Processing* (pp. 35-57): Wiley-Blackwell.

Radford, S. J., & Dickinson, E. (2004). Depletion flocculation of caseinate-stabilised emulsions: what is the optimum size of the non-adsorbed protein nano-particles? *Colloids and Surfaces A: Physicochemical and Engineering Aspects, 238*(1), 71-81. doi:https://doi.org/10.1016/j.colsurfa.2004.02.020

Reidy, P. T., Walker, D. K., Dickinson, J. M., Gundermann, D. M., Drummond, M. J., Timmerman, K. L., . . . Rasmussen, B. B. (2013). Protein Blend Ingestion Following Resistance Exercise Promotes Human Muscle Protein Synthesis. *J Nutr, 143*(4), 410-416. doi:10.3945/jn.112.168021

Robins, M. M. (2000). Emulsions — creaming phenomena. *Current Opinion in Colloid & Interface Science, 5*(5), 265-272. doi:https://doi.org/10.1016/S1359-0294(00)00065-0

Roesch, R. R., & Corredig, M. (2005). Heat-induced soy-whey proteins interactions: Formation of soluble and insoluble protein complexes. *Journal of Agricultural and Food Chemistry, 53*(9), 3476-3482. doi:10.1021/jf048870d

Roesch, R. R., & Corredig, M. (2006). Study of the effect of soy proteins on the acid-induced gelation of casein micelles. *Journal of Agricultural and Food Chemistry, 54*(21), 8236-8243. doi:10.1021/jf060875i

Roesch, R. R., Juneja, M., Monagle, C., & Corredig, M. (2004). Aggregation of soy/milk mixes during acidification. *Food Research International, 37*(3), 209-215. doi:10.1016/j.foodres.2003.11.003

Sabaté, J., & Soret, S. (2014). Sustainability of plant-based diets: back to the future. *The American journal of clinical nutrition, 100*(suppl_1), 476S-482S. doi:10.3945/ajcn.113.071522

Salopek, B., Krasić, D., & Filipović, S. (1992). Measurement and Application of Zeta-potential. *Rudarsko-geološko-naftni zbornik, 4*, 141-157.

Sava, N., Van der Plancken, I., Claeys, W., & Hendrickx, M. (2005). The Kinetics of Heat-Induced Structural Changes of β-Lactoglobulin. *Journal of Dairy Science, 88*(5), 1646-1653. doi:https://doi.org/10.3168/jds.S0022-0302(05)72836-8

Schägger, H. (2006). Tricine-SDS-PAGE. *Nature protocols, 1*(1), 16-22.

Schellman, J. A. (1997). Temperature, stability, and the hydrophobic interaction. *Biophysical Journal, 73*(6), 2960-2964. doi:https://doi.org/10.1016/S0006-3495(97)78324-3

Scheraga, H. A., Nemethy, G., & Steinberg, I. Z. (1962). The contribution of hydrophobic bonds to the thermal stability of protein conformations. *Journal of Biological Chemistry, 237*, 2506-2508.

Schindelin, J., Arganda-Carreras, I., Frise, E., Kaynig, V., Longair, M., Pietzsch, T., . . . Schmid, B. (2012). Fiji: an open-source platform for biological-image analysis. *Nature methods, 9*(7), 676.

Sharifizadeh, A., Saboury, A. A., Moosavi-Movahedi, A. A., Salami, M., & Yousefi, R. (2012). A new aspect to chaperone-like activity of bovine β-casein by protein–protein interactions study. *International Journal of Biological Macromolecules, 51*(5), 901-907. doi:https://doi.org/10.1016/j.ijbiomac.2012.08.002

Shewry, P. R., & Casey, R. (1999). Seed Proteins. In P. R. Shewry & R. Casey (Eds.), *Seed Proteins* (pp. 1-10). Dordrecht: Springer Netherlands.

Shewry, P. R., Napier, J. A., & Tatham, A. S. (1995). Seed storage proteins: structures and biosynthesis. *The Plant Cell, 7*(7), 945-956.

Shridhar, K. S. (2012). Protein Solubility and Functionality. In *Food Proteins and Peptides* (pp. 95-124): CRC Press.

Silva, J. V. C., Balakrishnan, G., Schmitt, C., Chassenieux, C., & Nicolai, T. (2018). Heat-induced gelation of aqueous micellar casein suspensions as affected by globular protein addition. *Food Hydrocolloids, 82*, 258-267. doi:https://doi.org/10.1016/j.foodhyd.2018.04.002

Silva, J. V. C., Cochereau, R., Schmitt, C., Chassenieux, C., & Nicolai, T. (2018). Heat-induced gelation of mixtures of micellar caseins and plant proteins in aqueous solution. *Food Research International*. doi:https://doi.org/10.1016/j.foodres.2018.09.058

Silva, J. V. C., Jacquette, B., Amagliani, L., Schmitt, C., Nicolai, T., & Chassenieux, C. (2019). Heat-induced gelation of micellar casein/plant protein oil-in-water emulsions. *Colloids and Surfaces A: Physicochemical and Engineering Aspects, 569*, 85-92. doi:10.1016/j.colsurfa.2019.01.065

Singh, H. (2011). Functional Properties of Milk Proteins. In *Encyclopedia of Dairy Sciences* (2 ed., pp. 887-893). San Diego: Academic Press.

Srivastava, N. (2020). *Mintel Patent insights: next-gen plant protein ingredients*. Retrieved from https://www.mintel.com/

St. Angelo, A. J., Yatsu, L. Y., & Altschul, A. M. (1968). Isolation of edestin from aleurone grains of Cannabis sativa. *Archives of Biochemistry and Biophysics, 124*, 199-205. doi:http://dx.doi.org/10.1016/0003-9861(68)90320-2

Stone, A. K., Karalash, A., Tyler, R. T., Warkentin, T. D., & Nickerson, M. T. (2015). Functional attributes of pea protein isolates prepared using different extraction methods and cultivars. *Food Research International, 76, Part 1*, 31-38. doi:http://dx.doi.org/10.1016/j.foodres.2014.11.017

Stumpe, M. C., & Grubmüller, H. (2007). Interaction of Urea with Amino Acids: Implications for Urea-Induced Protein Denaturation. *Journal of the American Chemical Society, 129*(51), 16126-16131. doi:10.1021/ja076216j

Sun, C., Gao, Y., & Zhong, Q. (2018a). Effects of acidification by glucono-delta-lactone or hydrochloric acid on structures of zein-caseinate nanocomplexes self-assembled during a pH cycle. *Food Hydrocolloids, 82*, 173-185. doi:https://doi.org/10.1016/j.foodhyd.2018.04.007

Sun, C., Gao, Y., & Zhong, Q. (2018b). Properties of Ternary Biopolymer Nanocomplexes of Zein, Sodium Caseinate, and Propylene Glycol Alginate and Their Functions of Stabilizing High Internal Phase Pickering Emulsions. *Langmuir, 34*(31), 9215-9227. doi:10.1021/acs.langmuir.8b01887

Tanford, C. (1962). Contribution of Hydrophobic Interactions to the Stability of the Globular Conformation of Proteins. *Journal of the American Chemical Society, 84*(22), 4240-4247. doi:10.1021/ja00881a009

Tang, C.-H., & Liu, F. (2013). Cold, gel-like soy protein emulsions by microfluidization: Emulsion characteristics, rheological and microstructural properties, and gelling

mechanism. *Food Hydrocolloids, 30*(1), 61-72. doi:https://doi.org/10.1016/j.foodhyd.2012.05.008

Tang, C.-H., Ten, Z., Wang, X.-S., & Yang, X.-Q. (2006). Physicochemical and Functional Properties of Hemp (Cannabis sativa L.) Protein Isolate. *Journal of Agricultural and Food Chemistry, 54*(23), 8945-8950. doi:10.1021/jf0619176

Teh, S. S., Bekhit, A. E. D. A., Carne, A., & Birch, J. (2016). Antioxidant and ACE-inhibitory activities of hemp (Cannabis sativa L.) protein hydrolysates produced by the proteases AFP, HT, Pro-G, actinidin and zingibain. *Food Chemistry, 203*, 199-206. doi:10.1016/j.foodchem.2016.02.057

Ustunol, Z. (2014). Physical, Chemical, and Processing-Induced Changes in Proteins. In *Applied Food Protein Chemistry* (pp. 23-46): John Wiley & Sons, Ltd.

Vinceković, M., Ćurlin, M., & Jurašin, D. (2014). Impact of Cationic Surfactant on the Self-Assembly of Sodium Caseinate. *Journal of Agricultural and Food Chemistry, 62*(34), 8543-8554. doi:10.1021/jf5016472

Visschers, R. W., & De Jongh, H. H. J. (2005). Disulphide bond formation in food protein aggregation and gelation. *Biotechnology Advances, 23*(1), 75-80. doi:10.1016/j.biotechadv.2004.09.005

Vojdani, F. (1996). Solubility. In G. M. Hall (Ed.), *Methods of testing protein functionality* (pp. 11-60). London.

Vreeker, R., Hoekstra, L. L., den Boer, D. C., & Agterof, W. G. M. (1992). Fractal aggregation of whey proteins. *Food Hydrocolloids, 6*(5), 423-435. doi:https://doi.org/10.1016/S0268-005X(09)80028-3

Wang, L., Xue, J., & Zhang, Y. (2019). Preparation and characterization of curcumin loaded caseinate/zein nanocomposite film using pH-driven method. *Industrial Crops and Products, 130*, 71-80. doi:https://doi.org/10.1016/j.indcrop.2018.12.072

Wang, L., & Zhang, Y. (2017). Eugenol Nanoemulsion Stabilized with Zein and Sodium Caseinate by Self-Assembly. *Journal of Agricultural and Food Chemistry, 65*(14), 2990-2998. doi:10.1021/acs.jafc.7b00194

Wang, Q., Jin, Y., & Xiong, Y. L. (2018). Heating-aided pH Shifting Modifies Hemp Seed Protein Structure, Cross-linking, and Emulsifying Properties. *Journal of Agricultural and Food Chemistry*. doi:10.1021/acs.jafc.8b03901

Wang, Q., & Xiong, Y. L. (2019). Processing, Nutrition, and Functionality of Hempseed Protein: A Review. *Comprehensive Reviews in Food Science and Food Safety, 0*(0). doi:10.1111/1541-4337.12450

Wang, R., Xu, P., Chen, Z., Zhou, X., & Wang, T. (2019). Complexation of rice proteins and whey protein isolates by structural interactions to prepare soluble protein composites. *LWT - Food Science and Technology, 101*, 207-213. doi:https://doi.org/10.1016/j.lwt.2018.11.006

Wang, T., Xu, P., Chen, Z., & Wang, R. (2018). Mechanism of structural interplay between rice proteins and soy protein isolates to design novel protein hydrocolloids. *Food Hydrocolloids, 84*, 361-367. doi:https://doi.org/10.1016/j.foodhyd.2018.06.024

Wang, T., Xu, P., Chen, Z., Zhou, X., & Wang, R. (2018). Alteration of the structure of rice proteins by their interaction with soy protein isolates to design novel protein composites. *Food & Function, 9*(8), 4282-4291. doi:10.1039/C8FO00661J

Wang, T., Yue, M., Xu, P., Wang, R., & Chen, Z. (2018). Toward water-solvation of rice proteins via backbone hybridization by casein. *Food Chemistry, 258*, 278-283. doi:https://doi.org/10.1016/j.foodchem.2018.03.084

Wang, T., Zhang, H., Wang, L., Wang, R., & Chen, Z. (2015). Mechanistic insights into solubilization of rice protein isolates by freeze-milling combined with alkali pretreatment. *Food Chemistry, 178*, 82-88. doi:10.1016/j.foodchem.2015.01.057

Wang, X.-S., Tang, C.-H., Yang, X.-Q., & Gao, W.-R. (2008). Characterization, amino acid composition and in vitro digestibility of hemp (Cannabis sativa L.) proteins. *Food Chemistry, 107*(1), 11-18. doi:10.1016/j.foodchem.2007.06.064

Webb, M. F., Naeem, H. A., & Schmidt, K. A. (2002). Food Protein Functionality in a Liquid System: A Comparison of Deamidated Wheat Protein with Dairy and Soy Proteins. *Journal of Food Science, 67*(8), 2896-2902. doi:10.1111/j.1365-2621.2002.tb08835.x

Wilde, P. J., & Clark, D. C. (1996). Foam forming and stability. In G. M. Hall (Ed.), *Methods of testing protein functionality* (pp. 112-152). London: Blackie Academic & Professional.

Wong, B. T., Zhai, J., Hoffmann, S. V., Aguilar, M.-I., Augustin, M., Wooster, T. J., & Day, L. (2012). Conformational changes to deamidated wheat gliadins and β-casein upon adsorption to oil–water emulsion interfaces. *Food Hydrocolloids, 27*(1), 91-101. doi:https://doi.org/10.1016/j.foodhyd.2011.08.012

Wong, D., Vasanthan, T., & Ozimek, L. (2013). Synergistic enhancement in the co-gelation of salt-soluble pea proteins and whey proteins. *Food Chemistry, 141*(4), 3913-3919. doi:http://dx.doi.org/10.1016/j.foodchem.2013.05.082

Wouters, A. G. B., Rombouts, I., Fierens, E., Brijs, K., & Delcour, J. A. (2016). Relevance of the Functional Properties of Enzymatic Plant Protein Hydrolysates in Food Systems. *Comprehensive Reviews in Food Science and Food Safety, 15*(4), 786-800. doi:10.1111/1541-4337.12209

Xiao, J., Wang, X. a., Perez Gonzalez, A. J., & Huang, Q. (2016). Kafirin nanoparticles-stabilized Pickering emulsions: Microstructure and rheological behavior. *Food Hydrocolloids, 54*, 30-39. doi:https://doi.org/10.1016/j.foodhyd.2015.09.008

Ye, A., Flanagan, J., & Singh, H. (2006). Formation of stable nanoparticles via electrostatic complexation between sodium caseinate and gum arabic. *Biopolymers, 82*(2), 121-133. doi:https://doi.org/10.1002/bip.20465

Yerramilli, M., Longmore, N., & Ghosh, S. (2017). Improved stabilization of nanoemulsions by partial replacement of sodium caseinate with pea protein isolate. *Food Hydrocolloids, 64*, 99-111. doi:http://dx.doi.org/10.1016/j.foodhyd.2016.10.027

Yin, S.-W., Tang, C.-H., Cao, J.-S., Hu, E.-K., Wen, Q.-B., & Yang, X.-Q. (2008). Effects of limited enzymatic hydrolysis with trypsin on the functional properties of hemp (Cannabis sativa L.) protein isolate. *Food Chemistry, 106*(3), 1004-1013. doi:http://dx.doi.org/10.1016/j.foodchem.2007.07.030

Yin, S.-W., Tang, C.-H., Wen, Q.-B., & Yang, X.-Q. (2007). Properties of cast films from hemp (Cannabis sativa L.) and soy protein isolates. A comparative study. *Journal of Agricultural and Food Chemistry, 55*(18), 7399-7404.

Yong, Y. H., & Foegeding, E. A. (2008). Effects of Caseins on Thermal Stability of Bovine β-Lactoglobulin. *Journal of Agricultural and Food Chemistry, 56*(21), 10352-10358. doi:10.1021/jf801658u

Yong, Y. H., & Foegeding, E. A. (2010). Caseins: Utilizing Molecular Chaperone Properties to Control Protein Aggregation in Foods. *Journal of Agricultural and Food Chemistry, 58*(2), 685-693. doi:10.1021/jf903072g

Young, V. R., & Pellett, P. L. (1994). Plant proteins in relation to human protein and amino acid nutrition. *The American journal of clinical nutrition, 59*(5), 1203S-1212S. doi:10.1093/ajcn/59.5.1203S

Zaidel, D. N. A., Chronakis, I. S., & Meyer, A. S. (2013). Stabilization of oil-in-water emulsions by enzyme catalyzed oxidative gelation of sugar beet pectin. *Food Hydrocolloids, 30*(1), 19-25. doi:https://doi.org/10.1016/j.foodhyd.2012.04.004

Zeng, T., Wu, Z.-l., Zhu, J.-Y., Yin, S.-W., Tang, C.-H., Wu, L.-Y., & Yang, X.-Q. (2017). Development of antioxidant Pickering high internal phase emulsions (HIPEs) stabilized by protein/polysaccharide hybrid particles as potential alternative for PHOs. *Food Chemistry, 231*, 122-130. doi:https://doi.org/10.1016/j.foodchem.2017.03.116

Zhang, X., Fu, X., Zhang, H., Liu, C., Jiao, W., & Chang, Z. (2005). Chaperone-like activity of β-casein. *The International Journal of Biochemistry & Cell Biology, 37*(6), 1232-1240. doi:https://doi.org/10.1016/j.biocel.2004.12.004

Zhu, Q., Lu, H., Zhu, J., Zhang, M., & Yin, L. (2019). Development and characterization of pickering emulsion stabilized by zein/corn fiber gum (CFG) complex colloidal particles. *Food Hydrocolloids, 91*, 204-213. doi:https://doi.org/10.1016/j.foodhyd.2019.01.029

Zou, Y., Pan, R. T., Wan, Z. L., Guo, J., Wang, J. M., & Yang, X. Q. (2017). Gel-like emulsions prepared with zein nanoparticles produced through phase separation from acetic acid solutions. *International Journal of Food Science and Technology, 52*(12), 2670-2676. doi:10.1111/ijfs.13558

MASSEY UNIVERSITY
GRADUATE RESEARCH SCHOOL

STATEMENT OF CONTRIBUTION
DOCTORATE WITH PUBLICATIONS/MANUSCRIPTS

We, the candidate and the candidate's Primary Supervisor, certify that all co-authors have consented to their work being included in the thesis and they have accepted the candidate's contribution as indicated below in the *Statement of Originality*.

Name of candidate:	Chih-Chieh Chuang
Name/title of Primary Supervisor:	Aiqian Ye
Name of Research Output and full reference:	
Chuang, C.-C., Anema, S. G., Ye, A., & Loveday, S. M. (2020). Hemp globulin forms colloidal nanocomplexes with sodium caseinate during pH-cycling. Food Research International. Under revision.	
In which Chapter is the Manuscript /Published work:	Chapter 6
Please indicate:	
• The percentage of the manuscript/Published Work that was contributed by the candidate:	85
and	
• Describe the contribution that the candidate has made to the Manuscript/Published Work:	
The candidate designed and carried out the experiments. The candidate prepared the first draft of the manuscript and drafted answers to reviewers' comments during the peer-review process.	
For manuscripts intended for publication please indicate target journal:	
Candidate's Signature:	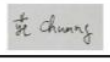 Digitally signed by 86be710-6c04-460c-adb5-0e7b1b3f06a DN: CN=86be710-6c04-460c-adb5-0e7b1b3f06a Reason: I am approving this document with my legally binding signature Location: Palmerston North Date: 2021.01.21 22:23:06+1700' Foxit Reader Version: 10.1.1
Date:	21/01/2021
Primary Supervisor's Signature:	Aiqian Ye Digitally signed by Aiqian Ye DN: cn=Aiqian Ye, c=NZ, o=Massey University, ou=SF&AT, email=a.m.ye@massey.ac.nz Date: 2021.01.26 08:59:37 +13'00'
Date:	26/01/2021

(This form should appear at the end of each thesis chapter/section/appendix submitted as a manuscript/ publication or collected as an appendix at the end of the thesis)

MASSEY UNIVERSITY
GRADUATE RESEARCH SCHOOL

STATEMENT OF CONTRIBUTION
DOCTORATE WITH PUBLICATIONS/MANUSCRIPTS

We, the candidate and the candidate's Primary Supervisor, certify that all co-authors have consented to their work being included in the thesis and they have accepted the candidate's contribution as indicated below in the *Statement of Originality*.

Name of candidate:	Chih-Chieh Chuang
Name/title of Primary Supervisor:	Aiqian Ye
Name of Research Output and full reference:	
Chuang, C.-C., Ye, A., Anema, S. G., & Loveday, S. M. (2020). Concentrated Pickering emulsions stabilised by hemp globulin–caseinate nanoparticles: tuning the rheological properties by adjusting the hemp globulin: caseinate ratio. Food & Function.	
In which Chapter is the Manuscript /Published work:	Chapter 7
Please indicate:	
• The percentage of the manuscript/Published Work that was contributed by the candidate:	85
and	
• Describe the contribution that the candidate has made to the Manuscript/Published Work:	
The candidate designed and carried out the experiments. The candidate prepared the first draft of the manuscript and drafted answers to reviewers' comments during the peer-review process.	
For manuscripts intended for publication please indicate target journal:	
Candidate's Signature:	Chuang — Digitally signed; Reason: I am approving this document with my legally binding signature; Location: Palmerston North; Date: 2021.01.21 22:25:16 +13'00'; Foxit Reader Version: 10.1.1
Date:	21/01/2021
Primary Supervisor's Signature:	Aiqian Ye — Digitally signed by Aiqian Ye; DN: cn=Aiqian Ye, c=NZ, o=Massey University, ou=SF&AT, email=a.m.ye@massey.ac.nz; Date: 2021.01.26 09:00:01 +13'00'
Date:	26/01/2021

(This form should appear at the end of each thesis chapter/section/appendix submitted as a manuscript/ publication or collected as an appendix at the end of the thesis)